Stony Brook University

NET N_2 FLUXES IN MUDDY SEDIMENTS OF GREAT PECONIC BAY: RATES, PATHWAYS & CONTROLS

A Dissertation Presented

by

Stuart Waugh

to

The Graduate School

in Partial Fulfillment of the

Requirements

for the Degree of

Doctor of Philosophy

in

Marine and Atmospheric Sciences

Stony Brook University

December 2015

Stony Brook University

The Graduate School

Stuart Waugh

We, the dissertation committee for the above candidate for the

Doctor of Philosophy degree, hereby recommend

acceptance of this dissertation.

Robert C. Aller, Dissertation Advisor
Distinguished Professor, School of Marine & Atmospheric Sciences

Bruce J. Brownawell , Chair of the Defense
Associate Professor, School of Marine & Atmospheric Sciences

Robert M. Cerrato
Associate Professor, School of Marine & Atmospheric Sciences

John E. Mak
Professor, School of Marine & Atmospheric Sciences

Anne E. Giblin
Senior Scientist, Marine Biological Laboratory

This dissertation is accepted by the Graduate School

Charles Taber
Dean of the Graduate School

Abstract of the Dissertation

NET N_2 FLUXES IN MUDDY SEDIMENTS OF GREAT PECONIC BAY: RATES, PATHWAYS & CONTROLS

by

Stuart Waugh

Doctor of Philosophy

in

Marine and Atmospheric Sciences

Stony Brook University

2015

Depending on its form, nitrogen (N) can exert a dominant control on marine productivity and ecosystem structure. Multiple geochemical processes are involved in redox transformations of nitrogen (N) in marine sediments. In coastal benthic environments, a number of abiotic and biological environmental factors control the extent to which these processes are relevant and therefore the outcomes of sedimentary N transformations. This dissertation seeks to quantify rates of net N remineralization in and fluxes from the un-vegetated, muddy sediments of Great Peconic Bay (GPB), NY and describe the relevance of the biogeochemical processes involved.

Direct measurements of sediment – water solute fluxes (O2, N_2, NH_4^+ & NO_3^-/NO_2^-) were made both *ex-situ* and *in-situ* with benthic chambers; N & ΣCO_2 remineralization was measured in anoxic incubations. Seasonal flux and remineralization patterns were investigated. Although GPB sediment produced net N_2 (g) over each seasonal period measured, N_2 fixation was found to have had a measureable impact on gross N_2 fluxes especially when rates were low in spring periods. N_2 production was influenced by temperature, reactive substrate availability, bio-irrigation (by *Amphioplus abditus* & *Squilla empusa*) and the presence of benthic algae. Estimates of sedimentary N remineralization were consistent with ΣCO_2 production and approximated separately measured N fluxes (N_2, NH_4^+ & NO_3^-/NO_2^-). ^{15}N tracer experiments demonstrated denitrification was the dominant N_2 production pathway and anammox contributed < 10% to net N_2 production.

There is evidence from previous studies denitrification is susceptible to environmental contaminants. This research investigated what impacts environmentally relevant concentrations of different classes of the commonly-used quaternary ammonium surfactant compounds (QACs) and Cu - alone and

in combination- have on denitrification in GPB mud sediments. Highly adsorbent QACs were not found to impact N_2 production in the fine-grained sediments of GPB but Cu was shown to often inhibit N_2 production. Thus, increasing anthropogenic contaminant inputs could alter the benthic N cycle.

To gain a preliminary understanding of how GPB sediments process modern-day N loadings into the GPB estuary, N_2 flux estimates were compared with estimates of atmospheric and groundwater N inputs into the bay. These estimates show sedimentary N_2 fluxes substantially reduce anthropogenic N loadings but do not eliminate them under some likely scenarios.

DEDICATION PAGE

To the memory of my father, Ralph Stuart Waugh, who showed me the beauty of the oceans and to my son, Henry Waugh, who realizes the value of unspoiled nature even at his early age.

TABLE OF CONTENTS

LIST OF TABLES

ACKNOWLEDGMENTS

I thank Robert C. Aller, my advisor, from whom I have learned not only how to study marine sediments but more broadly how to harness curiosity. Bob teaches by setting examples of excellence and integrity not only in scientific pursuits but, equally importantly, in navigating life. I am also grateful for the financial support of his lab over a number of years.

I acknowledge the members of my committee all of whom contributed to the development of my dissertation. Earning a Ph.D. is not a solitary achievement and each of my committee members has helped me to grow as a scientist. Specifically, I would like to acknowledge: John Mak for his incisive questions which allowed me to build a dissolved gas analyzer capable of measuring dissolved N_2 (g); Robert Cerrato for his patient explanations of alternate statistical methods with which to effectively weigh the importance of trends and differences in my results; Bruce Brownawell for sharing some of his extensive knowledge of general, organic and analytical chemistry and for helping me develop the experimental design used in chapter 6; and Anne Giblin who far exceeded the responsibilities of an external advisor in advising me on the development of experimental designs and measurement protocols.

Christina Heilbrun, manager of the Aller lab, has assisted me on countless occasions in everything from measuring ΣCO_2 and O_2, cleaning-up after a barrage of sediment processing, explaining methods to listening to trial presentations and proofing scientific drafts. I cannot begin to thank her sufficiently.

Brian Gagliardi, manager of the research vessels in Southhampton, was instrumental in the effective and safe collection of sediment samples in Great Peconic Bay. Additionally, I was able to focus on sediment sampling and processing because of the help of competent dive partners including Chuck Wall, Debbie Aller, Lisa Jackson and Amanda Tinoco. Tracey Evans, formerly of the Mak lab, provided invaluable help in joining together glass and steel in a seamless way during the development of the dissolved gas analyzer.

I was fortunate to have shared the company of a number of lab-members during my research. Aleya Kaushik, Zhenrai Cao, Shaily Rahman and Isaac Klingensmith have all given me indelible memories of their generosity, hard work and dedication to science.

Finally, I thank the faculty of the School of Marine and Atmospheric Sciences for fostering a great learning environment; in particular, I acknowledge Kirk Cochran, Cindy Lee, Qingzhi Zhu and Mary Scranton for their roles in my development as a scientist.

CHAPTER ONE: INTRODUCTION

Multiple geochemical processes are involved in redox transformations of nitrogen (N) in marine sediments. In coastal environments, a large number of abiotic and biological environmental factors control the extent to which these processes are relevant and therefore the outcomes of N transformations within the sediments. This dissertation seeks to quantify rates of net N_2 fluxes in the un-vegetated, muddy sediments of Great Peconic Bay (GPB), NY and describe the relevance of the biogeochemical processes involved.

The initial motivation for the research with which this dissertation began was to see whether instances of net benthic N_2 fixation could be found in Great Peconic Bay (GPB). Net N_2 fixation (loss of N_2 from solution) had been reported in sediments at several sites in Texas estuaries (Garner et al 2006; McCarthy et al 2008) and in Narragansett Bay (Fulweiler et al 2007) using membrane inlet mass spectrometry (MiMS). Although earlier work had described N_2 fixation in coastal sediments (e.g., Jones 1982), its significance was thought limited by inhibitory NH_4^+ concentrations (Howarth 1988 (b)) and consequently confined to surficial microbial mats (e.g., Joye & Paerl 1993; Paerl et al 1996) or to rhizospheres of sea- and marsh- grass meadows (e.g., McGlathery et al 1998; Currin et al 1996).

The mid-bay station in Narragansett Bay, where Fulweiler et al (2007 & 2014) collected sediment samples upon which much of their findings (and subsequent confirmations) of net N_2 fixation were based, is only ~ 120 km from the GPB station where sediments for this investigation were sampled. And, as the sites are within 1° latitude of each other, they experience the same climate. Further, the benthic environments at each site share many common characteristics including similar overlying water depth, tidal influence, salinity and variation in salinity, grain size and lack of vegetation (Table 1.1). Consequently, GPB sediment provided a comparable setting in which to investigate the balance between N_2 production and N_2 fixation.

1.1 The sedimentary N cycle.

The N cycle in marine sediments is described in Fig. 1.1 Although there is increasing evidence of the relevance of benthic N_2 fixation in coastal marine sediments (see below), N is generally delivered to the seabed as particulate organic nitrogen (PON). The complexity of remineralization of PON to NH_4^+ depends on structure of nitrogenous molecules involved but the fundamental process as described by Herbert (1999) consists of the hydrolysis of proteins to amino acids which are subsequently deaminated to NH_4^+. A diverse group of

ammonifying bacteria produce the necessary hydrolytic enzymes. The recycled NH_4^+ can diffuse along concentration gradients, become assimilated by benthic biomass, adsorb onto particles or become oxidized.

Nitrification is the biological oxidation of remineralized NH_4^+ in a sequential process (first to NO_2^- and subsequently to NO_3^-) in which obligate chemolithoautotrophic microbes fix CO_2 using reduced N substrates for energy (Ward 2008). Because NH_4^+ has the same oxidation state as proteins and is consequently available to phytoplankton and heterotrophic bacteria without costly transformations, nitrifying microbes must compete for it with other NH_4^+ consuming microbes (Ward 2008). Also because nitrification is an obligately aerobic process, it can only occur in the oxygenated zone of sediments. By increasing oxygenated volumes in sediments, bio-irrigation increases nitrification (Aller 1988; 2001). Because nitrification does not change the inventory of biological available N itself, this dissertation discusses it only as a part of the coupled nitrification - denitrification process.

Oxidized N species can be reduced in sediments by several pathways to N_2 (g), which is biologically unavailable to most organisms, or to NH_4^+ through dissimilatory reduction of nitrate to ammonia (DRNA) which conserves biologically available N in the ecosystem (Giblin et al 2014). As a competing process to N_2 production, DRNA has enormous relevance to whether N is lost or conserved within a sedimentary system. DRNA can occur either through heterotrophic or chemolithoautotrophic (NO_3^- oxidizes sulfide or other reduced products) processes but the environmental controls which trigger DNRA or N_2 production are not fully understood (Giblin et al 2014). DNRA was not investigated in this dissertation. Instead the scope of research was constrained to investigating how biologically available N was produced and lost in the system not how it was conserved. Transformations between dissolved inorganic nitrogen (DIN) species are considered only in so far as they affect the quantity of N_2 produced and consumed.

1.1.1 N_2 production pathways.

While several thermodynamically favorable, chemolithotrophic reactions coupling (1) NO_3^- and dissolved metal ions (Hulth et al 2005) and (2) Mn- oxides and NH_4^+ to produce N_2 (Luther et al 1997; Anschutz et al 2000) have been proposed or inferred from solute distributions in porewater, only two primary pathways of sedimentary N_2 production have been widely documented in marine sediments: denitrification and anammox.

(i) Denitrification. Dentrification is a multi-step reductive process whereby facultative anaerobic, heterotrophic microbes (from both *Archaea* and *Bacteria*) sequentially utilize N oxides as terminal electron acceptors in a respiratory sequence resulting in the transformation of biologically available NO_3^-

to N_2 gas if carried to completion (Zumft 1997). The denitrification pathway transforms N species according to the following reductive sequence:

$$NO_3^- \rightarrow NO_2^- \rightarrow NO \rightarrow N_2O \rightarrow N_2$$

Denitrification requires nitrate as a substrate but is inhibited by oxygen even at low (O_2 < 10 μM) ambient concentrations. Consequently, denitrification takes place along oxic/anoxic boundaries and micro-environments such as occur in coastal marine sediments. The reaction describing denitrification as a heterotrophic process can be summarized as:

$$5C_6H_{12}O_6 + 24NO_3^- \rightarrow 12N_2 + 24HCO_3^- + 6CO_2 + 18H_2O$$

(ii) Anammox. Bacteria compete for NO_3^- in a number of other processes in marine sediments in addition to denitrification (e.g., Hulth et al, 2005). Anaerobic ammonium oxidation (anammox) is a chemolithoautotrophic process mediated by obligatory anaerobic bacteria belonging to a branch of *Planctomycetales* (Dalsgaard et al 2005) whereby

$$NO_2^- + NH_4^+ \rightarrow N_2 + 2H_2O$$

The applicability of this reaction to marine sediments was demonstrated by ^{15}N tracer experiments in which the one:one NH_4^+:NO_3^- stoichiometry can be observed in the isotopic products of $^{15}NH_4^+$ & $^{14}NO_3^-$ additions to sediments (Dalsgaard & Thamdrup 2002). Because of the high capacity of marine sediments to reduce NO_3^- to NO_2^-, anammox is not generally limited by low concentrations of intermediate NO_2^- itself (Dalsgaard & Thamdrup 2002).

The relative importance of anammox to total N_2 production (*ra%*) is particularly important in sediments where NO_3^- concentrations in overlying bottomwaters are stable and high (Rysgaard et al 2004; Risgaard- Petersen et al 2004; Dalsgaard et al 2005; Risgaard- Petersen et al 2005; Nicholls & Trimmer 2009). The distinction may derive from differences between metabolic flexibility of denitrifying bacteria compared to anammox bacteria. As facultative anaerobic heterotrophs, denitrifying bacteria have a greater ability to adapt to variable environmental conditions than do anammox bacteria which are obligate anaerobes whose metabolism relies solely on conversion of NO_2^- and NH_4^+ to N_2 and whose growth rates are slow (Strous 1999). Spatially, *ra%* increases with water-column depth (decreasing C_{org} deposition); multiple studies have shown higher *ra%* on continental shelves/ slopes and low or no *ra%* in coastal systems (e.g., Engstrom et al 2005; Nicholls & Trimmer 2009; Thamdrup & Dalsgaard 2002; Trimmer et al 2013; Brin et al 2014). In part, the spatial pattern in *ra%* is determined by more variable denitrification rates relative to more stable anammox rates (Thamdrup & Dalsgaard 2002; Trimmer & Nicholls 2009) but competition for N substrate may render near-shore sediments less stable environments for anammox bacteria. Rates of N_2 production by anammox have

little correlation with temperature nor have strong seasonal patterns been reported (e.g., Neubacher et al 2011 & Brin et al 2014).

1.1.2 Controls on sedimentary N_2 production.

Controls on sedimentary N_2 production include temperature and salinity, the availability of NO_3^-/NO_2^-, O_2 penetration depth, the quantity and proteinaceous (N-rich) character of organic carbon undergoing remineralization and the activity of macrofauna, macrophytes and benthic micro-algae (e.g., Seitzinger 1988; Cornwell et al 1999). These controls exert influences on N_2 production on both a diurnal and seasonal basis (Kemp et al 1990). Because the GPB seabed lacks macrophytes within the depths investigated here, their influence is not specifically described; macrofaunal influence on N_2 production is reviewed in chapter 3. Remaining controls are discussed in the context of their significance to N_2 production in GPB sediments in chapter 2.

1.1.3 N_2 Fixation.

The fixation of N_2 to NH_3 is accomplished by a widely diversified group of prokaryotes all of which share the nitrogenase enzyme required for N_2 fixation (Postgate 1982). The enzyme catalyzes biological fixation of N_2 to NH_3 with concomitant evolution of H_2 according to the equation:

$$N_2 + 8H^+ + 8e^- \rightarrow 2NH_3 + H_2$$

Nitrogenase consists of two metalloproteins: a large one containing Mo/Fe and sulfide and a smaller one containing Fe and S (Postgate 1982). As O_2 damages these proteins, diazotrophs including aerobic N_2 fixers have evolved physiological strategies such as conformational structures or formation of heterocysts to protect the enzyme (Postgate 1982).

In benthic environments, N_2 fixation is carried out by photoautotrophs as well as aerobic and anaerobic heterotrophs (Capone 1988). The ability of sulfate reducing bacteria (SRBs) to fix N_2 (e.g., Riederer- Henderson & Wilson 1971) and its occurrence in sediments (e.g., Jones 1982) has been known for many decades. N_2 fixation coupled to sulfate reduction has also been reported in rhizopheres of sea-grasses (Welsh et al 1996; McGlathery et al 1998) and in microbial mats (Steppe & Paerl 2002).

Benthic N_2 fixation is generally more relevant than planktonic N_2 fixation in coastal marine systems perhaps because of the greater sedimentary bioavailability of metal cofactors necessary for nitrogenase (e.g., in reducing conditions in sediments Mo speciates to reduced (but soluble) forms which may be more bioavailable than molybdate (the stable species of Mo in oxic seawater) (Howarth et al 1988 (b)). Besides essential trace metals and O_2, a number of environmental controls regulate the extent of nitrogenase activity in and on

sediments. Because of its high metabolic cost, heterotrophic N_2 fixation is limited by C availability (e.g. Jones 1982; Howarth et al 1988 (a); Welsh et al 1996; McGlathery et al 1998; Bertics et al 2013). Temperature also directly regulates N_2 fixation (e.g., Jones 1982; Bertics et al 2013) as does irradiance in the case of cyanobacteria (Capone 1988) although photosynthesis may inhibit fixation by generating O_2 (Gao et al 2014).

Dissolved inorganic nitrogen (DIN) constrains N_2 fixation due to allosteric inhibition of the glutamine synthetase which is required for the synthesis of nitrogenase (Postgate 1982; Yoch & Whiting 1986). N_2 fixation has been shown to increase with decreasing NH_4^+ concentrations in experimental sediment cores (Carpenter & Carbone 1982 (a)); further, some field studies have observed inverse relationships between NH_4^+ concentrations in overlying water and rates of N_2 fixation from microbial mats on the sediment surface (e.g. Joye & Paerl 1993).

Nevertheless, a number of field studies have reported N_2 fixation in sediments with high concentrations of NH_4^+ (e.g., Haines et al 1981; Bertics et al 2010 & 2013) or documented concomitant N_2 production and fixation in proximate sediments (e.g., Haines et al 1981; Fulweiler et al 2007; Bertics et al. 2012). In vegetated sediments, heterotrophic N_2 fixing microbes (e.g., SRBs) are able to take advantage of carbon from plant exudates or detritus while benefitting from plant uptake of otherwise inhibiting NH_4^+ (Welsh et al 1996; McGlathery et al 1998). Bertics et al 2010 proposed sediments proximate to active macro-faunal burrows as another class of sites of intensive N_2 fixation carried out by SRBs. Although active burrows are irrigated with oxygenated water and surrounded by NH_4^+ gradients, N_2 fixation may occur near the redox gradient surrounding burrows where oxygen has been consumed and coupled nitrification-denitrfication has limited availability of inhibiting DIN.

1.2 Organization of the dissertation.

N_2 fluxes were measured together with O_2, NH_4^+ and NO_3^-/NO_2^- sedimentary fluxes[1]. These results are analyzed in chapter 2 to determine their seasonality and the relevance of temperature, sedimentary oxygen demand (SOD) and irradiance on N fluxes rates and their seasonality. To ensure fluxes were measured as close as practical to natural conditions, benthic chambers were used *in-situ* in addition to *ex-situ* cores to incubate sediment samples and a contrast of results from each method is also included in chapter 2. Measurements and experiments investigating the influence of bio-irrigation by indigenous populations of *Amphioplus abditus* and *Squilla empusa* on N_2 production is described in chapter 5.

[1] Sedimentary O_2 influx is described either as O_2 flux or sedimentary oxygen demand (SOD) in this dissertation. The terms have identical meanings; usage is determined by whichever term is most succinct in context.

As the research proceeded, a pattern began to emerge in estimates of seasonal N_2 flux values and it became clear a separate method was necessary to quantify the proportion of gross N_2 fixation subsumed within the net N_2 flux numbers obtained by MiMS. Acetylene reduction assays (ARAs) were subsequently carried out for this purpose. These experiments and the likely importance of N_2 fixation in GPB sediments are discussed in Chapter 3. This chapter also describes ^{15}N tracer experiments conducted to ascertain the relevance of anammox or other processes capable of oxidizing NH_4^+ (e.g., oxidation by MnO_2) to produce N_2.

A priority in this research was to reconcile N flux estimates with N remineralization estimates which were obtained by non-steady state, anoxic, whole core incubations which rely on a completely different experimental approach than the closed core incubations used to obtain flux measurements. The idea behind this two- pronged approach which is described in Chapter 4 was to investigate how consistent dissolved N production estimates were compared with flux estimates. The degree of consistency between flux and production rates should provide a measure of the accuracy of each estimate beyond the regression analysis carried out for these rates.

There is evidence from multiple areas of research that denitrification is susceptible to environmental contaminants (Bollag & Barabasz 1979; Holtan-Hartwig et al 2002; Magalhaes et al 2011; & Tezel et al 2008 & 2010). Chapter 6 describes investigations to determine what impacts environmentally relevant concentrations of different classes of the commonly used quaternary ammonium surfactant compounds (QACs) and the heavy metal contaminant Cu - alone and in combination- have on denitrification in GPB mud sediments. Finally, chapter 7 summarizes the findings of this dissertation and discusses its estimates of N fluxes in the content of modern-day inputs of N loadings into larger GPB estuary.

1.3 The benthic environment of Great Peconic Bay.

There has been little description of the biogeochemistry of GPB sediments in the published literature. Most available information on GPB sediments is contained in 3 reports prepared for the Peconic Estuary Program (PEP) or the Suffolk County Department of Health Services in its capacity as an administrator of the PEP.

GPB consists of a central mud basin with a fringing sand border of coarse-grained material (Fig. 1. 2). This investigation centered on muddy sediments sampled near a station at 40° 56’ 055” and 72° 29’ 877”. Estimates of grain size in this investigation are from samples taken by Cerrato et al (2010) with a van Veen grab near the GPB station where incubated sediment was collected; these researchers reported the sediments have mean phi (Φ) values ~ 8.1 – 8.5

characterizing them as fine-grained silt-clay. The sediment here are impermeable. Salinity was estimated in February and May 2014 by conductivity measurements which revealed porewater values which were roughly constant or slightly higher than salinity in GPB bottomwater (Fig. 1.2). Sediment accumulation rates calculated from excess ^{210}Pb were estimated in a range from 0.09 to 0.2 cm yr^{-1} (Cochran et al 2000).

Muds in GPB are heavily bio-irrigated. In unpublished research adjunct to this dissertation, the particle mixing coefficient D_B., based on Be^7 (1/2 life = 53d) inventories to 4 cm, was found to generally vary between 10- 50 cm^2 yr^{-1} indicating upper sediment intervals are mixed by infauna on time scales of a week to just over a month (R.C. Aller, NY Sea Grant Final Report (2012)). In addition to diverse polychaetes, this investigation found dense populations from the family *Amphiuridae* and the genus *Squilla*. Burrow ventilation of amphiurid brittlestars has been described by Woodley (1975) and the observed activity of the *Amphiuridae* closely resembles the ventilation of these brittlestars. Since the only species within *Amphiuridae* identified by Cerrato et al (2010) in GPB was *Amphioplus abditus*, the *Amphiuridae* populations found in GPB sediments will be referred to as *A. abditus* or *Amphioplus* in this dissertation. The *Squilla* populations were similar to descriptions of the species *Squilla empusa* by Meyer (1979) in Narragansett Bay and the *Squilla* observed in GPB will be assumed to be *S. empusa*. Because of their size relative to flux sub-cores or benthic chambers, *A. abditus* were frequently present in sediment samples from which flux estimates were measured whereas, for the same reason, *S. empusa* were systematically excluded. Consequently, the flux estimates of this investigation apply to GPB bulk sediments but do not take account of the specific biogeochemistry of *S. empusa* burrows. However, the likely impact of *Squilla* is addressed through direct analyses of burrow lumen water (Chapter 5).

Cochran et al (2000) reported C and N values from organic source material adjusted for calcium carbonate for sediments collected at sites with GPS coordinates very near the station where sediments were collected for this investigation. % organic C and % organic N obtained from sediment in the upper 5 cm of box cores were 1.98% (+/- 0.15/ 0.08 %) and 0.18% (+/- 0.02/ 0.02 %) respectively implying a C:N ratio of bulk organic source material of 11 in fall 1997 and % organic C and % organic N of 1.69% (+/- 0.03/ 0.07 %) and 0.18% (+/- 0.01/ 0.01 %) in the upper 4 cm of sediment in box cores implying a C:N ratio of organic source material of 9.0 in spring 1998. In contrast, measurements from gravity cores from fall 1997 showed % organic C and % organic N of 1.73% (+/- 0.12/ 0.26 %) and 0.30% (+/- 0.09/ 0.08 %) in the upper 14 cm implying a C:N ratio of organic source material of 5.8, and 1.84% and 0.39% in the upper 3 cm, implying a C:N ratio of bulk organic source material of 4.7.

Howes et al (1998) presented the only previously available measurements of seasonal sediment oxygen demand (SOD) and nutrient fluxes (NH_4^+, NO_3^- & $PO_4^=$) from GPB sediments. The seasonal pattern in sediment metabolism

reported resembles values for other temperate estuaries; i.e., low but increasing from spring through summer. NO_3^- was negative in July perhaps reflecting low O_2 penetration into sediments. Overall annualized fluxes between Howes et al (1998) and this study are also similar (Table 2.1).

1.4 TABLES & FIGURES

Table 1.1

Comparison of Narragansett Bay mid-bay site & GPB station

		mid-Bay (NB) *		**GPB**	**GPB reference**
Grain character/ Grain size		Silt-clay (70%+); clay (20%)		Silt Φ = 8.1- 8.5	This study Cerrato et al (2010)
Water depth		7- 8 m		7.6	This study
Organic %		4%		1.84%- C 0.18%- N (upper 4 cm)	Cochran et al (2000)
C:N (surficial sediments)		9.5- 13.9		9.0- 11 (box-cores)	Cochran et al (2000)
Light at bottom		4- 80 µmol m^{-2} s^{-1}		8- 80 µmol m^{-2} s^{-1}	This Study
Macrobenthos		*Mediomastus* (deposit feeding-polychaete); *Nucula* (bivaluve)		primarily *Amphioplus abditus* & *Squilla empusa*	This Study

* all references for mid-bay Naragansett Bay from Nixon et al (2009)

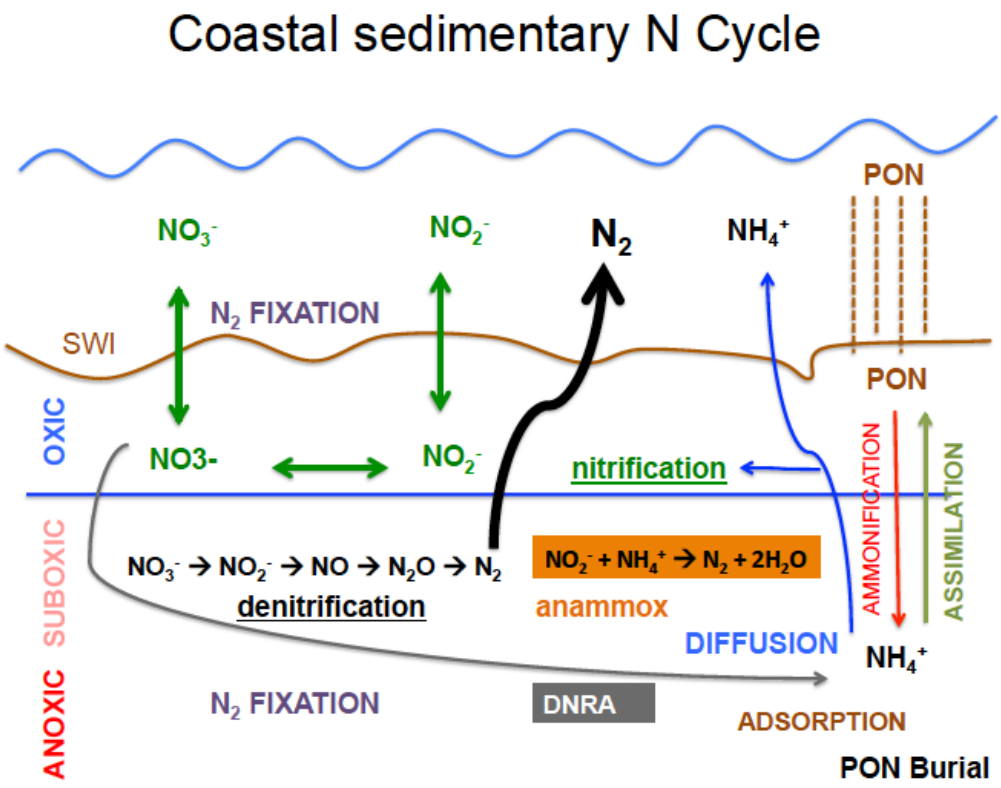

Fig. 1.1 Schematic of coastal sedimentary N cycle

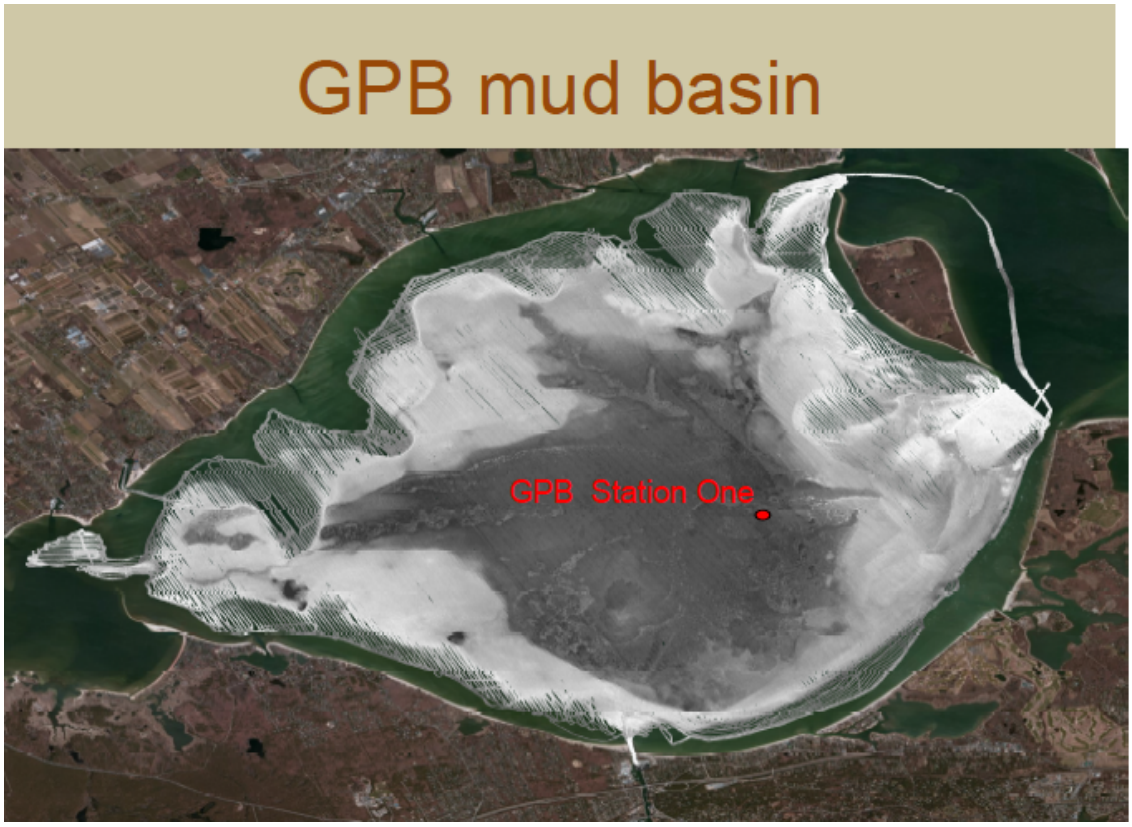

Fig. 1.2 Map of GPB mud basin. Darker shading reflects fine-grained silt; lighter striations reflect coarser grained material. Benthic sonar map by Flood & White; School of Marine & Atmospheric Sciences, Stony Brook Uinversity (unpubl).

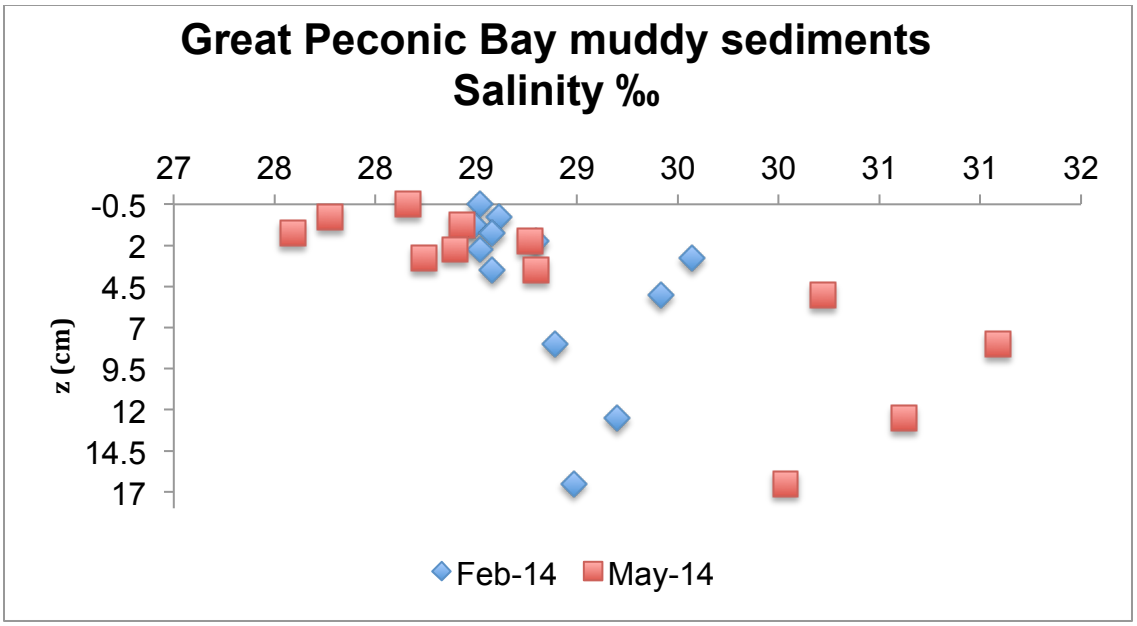

Fig. 1.3 Depth Profiles of salinity in GPB porewater. Values obtained **from** chlorinity titration of porewater. Conductivity measurements were converted to salinity by assuming stable seawater compositions and using a Cl ‰ conductivity^{-1} ratio = .03546 and multiplying Cl ‰ by 1.80655. Negative value on depth scale corresponds to overlying bottomwater salinity value.

CHAPTER TWO: NET O_2 & N FLUXES IN GPB MUDDY SEDIMENTS

2.1 INTRODUCTION

2.1.1 Overview & published rates of net N_2 flux.

This chapter describes N_2 dynamics in muddy sediments in Great Peconic Bay (GPB) as measured by net sedimentary fluxes of N_2. In addition to documenting N_2 fluxes and how these rates respond to abiotic and biotic environmental variables, measurements of NH_4^+, NO_3^-/NO_2^- (referred to as NO_3^-) and O_2 fluxes are also presented to further elucidate biogeochemical context and controls on net N_2 production. Measurements were obtained both from sediment incubations carried out *ex situ* in cores and *in-situ* using benthic chambers. Because the *in-situ* incubations revealed net rates of N_2 production and relationships between N_2 , NH_4^+, and O_2 fluxes which were not observed *ex situ*, this chapter also includes a discussion of these differences and published comparisons between the two incubation methods. Benthic N and O_2 fluxes were also measured in sediment from Smithtown Bay, Long Island Sound and the similarities and differences between the two estuarine sites are examined.

Estuarine sediments can be subject to a continually changing regime of irradiance and corresponding changes in activity of benthic macrophytes and micro-algae as well as to varying bottomwater O_2 & NO_3^- concentrations. Devol (2015) has tabulated the range of most common net N_2 fluxes on continental shelves at 0.5- 2.0 mmol m^{-2} d^{-1} whereas comparable net N_2 fluxes in estuarine sediments are 0.5- 5.0 mmol m^{-2} d^{-1} (Joye & Anderson 2008). This difference in ranges points to the multiple, dynamic factors which influence rates of N_2 production or consumption in estuaries.

2.1.2 Controls on sedimentary N_2 production.

(i) Nitrate source. In some coastal systems with high bottomwater NO_3^- concentrations, sedimentary N_2 production is driven by influx of NO_3^- from the overlying water to the sediments where it is reduced (Cornwell et al 1999). As will be shown, N_2 flux using water column sourced NO_3^- is not likely a generally occurring process in GPB sediments. The oxidant substrate for N_2 production in GPB sediments is considered autochthonous and coupled to sedimentary nitrification of NH_4^+ derived from the remineralization of organic matter in this study.

(ii). The effects of temperature and salinity on N_2 production. Field studies have not found a straightforward linear relationship between temperature and N_2 production (Seitzinger 1988; Fulweiler & Nixon 2012). Seitzinger (1988) observed close to a doubling of the rate of N- N_2 production from 0.94 to 1.66 mmol m^{-2} d^{-1} when temperatures increased from 3° C to 10° C in March in Narragansett Bay and no further increases in rates as temperatures increased to 20° C. But seasonal field studies alone cannot isolate temperature effects from the effects of other controls which may co-vary with temperature (e.g., organic matter deposition, O_2 penetration depth, bio-irrigation).

Ionic strength affects competition for cation exchange sites in sediments and increases in salinity lower NH_4^+ adsorption capacity (Seitzinger 1991; Rysgaard et al 1999; Weston 2010). Less NH_4^+ adsorbs in marine systems than in lakes (Seitzinger 1988). Salinity changes from 0 to 10 have the largest effect on NH_4^+ adsorption equilibrium (Rysgaard et al 1999). Several researchers have found changes in salinity are inversely related to nitrification (e.g., Seitzinger et al 1991; Rysgaard et al 1999), and N_2 production coupled to it even in NO_3^- replete porewater (Rysgaard et al 1999; Giblin et al 2010). These findings suggest salinity exerts a direct, physiological effect on nitrifying and denitrifying organisms independent of NH_4^+ partitioning equilibrium (Rysgaard et al 1999). This inhibition of nitrification was also observed to occur only between salinity values of 0- 10 ppt (Rysgaard et al 1999). Salinities in GPB were observed to vary between 25-30 over the course of this study and no significant impacts of salinity on either NH_4^+ fluxes or N_2 production were observed. Consequently, the effects of salinity on N cycling will not be discussed further in this chapter.

(iii) The effects of bottomwater O_2 concentrations and O_2 penetration depth on sedimentary N_2 production. Bottomwater O_2 concentration forms one end of a concentration gradient which decreases as it extends into sediments; higher bottomwater O_2 concentrations raise the O_2 diffusive flux into the sediments and deepen O_2 penetration depth. Deeper O_2 penetration into sediments enhances nitrification of NH_4^+ (Hansen et al 1981) and thereby increases N_2 production coupled to nitrification (Rysgaard et al 1994). Deeper O_2 penetration into sediments increases nitrification as NH_4^+ porewater concentrations generally increase with depth.

Because a micro-sensor- based system necessary to measure O_2 penetration depth in the sensors was unavailable, this study analyzed bottomwater O_2 concentrations against N_2 production values as a surrogate for O_2 penetration depth. O_2 bottomwater concentrations (and oxygen penetration depths) may not correlate well with N_2 production. In winter, cold temperatures will increase O_2 solubility and because there is little biological demand for O_2 , its penetration depth should deepen. But at winter temperatures approaching zero, rates of denitrification are low (Seitzinger 1988 and data in this study). Winter data-points will consequently most likely plot as an outlier to a positive correlation between O_2 bottomwater (or O_2 penetration depth) and N_2 production. Further,

photosynthesis may complicate the correlation between O_2 bottomwater concentrations and N_2 production if competition for NH_4^+ between benthic microalgae and N_2 producers attenuates nitrification.

(iv) The effects of sediment metabolism on N_2 production. When NO_3^- is not supplied to the sediments from overlying water, its only source in sediments is from oxidation of NH_4^+ supplied by remineralization of organic matter. In this study, NO_3^- concentrations were low (< 2 uM). Low NO_3^- concentrations need not constrain N_2 production rates as long as NH_4^+ and O_2 concentrations are not limiting. Available NH_4^+ depends not only on the rate of ammonification of reduced organic N (N_{org}) but also on the quantity and proteinaceous character of organic matter deposited on the seabed (Sloth et al 1995; Eyre et al 2013). All else equal, additions of organic matter with marine C:N ratios will increase N_2 production (Fulweiler et al 2008) by increasing available N substrate until O_2 depletion attenuates nitrification (Billen 1982; Jenkins & Kemp 1984; Kemp et al 1990). At high organic matter loadings, sulfide may inhibit nitrification and thereby reduce or eliminate N_2 production (Joye & Hollibaugh 1995).

Multiple researchers have reported seasonal depressions in rates of N_2 production in summer or in periods of high sediment metabolism (e.g., in Danish coastal sediments (Hansen et al 1981); in Mediterranean lagoons (Dedieu et al 2007); in Chesapeake Bay (Jenkins & Kemp 1984; Kemp et al 1990); in Florida Bay (Gardner & McCarthy 2009; and in Moreton Bay, Australia (Ferguson & Eyre 2013). Although the same controls on N cycling apply in coastal waters of northern Europe, seasonal N_2 production and DIN fluxes are also influenced by NO_3^- availability in highly eutrophic bottomwater (Rysgaard et al 1995). In general, summer depressions of N_2 production have been related to high organic matter loading & high SOD reducing available O_2 and thereby the rate of nitrification or increasing inhibitory sulfide.

(v) The effects of benthic micro-algae on sedimentary N cycling. Experimental and field studies have documented differing effects of the activity of benthic micro-algae on N cycling. Photosynthesis can deepen O_2 penetration depth thereby enhancing nitrification; concomitantly, benthic micro-algae compete with denitrifying bacteria for available NH_4^+ (Risgaard- Petersen 2003). Benthic micro-algae can compete for bio-available N in dark and light conditions (Risgaard- Petersen 2003). Where N is not limiting (either because of NO_3^- in the overlying water or because of remineralization of proteinaceous organic material in the sediments), the presence of benthic micro-algae can increase O_2 penetration depth, N_2 production coupled to nitrification (Risgaard- Petersen et al 1994; Rysgaard et al 1995; An & Joye 2001; & Porubsky et al 2008). Where N is limiting, benthic micro-algae may compete for NH_4^+ with nitrifiying bacteria thereby limiting nitrification and N_2 production (e.g., Ferguson et al 2004; Rysgaard et al 1995; Risgaard-Petersen et al 2004; & Risgaard- Petersen et al 2005). The effects of benthic micro-algae on N cycling may occur over diurnal

cycles with changes in ambient bottomwater light (e.g., Risgaard-Petersen et al 2004) or over seasonal cycles with changes in the availability of N in combination with irradiance (e.g., Rysgaard et al 1995).

Several studies have indicated assimilation by benthic micro-algae is a major pathway of N removal in coastal sediments relative to denitrification (e.g., Sundback & Miles 2000; Ferguson et al 2004). Since bacteria may also periodically store N (e.g., Aller 1994, Lomstein et al 1998, Sayama 2001), there may be a three way competition between BMA, nitrifying bacteria and heterotrophic bacteria for NH_4^+ which will control whether the N in NH_4^+ ultimately fluxes from the sediments as NH_4^+, NO_3^- or N_2 or is incorporated in biomass. N assimilation by bacteria and BMA and subsequent grazing by protozoa and meio-fauna can shunt a portion of N out of the microbial loop and inorganic N cycle to higher trophic levels (Ferguson et al 2004).

2.2 METHODS.

2.2.1 Incubations.

Sediment incubations were carried out to measure fluxes from GPB sediments both *ex-situ*- in the lab- in October 2012, June 2013, November 2013, February 2014, May 2014 and September 2014 and *in-situ* with benthic chambers in October 2012, June 2013, May 2014 and September 2014. Rates of net N_2 fluxes, SOD and ΣCO_2, NH_4^+, NO_3^-/NO_2^- and $HPO_4^=$ fluxes were measured (although measurements of $HPO_4^=$ are not presented). These sampling times span a range of seasonal temperature and productivity conditions.

Ex situ sediment incubations were conducted in a temperature-controlled room at in-situ temperatures in 9.4 cm (ID) X 25.5 cm cylindric plexiglass sub-cores. Sediments were retrieved in 11.5 cm X 29.5 cm (ID) rectangular plexiglass box-cores by scuba-divers which were transported (transport time ~ 2 hours) to the lab in large containers filled with unfiltered GPB seawater. These large containers were aerated and, typically, box- cores were stored at least overnight before starting incubation procedures. Intact sediment samples for incubation were taken by inserting sub-cores vertically in the box-cores. Overlying water was replaced in the sub-cores twice before commencing incubations. Sub-cores were filled to approximately two-thirds of their height creating an overlying water volume of ~ 600 ml. Overlying water was stirred by magnets attached to sub-core covers and driven by a large, externally rotating magnet. Covers had in- and out-take vents fitted with leur- locks for sampling and replacing overlying seawater.

In-situ incubations were carried out in 6.98 cm X 30.5 cm cylindrical acrylic benthic chambers inserted into sediments to two-thirds of the height of the chambers. For incubations in October 2012 and June 2013, these heights

(marked by tape) were used to calculate overlying water volumes. In May and September 2014, benthic chambers were capped from the bottom and retrieved. Overlying water volume was measured in the lab. In addition to leur- lock vents (in- and out- take), covers of the benthic chambers were fitted with battery-driven, gear- box motors contained in a waterproof PVC pipe housing. These motors rotated magnets positioned less than 1 cm above the acrylic covers which propelled magnetic bars inside the chambers. The rotating magnet inside the chamber drove a 4 pronged plastic impeller which stirred overlying water. This stirring apparatus was tested multiple times in the lab to ensure sufficient battery capacity and to check that mixing of the overlying water did not disturb the sediment.

2.2.2 Measurements

(i) N_2 measurement. N_2/Ar ratios in water samples were measured using a modified Membrane Inlet Mass Spectrometry (MiMS) method and Faraday detection (Kana et al 1994). N_2 values were calculated by multiplying the measured ratios by the equilibrium value of Ar derived from Hamme & Emerson (2003).The quadrapole mass spectrometer used was a Prisma 2000 coupled with a Pfeiffer turbo-pump. The gas delivery line was fitted with a copper-reduction furnace (WATLOW) after the liquid nitrogen trap. Because the mass spec could only be accessed thru a narrow- bore multi-port valve which accommodated another line to the mass spec, the line's volume was designed to be as low as feasible and consisted of 1/8" quartz tubing and stainless steel tubing comprising the liquid N_2 trap and connecting to the membrane inlet.

This lower volume gas delivery system enabled rapid enough response time to allow the N_2/Ar signal to stabilize and run for approximately four minutes before the sample was consumed. All N_2/Ar samples were withdrawn without bubble formation from bottomwater overlying sediment by syringe and transferred to glass 12.5 ml Exetainers. Samples from benthic chambers were transferred to Exetainers immediately after scuba divers return to ship; samples from lab incubations were immediately transferred after sampling by syringe. Approximately, 16 ml of overlying water was used to overfill Exetainers; the remaining sample (~ 5 ml) was filtered (20 µm polycarbonate) (1) to 25 ml plastic scintillation vials and immediately frozen (T ~ 0° C) for NO_3^- & NH_4^+ analysis and (2) the remainder split between 1 ml syringes for ΣCO_2 measurement and snap-cap vials for $HPO_4^=$ measurement after acidification with trace metal grade HCl.

(ii) Measurement of nutrients and ΣCO_2. Overlying water for flux measurements was sampled by syringe and filtered (0.2 um polysulfone mesh). NH_4^+ was measured colorimetrically by the phenolhypochlorite method (Solorzano 1969); NO_3^- (after reduction with VCl_3) and NO_2^- were measured colorimetrically as NO_2^- after treatment with Griess reagent (Doane & Howarth 2003). NO_2^- was not measured separately; all references to NO_3^- in this

dissertation include both NO_3^- and NO_2^-. ΣCO_2 was measured using a flow injection analysis system with conductivity detection (Hall & Aller 1992).

(iii). O_2 measurements. O_2 was measured using a modified Winkler titration (Strickland & Parsons 1972). 10ml water samples were taken from incubations using 10ml plastic syringes. In lab incubations, reacted samples were titrated with thiosulfate typically within 15 minutes. Samples from benthic incubations in September May 2014 were titrated upon return to the lab several hours after on-board treatment with Winkler reagents. Samples from benthic incubations in October 2012 and June 2013 were fixed immediately after sampling in the field and were titrated within several days. On these two occasions, measurements of O_2 concentrations were discovered to be too low relative to equilibrium gas values to be accurate. To correct these measurements, GPB seawater samples were taken in 10 ml plastic syringes at *in-situ* temperatures recorded during sampling in October 2012 and June 2013; triplicate samples were then measured by Winkler titration immediately and after waiting periods equivalent to those lapsed during the October 2012 and June 2013 sampling periods. Rates of decay derived from a regression of these measured values was then used to correct original October 2012 measurements. As corrected values for the June 2013 measurements were still not consistent with equilibrium gas values, the data was not reported or incorporated in further analysis.

(iv). Comparison of sedimentary O_2 & N fluxes against changes in corresponding values in bottomwater. Concomitant with measurements of sedimentary fluxes, corresponding measurements (N_2, NH_4^+, NO_3^-/NO_2^- fluxes & SOD) in bottomwater incubated in acrylic sub-cores of similar dimensions were made. Bottomwater was filtered to remove macro-algae (44 µm mesh) in *ex-situ* measurements only. The intended purpose of these measurements was to distinguish sedimentary fluxes from changes in N and O_2 values occurring in bottomwater and not to serve as analytical blanks.

(v). Light versus dark incubations. Sediments were incubated in both light and dark conditions. From October 2012 through the May 2014, artificial light was measured with a QSL- 100 (Quantum Scale Irradiance) meter from Biospherical Instruments. The instrument measured photosynthetically active radiance (PAR) generated by one or two light arrays positioned on the side of the bench in the temperature- controlled room where incubations took place. Unlike on the seabed, light was not radiating from directly above on the sediment surface but from a low lateral angle. PAR in overlying water of the incubating sediment cores in the lab was measured at ~ 25 & 30 µE m^{-2} s^{-1} with only a single side-light array on. A range of PAR values at 6.5 meters depth was calculated based on estimates of PAR at 42° latitude seasonally. Beer's Law was used to calculate light attenuation with an attenuation coefficient derived as (1.7/Secchi depth) which was measured and varied over the sampling periods between 2- 3 meters. The range of seabed PAR was estimated between 8- 80 µE m^{-2} s^{-1} .

While lighting options in the temperature controlled room were limited to using one or two lamps, the single array generated irradiance in the low to middle range of calculated possible values and generally matched the author's impression of ambient bottomwater light. Since seasonal changes in water-column turbidity generally had opposite effects on benthic PAR to changes in solar irradiance, artificial light levels were not change from one incubation period to another.

From September 2014, light reaching within ~18 cm of the GPB sediment surface was measured in LUX with a micro-sensor from Onset Computer Corp. Artificial light in the lab incubation room was set so as to approximate *in-situ* LUX based on these measurements.

2.2.3 Flux Calculations and Statistical Analysis.

Flux measurements were calculated by linear regression of concentrations as a function of time (generally around 24 hours) in incubations; fluxes and associated regression analyses (i.e., p- values) are detailed in Appendix 2.1. In many cases and, especially for the *in-situ* measurements, incubations were limited to 3 time-points; in these cases, degrees of freedom were limited to df= 1; critical value thresholds for t- distributions were high and statistical significance (at p = 0.05) was difficult to achieve. Concentration values were always screened for consistency among replicates and, in the case of dissolved gases, for reasonableness relative to equilibrium values. In some instances, flux estimates were excluded from further analysis based on these assessments. Statistical significance (.05) of incubation regression was not used as a threshold to decide on inclusion or exclusion of flux values from analysis. P- values are provided as an indication of the trend in sequential incubation values. For NH_4^+ and NO_3^- /NO_2^- fluxes especially, p-values frequently exceeded critical significance thresholds (either at $\alpha = 0.05$ or = 0.10). These results often occur at low DIN concentrations and are not surprising in incubations of estuarine sediments where DIN is not only produced but rapidly consumed as well. In contrast to more consistent trends in net N_2 production and SOD, NH_4^+ values often showed one or more outlying data points in a time-series. These outliers which were neither consistently above or below trend could reflect analytical error. Alternately, they could indicate counter-trend production or consumption of NH_4^+ in a dynamic microbial environment.

Comparison of flux values (1) *in-situ* and *ex-situ* (2) in dark and light conditions and (3) in incubated bottomwater versus sediment were evaluated by two-sample *t- tests*. Comparisons of seasonal means of flux values were assessed for homogeneity of variance by Barlett's test. Because outcomes of the Barlett's tests consistently showed heterogeneity of variances in flux values, statistical significance of differences between seasonal means was assessed by an approximate test of equality of means (Games and Howell method in Rohlf

and Sokal 1969). Unlike ANOVA, this test does not require homogeneous variances between seasonal flux values.

2.3 RESULTS

2.3.1 O_2 & N fluxes: average rates and seasonal patterns.

Average SOD, N- N_2, NH_4^+ and NO_3^-/NO_2^- flux rates in this study were 18, 1.4, 0.93 and 0.05 mmol m^{-2} d^{-1} ; corresponding annualized SOD, N- N_2, NH_4^+ and NO_3^-/NO_2^- flux rates were 17, 1.1, 0.99 and 0.03 mmol m^{-2} d^{-1} (Table 2.1). The slightly lower annualized flux rates for SOD, N-N_2 and NO_3^-/NO_2^- result primarily from equal weighting of low winter values whereas overall averages include fewer samples of winter values than other periods with higher values. NH_4^+ rates were higher on an annualized than average basis reflecting a higher weight of high spring and summer NH_4^+ rates relative to more numerous but low fall NH_4^+ rates. Rates include all incubation results measured *in-situ* and *ex-situ* and in dark and light conditions. Average seasonal SOD, N- N_2, NH_4^+ and NO_3^-/NO_2^- flux rates are charted in Fig. 2.1; periodic flux rates are charted in Fig. 2.2.

Sediment oxygen demand (SOD) was lowest in winter (4.4 mmol m^{-2} d^{-1}), highest in spring and summer (28 & 20 mmol m^{-2} d^{-1} respectively) and declined in fall (12 mmol m^{-2} d^{-1}) (Fig. 2. 1 (a)). Spring SOD is higher than would be expected based on simple T dependence likely reflecting higher deposition of organic matter. An equality of means test (Games and Howell method) showed significant differences between rates in all seasonal periods except those in spring and summer and in fall and winter.

Net N- N_2 production from GPB sediments followed a seasonal pattern (Fig. 2.1 (b)). Summer and fall rates of net N_2 release averaged 1.50 (+/- 0.38 SD) and 1.78 (+/- 0.38 SD) N- N_2 mmol m^{-2} d^{-1} respectively. At a temperature of ~ 0° C in February, sediment produced close to no N- N_2 (0.06 mmol m^{-2} d^{-1}). Mean N_2 production in spring periods averaged 1.06 mmol N- N_2 m^{-2} d^{-1} and was much more variable (+/- 1.21 SD) than in the summer and fall periods. Lab incubations in May 2014 produced negative N_2 fluxes reflecting net N_2 consumption (-0.08 N-N_2 mmol m^{-2} d^{-1}); daylight *in-situ* incubations in benthic chambers generated high N_2 levels (2.49 N-N_2 mmol m^{-2} d^{-1}) during this same period. An equality of means test (Games and Howell method) showed significant differences between summer and fall rates with those in winter. Differences between spring and any other periods were not significant because of the high variance of results within the spring period.

NH_4^+ fluxes were greatest in summer (2.7 mmol m^{-2} d^{-1}), declined in the fall (0.20 mmol m^{-2} d^{-1}) to reach close to zero in winter (0.10 mmol m^{-2} d^{-1}) and rose again in spring (0.85 mmol m^{-2} d^{-1}). (Fig. 2. 1 (c)). NH_4^+ fluxes differed in direction in the spring in 2013 and 2014. June 2013 NH_4^+ fluxes averaged 1.93

mmol m^{-2} d^{-1}; in contrast, May 2014 NH_4^+ fluxes averaged -0.23 mmol m^{-2} d^{-1}- i.e., fluxes were into sediment or onto its surface (Fig. 2.2 (b)). An equality of means test (Games and Howell method) showed significant differences between summer NH_4^+ fluxes and rates in other periods but identified no differences among rates in these other periods.

Benthic NO_3^- fluxes averaged 0.03 mmol m^{-2} d^{-1} and varied around this mean within a very small range (+/- 0.21 mmol m^{-2} d^{-1} SD) (Fig. 2. 2 (d)). In spring, net NO_3^- was consumed or fluxed into the sediments; during other periods, mean fluxes were from the sediments. An equality of means test (Games and Howell method) showed no significant differences in NO_3^- flux rates between any periods.

N_2 production is almost completely derived from denitrification and not anammox in GPB sediments (see Chp 3). Denitrification efficiency **(**DE) (defined as N-N_2 flux/(N-N_2 flux + DIN flux)) showed a seasonal pattern primarily driven by changes in NH_4^+ fluxes which were more variable than N_2 release (Fig. 2.2 (b)). Overall measured DE was 0.6 (Fig. 2.3 (a)). In winter, all N flux rates were low and the ratio was not particularly meaningful as it could be easily affected by small changes in any of the components. Denitrification efficiency in the fall was at its highest and most stable, reflecting steady N_2 production and low NH_4^+ fluxes. The vastly different outcomes in the spring data from May 2014 and June 2013 result from the NH_4^+ fluxes. Low DE in summer is driven by high NH_4^+ export (Fig. 2.3 (b)).

Figure 2.4 (a) illustrates contrasting benthic N patterns found in May 2014 and June 2013. In May 2014 *in-situ* incubations, NH_4^+ was consumed in bottomwater on a net basis; despite this demand for NH_4^+, N-N_2 fluxes were high in May 2014 whereas N was primarily exported as NH_4^+ in June 2013 and N-N_2 flux was low . Measurements of GPB seawater incubated *in-situ* showed substantial ΣCO2 consumption in each period (Fig 2.4 (b)). Seawater in the bay was unusually clear during the spring of 2014 and benthic diatoms were abundant on the seabed and on the surface of retrieved sediment (Fig. 2.5). NH_4^+ fluxes for this period under light conditions averaged -1.24 mmol m^{-2} d^{-1} *in-situ* and -0.02 mmol m^{-2} d^{-1} in the lab whereas NH_4^+ dark fluxes in the lab averaged 0.37 mmol m^{-2} d^{-1}. It is probable these fluxes reflect NH_4^+ assimilation by benthic micro-algae on the sediment surface of the cores and benthic chambers. The June 2013 ΣCO2 data also indicate signs of benthic photosynthesis. It is not clear why in one period showed high N-N_2 and negative NH_4^+ flux and the other low N-N_2 and NH_4^+ efflux. It is unlikely the reasons for this divergence related to O_2 limitation on coupled nitrification denitrification in June 2013 as bottomwater O_2 concentrations were > 235 uM.

2.3.2 Relationships between net N_2 fluxes and seasonal variables.

(i) Relationship of N_2 fluxes with bottomwater oxygen and porewater NO_3^-. No trends were found between seasonal averages of N_2 fluxes and bottomwater oxygen (F-stat= 1.5, df= 7 & p- value**=** 0.26) or N_2 fluxes and NO_3^- concentrations in the upper 0.5 cm of sediment porewater (F-stat= 0.93, df= 6 & p-value= 0.37).

(ii) Relationship of N fluxes with temperature. At ~ 0°C, sediment biological activity was dormant; net N-N_2 production, NH_4^+ and NO_3^- fluxes approached zero (0.05; 0.04; & 0.01 mmol m^{-2} d^{-1}) and SOD was low (4.4 mmol m^{-2} d^{-1}). Between 0° and ~ 8 °C (the next lowest sampling temperature for GPB), net N- N_2 production increased by more than 1 mmol m^{-2} d^{-1}. Above ~ 8° C, net N_2 production had no significant trend with bottomwater temperatures (Fig. 2.6 (a)). N_2 values from Smithtown Bay also do not show any relationship between net release and temperature.

Regressions of NH_4^+ fluxes and SOD against *in-situ* bottomwater temperatures in GPB were significant (p values = .01 and < .05 respectively) (Fig. 2.6 (b) and (c)). The regression lines on the graphs shown are for GPB data only; nevertheless, the Smithtown Bay SOD values fit the GPB regression line closely. The regression of SOD against temperature (Fig. 2.6 (c)) is consistent with high mean in spring SOD relative to summer SOD shown in chart 2.2 (a) as both SOD & temperature in June 2013 were high. NH_4^+ measurements from Smithtown Bay sediment incubations do not show the trend with temperature reflected in the GPB data. This result partly derives from one measurement of an NH_4^+ influx into the sediments in a single incubation at the highest temperature (22° C); without this data-point, the STB data would show a low but positive relationship with T. NO_3^- fluxes values had no relationship with bottomwater temperatures (data not shown).

(iii) Relationship of N fluxes with measures of sediment metabolism. Sediment metabolism was measured by sediment oxygen demand (SOD) in this study. N flux values did not produce robust linear relationships when regressed against SOD. Fig. 2.7 illustrates geometric mean regressions (type II) against SOD for (a) N_2 (b) NH_4^+ and (c) TNF (total nitrogen flux: N_2 + NH_4^+ + NO_3^-/NO_2^-) fluxes. These regressions include all measured data points; i.e, all flux values from *in-situ* and *ex-situ* incubations and from both light and dark incubations. Data measured from STB sediments is shown to illustrate the similar N versus O_2 relationships for sediments from each estuary. The regression lines shown on these charts are derived from GPB data only; Smithtown Bay data are only superimposed on graphs.

Fig. 2.8 color-codes N versus O_2 relationships by temperature. The charts show 3 clusters where N fluxes have different relationships with SOD and T. N_2, NH_4^+ & TNF fluxes are low at low SOD likely reflecting low overall microbial

activity as T approaches zero. At intermediate values of T and SOD, N fluxes are variable and likely not constrained by T or SOD but by more complex and varying redox conditions in the sediments. At high T and SOD values, N-N_2 and NH_4^+ fluxes are low relative to intermediate T and SOD values. In this range, N-N_2 fluxes likely reflect more constrained nitrification and NH_4^+ fluxes likely reflect more biological competition for NH_4^+ than at intermediate T and SOD values.

2.3.3 Seasonal & diurnal controls on N_2 Production: dark versus light incubations.

In the October 2012 *in-situ* incubations, benthic chambers were left on the seabed for ~ 24 hours. The incubations produced sharp increases in N-N_2 flux (10 mmols m^{-2} d^{-1}) during daylight hours; production at night slowed significantly (p value= .02) and averaged only 0.5 mmols m^{-2} d^{-1} over the 24 hour period (Fig. 2.9 (a)). This in-situ dichotomy was not replicated in the lab between dark and light incubations in October 2012 (Fig. 2.9 (b)). *In-situ* incubations in May and September 2014 were only carried out in daylight and high rates (> 4 mmol m^{-2} d^{-1}) of N-N_2 production were measured in May 2014 (Fig. 2.9 (c)). These high daylight fluxes in October 2012 and May 2014 (n= 5) occurred together with signs of photosynthesis in the benthic environment (Fig. 2.9 (c)). SOD and in ΣCO_2 production in bottomwater was either low or negative (reflecting O_2 production or ΣCO_2 consumption); and net NH_4^+ fluxes were low or negative (reflecting NH_4^+ consumption) (Fig. 2.9 (c)). The benthic environment in May 2014 was characterized by obvious colonies of benthic diatoms (Fig. 2.6).

Nevertheless, it is not certain these higher *in-situ* daylight N-N_2 flux rates are connected with activity due to light. In June 2013 photosynthetic activity was apparent in ΣCO_2 consumption in bottomwater, yet *in situ* N-N_2 production was not meaningfully different between daylight and nighttime hours (*t- test*, p value > .05). The Sep 2014 data did not clarify whether light had a strong impact on N-N_2 production; N-N_2 flux was moderate and there were no clear signs of photosynthetic activity (Fig. 2.9). Results from *ex-situ* (only) incubations showed no significant differences (*t- tests*, p-values > .05) in N_2 production, NH_4^+ or NO_3^- fluxes between light and dark incubations (Table 2.2). Sufficient light was provided to these light incubations to support photosynthesis as evidenced by the lower SOD rates in light cores compared with dark cores. Yet no corresponding differences in N fluxes between dark and light incubations were found. Consequently, the higher N-N_2 flux rates found in some *in-situ* daylight incubations may reflect influences other than light conditions - for example- macro-faunal activity.

2.3.4 Comparisons between *in-situ* and *ex-situ* incubations.

In most periods (i.e. 8/11 datasets), *in- situ* incubations yielded higher mean net flux rates for N_2, NH_4^+ and SOD than *ex-situ* incubations although differences were infrequently significant (Table 2.3). NO_3^- results showed no

significant differences between *ex-situ* and *in-situ* as rates in both cases were close to zero.

To try to determine whether the overall bias towards higher flux rates *in-situ* compared with *ex-situ* arose from the site of incubation or the type of cylinder used, benthic chambers from the September 2014 *in-situ* incubations were capped from the chamber-bottom at the seabed and returned to the lab where they were incubated once again the following day (Table 2.4). Overall Sep 2014 flux rates were higher measured *in-situ* than *ex-situ* (in sub-cores) except in the case of NO_3^- fluxes which were all close to zero. Mean rates of net N_2 fluxes from lab-based benthic chamber incubations were closer to those measured in sub-cores than those measured *in-situ*; however, differences were not significant (Table 2.4). SOD were significantly higher measured *in-situ* than *ex-situ* in cores (Table 2.4); however, SOD was higher still in benthic chambers measured in the lab compared with *in-situ* measurements (this difference was significant at the α= 0.10 level). *In-situ* NH_4^+ fluxes were significantly higher than all *ex-situ* fluxes; NH_4^+ fluxes in cores were higher than *ex-situ* benthic chamber NH_4^+ fluxes (Table 2.4).

Results of this *in-situ* versus *ex-situ* comparison of N_2 and NH_4^+ fluxes support the notion the site of incubation influences outcomes more than the vessels used although in the case of the N_2 fluxes the differences in rates between the comparison groups were not significant. The results of SOD incubations show the highest rates occur in benthic chambers regardless of location although the reason for the increase in SOD from *in-situ* to *ex-situ* conditions is not clear. Measurements were made in daylight *in-situ* and in the lab with artificial light calibrated to replicate *in-situ* conditions based on Lux measurements taken with HOBO light sensors. If light had a deterministic control over SOD in these incubations, *ex-situ* results between cores and benthic chambers should have been closer.

2.3.5 Comparison of sedimentary fluxes with changes in corresponding values in bottomwater.

Table 2.5 compares net sedimentary fluxes of N_2, NH_4^+ and NO_3^-/NO_2^- and SOD against similarly calculated changes in corresponding values in bottomwater collected and incubated concomitantly. The purpose of these measurements was to distinguish sedimentary fluxes from changes in N and O_2 values occurring in bottomwater and not to serve as analytical blanks. Changes in N_2 and O_2 concentrations in bottomwater were generally close to zero or at least small relative to corresponding changes in sediment incubations. In several specific measurement periods, differences were not significant (p value > 0.05) because means of net sedimentary N_2 production and SOD were low and therefore close to values from bottomwater incubations.

NH_4^+ and NO_3^-/NO_2^- fluxes often did not show significant differences compared with corresponding changes in overlying bottomwater values. In the case of NO_3^-/NO_2^- fluxes, both sedimentary and bottomwater values were close to zero. Lack of a significant differences between NH_4^+ data-sets likely points to common demand for or production of NH_4^+ within GPB sediments, on the sediment: water interface and in GPB bottomwater.

2.3.6 N results compared with published values.

Table 2.1 compares fluxes of N- N_2, NH_4^+ and NO_3^-/NO_2^- measured in GPB and SB against averages of published fluxes complied in Fennel et al (2009) and other relevant publications. The mean and median N_2 fluxes for all (657) data points in Fennel et al (2009) were 2.2 and 1.5 mmol m^{-2} d^{-1}; however, these parameters include measurements from lakes and values calculated from NH_4^+ production or SOD which require stoichiometric assumptions to derive N_2 flux estimates. The article included a database modified here to (I) exclude all non-marine data points and those not directly measured; (II) average data-points aggregated by geographic study area to reduce the overall average bias toward studies with large numbers of measurements. Modified (II) fluxes in Fennel et al (2009) of N- N_2, NH_4^+ and NO_3^-/NO_2^- on this basis average 1.1; 0.95 and -0.60 mmol m^{-2} d^{-1} respectively.

2.4 DISCUSSION

2.4.1 Seasonality of fluxes.

GPB muddy sediments are distinguished from many estuarine sediments by low net N_2 fluxes in the winter and highly variable net N_2 fluxes in the spring. This high variability in spring relative to other seasons likely reflects patchiness in controlling factors and the influence of N_2 fixation (see Chp. 4). N_2 production in summer and fall show no significant differences between one another. These results contrasts with multiple studies showing a seasonal depression in absolute N_2 fluxes in summer: e.g., in Danish coastal sediments (Hansen et al 1981); in Mediterranean lagoons (Dedieu et al 2007); in Chesapeake Bay (Jenkins & Kemp 1984; Kemp et al 1990); in Florida Bay (Gardner & McCarthy (2009) and in Moreton Bay, Australia (Ferguson & Eyre 2013). Reported seasonal patterns in N_2 production in Narragansett Bay differ; e.g., Fulweiler & Nixon (2012) found little correlation with seasonal variables such as temperature or SOD under *in-situ* conditions whereas Brin et al (2014) have found strong correlations between potential N_2 production and temperature and SOD using $^{15}N\text{-}NO_3^-$ amendments to sieved and homogenized sediments.

2.4.2 Controls on the seasonality of N_2 production.

(i) The effect of temperature on N cycling. The absence of net sedimentary N_2 production during the winter in GPB derives from depressed microbial activity near ~0° C (0.4° C); few or no measurements at temperatures this low have been published for other temperate estuaries. As discussed in Chp.4, inventories of labile reduced organic N were not depleted over the winter period measured (February 2014). The absence of a direct relationship between N_2 production and temperature at temperatures above ~ 5° C in STB and ~ 8 ° C in GPB echoes Seitzinger (1988) who observed rates of N_2 production increased ~ twofold when temperatures increased from 3° C to 10° in Narragansett Bay sediments and with Fulweiler and Nixon (2012) who found ambiguous relationships between N_2 production and temperature at temperatures above 10° C (again for N.B.). The N_2 fluxes and water temperatures in in Smithtown Bay likewise show no direct relationship. Combined, these results underscore that N_2 fluxes in estuarine systems are determined by multiple controls. The positive trends between water temperatures and NH_4^+ fluxes and SOD observed largely agree with published studies (e.g., Kemp et al 1990; Boynton & Kemp 2008).

(ii) The effect of sediment metabolism on N_2 production. A regression (geometric mean type (II)) of measured net N- N_2 fluxes against SOD from GPB sediments produced a slope similar to the one described by Seitzinger & Giblin (1996) (N_2 flux ($N\text{-}N_2$ mol m^{-2} d^{-1}) = 0.116 * SOD (O_2- mol m^{-2} d^{-1}) (R = 0.80)) but did not result in a robust linear relationship (Fig. 2.7):

$$N_2 \text{ flux } (N\text{-}N_2 \text{ mol } m^{-2} d^{-1}) = .13^* \text{ SOD } (O_2\text{- mol } m^{-2} d^{-1}) - 1.16; (R= .25).$$

Since the GPB data included negative N_2 flux rates, the Y intercept was not forced to zero at the X axis. The data used by Seitzinger & Giblin (1996) consisted of SOD values from < 5 to ~ 50 mmol m^{-2} d^{-1}, a range similar to GPB, but contained higher N_2 production values at the high end of the SOD range than those from GPB incubations. As discussed above, these low GPB $N\text{-}N_2$ fluxes likely reflected lower nitrification at higher SOD levels. Although O_2 in bottomwater was never observed below ~ 230 µM, high SOD could indicate high biological demand for N which would constrain nitrification. The Seitzinger & Giblin (1996) continental shelf data came from depths of 16 to 106 m, whereas the GPB sediments are from 8 m depth and receive variable light depending on water column turbidity. Consequently, O_2 and N dynamics in surficial GPB sediments are subject to production and consumption patterns by benthic autotrophs which may not be typical of sediments on many continental shelves. The lower GPB $N\text{-}N_2$ fluxes compared to the data in Seitzinger & Giblin (1996) could reflect the activity of more diverse consumers of N substrate prevalent in shallower sediments than on continental shelves.

The lack of a linear relationship between N_2 production and SOD was also observed by Fulweiler and Nixon (2012) in Narragansett Bay sediments.

However, others have found robust relationships (e.g., Eyre, Maher & Squire 2013). In the case of the GPB data-set, the lack of robust correlation between N_2 production and SOD reflects the multiple controls which can influence N_2 production at any one time (e.g., T, C_{org} flux, O_2, bioturbation and assimilation of N by biomass).

A regression of N_2 against SOD in sieved, homogenized sediment without macro-fauna used for blanks in toxicity experiments and incubated in the dark produced a robust linear trend (N_2 production = 0.17 SOD + .01 (mmol m^{-2} d^{-1}) R^2= .89. Chp. 6; Fig. 6.10 (a)). The steeper slope of the regression compared against Seitzinger & Giblin (1996) likely reflects lower SOD which is probably the consequence of short cores (lower z) used in only in these toxicity experiments. Less sediment depth would generate less remineralized reduced solute products and therefore require less oxygen. Stripped of bio-irrigation and photoautotrophic O_2 demand, the relationship between SOD and N_2 production becomes more linear.

The lower rate of N_2 production from STB incubations collected in September 2013 compared with May 2012 is opposite to the seasonal pattern reflected in GPB sediments where N_2 production rises from spring to summer. STB bottomwater O_2 was lower in September 2013 compared with May 2012 but remained over 250 uM. The STB N_2 production values mirror the lower N_2 production in summer than in spring reported frequently in Chesapeake Bay and associated with lower O_2 availability (Jenkins & Kemp 1984; Kemp et al 1990).

(iii) Light versus dark incubations. High rates of N_2 production and NH_4^+ consumption during daylight measured in benthic chambers *in-situ* in October 2012 and May 2014 reflect the dynamic nature of N cycling in GPB sediments. These *in-situ* daylight results suggest intense cycling of N by nitrifying and N_2 producing microbes and, at least in the May 2014 *in-situ* incubations, with simultaneous consumption of NH_4^+ by benthic algae (Fig 2.4). Numerous field studies have demonstrated when N substrate is available, the presence of benthic micro-algae in light will enhance denitrification (e.g., Risgaard- Petersen et al 1994; Rysgaard et al 1995; An & Joye 2001 and Porubsky et al 2008). High rates of *in-situ* N_2 production and concomitant NH_4^+ consumption were never replicated in lab incubations in which NH_4^+ was generally effluxed. Artificial light in the lab was calibrated to approximate *in-situ* irradiance at the GPB station and the supplied irradiance was sufficient to stimulate photosynthesis in 5 out of 6 incubation periods (as evinced by SOD averaging > 30% greater in dark incubations than light incubations).

(iv) The seasonal DE pattern. The seasonal pattern observed in the DE ratio in fluxes from GPB sediments is driven by NH_4^+ fluxes which vary more than N_2 production. During the summertime, a decrease in DE is brought about not by a decrease in N_2 production from spring or fall averages but by an increase of NH_4^+ efflux. NO_3^- fluxes remained in low summer and there was no

accumulation of NO_3^- inventories in porewater observed. So in summer as ammonification of reduced N from the remineralization of organic matter increased (see Chp. 4), a threshold was reached beyond which NH_4^+ was preferentially effluxed rather than nitrified.

Low O_2 availability or sulfide inhibition may explain low rates of nitrification (Hansen et al 1981); but in these GPB incubations, O_2 bottomwater concentrations remained above 225 uM (with one exception at 208 uM) even in summer and sulfide gas (not measured) was never observed in sampling flux cores. But there are other explanations for preferential NH_4^+ efflux in summer.

The enzyme responsible for the first step in the nitrification pathway oxidizing NH_3 to hydroxylamine is ammonia monooxygenase AMO (McCarty 1999). There is ample evidence from the soil sciences literature that a broad spectrum of substrates can be oxidized by AMO (McCarty 1999) and competition at this site could inhibit nitrification. In addition to organic compounds (e.g., methane), there are a number of sulfides (e.g. methyl sulfide) which can compete in soils at this active site. Additionally, AMO likely requires copper as a co-factor at the active site in the enzyme (McCarty 1999; Ward 2008) but there has been no published research this author is aware of which investigates whether well-documented seasonal attenuation in nitrification could be the result of copper limitation. Research investigating copper limitation in denitrifying bacteria in seawater suggest copper could be a regulating trace element in the water column (Granger et al 2003).

(v) Summary of factors affecting seasonality of N fluxes.
Regressing net N_2 fluxes against single control variables like bottomwater O_2, porewater NO_3^- or SOD did not yield tight fits; instead multiple controls influence the set of redox reactions involved in N_2 production coupled to nitrification. The seasonality in net N_2 fluxes demonstrated in this study derives from low N_2 production in the winter and highly variable net production in the spring. Net N_2 production in summer and fall show no significant differences. The low values for winter N_2 production are the result of generally low microbial activity brought about by 0° C temperature; NH_4^+ production estimates discussed in Chp.4 showed sedimentary NH_4^+ inventories were not depleted of reduced labile organic N.

The highly variable net N_2 flux in the spring follows from elevated rates of net production found in some *in-situ* incubations and low and negative rates found in lab cores and other *in-situ* incubations. The high rates of net N_2 production occur with influxes of NH_4^+ and, at least in May 2014, with high levels of benthic micro-algae. In other incubations of spring sediment, net N_2 fluxes rates were negative suggesting the occurrence of N-fixation. Because MiMS was used to measure N_2, it is possible N_2 fixation could be disguised in net N_2 production numbers. Alternately, the negative N_2 fluxes might be attributable to analytical error. Not all the negative N_2 flux values were derived from statistically

significant regressions often because it was only feasible to take a low number (3) of time-points especially in the case of *in-situ* incubations. The largest negative N_2 flux number was -0.42 mmol m^{-2} d^{-1} which was significant (p-value < 0.05).

2.4.3 Experiment with additional lamp.

During the May 2014 lab measurements, an extra set of incubations were carried out with an additional lamp which increased irradiance in the overlying water of the lab cores from a range 25- 30 µE m^{-2} s^{-1} to a range between 86- 150 µE m^{-2} s^{-1}. The additional light resulted in a change in O_2 flux from SOD of 10 mmol m^{-2} d^{-1} under usual light to O_2 production (i.e., O_2 efflux) of 6.0 mmol m^{-2} d^{-1}. Only one core showed SOD under elevated light and this core had a brittlestar (*Amphioplus Abiditus;* see chapter 5*)* actively ventilating; the two cores which showed O_2 production had no apparent macro-fauna. The cores showed close-to-zero or negative N_2 fluxes under usual light (0.16 mmol m^{-2} d^{-1} average). In the incubations with the additional light, average N_2 production became positive (0.36 mmol m^{-2} d^{-1} average of the cores without *Amphioplus*); when light was extinguished N_2 fluxes again turned negative (-0.31 mmol m^{-2} d^{-1} average of the cores without *Amphioplus*). N_2 fluxes in the core with the *Amphioplus* averaged -0.05 mmol m^{-2} d^{-1} under usual light, 0.12 mmol m^{-2} d^{-1} in the incubation with the additional lamp and 0.09 mmol m^{-2} d^{-1} when the light was extinguished. The differences in N_2 fluxes measured under initial light, additional light and dark were all significant (p value <= 0.05).

Unlike in the May 2014 *in-situ* incubations, the lab incubations for this period showed low or negative N_2 production. The May 2014 experiment with additional light suggest N fixation occurred in these incubations. The incremental light resulted in O_2 production in place of SOD in sediment cores incubated in the dark or with one lamp. N fixation is inhibited by O_2 (Capone 1988). In this enhanced oxygen setting, net N_2 flux turned from slightly negative to positive; when the light was extinguished, N_2 production once again turned negative. In order to test the hypothesis N fixation occurs in GPB sediments and therefore reduces gross N_2 production in MiMS analysis, acetylene reduction assays were carried out on GPB sediments in November 2014 and May 2015. These experiments are described in chapter 3 of this dissertation.

2.4.4 Comparison between *in situ* and *ex situ* flux estimates.

Several researchers measured higher sedimentary fluxes *in-situ* in benthic chambers than *ex- situ* in cores ((NH_4^+, NO_3^-/NO_2^- & SOD) Glud et al 1998; & (NO_3^-/NO_2^- & SOD) MacReadie et al. 2006); Nielsen & Glud (1996) reported similar denitrification rates from *in-situ* and lab- based incubations. This study generally found higher N_2 , NH_4^+ and O_2 fluxes in *in-situ* incubations than in *ex-situ* ones; however, differences were only infrequently significant. NO_3^- fluxes

(which were small) were not significantly different from each-other regardless of the incubation method used.

Glud et al (1998) attributed the higher fluxes in chambers to edge effects (i.e. the ratio of cylinder circumference to surface area, or equivalently, 2x the curvature of the cylinder) excluding bio-irrigating infauna to a greater extent in cores (edge effect ~ 0.41 cm^{-1}) versus chambers (edge effect ~ 0.13 cm^{-1}). The results of this study largely agreed with Glud et al (1998) even though edge ratios (2/radius) for the chambers used was lower (0.29 cm^{-1}); the ratios for the cores was similar (0.43 cm^{-1}). In this research, N_2 production, SOD & NH_4^+ fluxes were higher in incubations with higher densities of *Amphioplus abditus* than in those with lower densities (Chp. 5; this dissertation). Higher densities of *A. abiditus* were sometimes found in low edge benthic chambers and sometimes in high edge cores. The controlling variable was macro-faunal density; whether vessel geometry may have affected macro-faunal activity was not determined.

2.5 TABLES & FIGURES

Table 2.1 Summary of published & measured N fluxes. Results in this study include in-situ and ex-situ measurements in both dark and light conditions. The mean N_2 production for GPB sediments calculated as an annualized rate is lower than average of all measured rates because there are less data-points for winter months. Ranges specified for GPB sediments are derived from sampling period averages; ranges from Smithtown Bay are derived from individual flux measurements as sediment was only collected from the site on 3 occasions. The mean and median N_2 fluxes for all (657) data points in Fennel et al (2009) were 2.2 and 1.5 mmol m^{-2} d^{-1}; however, these parameters include measurements from lakes and values calculated from NH_4^+ production or SOD which require stoichiometric assumptions to derive N_2 flux estimates. The article included a database modified here to * (I) exclude all non-marine data points and those not directly measured; ** (II) average data-points aggregated by geographic study area to reduce the overall average bias toward studies with large numbers of measurements.

		mean net flux rates (mmols m^{-2} d^{-1})			
Study:	sediment	SOD	N- N_2	NH_4^+	NO_3^-
Fennel et al (2009) *	marine	27	2.2	2.0	-0.69
*modified (I)	marine	16	1.4	0.99	-0.52
*modified (II)	marine	10	1.1	0.95	-0.60
			Range (mmols m^{-2} d^{-1})		
Devol (2015)	shelves		0.5 – 2.0		
Joye & Andersen (2008)	estuaries		0.5 – 5.0		
		mean net flux rates (mmols m^{-2} d^{-1})			
GPB- this study (average & range)	estuary	18 (4- 39)	1.4 (0.06-2.8)	0.93 (-0.4- 3.6)	0.05 (-0.1- .23)
GPB-this study (annualized)	estuary	17	1.1	0.99	0.03
GPB Howes et al (2000)	estuary	25	N-A	1.2	0.16
Smithtown Bay- this study (average & range)	estuary	15 (7- 26)	1.48 (0.39- 2.5)	0.41 (-0.15- 1.2)	0.23 (-.08- 1.0)

Table 2.2 Comparison of net fluxes of *ex-situ* incubations under dark & light conditions. Applied light PAR values ~ 25 - 30 µE m^{-2} s^{-1}. P-values from *t-tests*: n= 3 all samples.

	$N\text{-}N_2$ (mmol/m^2-d)			O_2 (mmol/m^2-d)			NH_4^+ (mmol/m^2-d)			NO_3^- (mmol/m^2-d)		
period	dark	light	p	dark	light	p	dark	light	p	dark	light	p
9-14	1.20	1.00	.68	21.5	15.8	.02	4.43	3.21	.13	0.61	0.08	.00
5-14	0.01	- .32	.28	12.8	10.0	.68	0.37	-0.02	.06	-0.01	-0.13	.25
2-14	0.06	0.06	.99	5.13	3.55	.04	0.11	0.08	.73	0.01	0.02	.73
11-13	1.14	1.12	.95	16.0	10.3	.08	-0.30	-0.49	.71	0.30	0.16	.15
6-13	1.05	0.62	.32	48.7	29.2	.05	1.76	2.09	.67	-0.14	-0.15	.96

Table 2. 3 Comparison of net fluxes measured in *ex-situ* and *in-situ* incubations. P-values from *t-tests*: n= 3 all samples. (bc= *in-situ* benthic chamber; lab= *ex-situ* sub-cores).

	N_2 (mmol m^{-2}-d^{-1})			O_2 (mmol m^{-2} d^{-1})			NH_4^+ (mmol m^{-2} d^{-1})			NO_3^- (mmol m^{-2} d^{-1})		
Period	bc	lab	p	bc	lab	p	bc	lab	p	bc	lab	p
09-14	1.02	0.50	0.40	23.7	15.8	0.08	6.05	3.21	0.02	-0.01	0.08	.40
05-14	3.27	-0.16	0.05	21.9	10.0	0.24	-1.42	-0.02	0.03	-0.16	-0.13	.71
06-13	0.15	0.44	0.29				1.77	1.73	0.80	0.00	-0.15	.08
10-12	1.01	0.33	0.14	14.9	16.9	0.34	1.03	-0.42	0.01	0.12	-0.04	.23
All	1.71	0.28	<.03	21.6	13.5	<.02	1.87	1.17	0.58	0.00	-0.07	.26
Light only	2.41	0.24	<.01	23.7	13.5	<.02	2.05	1.27	0.52	-0.05	-0.08	.58

Table 2.4 Analysis of differences between sedimentary flux rates measured in incubations (1) *in-situ* in benthic chambers ; (2) *ex- situ* in benthic chambers; and (3) *ex-situ* in sub-cores in September 2014. Values for bc's in lab & cores in lab are different when compared against each-other than when compared against bc's in-situ. The reason for the differences is fluxes from bc's in-situ were daylight only fluxes; consequently, they are compared only against lab fluxes incubated in light. Comparisons of bc's and cores incubated in the lab were made on as wide a data-set as available and therefore included both dark and light incubations. Dimensions of incubation vessels are given in the text. P-values from *t-tests*: n= 3 all samples.

	N_2 (mmol m^{-2}-d^{-1})			O_2 (mmol m^{-2} d^{-1})		
	bc (in-situ)	**cores (lab)**	**p-value**	**bc (in-situ)**	**cores (lab)**	**p-value**
in-situ vs lab (light only)	1.02	0.50	0.40	23.7	15.8	0.08
	bc (in-situ)	**bc (lab)**	**p-value**	**bc (in-situ)**	**bc (lab)**	**p-value**
in-situ vs bc's in lab (light only)	1.02	0.62	0.52	23.7	38.2	0.07
	bc (lab)	**cores (lab)**	**p-value**	**bc (lab)**	**cores (lab)**	**p-value**
lab: bc's vs cores (L&D)	0.52	0.55	0.84	32.2	18.6	0.02
	NH_4^+ (mmol m^{-2} d^{-1})			NO_3^- (mmol m^{-2} d^{-1})		
	bc (in-situ)	**cores (lab)**	**p-value**	**bc in-situ**	**sub-cores**	**p-value**
in-situ vs lab (light only)	6.0	3.2	0.02	-0.01	0.08	0.37
	bc (in-situ)	**bc (lab)**	**p-value**	**bc in-situ**	**bc lab**	**p-value**
in-situ vs bc's in lab (light only)	6.0	2.1	0.01	-0.01	-0.05	0.73
	bc (lab)	**cores (lab)**	**p-value**	**bc lab**	**sub-cores**	**p-value**
lab: bc's vs cores (L&D)	1.8	3.8	0.02	-0.05	0.35	0.10

Table 2.5 Comparison of sedimentary fluxes and changes in corresponding values in bottomwater. Concomitant with measurements of sedimentary fluxes, corresponding measurements were made of filtered (44 µm mesh) GPB seawater in acrylic sub-cores of similar dimensions. P-values from *t-tests*: n= 3 (sediment fluxes); n= 1 (bottomwater).

	N_2 (mmol m^{-2}-d^{-1})			SOD (mmol m^{-2} d^{-1})			NH_4^+ (mmol m^{-2} d^{-1})			NO_3^- (mmol m^{-2} d^{-1})		
period	sed	BW	p	sed	BW	p	sed	BW	p	sed	BW	p
0914	0.66	0.02	.08	25	5.7	.01	3.6	1.8	.10	.11	0.15	.77
0514 *	0.76	0.12	.63	17	0.65	.04	-0.23	-0.65	0.53	-.09	0.10	.04
0214	0.03	-0.10	.10	4.3	0.02	<.01	0.10	0.03	0.33	.01	0.00	.61
1113	0.56	0.10	.04	13	0.42	<.01	-0.40	-0.18	0.61	.23	0.05	.22
0613	0.29	-0.04	.07	39	1.1	<.01	2.23	0.37	<.01	-.07	-0.09	.27
1012	0.67	0.06	.14	14.0	-3.1	<.01	0.17	-0.03	0.81	.02	-0.01	.83

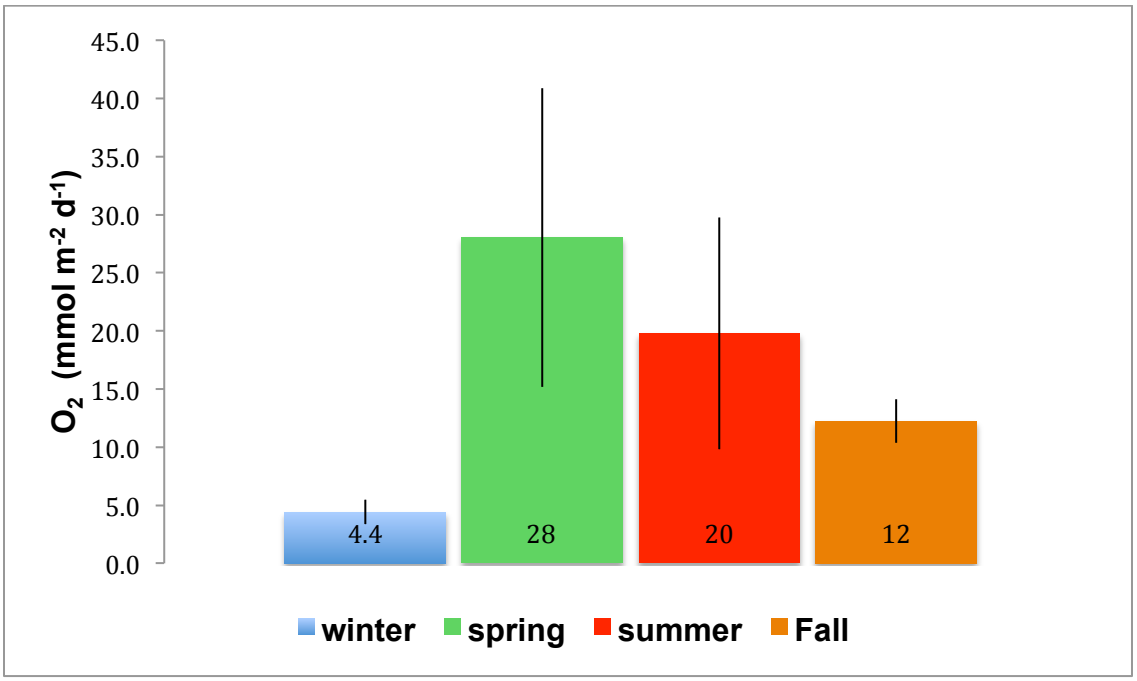
45.0
40.0
35.0
30.0
25.0
20.0
15.0
10.0
5.0
0.0
O2 (mmol m-2 d-1)
4.4
28
20
12
winter
spring
summer
Fall

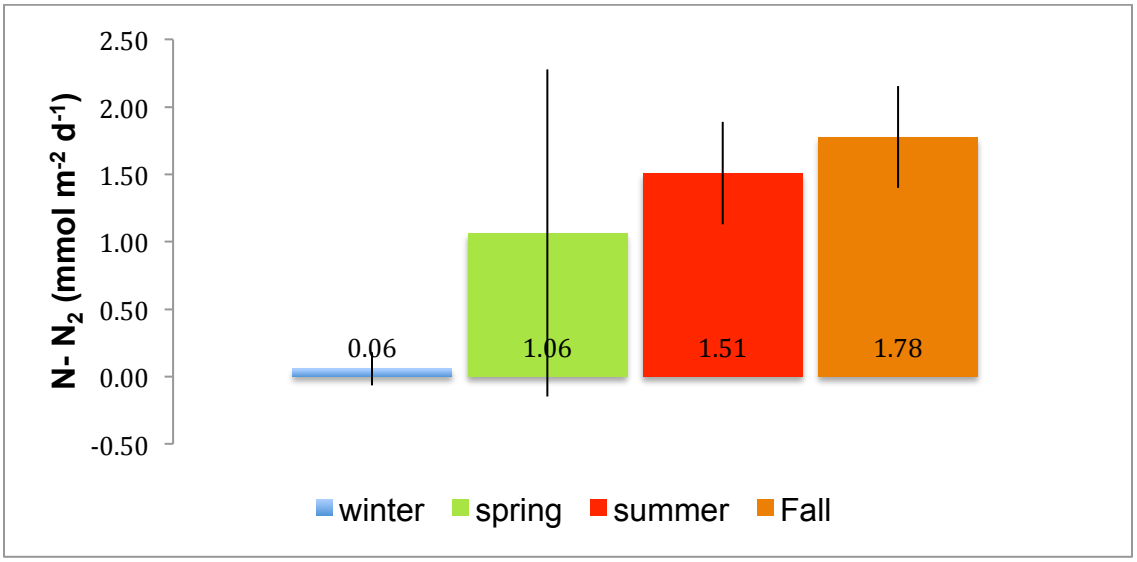
2.50
2.00
1.50
1.00
0.50
0.00
-0.50
N- N2 (mmol m-2 d-1)
0.06
1.06
1.51
1.78
winter
spring
summer
Fall

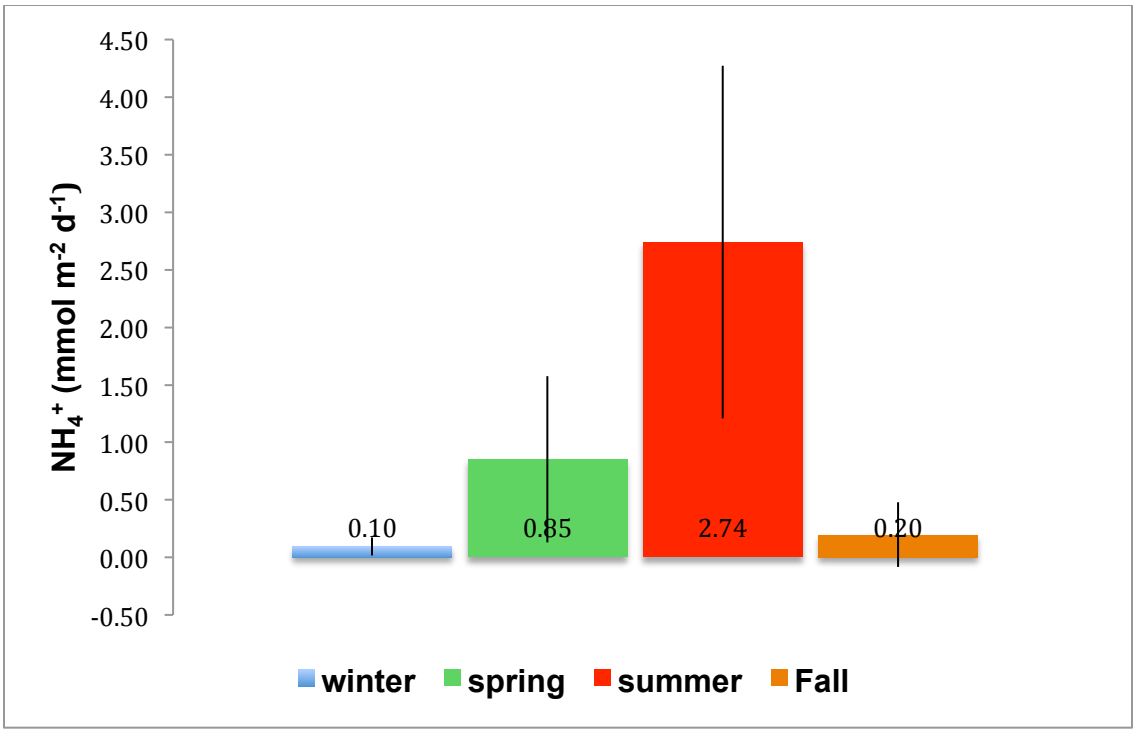

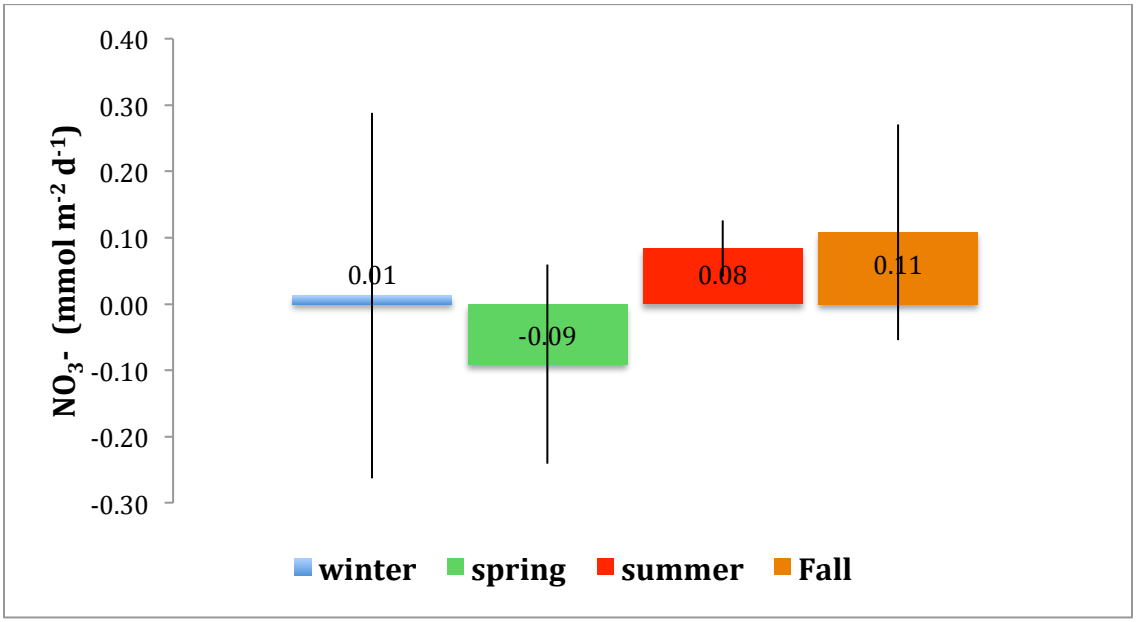

Fig. 2.1 (a) **Seasonal means of SOD; (b) Seasonal means of N_2 fluxes; (c) Seasonal means of NH_4^+ fluxes; & (d) Seasonal means of NO_3^- fluxes.** Means of replicates from each sampling period are averaged by season; error bars are period weighted standard deviations of replicate incubations. Spring SOD is higher than would be expected based on simple T dependence likely reflecting higher deposition of organic matter.

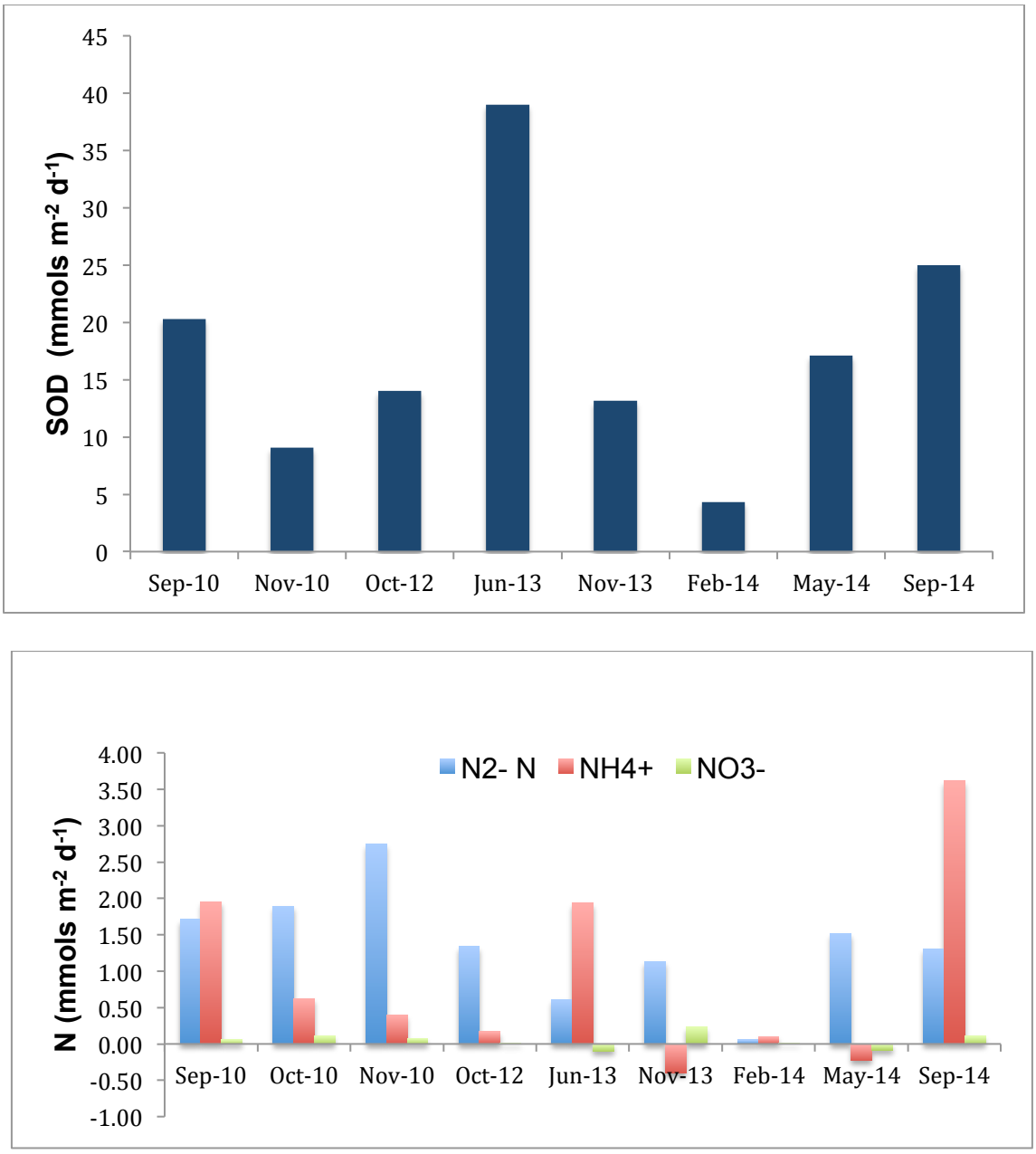

Fig. 2.2 (a) Period means of measured SOD. (b) Period means of measured N fluxes. Note: N_2 is stable relative to NH_4^+ fluxes generally; NH_4^+ fluxes are divergent in spring periods.

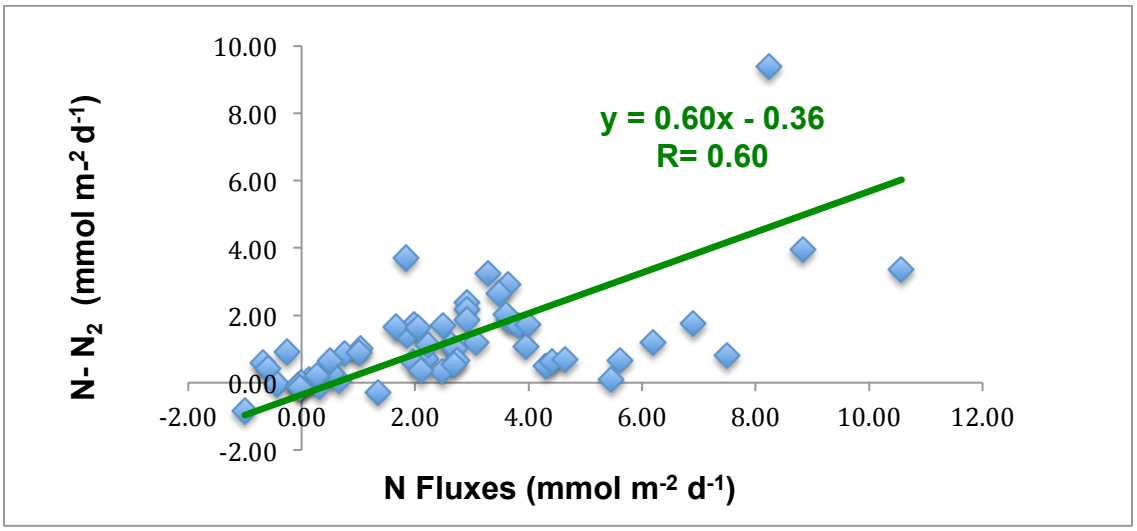

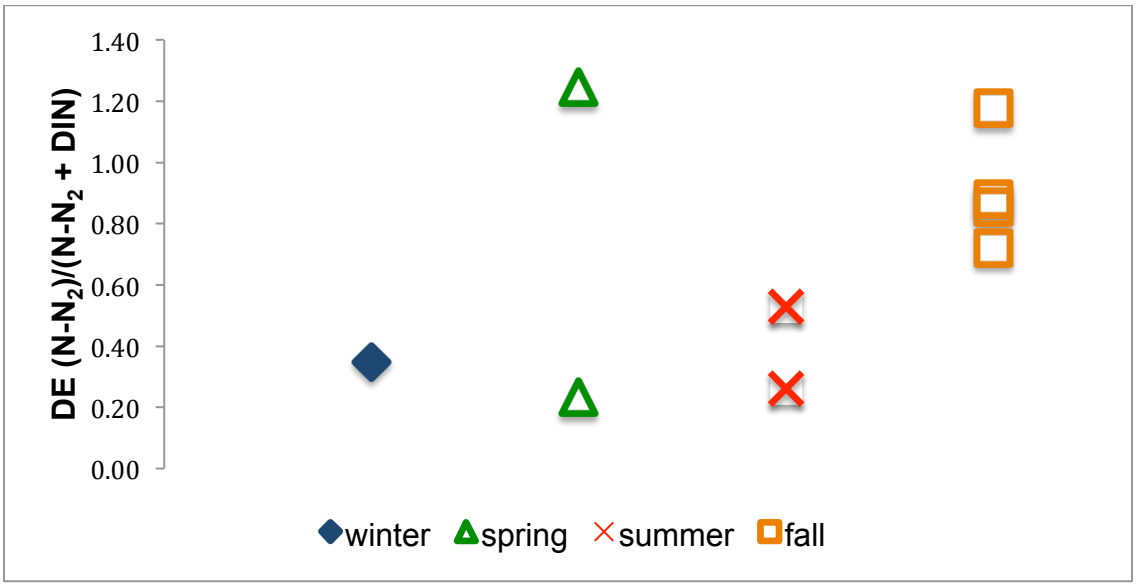

Fig. 2.3 (a) Average denitrification efficiency ($N\text{-}N_2/(N\text{-}N_2 + DIN)$). (b) Seasonality of denitrification efficiency. (ratios > 1 result from small negative DIN fluxes.

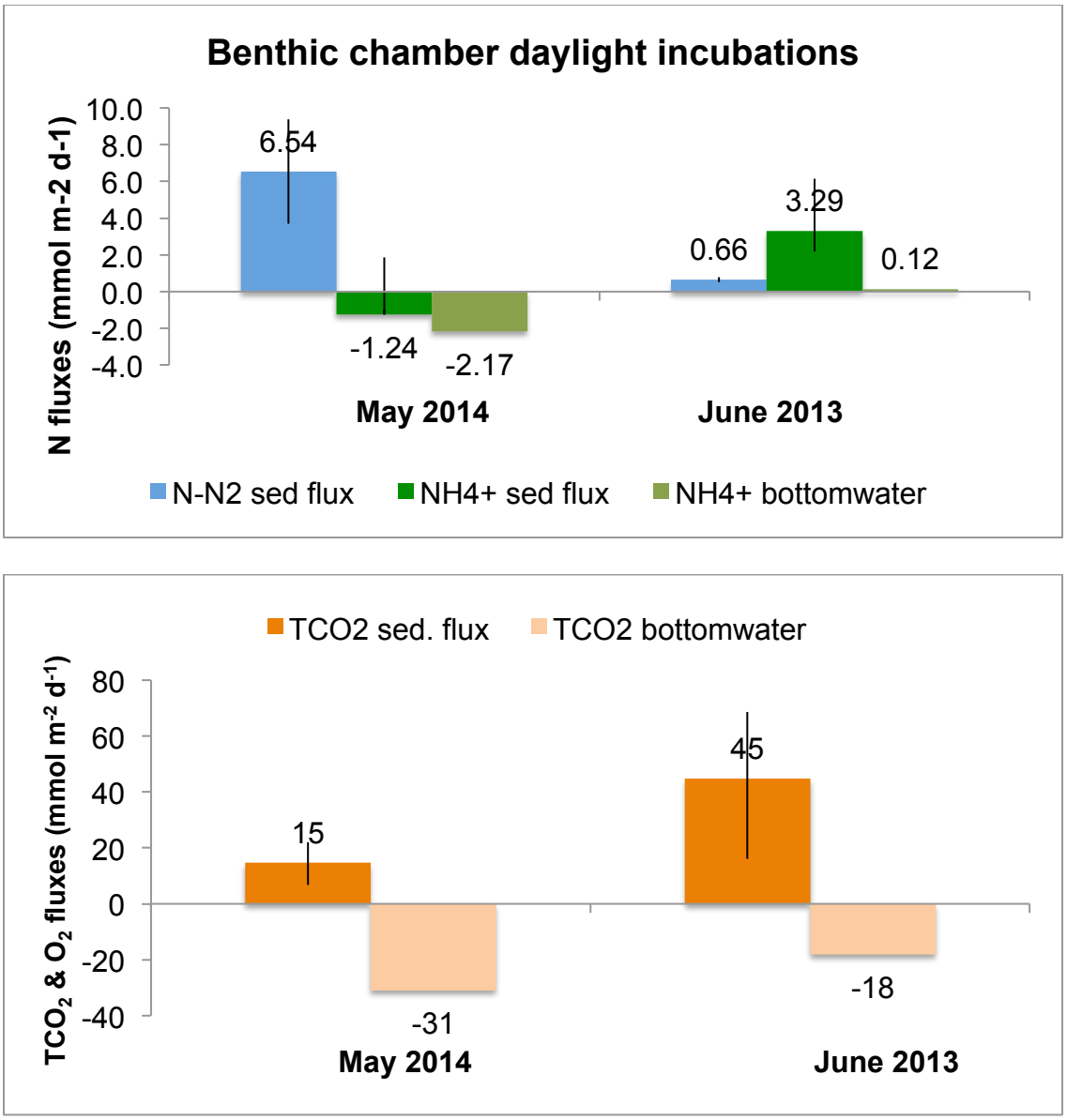

Fig. 2.4 (a) Comparison of daylight *in-situ* N fluxes in June 2013 & May 2014. (b) Comparison of daylight *in-situ* ΣCO_2 fluxes in June 2013 & May 2014. Although there was evidence of the presence of benthic algae in each period (i.e., ΣCO_2 was consumed in bottomwater), N fluxes showed opposite trends in each period.

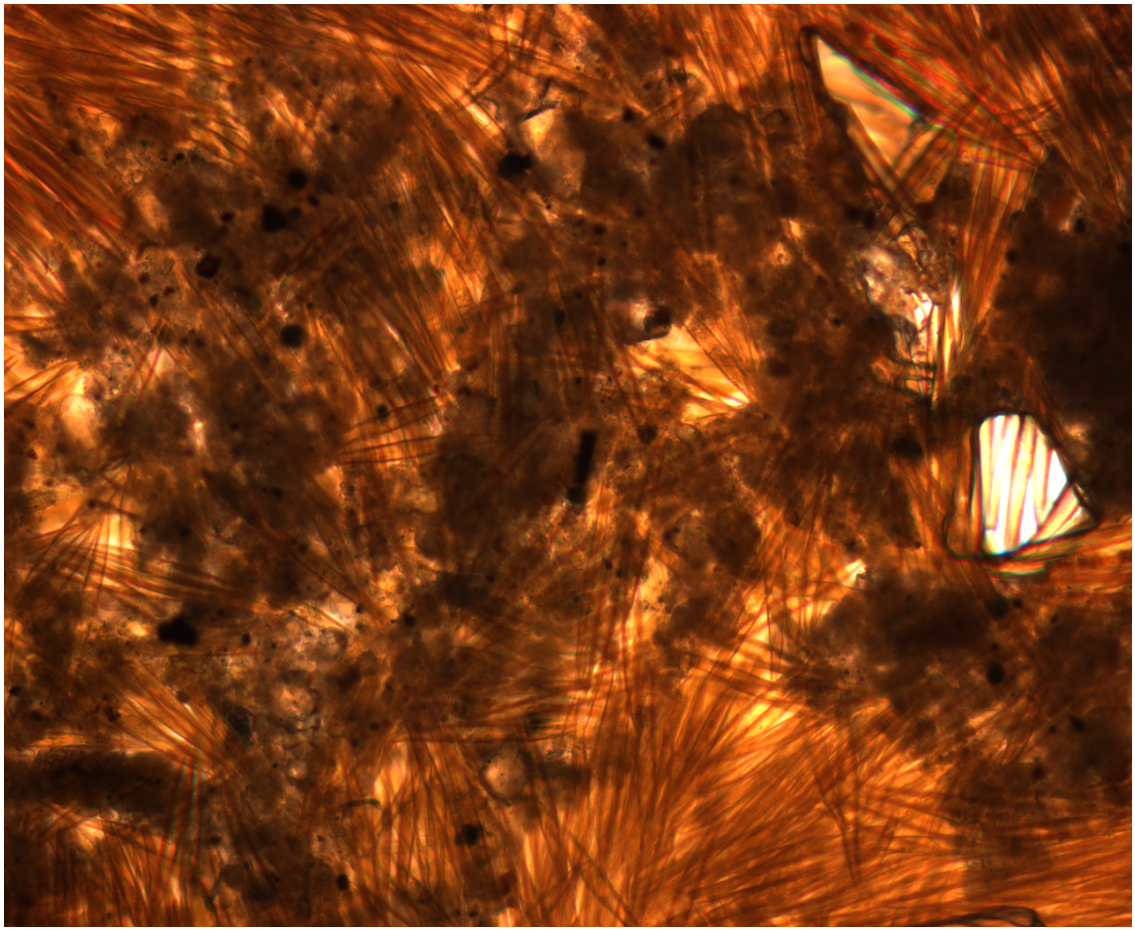

Fig. 2.5 Microscope image benthic diatom clusters which covered GPB sediment in sub-cores and benthic chambers in May 2014.

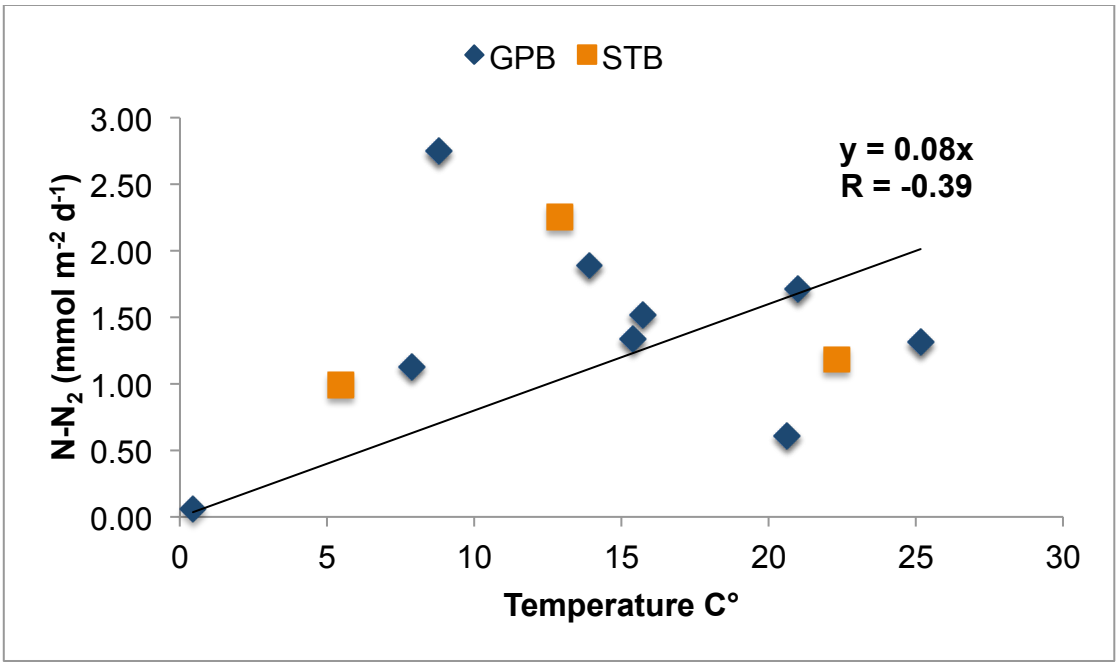
GPB
STB
y = 0.08x
R = -0.39
N-N2 (mmol m-2 d-1)
3.00
2.50
2.00
1.50
1.00
0.50
0.00
0
5
10
15
20
25
30
Temperature C°

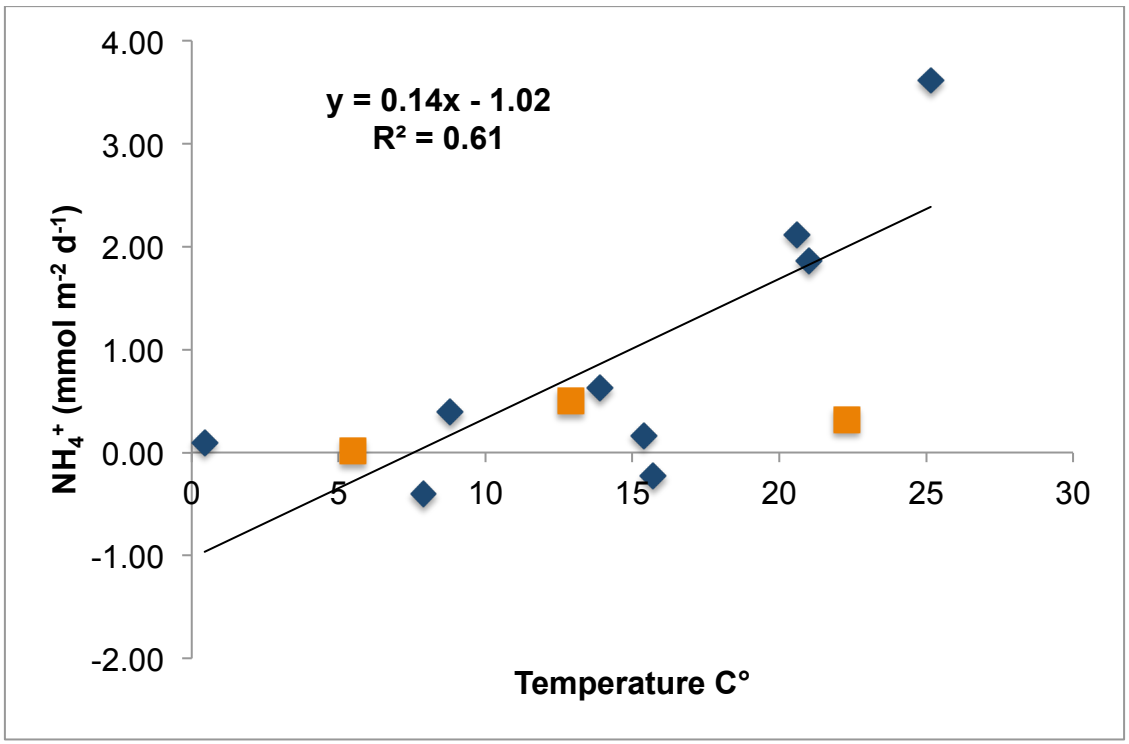
y = 0.14x - 1.02
R² = 0.61
NH4+ (mmol m-2 d-1)
4.00
3.00
2.00
1.00
0.00
-1.00
-2.00
0
5
10
15
20
25
30
Temperature C°

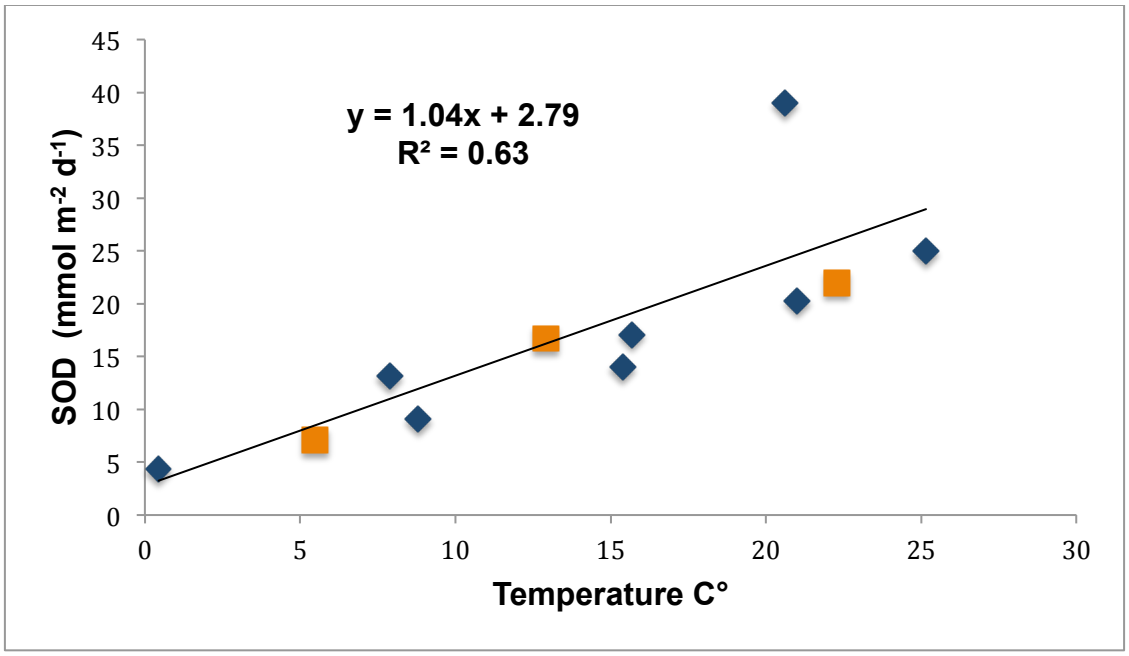

Fig. 2.6 (a) Relationship between N- N_2 fluxes & temperature. The direct relationship between temperature and period average N-N_2 fluxes derives only from the near-zero value of N-N_2 production at T= 0° C. N-N_2 flux values show an insignificant negative correlation with temperatures if the T= 0° C data point is excluded. **(b) Relationship between NH_4^+ fluxes & temperature.** Period average NH_4^+ fluxes in GPB sediments show a direct correlation with temperature as expected for products and reactants involved in heterotrophic microbial activity. NH_4^+ fluxes from Smithtown Bay sediments do not show a trend with temperature largely reflecting a low average flux value at T= 22.3° C. This low value reflects one data point showing an influx of NH_4^+. **(c) Relationship between SOD and temperature.** This regression is consistent with high mean SOD in spring SOD shown in chart 2.2 (a) as both SOD & temperature in June 2013 were high. Regressions derive only from GPB data in all cases.

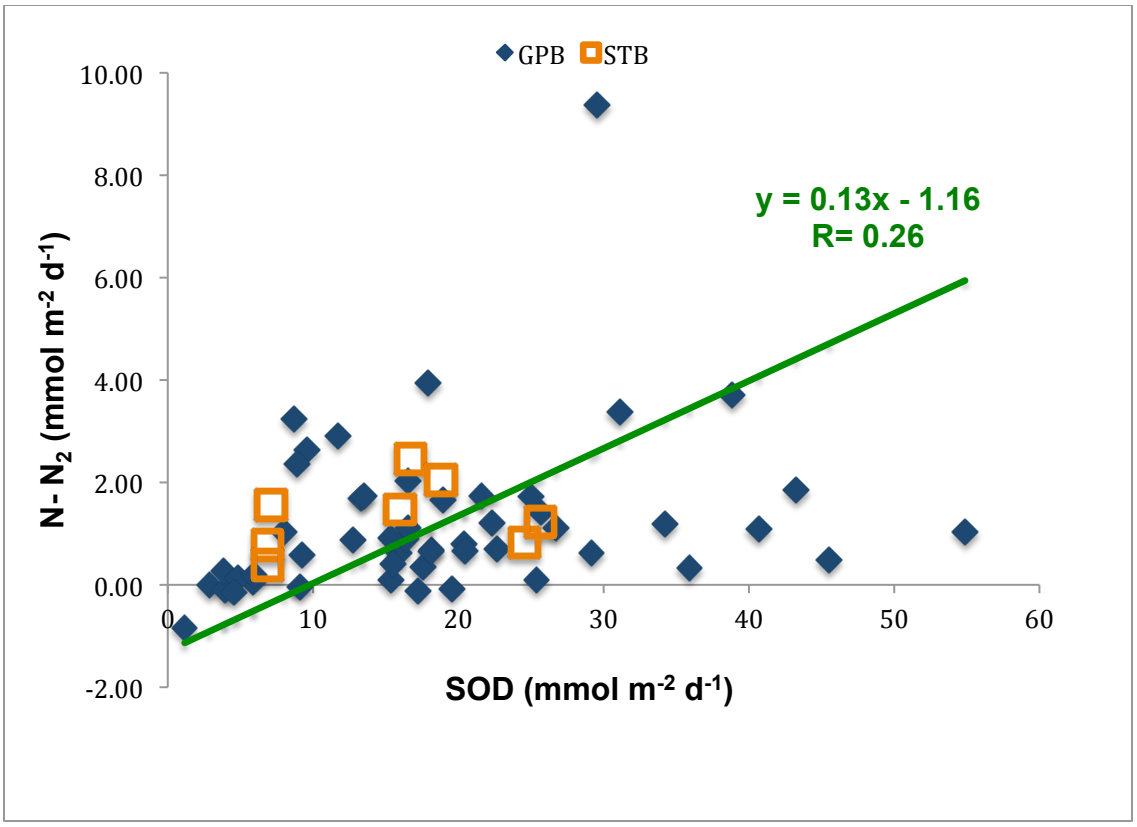
GPB
STB
y = 0.13x - 1.16
R= 0.26
N- N2 (mmol m-2 d-1)
SOD (mmol m-2 d-1)
10.00
8.00
6.00
4.00
2.00
0.00
-2.00
0
10
20
30
40
50
60

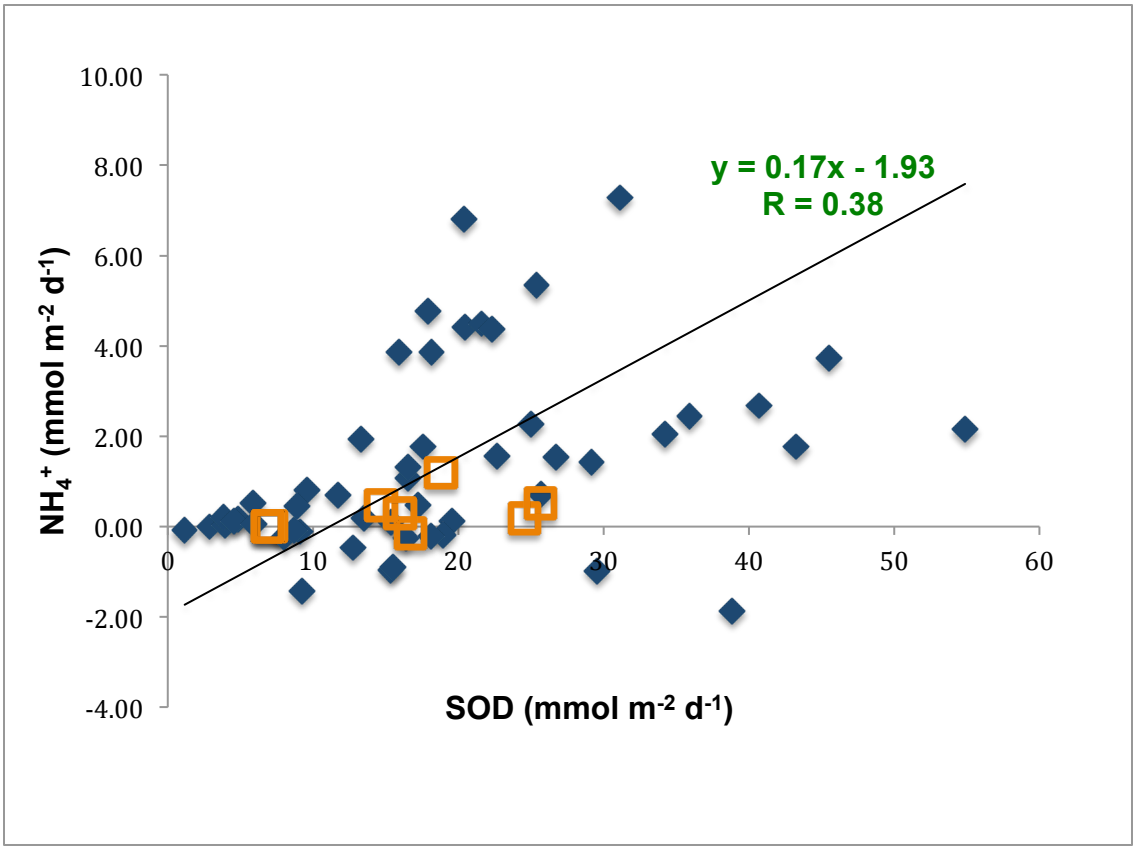
y = 0.17x - 1.93
R = 0.38
NH4+ (mmol m-2 d-1)
SOD (mmol m-2 d-1)
10.00
8.00
6.00
4.00
2.00
0.00
-2.00
-4.00
0
10
20
30
40
50
60

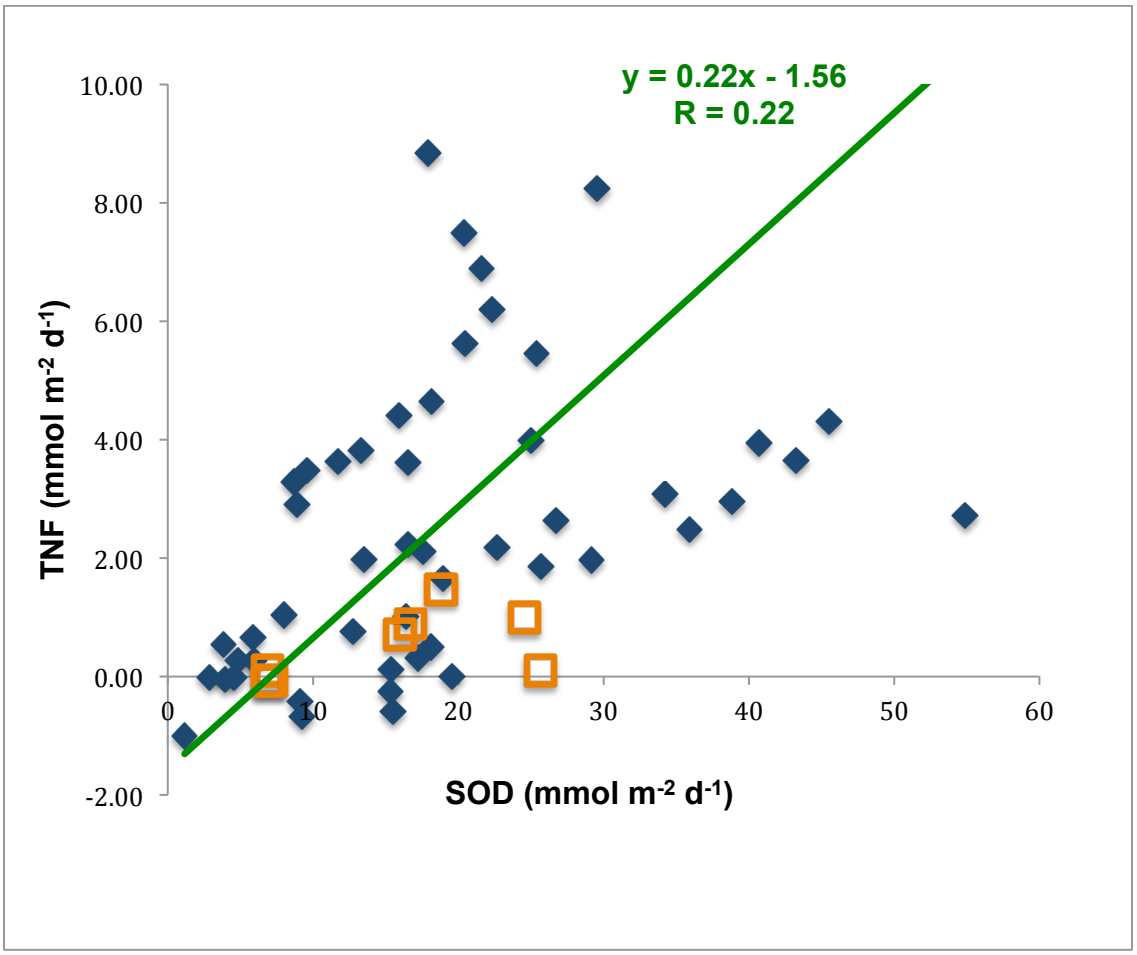

Fig. 2.7 (a) Correlation between N- N_2 fluxes and SOD. (b) Correlation between NH_4^+ fluxes and SOD. (c) Correlation between TNF and SOD. Both N-N_2 and NH_4^+ fluxes show a tailing-off at SOD > 30 mmol m^{-2} d^{-1}. At high SOD, nitrification may be inhibited limiting N_2 production and biological demand may limit NH_4^+ flux.

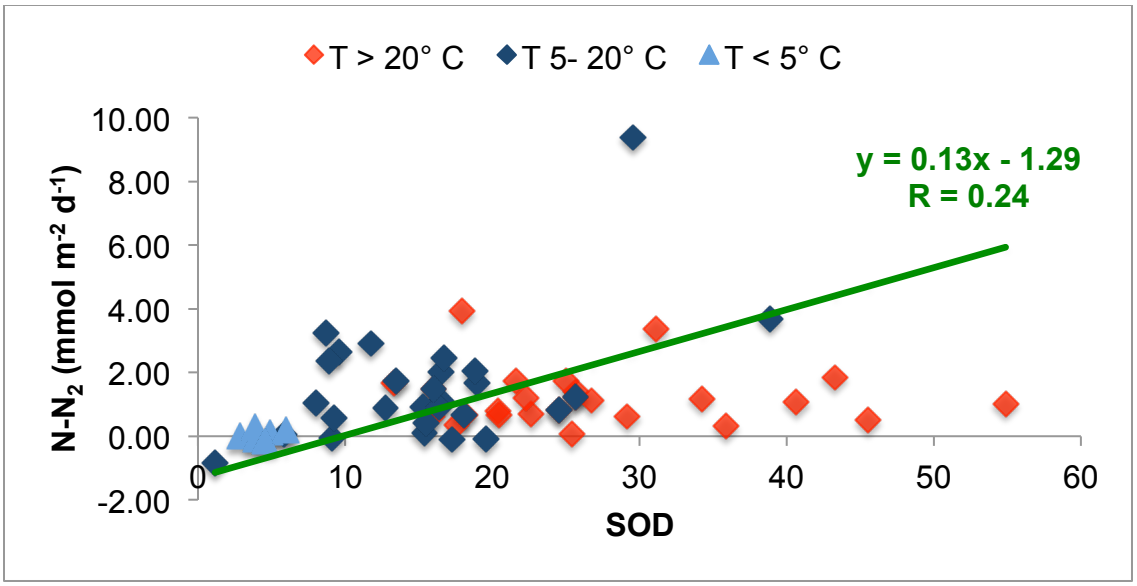
T > 20° C
T 5- 20° C
T < 5° C
10.00
8.00
6.00
4.00
2.00
0.00
-2.00
N-N2 (mmol m-2 d-1)
0
10
20
30
40
50
60
SOD
y = 0.13x - 1.29
R = 0.24

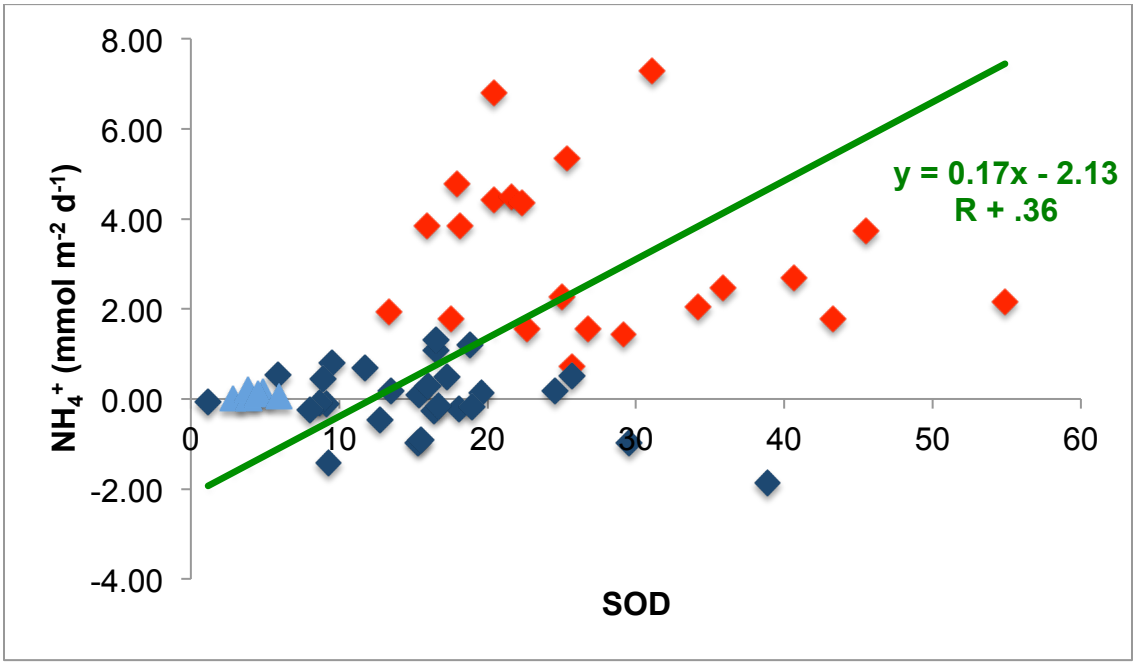
8.00
6.00
4.00
2.00
0.00
-2.00
-4.00
NH4+ (mmol m-2 d-1)
0
10
20
30
40
50
60
SOD
y = 0.17x - 2.13
R + .36

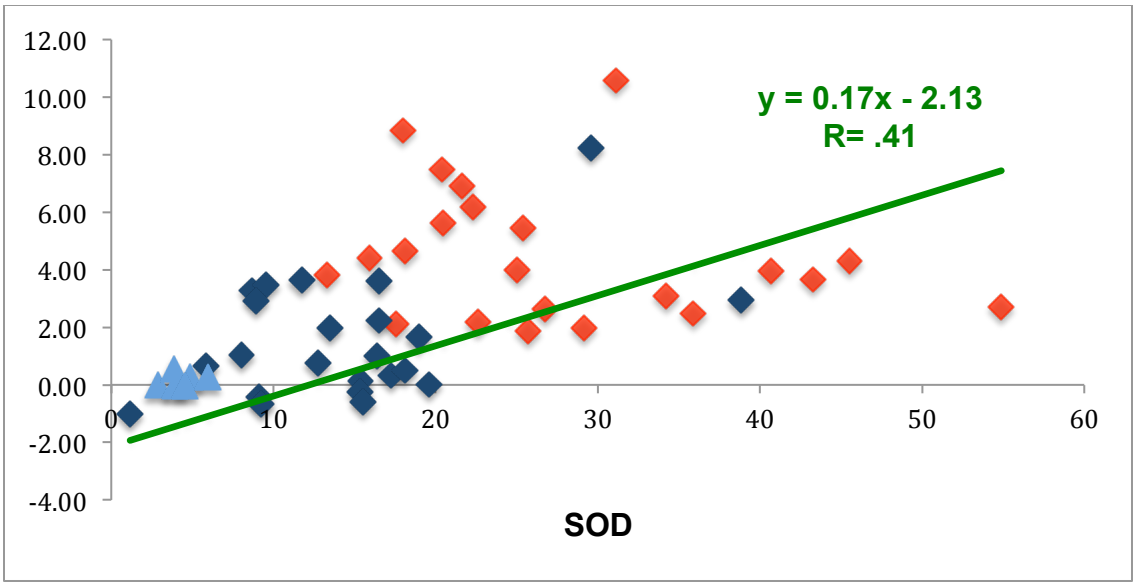

Fig. 2.8 (a) Correlation between N- N_2 fluxes & SOD color-coded for temperature ranges. (b) Correlation between NH_4^+ fluxes & SOD color-coded for temperature ranges. (c) Correlation between TNF values & SOD color-coded for temperature ranges

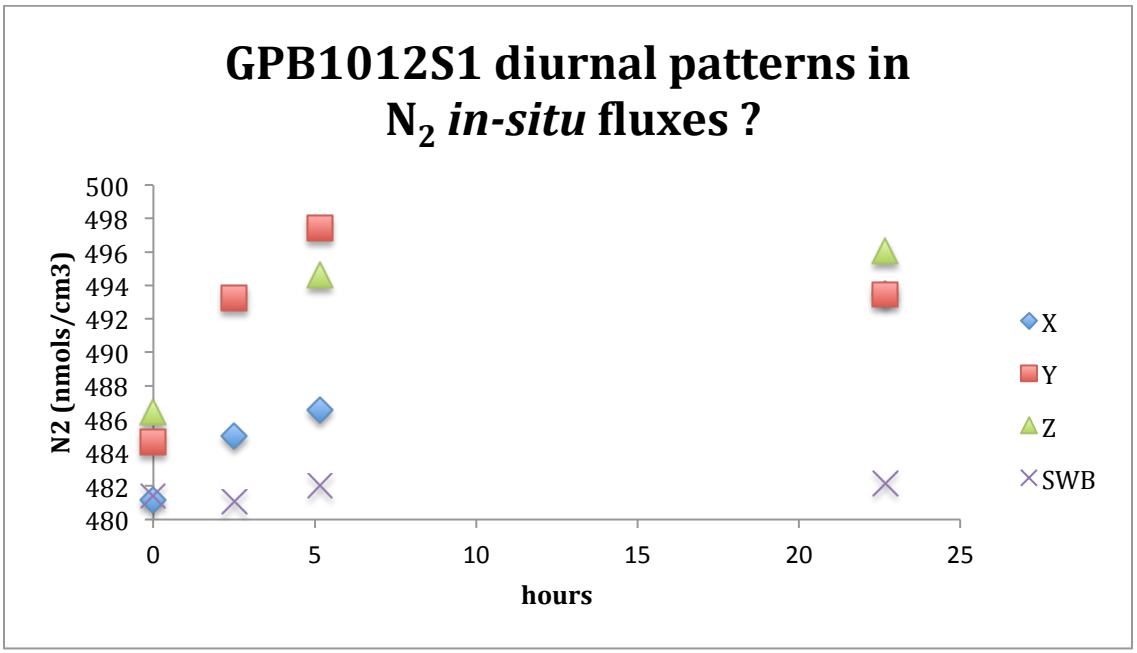
GPB1012S1 diurnal patterns in
N2 in-situ fluxes ?
N2 (nmols/cm3)
500
498
496
494
492
490
488
486
484
482
480
0
5
10
15
20
25
hours
X
Y
Z
SWB

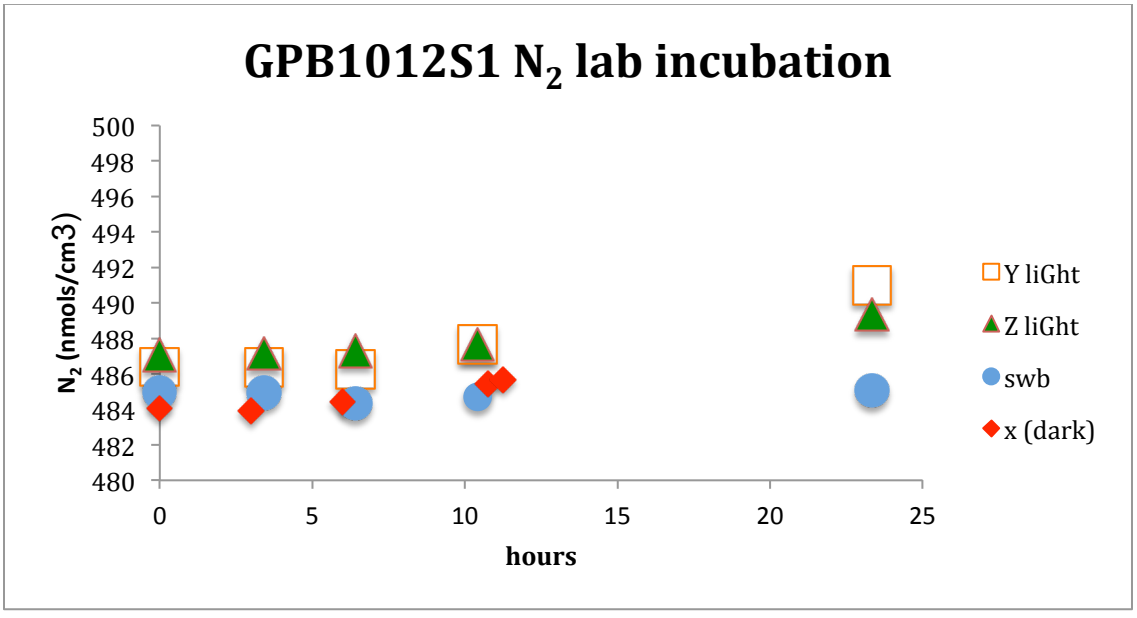
GPB1012S1 N2 lab incubation
N2 (nmols/cm3)
500
498
496
494
492
490
488
486
484
482
480
0
5
10
15
20
25
hours
Y liGht
Z liGht
swb
x (dark)

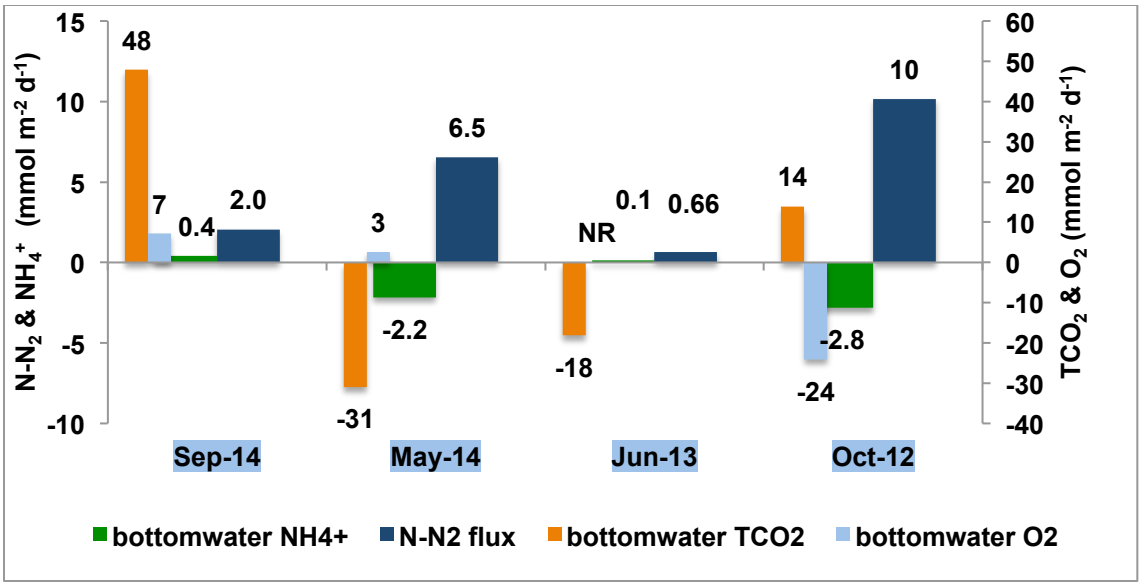

Fig. 2.9. (a) Summary of daylight *in-situ* incubations from October 2012. Large gains in N- N_2 production occur in daylight but not at night. **(b) *Ex-situ* incubations in light and dark conditions from October 2012**. The dichotomy in *in-situ* N2 flux rates was not found in dark and light lab incubations. **(c) Summary of daylight *in-situ* N-N_2 flux and changes in ΣCO_2, O_2 & NH_4^+ bottomwater values.** Large daylight gains in N-N_2 production occurred concomitant with signs of photosynthesis (ΣCO_2 & NH_4^+ consumption & O_2 production- i.e. negative O_2 flux- in bottomwater) only in May 2014 & October 2012.

CHAPTER THREE: N_2 PRODUCTION PATHWAYS & N_2 FIXATION

In chapter 2, net N_2 production was treated as a single, uniform process. This chapter examines the relative importance of the primary pathways for N_2 production, anammox and denitrification, and the role of N_2 fixation as a sink for N_2 in GPB mud sediments. Estimates of N_2 fixation using the acetylene reduction method are used to address how gross N_2 production may deviate from measured net N_2 production and how the difference may vary seasonally.

3.1 PATHWAYS OF N_2 PRODUCTION

3.1.1 INTRODUCTION

The basic biogeochemistry of denitrification and anammox processes in marine sediments was described in chapter 1. The capacity of GPB sediments to produce N_2 by these pathways and the relative contribution of each one to total N_2 production was measured following a general approach for ^{15}N tracer amendments to sediment incubations designed by Thamdrup & Dalsgaard (2002) and modified by Koop-Jacobsen & Giblin (2009).

The purpose of these ^{15}N tracer experiments was to constrain the degree to which the anammox reaction contributes to N_2 production in GPB mud sediments. The investigation was not designed to address questions about environmental controls (e.g. temperature, rate of carbon remineralization) on the importance of each process.

3.1.2 METHODS

^{15}N tracer experiments.

(i) Incubations. Tracer experiments were carried out on sediment collected in November 2014, May 2015 and July 2015 (3 separate sets); protocols evolved during the course of this work as experience was gained in obtaining reasonable isotopic values.

Samples for ^{15}N incubations were removed from the upper 3 cm of GPB deposits in November 2014 and May 2015 and from the upper 2 cm in July 2015. Box-cores were collected by divers and stored in aerated containers of GPB seawater at *in-situ* temperatures for periods of two weeks or less. Prior

measurements of GPB sediment indicated the surficial zone of nitrate reduction occurs between 0.5- 1 cm although bio-irrigation can create pockets of enhanced nitrate concentrations at all depths, particularly the upper ~ 20 cm (Appendix 3.1 (a-f)).

Slurries were created by combining sediment and de-oxygenated GPB seawater in a N_2 chamber. Seawater was de-oxygenated by sparging with a N_2/CO_2 gas mix and was confirmed anoxic by Winkler titration. Slurries were mixed in sediment:anoxic seawater proportions given in Table 3.1, initially in Exetainers and in the last two incubation sets in July 2015 in 62 ml serum vials. In the third set of July 2015 incubations, sediments samples were weighed individually and mixed with anoxic seawater in a N_2 chamber. Previously, slurries were mixed and poured into incubation vessels. Slurries were subsequently sealed with no headspace and pre-incubated overnight at *in-situ* temperatures to remove any indigenous NO_3^- except in the case of the November 2014 experiments where slurries were not pre-incubated.

Isotopic tracers used were (1) Isotec $^{15}NH_4Cl$ 98+ atom % ^{15}N (39466-62-1) and (2) Isotec $K^{15}NO_3^-$ ^{15}N 98+ % ^{15}N (CAS 57654-83- 8). From the pre-incubated slurries, three parallel series were incubated with amendments as follows: (1) 300 µM $^{15}NH_4Cl$; (2) 300 µM $^{15}NH_4Cl$ plus 300 µM $^{unlabeled}NaNO3$ and (3) 300 µM $Na^{15}NO_3^-$ (Thamdrup & Dalsgaard 2002; Engstrom et al 2005). In order to confirm $^{29}N_2$ outcomes were not limited by available NH_4^+ in the $^{15}NO_3^-$ incubations, the final set of July 2015 experiments included incubations amended with 300 uM $Na^{15}NO_3^-$ and 300 uM unlabeled NH_4Cl. Amended slurries were agitated on a shaker table in a cold-room at *in-situ* temperatures over the course of the incubated periods which generally ran ~ 24 hours (the November 2014 incubations included a 41 hour time-point). Time-point values in early experiments were established by terminating the incubations with injections of $HgCl_2$ (Table 4.1). After injection of $HgCl_2$, samples were returned to the shaker table for at least 3 hours. Prior to measurement, samples were allowed to decant. Overlying water was then pumped thru the MiMS apparatus and measured on a quadrupole mass spec with its penning gage disconnected.

Subsequent to the first set of July 2015 incubations, ^{15}N tracers were added to slurries at planned intervals ahead of sample measurement thereby establishing incubated periods and obviating the need for use of a terminating biocide. 62 ml serum vials allowed separate (~ 4 g) sediment samples to be introduced directly rather than as a bulk slurry as was necessary using Exetainers. With these simple procedural improvements, significant linear regressions of isotopic products were obtained from all ^{15}N tracer experiments in the last July 2015 experiments.

(ii) Interpretation of results. Single $^{15}NH_4^+$ additions determine whether pre-incubated sediments contained oxidants (e.g., Mn_2-oxides) capable of oxidizing NH_4^+ to directly produce N_2 or whether coupled nitirification/

denitrification occurred. If N_2 was not produced, the parallel incubation (which is identical except for the addition of $^{unlabeled}NaNO_3^-$) isolates NO_3^- as the only oxidant of any N_2 produced. Amendments of $^{15}NH_4^+$ and $^{unlabeled}NO_3^-$ can produce not only $^{29}N_2$ but also $^{28}N_2$ (from added $^{14}NO_3^-$ & indigenous $^{14}NH_4^+$) by anammox and so can not quantify the extent of N_2 produced by anammox under natural conditions but only whether the process can occur in the sediments.

Quantification of anammox, denitrification and the relative contributions of each process to N_2 production was based on measurements of $^{29}N_2$ and $^{30}N_2$ after $^{15}NO_3^-$ additions to pre- incubated slurries. N_2 produced by anammox in incubations without added NH_4^+ was constrained by indigenous NH_4^+ concentrations and N_2 produced by denitrification was constrained by amended NO_3^- concentrations (pre-incubation eliminated indigenous NO_3^-). At amended levels, NO_3^- was not likely to limit anammox (NH_4^+ concentrations in porewater are << 300 uM); however, such excess NO_3^- concentrations produced N_2 levels which are 'potential' rather than an approximation of *in-situ* N_2 production. Relative rates of anammox and denitrification are assumed to be unaffected by the additions and to reflect *in-situ* proportions.

In each period, time-point values of $^{29}N_2$ and $^{30}N_2$ products in nmol g sed.$^{-1}$ were plotted against hours incubated; where regressions resulted in significant trends (p values < 0.05), rates of anammox and denitrification were calculated from the slopes of these trends and adjusted for tracer impurities according to equations in Koop- Jakobsen & Giblin (2009). Anammox as a percentage of total N_2 production (*ra%*) was calculated as the rate of $^{29}N_2$ production over the combined rates of $^{29}N_2$ & $^{30}N_2$ production. Rates of isotopic N production could not be calculated for the November 2014 & May 2015 incubations.

3.1.3 RESULTS

$^{29}N_2$ values did not show increasing trends in any incubations with single additions of $^{15}NH_4^+$ thereby confirming after pre-incubation sediment slurries contained nothing capable of producing N_2 by oxidizing NH_4^+ (Fig. 3.2 (a); Fig 3.3 (a); Fig 3.4 (a) & Fig. 3.5 (a)). Only in the third set of July 2015 incubations did a combined addition of $^{15}NH_4^+$ & unlabeled NO_3^- produce a significantly increasing trend in $^{29}N_2$; more frequently, these incubations showed $^{29}N_2$ values which varied around a mean (Fig. 3.1 (a); Fig. 3.2 (a); Fig 3.3 (a); Fig 3.4 (a) & Fig. 3.5 (a)). $^{15}NO_3^-$ amended incubations showed large increases in $^{30}N_2$ and no or small increases in $^{29}N_2$ indicating denitrification but little anammox (Fig. 3.1 (b); Fig. 3.2 (b); Fig 3.3 (b); Fig 3.4 (b) & Fig. 3.5 (b)). The relative contribution of anammox to total N_2 production (*ra%)* was consistently below 10% in all incubations measured (Table 3.1).

In all 3 sets of July incubations, $^{30}N_2$ values showed increases in trend over the period incubated; $^{29}N_2$ values show either no or only slowly increasing

trends. All regression of $^{29}N_2$ & $^{30}N_2$ products in $^{15}NO_3^-$ amended incubations were significant; statistical output from regression analysis is shown in captions of individual charts. In the first 2 sets of incubations, sediments were slurried in bulk and poured into incubation vessels; after incubation and measurement, samples were dried and weighed. While the procedure was intended to provide (with constant stirring) uniform sediment: aqueous volume mixes in each sample, dried sediment weights varied more than expected (coefficient of variation ~ 18% in set 1) and showed several outliers in set 2. Normalizing isotopic product values by these dry weights improved the R^2 values of the N_2 production regressions of $^{30}N_2$ in the $^{15}NO_3^-$ amended incubations where N_2 production was clearly a function of sediment quantity. For $^{29}N_2$ values where there were no significant trends over the incubation periods, normalizing these values showed little or no improvement in regression fit and in one case increased volatility. The contrast in these outcomes underscores how $^{30}N_2$ values were clearly related to sediment quantity while the $^{29}N_2$ values were not. For the first and second set of July incubations, regressions of isotopic N product values for $^{15}NO_3^-$ additions are shown normalized to dry sediment weight and $^{29}N_2$ values for $^{15}NH_4^+$ and $^{15}NH_4^+$ & unlabeled NO_3 are shown in nmol ml^{-1} (Fig. 3.2 & Fig. 3.3).

To investigate whether NH_4^+ limitation could inhibit $^{29}N_2$ growth, an additional incubation set was carried out in July 2015 with combined additions of 300 µM $^{15}NO_3^-$ and 300 µM unlabeled NH_4^+. As reflected in figure 3.1 (c), results of this experiment showed close agreement with results from $^{15}NO_3^-$ only additions. This comparison provides strong evidence the low anammox rates were not affected by NH_4^+ limitation. As sediment was weighed and added to slurry vials individually in these incubations, there were no notable differences in regression outcomes whether expressed in molar amounts or normalized to sediment weight. Consequently, all regressions are shown only normalized to wet weight of sediment slurried.

Results obtained from November 2014 and May 2105 incubations were compromised by several procedural missteps. First, injection of ~ 20 uL of $HgCl_2$ in slurries (1.25 g wet sediment:12.6 ml Exetainers) appeared to fail to completely stop N_2 production in the May 2015 $^{15}NO_3^-$ incubations; i.e., the first two incubation values are close to average values for the entire incubation. Whether time-points were effectively established in the November 2014 incubations is uncertain.

Second, as with the first 2 sets of incubations in July 2015 samples for each incubation were slurried in bulk and siphoned into Exetainers. Unlike the July samples, actual sediment weights in individual slurries were not measured and may have varied from sample to sample. So $^{29}N_2$ and $^{30}N_2$ values from November incubations could not be normalized to sediment weight and apparent trajectories in $^{29}N_2$ and $^{30}N_2$ values in the first several time-points could reflect smaller sediment additions relative to samples used in later time-points.

Last, in contrast to the July $^{15}NO_3^-$ amended incubations which show linearly increasing $^{30}N_2$ throughout the incubation period, it is not clear from the isotopic product values whether NO_3^- was limiting in the November 2014 and May 2015 incubations. Isotopic product values reached an average value early on in these earlier incubations and thereafter showed no increase in trend. It is unlikely in these earlier experiments, the 300 µM NO3- was consumed by N2 production[2]. However, the absence of a continuous increase in $^{30}N_2$ in these incubations suggests a competing NO_3^- consumption reaction occurred. DNRA has the same delta free energy (ΔG^{of} = 358 kJ mol^{-1}) as anammox and only slightly less than the value for denitrification (Thamdrup 2012). Consequently, in the anoxic slurries DNRA could have consumed NO_3^- so as to limit gains in isotope product values in the November 2014 and May 2015 incubations. In the July experiments, the ratio of sediment: slurry volume was reduced and judging from the linear increases in isotopic products, NO_3^- was not limiting.

Because of the level of uncertainty as to the correct interpretation of results from November 2014 and May 2015 results, production rates were not quantified. However, graphs of the isotopic product values suggest rates of $^{29}N_2$ production were low relative to $^{30}N_2$ production (Fig. 4.1.4 (b) & Fig. 4.1.5 (b)).

[2] The highest N_2 production rate measured in any of these ^{15}N addition experiments was 0.56 nmol ml^{-1} hr^{-1}. Assuming a rate of 1 nmol ml^{-1} hr^{-1} (i.e., almost double the highest measured rate), the 300 uM NO_3^- additions would have lasted for 150 hours in a 12.6 ml Exetainer if only N_2 production was consuming it. As the incubations lasted at most 41 hours, N additions should have been sufficient in the absence of any other NO_3^- consuming processes in the slurries.

3.1.4 DISCUSSION

The results of all ^{15}N tracer addition experiments reflect a low contribution of anammox and a dominant role of dentrification in N_2 production. These results confirm expectations based on a number of field studies investigating the relative importance of anammox to N_2 production over the last 13 years. The list below illustrates the similarity of results reported for similar estuaries:

Study	**Research Area**	***ra%***
Brin, Giblin & Rich (2014)	Narragansett Bay	0- 4 %
Engstrom et al (2005)	Long Island Sound	4- 7 %
Nicholls & Trimmer (2009)	9 So. East English est.	1- 11 %
Risgaard-Petersen et al (2004)	Randers Fjord	5- 24 %
Risgaard-Petersen et al (2004)	Norsminde Fjord	0 %
This study	Great Peconic Bay	2- 9 %

3.1.5 TABLES & FIGURES: N_2 PRODUCTION PATHWAYS

Table 3.1 $^{15}N\text{-}NO_3^-$ Tracer Experiments Summary

				^{15}N-NO3- additions		
	Slurry mix Sed/total vol	time-point set by	Units	r (29N2) (p- value)	r (30N2) (p- value)	*ra%*
Nov 2014	3.33 g/12.6 ml Exetainer	20 uL HgCl2		Not Calc	Not Calc	Not Calc
May 2015	1.25 g/12.6 ml Exetainer	20 uL HgCl2		Not Calc	Not Calc	Not Calc
July 2015 (a)	1 g/12.6 ml Exetainer	100 uL HgCl2	nmol/ml-hr	.025 (.18)	.555 (.03)	4.3%
July 2015 (a)	1 g/12.6 ml Exetainer	100 uL HgCl2	nmol/g w sed hr			
July 2015 (b)	3.9 g/62 ml serum vial	Incubated hrs sequenced	nmol/ml	.010 (0.10)	.247 (<.01)	3.6%
July 2015 (b)	3.9 g/62 ml serum vial	Incubated hrs sequenced	nmol/g- w sed hr	1.62 (0.80)	17.4 (<.001)	3.6%
July 2015 (c)	3.9 g/62 ml serum vial	Incubated hrs sequenced	nmol/g- w sed hr	.420 (<.02)	6.33 (<.001)	6.2%
				^{15}N-NO3- & unlabeled NH_4^+		
July 2015 (c)	3.9 g/62 ml serum vial	Incubated hrs sequenced	nmol/g- w sed hr	0.351 (< .01)	6.02 (<.001)	5.5%

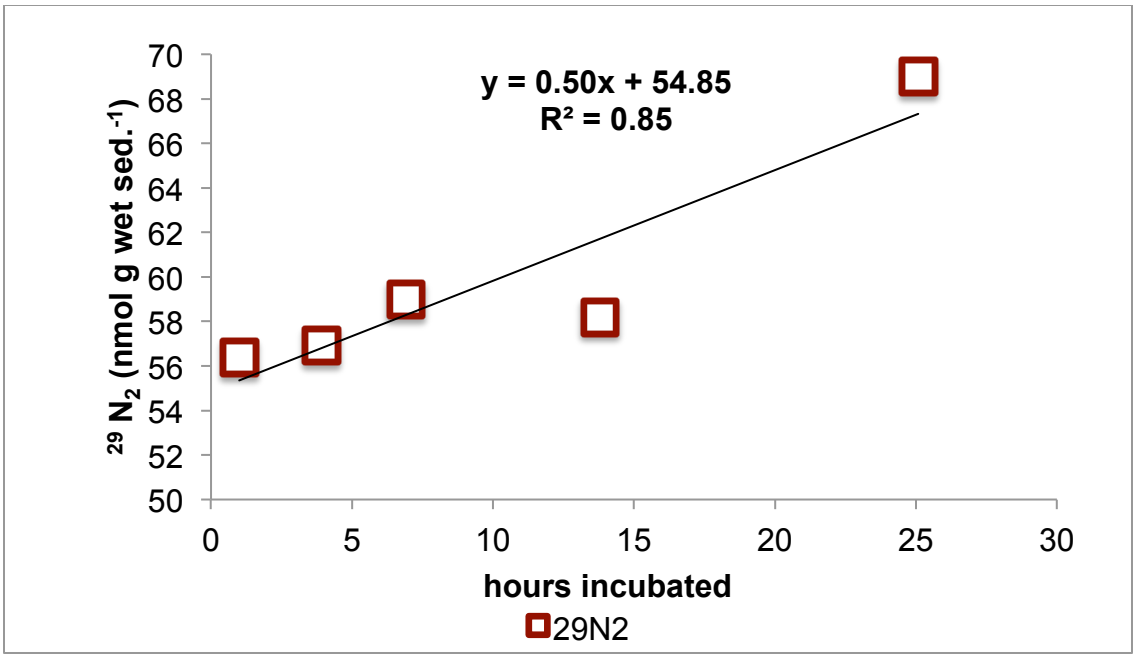
y = 0.50x + 54.85
R² = 0.85
29 N2 (nmol g wet sed.-1)
hours incubated
29N2

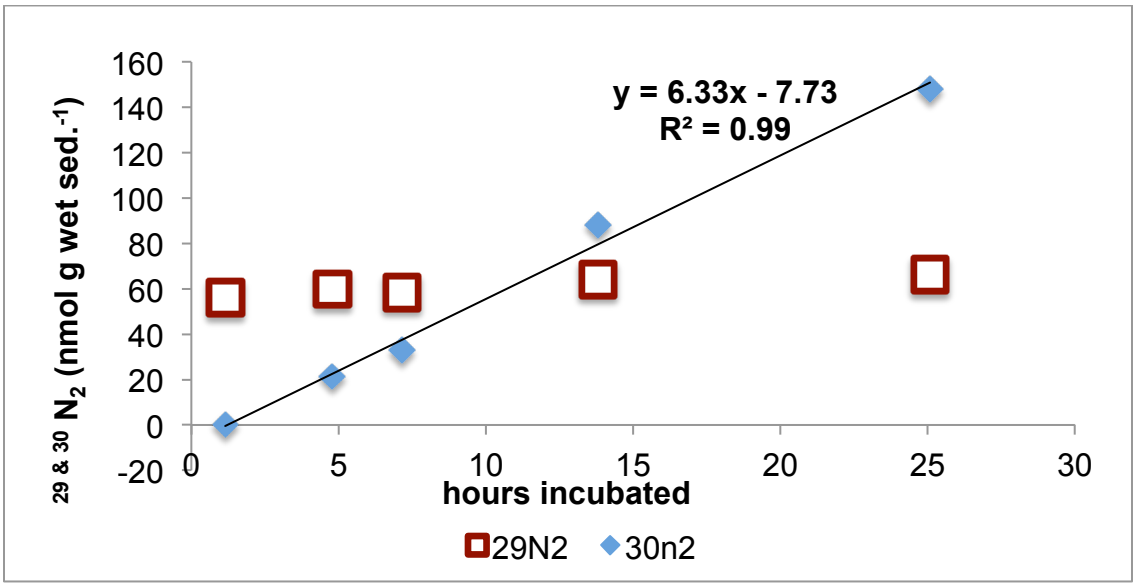
y = 6.33x - 7.73
R² = 0.99
29 & 30 N2 (nmol g wet sed.-1)
hours incubated
29N2
30n2

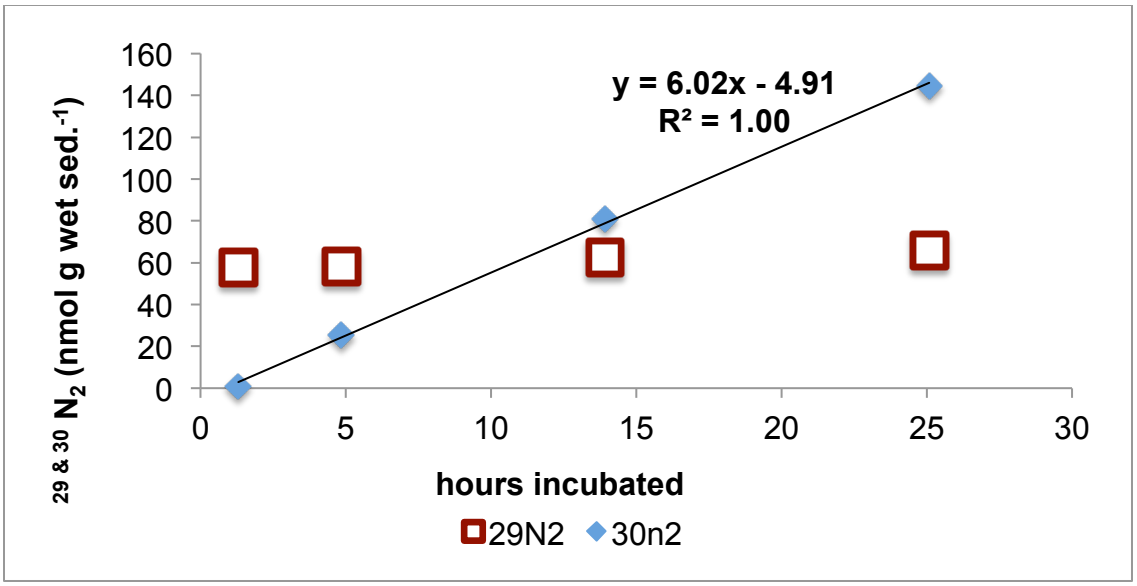

Figure 3.1 July 2015 third set of ^{15}N tracer experiments. (a) Trend in ^{29}N-N_2 w/ addition of 300 uM $^{15}NH_4^+$ & 300uM unlabeled NO_3^- (F- stat= 16.4, df=3 & p-value= .027); (b) Trend in ^{29}N- N_2 & ^{30}N-N_2 with addition of 300 uM ^{15}N-NO_3^- (F- stat= 406, df=3 & p-value < .001) and (c) Trend in ^{29}N- N_2 & ^{30}N-N_2 with addition of 300 uM $^{15}NO_3^-$ & 300 uM unlabeled NH_4^+ (F- stat= 1999, df=2 & p-value < .001). In all cases, ~ 3.9 g wet sediment were incubated in 62 ml serum vials; no biocide was necessary as samples were measured at incubation time-points. Charts show isotopic products normalized to grams wet sediment weighed in each incubation vial. Normalizing isotopic products to wet sediment weights instead of molar amounts measured does not change *ra%* nor significance of regressions. Additional NH_4^+ does not change the measured isotopic products from the incubation versus singly amended $^{15}NO_3^-$ indicating the incubation was not constrained by indigenous NH_4^+.

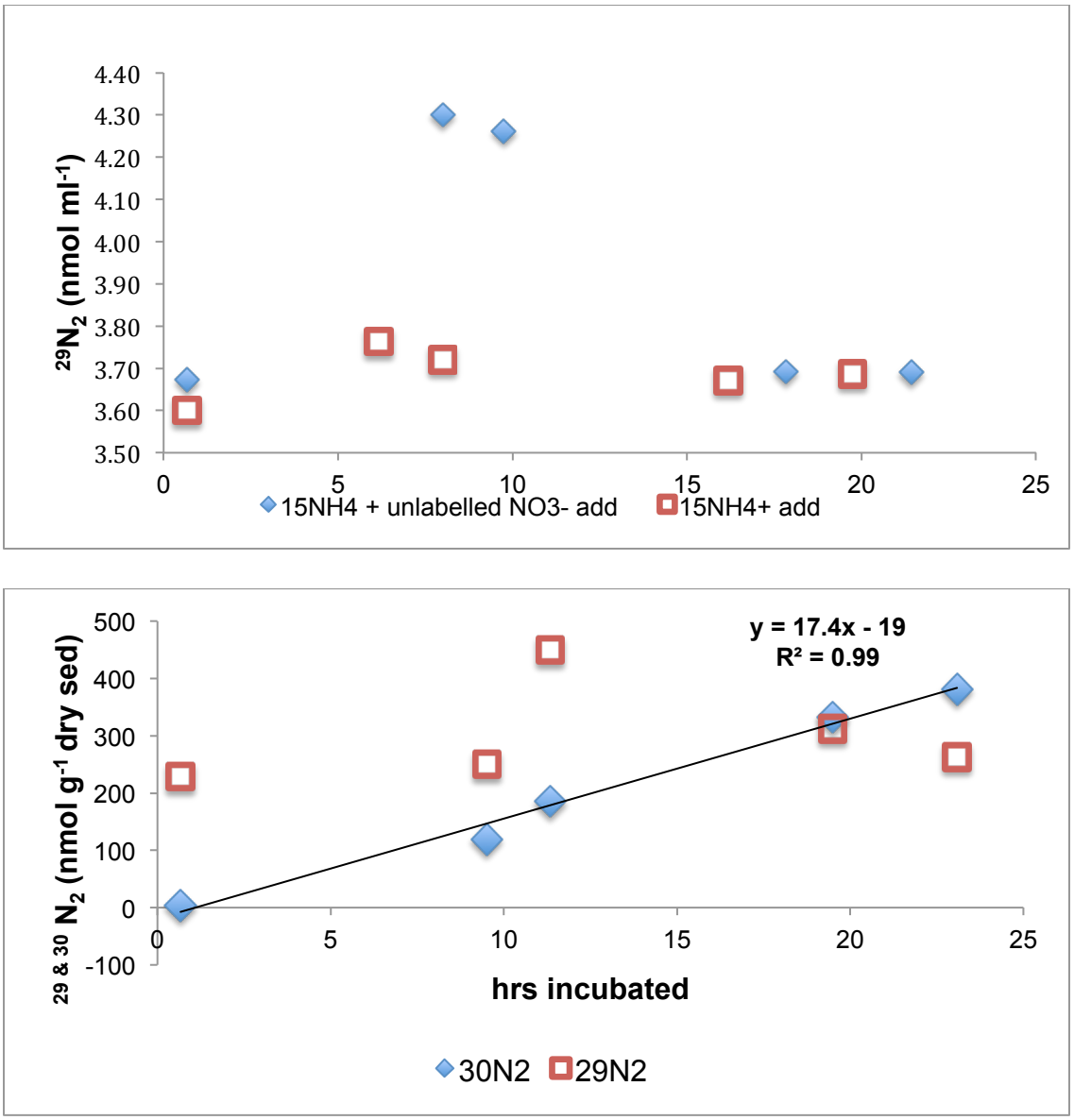

Figure 3.2 JULY 2015 second set of ^{15}N tracer experiments. (a) Trend in ^{29}N- N_2 w/ addition of (1) 300 uM $^{15}NH_4^+$ & (2) 300 uM $^{15}NH_4^+$& 300uM unlabeled NO_3^-; (b) Trend in ^{29}N- N_2 & ^{30}N-N_2 with addition of 300 uM ^{15}N-NO_3^- (F-stat= 269, df= 3 & p- value < .001). Incubations w/ 3.9 g wet sediment in 62 ml serum vials; no biocide was necessary as samples were measured at incubation time-points. Charts show isotopic products both in molar amounts measured for $^{15}NH_4^+$ additions and normalized to grams dry sediment for $^{15}NO_3^-$.

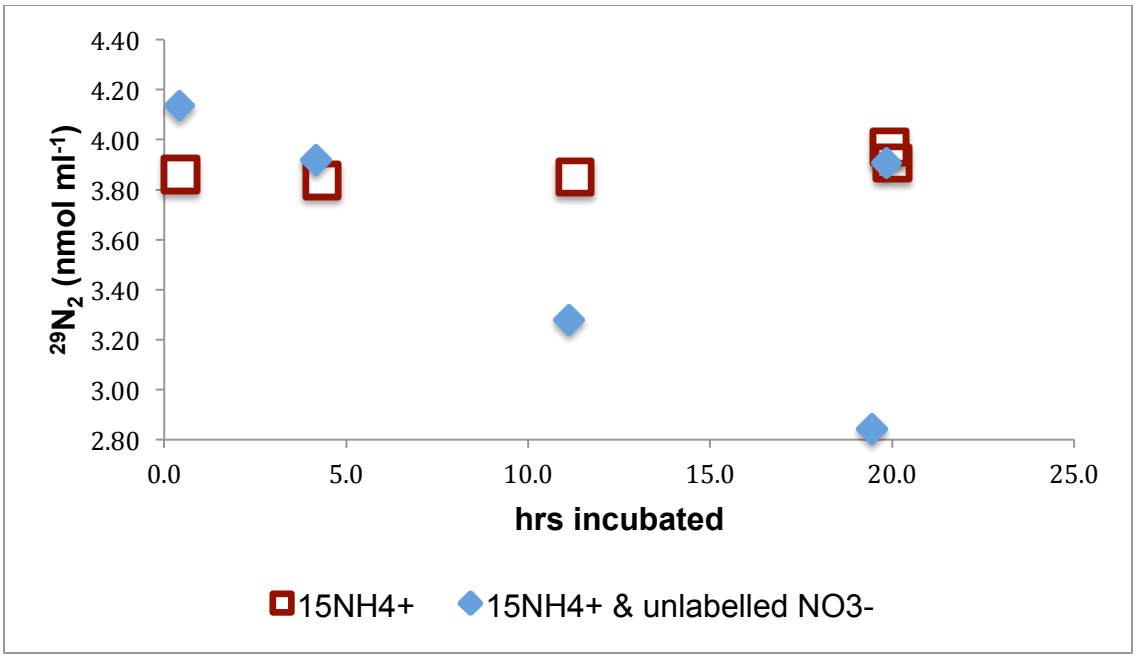

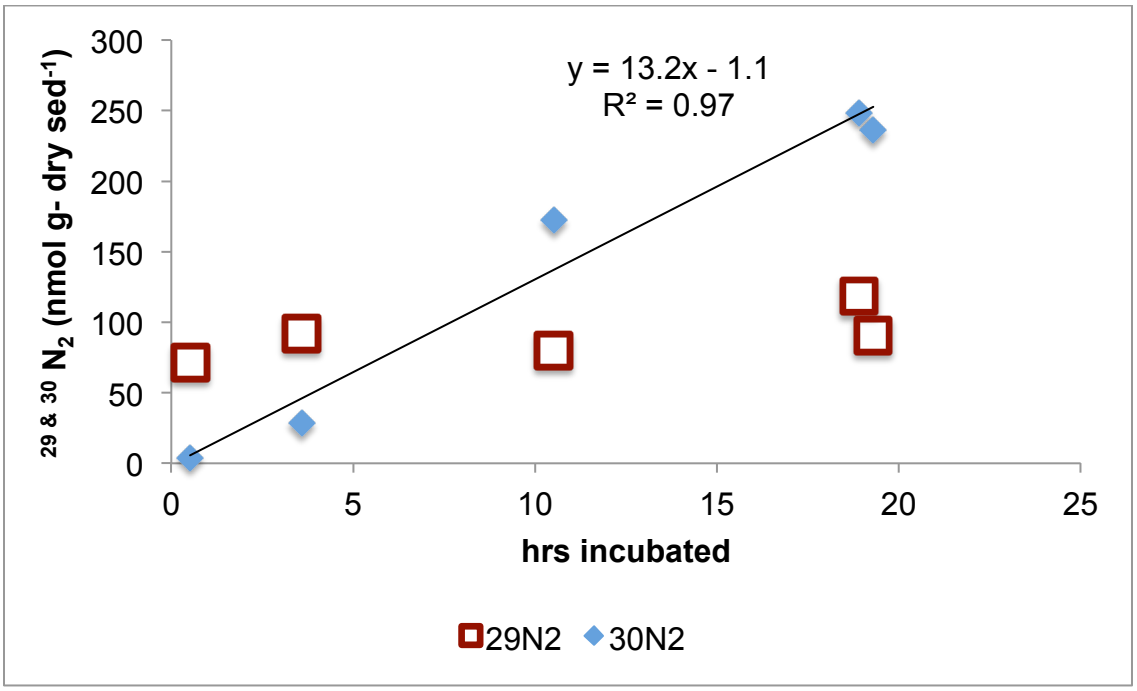

Figure 3.3 JULY 2015 first set of ^{15}N tracer experiments. (a) Trend in ^{29}N-N_2 w/ addition of (1) 300 uM $^{15}NH_4^+$ & (2) 300 uM $^{15}NH_4^+$& 300uM unlabeled NO_3^-; (b) Trend in ^{29}N- N_2 & ^{30}N-N_2 with addition of 300 uM ^{15}N- NO_3^- (F-stat 83.7, df=3 & p-value= .003). ^{15}N additions to sediment slurries in Exetainers (1 g /12.6 ml); each time-point established by addition of 100 uL of $HgCl_2$.

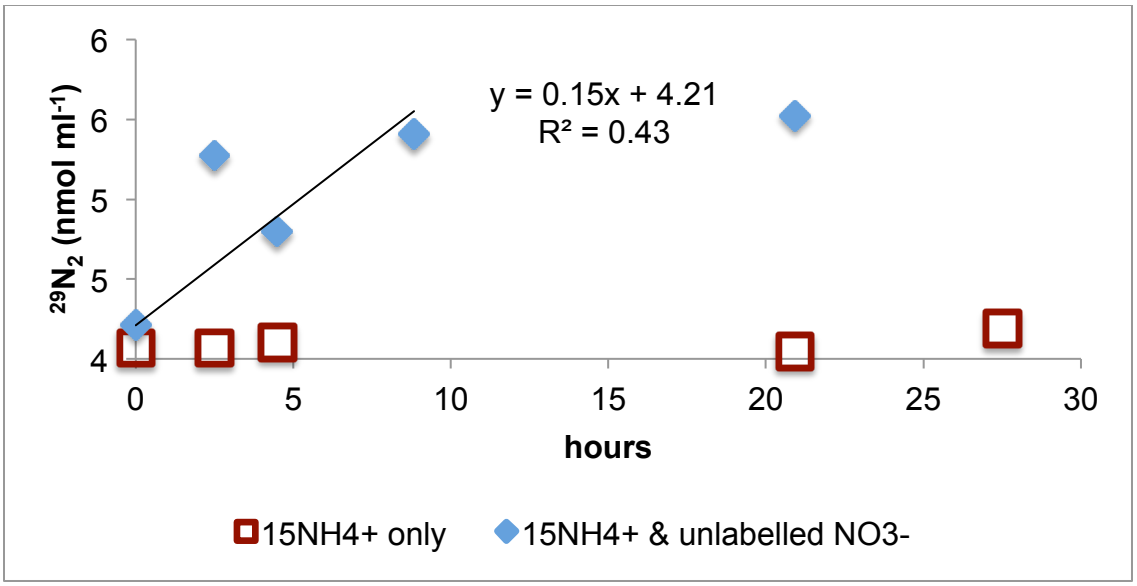

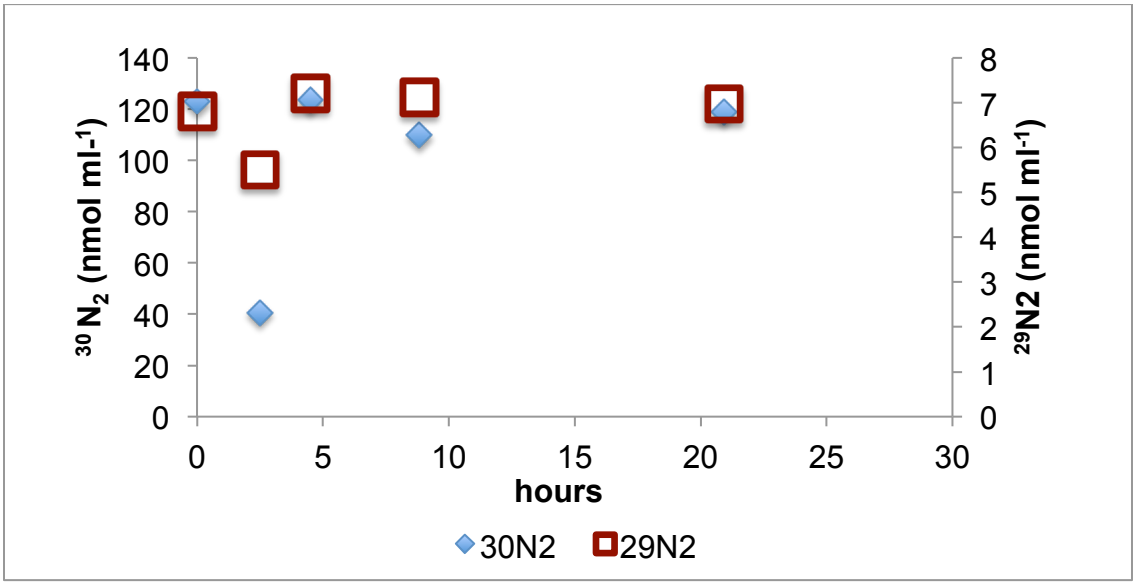

Figure 3.4 MAY 2015 ^{15}N Tracer experiments. (a) Trend in ^{29}N- N_2 w/ addition of (1) 300 uM $^{15}NH_4^+$ & (2) 300 uM $^{15}NH_4^+$& 300uM unlabeled NO_3^-; (b) Trend in ^{29}N- N_2 & ^{30}N-N_2 with addition of 300 uM ^{15}N- NO_3^-. ^{15}N additions to sediment slurries in Exetainers (1.25 g /12.6 ml); each time-point established by addition of 20 uL of $HgCl_2$.

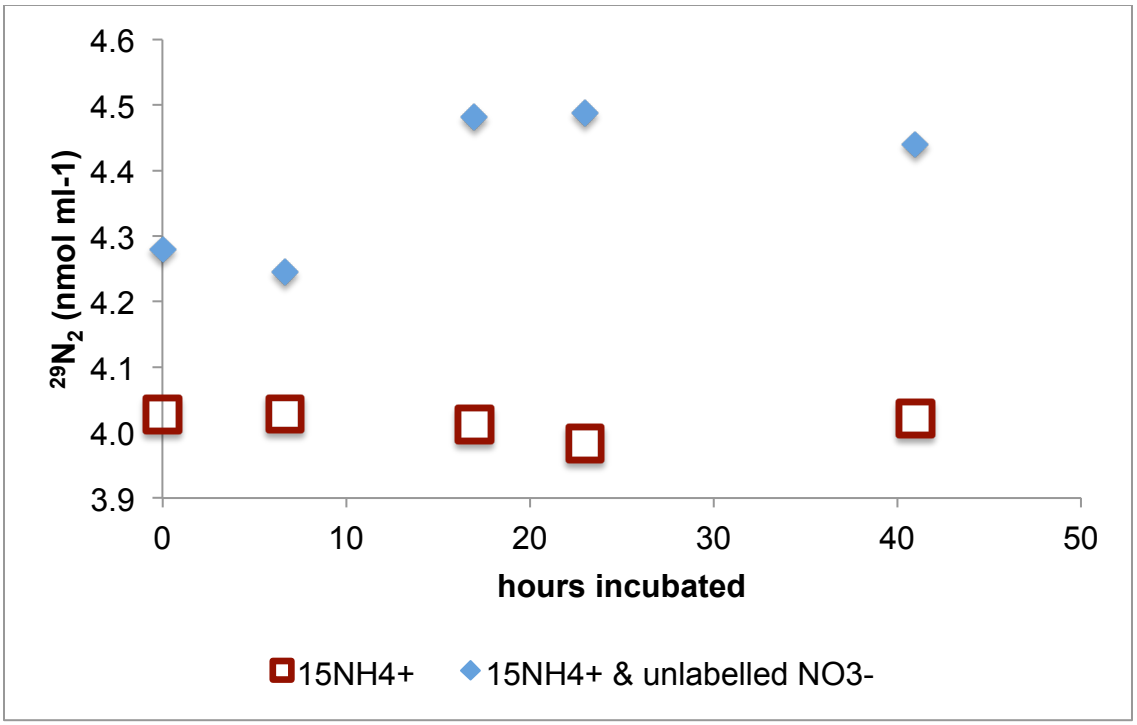

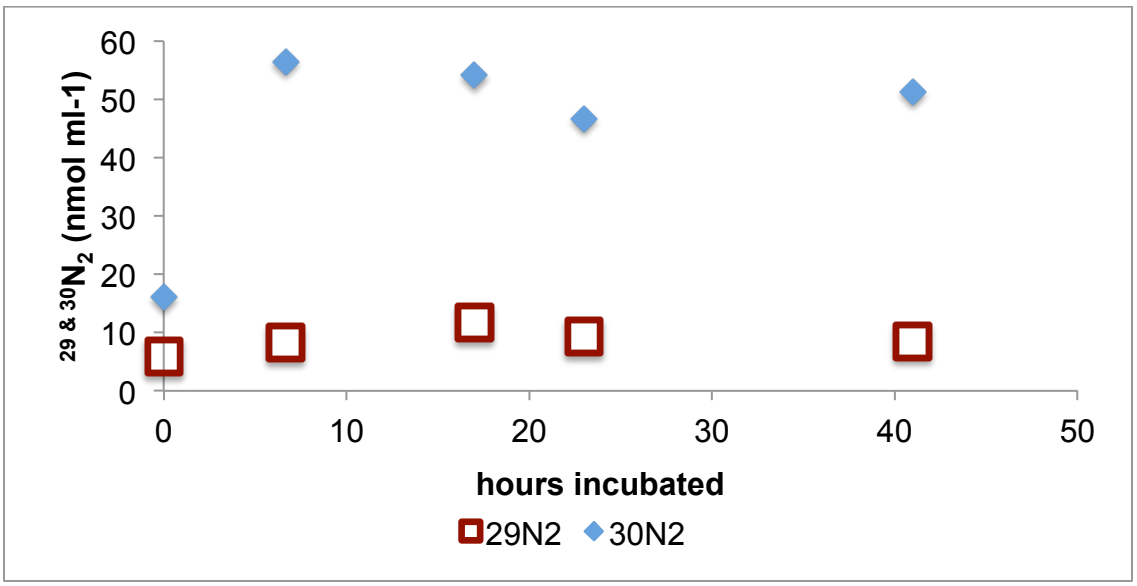

Figure 3.5 NOVEMBER 2014 ^{15}N tracer experiments. ^{1}(a) Trend in ^{29}N- N_2 w/ addition of (1) 300 uM $^{15}NH_4^+$ & (2) 300 uM $^{15}NH_4^+$& 300uM unlabeled NO_3^-; (b) Trend in ^{29}N- N_2 & ^{30}N-N_2 with addition of 300 uM ^{15}N- NO_3. ^{-15}N additions to sediment slurries in Exetainers (3.33 g /12.6 ml); each time-point established by addition of 20 uL of $HgCl_2$.

3.2 N_2 FIXATION

3.2.1 INTRODUCTION

Rates of N_2 fixation in non-vegetated sediments are generally low relative to rates reported for rhizospheres in sea grass meadows and salt marshes; (Howarth et al 1988 (a); McGlathery et al (1998); Welsh et al (1996); & Currin et al (1996)); in microbial mats (Herbert (1999)) and in burrows of thalassinidean shrimp (Bertics et al (2010)) (Table 4.2.1). For instance, McGlathery et al (1998) reported N_2 fixation rates 3 times higher in eelgrass rhizosphere than in nearby un-vegetated sediment; Currin et al (1996) reported N_2 fixation rates in *Spartina* marsh sediments exceeded rates in nearby un-vegetated sediments by 5- 10 times. A compilation of reported rates for un-vegetated estuarine sediments from 8 studies ranged from 0 to 0.127 m^{-2} d^{-1} (Herbert (1999); Bertics (2013) reported N_2 fixation rates for the upper 18 cm of sediment in seasonally hypoxic Eckernforde Bay ranging from 0.08 mmol m^{-2} d^{-1} to .22 mmol m^{-2} d^{-1} (Table 3.2).

While GPB sediments are populated with *S. empusa* which forms burrows similar to those described by Bertics et al (2010) and while microbial mats where observed in one spring sediment sampling, the objective here was to investigate the extent to which N_2 fixation may have reduced gross N_2 production in measurements of net N_2 flux rates in bulk sediments made with a membrane inlet mass spectrometer (MiMS). N_2 fixation was not directly measured in burrows of *S. empusa* or in sediments colonized with microbial mats. In the case of *S. empusa* burrows, burrow lumen water showed excess N_2 above bottom water during all seasons indicating no net N_2 fixation associated with deep tier bioturbation (Chapter 5).

3.2.2 METHODS

Acetylene reduction assays

In benthic estuarine environments, N_2 fixation could occur on the sediment-water interface or in the sediments. In GPB, the sediment surface is oxic while deeper sediments are characterized by redox gradients which occur vertically with depth and chaotically within microcosms created by infaunal activity. The gradients reflect oxic to anoxic conditions. Additionally, biological processes at the sediment-water interface could be influenced by variation in light.

To obtain an indication of benthic N_2 fixation in GPB sediments, acetylene reduction assays (ARAs) were carried out in November 2014 and May 2015. The procedures rely on the preference of the nitrogenase enzyme for C_2H_2 over N_2 and follow methods adopted from Capone (1993).

(i) Incubations. Incubations of intact sediment cores under appropriate light conditions would offer the most representative estimates of *in-situ* N_2 fixation. However, such incubations would not distinguish between sources of N_2 fixation; additionally, the approach poses considerably practical problems in achieving diffusion of C_2H_2 into intact sediment cores. Consequently, incubations were carried out using sediment slurries under different environmental conditions. To assess the influence of light and oxygen on N_2 fixation on the sediment:water interface, ARAs were carried out on samples from the upper 0.5 cm sediment interval in oxic light and dark conditions and anoxic dark conditions as well as on samples from the 0.5- 3 cm sediment interval in anoxic conditions. In addition to sediment incubations described above, controls (no C_2H_2 addition to sediment slurries) were incubated under oxic conditions for upper 0.5 cm interval GPB sediments and under anoxic conditions for the 0.5- 3 cm interval (May 2015 only). Additional ARAs were carried out on GPB seawater collected in May 2015 in both light and dark conditions.

May 2015 experiments. Sediment slurries were mixed in bulk on the basis of 96.5 g homogenized wet weight sediment (~ 70 ml): 145 ml GPB seawater and poured into 244 ml serum vials. The slurries were continually stirred in a beaker prior to pouring to achieve a homogenous sediment:water mix in the sample vials. Based on variations in measurements of dry sediment weights of slurries mixed in a similar way for ^{15}N additions (see prior section in this chapter), the mixing method may not have achieved a thoroughly homogenous mix among all ARA slurries. The slurry volumes left headspace of 29 ml in each vial thereby resulting in a gas: aqueous phase ratio of 0.12 using a porosity estimate of 0.8 to calculate dry sediment volume. For anoxic incubations, slurries were mixed in an N_2 chamber w/ de-oxygenated water created by sparging with a N_2/CO_2 gas mix (~.9995/.0005); de-oxygenation was confirmed anoxic by Winkler titration.

C_2H_2 was prepared from calcium carbide according to Postgate (1982) and kept in Tedlar gas bags. 2 ml of C_2H_2 was injected into the headspace (29 ml) of each slurry and the septa of each serum vial was subsequently briefly vented to the atmosphere with a narrow bore needle to equilibrate headspace pressure to 1 atm.

Because of the inhibitory or perverse effects of C_2H_2 on sediment metabolism (Capone 1993), durations of the assays were kept under 8 hours. Measurement samples were taken 5 times at roughly 2 hour intervals. All incubations were carried out at *in-situ* temperatures. Light incubations in May 2015 were carried out in a water-bath kept under a shady tree during the afternoon/evening and shaken frequently. The ambient light in this space was considered approximate to but not lower than ambient light conditions at 6.5 meter depth on the day of sediment retrieval based on impressions of the

diver/analyst. All other incubated samples were kept on a shaker table in the dark in a temperature controlled room.

Incubation time-points were established by injecting 500 uL of N_2 gas into the vial headspace and withdrawing 500 uL of sample gas by a glass air-tight syringe. The sample was then injected to a GC (HP 5890 Series II) with flame-ionization detection coupled with a Porapak R column (T = 90° C; pressure = 22 psi) using N_2 as a carrier gas. The C_2H_4 signal recorded was area under the curve C_2H_4 and C_2H_2 peaks were almost completely separated.

C_2H_4 standards were prepared by dilutions in septum vials of 1% ethylene mixture (Scotty's transportable 14L cylinder). Standard gas concentrations were calculated from the ideal gas law (i.e., PPMv * 22.41L/mol = mols injected). GC measurements consistently produced linear curves with tight fits ($R^2 > 0.98$) but standard values changed from day- to- day likely due to instrument variation (M.Scraton pers. comm) and slight differences in C_2H_4 gas standards which were prepared each measurement day. Temperature, pressure and flow rate settings were not altered within measurement periods but the GC was shut down between November 2014 and May 2015 and pressure settings between these periods were slightly different. Samples were valued based on a single standard curve for each of the 2 incubation periods. Accurate measurement of standards requires gas sample preparation and dilution skills which are not trivial. Single standard curves avoiding use of standard values which may have resulted from processing artifacts. Chart 4.4 shows standard curves used to value November 2014 and May 2015 samples together with alternate curves. In each period, curves were chosen from alternatives based on which one produced the highest trend in C_2H_4 as the purpose of the measurements was to investigate whether N_2 fixation could occur in the sediments. In the May 2015 data, using an alternate curve could have lowered the overall gain in C_2H_4 by a maximum of 30%. An alternate standard curve measured in November 2014 could have reduced gains in C_2H_4 by a multiple of 4; however, this curve was rejected as an artifact of processing error.

Sample molar C_2H_4 concentrations in the gas phase were estimated based on a linear regression of standard concentrations and adjusted to total (aqueous and gas phases) based on Capone (1993):

$[C_2H_4]$ sample (nmol/ml) (gas phase) * gas phase volume * SC

where SC = 1 + (α * aqueous volume/gas volume) &
α = Bunsen coeff (Breitbarth et al 2004).

Total C_2H_4 values in nmols were then normalized to wet sediment sample volumes.

November 2015 experiments. These experiments were based on similar principles to the May 2015 experiments. The primary differences were in (1) the way incubations were terminated and (2) the ratios of sediment: seawater and of gas: aqueous phase used. Anoxic slurries were carried out in 43 ml amber vials with silicon septa based on a wet weight sediment: GPB seawater mix of 13g: 17 ml leaving gas:aqueous phase ratio at ~ 0.28. Oxic slurries were carried out in 62 ml serum vials with rubber septa and based on a wet weight sediment: GPB seawater mix of 195.5g: 470 ml (i.e., 0.3 v/v mix) leaving a gas:aqueous phase ratio of ~ 0.19. In all of these earlier incubations, time-point values were established by with additions of $HgCl_2$ (60 uL per 43 ml vial in anoxic incubations and 80 uL per 62 ml vial in oxic incubations) and stored until measurement. Oxic light incubations were carried out in a temperature controlled room with lamps set to approximate average ambient *in-situ* light.

(ii) Conversion of C_2H_4 production to N_2 fixation. N_2 fixation was converted at a C_2H_4: N_2 ratio of 3:1 (Capone 1993).

(iii) Statistical analysis. In each period, time-point values in nmol cm^{-3} wet sediment were plotted against hours incubated and significant ($\alpha < .05$) C_2H_4 trends were compared in single- factor ANOVAs. Mans of data-sets with significant outcomes were subsequently compared for differences using a Tukey multiple comparison test.

3.2.3 RESULTS

(i) May 2015 incubations. C_2H_4 increases over the duration of all May 2015 incubations were linear (p values < 0.05) (Fig. 4.2.1 (a)). Variation among triplicates was also low. C_2H_4 production rates in the upper 0.5 cm sediment interval ranged between 0.063 – 0.113 nmols cm^{-3} wet sed. hr^{-1} depending on ambient light and oxygen conditions. Neither controls (sediment incubated with no C_2H_2 addition) nor seawater incubated in light and dark conditions produced C_2H_4 (Fig. 4.2.1 (b)).

Results of the Tukey multiple comparison test (Table 4.2) indicate C_2H_4 production in sediment from the 0.5- 3 cm depth interval was significantly (α = .05) higher than C_2H_4 production in sediment from the upper 0.5 cm depth interval except in the case of the oxic light incubation. C_2H_4 production in sediment from the upper 0.5 cm depth in oxic, light conditions was also significantly different than it was in anoxic, dark conditions although this difference resulted from only one outlying replicate measurement which may have arisen from analytical error.

To calculate an integrated C_2H_4 production rate over the upper 3 cm of sediment the average of oxic dark and light rates over the upper 0.5 cm was combined with the average rate from the 0.5- 3 cm depth interval. This C_2H_4

production rate was 0.31 nmol cm^{-2} hr^{-1} which is equivalent to ~ 0.075 mmol m^{-2} d^{-1}. Converting C_2H_4 values to N_2 values at a 3:1 ratio (Capone 1983) results in a N_2 fixation estimate of 25 umol m^{-2} d^{-1}. This rate should be regarded as a minimum as ARAs were not carried out on sediment at lower depth intervals.

(ii) November 2014 Incubations. Only 4 time-points were recorded for November 2014 incubations and for the anoxic 0.5 cm incubation the sample at one time-point value was destroyed. Only the oxic, dark ARA of the upper 0.5 cm sediments reflected a significant trend at the $\alpha = 0.05$ level although the anoxic upper 0.5 cm sediment interval reflected a significant trend at the $\alpha = 0.10$ level with only 3 data-points. The other incubations showed either no change (oxic, light in upper 0.5 cm sediment) or erratic values (anoxic 0.5- 3 cm sediment interval); data from these later incubations was excluded from further analysis. Consequently, C_2H_4 production in the upper 0.5 cm of sediments collected in November 2014 ranged from 0.068 nmol cm^{-3} wet sed. hr^{-1} in oxic, dark conditions to 0.179 nmol cm^{-3} wet sed. hr^{-1} in anoxic, dark conditions. Since these ARAs were not carried out in triplicate, the significance of the difference in these outcomes could not be assessed. A control (sediment under oxic conditions with no C_2H_2 addition) produced no C_2H_4.

Because of the erratic values measured in the 0.5- 3 cm sediment interval, C_2H_4 production rates could only be integrated for the upper 0.5 cm depth interval. Converting C_2H_4 values to N_2 as above produces a range of N_2 fixation rates from ~ 3 – 7 umol m^{-2} d^{-1} for this interval. The lack of a coherent trend in C_2H_4 values from the 0.5- 3 cm interval may be explained by analytical error in sample processing as these samples were among the first measured by ARA protocols which involve maintaining gases at a constant atmospheric pressure. Also the November 2014 incubations were also not run in triplicate.

3.3.4 DISCUSSION

May 2015 incubations with C_2H_2 additions demonstrate GPB sediments have the capacity to produce C_2H_4. The estimated N_2 fixation rate of 25 umol m^{-2} d^{-1} based on a 3:1 C_2H_4: N_2 conversion of measured C_2H_4 production represents ~ 10% of measured net N_2 production of sediments collected in May 2015. Gross N_2 production adjusted for N_2 fixation increases from 247 umol m^{-2} d^{-1} to 272 umol m^{-2} d^{-1}. The applicability of the assumed 3:1 C_2H_4: N_2 conversion ratio was not independently confirmed by isotopic measurements. Assuming the conversion ratio is appropriate, the N_2 fixation rate should be regarded as a minimum estimate because ARAs were not carried out at deeper sediment depth intervals than 3 cm. The depth of sediment in sub-cores used for flux measurements varied between 15 - 18 cm. If the estimated N_2 fixation rate was integrated over a 15 cm interval, N_2 fixation would represent 128 umol m^{-2} d^{-1} or ~ 52% of net N_2 production measured in sediments collected in May 2015. In this scenario, gross N_2 production would have risen from 247 umol m^{-2} d^{-1} (without

adjustment for N_2 fixation) to 375 umol m^{-2} d^{-1}. Sedimentary N_2 flux would still represent an N sink term. The use of a constant N_2 fixation rate for a depth interval from 0.5 cm to 15 cm is supported by the reports of nearly constant nitrogenase activity at similar depth intervals in non-vegetated sediments (e.g., McGlathery et al 1998).

C_2H_4 production rates measured in the upper 0.5 cm of sediment collected in November 2014 were similar to those measured from sediment collected in May 2015.. These measured N_2 fixation rates are also not dissimilar to those for non-vegetated sediments reported in published research (Table 4.2.1) (e.g., McGlathery et al (1998); Herbert (1999); Bertics et al (2013)). The measured May 2015 net N_2 flux rate (.25 mmol m^{-2} d^{-1}) was low relative to the measured average annualized net N_2 flux rate (.55 mmol m^{-2} d^{-1}) and compared with average summer and fall seasonal net N_2 flux rate (.82 mmol m^{-2} d^{-1}). Estimated N_2 fixation integrated to 15 cm sediment depth for May 2015 represents ~ 23% and ~ 16% of these net production rates.

As no significant differences were found between C_2H_4 production rates in light and dark oxic incubations and because no C_2H_4 production was measured in ARAs of GPB seawater, it seems unlikely the measured C_2H_4 production was fixed by cyanobacteria.

3.2.5 TABLES & FIGURES: N_2 FIXATION

Table 3.2 Comparison of estimates of N_2 fixation rates in this study with published estimates of benthic N_2 fixation rates

		N_2 fixation	Depth integrated	Reference:
Area	Sediment type	mmol m^{-2} d^{-1}	cm	
Eckernforde	unvegetated	0.08- 0.22	0- 18	Bertics et al (2013)
GPB mud	unvegetated	0.025	0- 3 (msd)	This study
GPB mud	unvegetated	0.153	0- 18 (est.)	This study
compilation	unvegetated	0- 0.13	NR	Herbert (1999)
compilation	cyano mats	0.16- 15	NR	Herbert (1999)
compilation	seagrass meadows	0.01- 10	NR	Herbert (1990)
Catilina Harbor	ghost shrimp burrows	0.8- 8.05	0- 10	Bertics et al (2010)
Bassin d' Arachon France	Seagrass meadows	0.01- .52	0- 5	Welsh et al (1996)
Limfjord, Denmark	Seagrass meadows	0.09- 0.43	0- 10	McGlathery et al (1998)
Tomales Bay, CA	Microbial mat	3	0- 1	Joye & Paerl (1998)
Beaufort Inlet, NC	Spartina marsh	3.6	0- 1	Currin et al (1996)

Table 3.3 ANOVA & Tukey multiple comparison tests for May 2015 incubations. Results show anoxic incubations of sediment from 0.5- 3 cm depth interval had significantly (α = .05) higher trend in C_2H_4 production (nmol C_2H_4 cm^{-3} wet sediment) than those from the upper 0.5 cm of sediment although the difference against light, oxic incubations was not significant. Results of light, oxic incubations were different from those of anoxic incubations in the upper 0.5 cm.

ANOVA on all May 2015 sediment samples (not blanks)

Means of increases in C_2H_4 ($nmol\ cm^{-3}$ wet sed.) during incubations

oxic (light)	oxic (dark)	dark_& anoxic (0- 0.5 cm)	(0.5- 3 cm)
0.0796	0.0790	0.0627	0.1026
0.0725	0.0831	0.0682	0.1082
0.1130	0.0878	0.0689	0.1110

	a	b	c	d
count (ni)	3	3	3	3
sum	0.27	0.25	0.20	0.32
mean	0.088	0.083	0.067	0.107
ΣX2/n	0.023	0.021	0.013	0.035
sum of squares	0.024	0.021	0.013	0.035

$\Sigma\Sigma Xij$	1.04	total DF	11
$\Sigma\Sigma X^2_{ij}$	0.093	groups DF	3
$C= (\Sigma\Sigma X)^2/N$	0.0896	error DF	8

Total sum of squares	$\Sigma\Sigma X^2_{ij}$- C	0.003559
Groups sum of squares	ΣX2/n -C	0.002522
Error sum of Squares		0.001037

Summary of Variance:

Source	SS	DF	MS
Total	0.003559	11	
Groups	0.002522	3	0.001
Error	0.001037	8	0.000

F Stat	groups MS/error MS	6.48
F (0.05, 3, 48)		3.42

H_0: $\mu_a = \mu_b = \mu_c = \mu_d$

Reject H_0

Tukey Multiple Comparisons Test

ranked means from May 2015 ANOVA

anoxic(l)	oxic (l)	oxic (d)	
0.107	0.088	0.083	0.067

SE 0.006573495

Critic value q (.05,8,2)= 3.26

	difference means	q	conclusion
anoxic (u) vs anoxic (l)	0.041	6.184	reject anoxic (u) = anoxic (l)
anoxic (u) vs oxic (d)	0.024	3.647	reject anoxic (l) = oxic (d)
anoxic (u) vs oxic (l)	0.019	2.870	accept anoxic (l) = oxic (l)
oxic (l) vs anoxic (u)	0.022	3.314	reject oxic (l) = anoxic (u)
xic (l) vs oxic (d)	0.005	0.777	accept oxic (l) = oxic (d)
oxic (d) vs anoxic (u)	0.017	2.537	accept oxic(d)= anoxic (u)

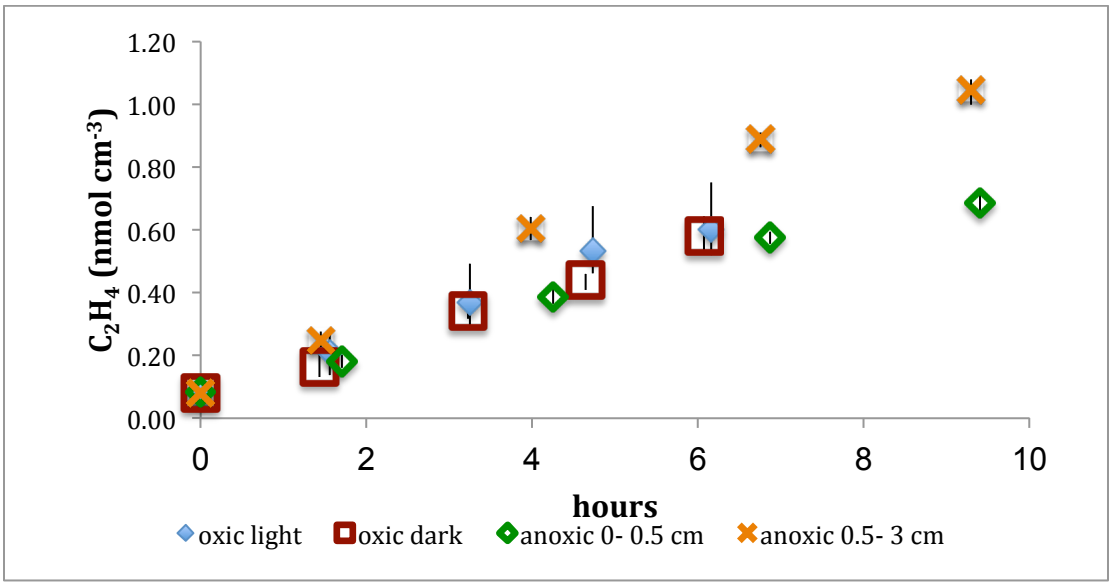

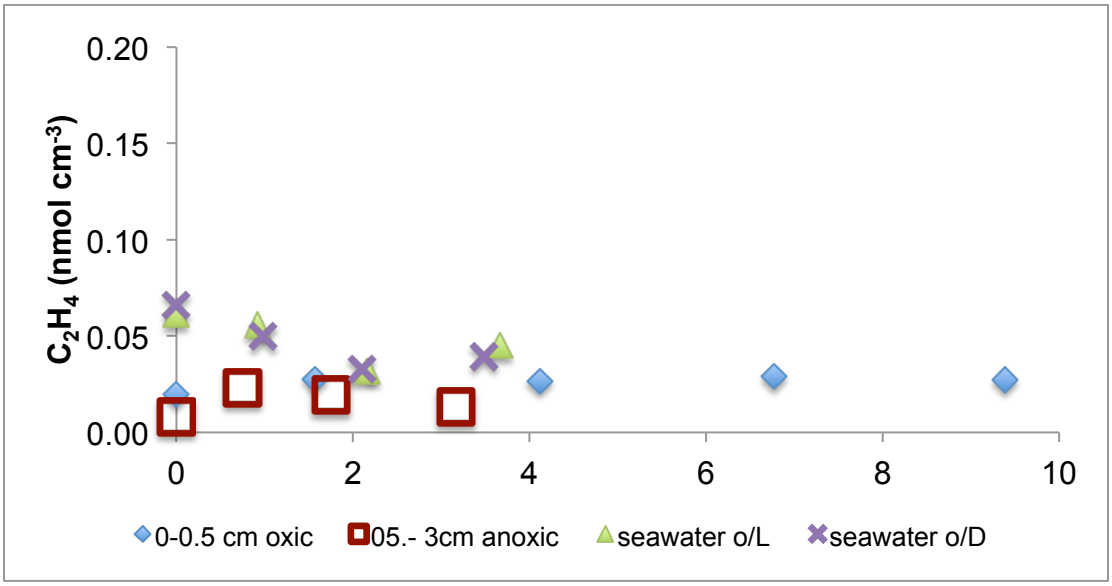

Fig. 3.6 (a) Acetylene Reduction Assays- May 2015: Samples. Increases in C_2H_4 from all May 2015 sediment ARAs were linear (oxic light: y= .088x + .081, R^2= .99; F-stat= 302, df= 3 & p-value < .001; oxic dark: y= .083x + .065, R^2= .99; F-stat= 520, df=3 & p-value < .001; anoxic upper: y= .067x + .086, R^2= .99; F-stat= 320, df=3 & p-value < .001; anoxic lower: y= .11x+ .11, R^2= .98; F-stat= 161, df= 3 & p-value = .001). Incubations were carried out in triplicate; symbols at each time-point are means. Error bars representing triplicate variability are difficult to detect under most symbols. **(b) Acetylene Reduction Assays- May 2015: controls & seawater.** Sediment blanks for 0.5 cm interval and 0.5- 3 cm interval where no C_2H_2 injected. C_2H_4 production in oxic seawater in light (L) & dark (D) conditions. Note Y-axis scale compared with sediment incubations. Effective sediment controls & seawater produced no C_2H_4

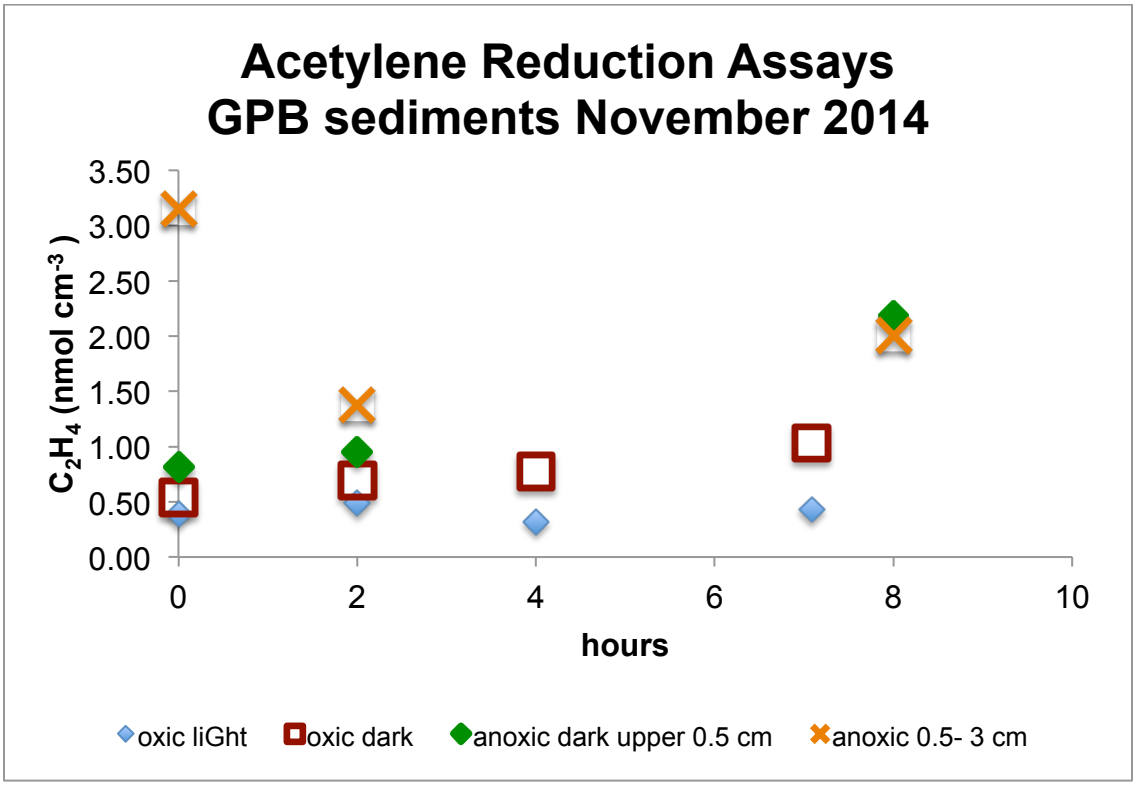

Fig. 3.7 Acetylene Reduction Assays- November 2014. Samples Incubations were not carried out in triplicate and consequently have no error bars.

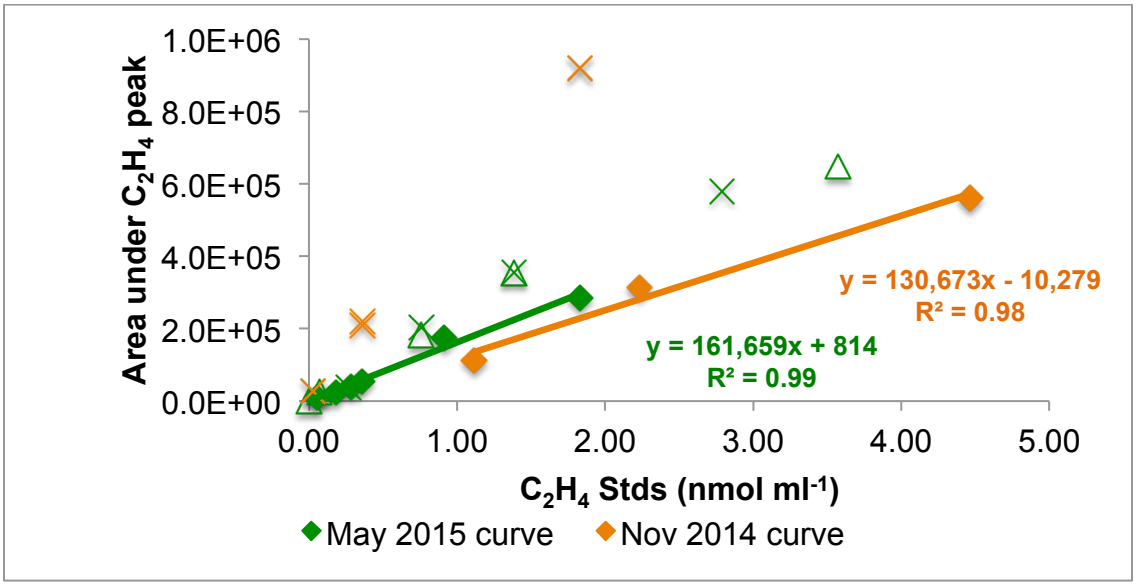

Fig. 3.8 **C_2H_4 Standard curves.** Alternate standard values are color-coded by period. The sharply increasing curve in November 2014 was rejected as due to gas processing error.

CHAPTER FOUR: N REMINERALIZATION & MASS BALANCES

4.1 INTRODUCTION.

N remineralization rate is a primary determinant of N cycle balances and ecosystem properties. In this study, N remineralization was estimated by three different proxies: (1) directly measured anoxic NH_4^+ production adjusted for adsorption ; (2) the N remineralization predicted from ΣCO_2 flux and a measured C:N production ratio; and (3) N remineralization estimated from SOD using measured O: ΣCO_2 and C:N production ratios. These N remineralization rates were used as the underlying N source term in different iterations of N mass balances. A comparison of SOD and C remineralization (by measured production and flux) was also included to provide a larger geochemical framework in which to assess N remineralization than one provided by the N terms themselves.

4.1.1 Mass balance equations.

Assuming N_2 fixation is not meaningful relative to other N terms, the steady-state equation describing the mass balance between remineralization of N_{org} and its fate within sediments can be simplified to:

$$N_{org\ remineralization} = N_{2\ net\ flux} + DIN_{\ flux} + \varepsilon \quad (I)$$

where ε represents an error term. $N_{2\ net\ flux}$ equals gross N_2 production minus N_2 fixation and $DIN_{\ flux}$ combines net NH_4^+ and NO_3^-/NO_2^- fluxes. In this investigation, all N terms are measured on a net basis.

In sediments within the euphotic zone, benthic macro-algae, benthic micro-algae and both heterotrophic and autotrophic bacteria compete for and assimilate N (Blackburn et al 1996; Eyre & Ferguson 2005; Ferguson et al 2004; Lomstein et al 1998; Risgaard-Petersen et al 2004; van Duyl et al 1993). In addition, grazing by meiofauna can shunt N further up the trophic chain with the effect that N release from biomass may not occur evenly but in pulses (Eyre & Ferguson 2005) or may be removed from the local ecosystem all together (e.g., as fish biomass). Time-scales required to measure N sources and sinks at steady state may not be congruent with practical measurement time-scales. To address non-steady N fluxes, equation (I) can be expanded to specify estimates of biological N assimilation:

$$N_{org}\ remineralization = N_{2\ net\ production} + DIN_{\ flux} + N_{\ assimilation} + \varepsilon \quad (II)$$

N assimilation by biomass was not directly measured in this study; instead it is treated as part of the residual term ε in equation (I).

4.1.2 N remineralization proxies

(i) N remineralization equated to NH_4^+ production. In the absence of benthic N_2 fixation, ammonification, the hydrolysis and deamination of $N_{org,}$ to produce NH_4^+, provides the only sedimentary source of reduced N substrate available to nitrifying microbes; consequently, N remineralization can be equated to NH_4^+ production if fixed N is measured separately[3]. When N_2 production is coupled to nitrification, NH_4^+ production provides the upper limit on gross N_2 production. NH_4^+ released in porewater can either undergo oxidation, diffuse along concentration gradients, become assimilated by sedimentary bacteria or benthic algae or adsorb onto particles.

Since NH_4^+ is a cation, it adsorbs to negatively charged particles in sediments found in clays or organic matter. Rosenfeld (1979) identified 3 pools of NH_4^+ which are in dynamic equilibrium with one-another in marine sediments and which can be defined by operational procedures used to recover NH_4^+: (1) porewater NH_4^+; (2) exchangeable NH_4^+ which can be extracted from particle associations with a 2N KCl leach and (3) fixed NH_4^+ which is tightly bound and requires liberation by a strong acid leach. The adsorption coefficient, K, describes the relationship between the quantity of exchangeable NH_4^+ relative to quantity of dissolved NH_4^+ in porewater.

Both ΣCO_2 and NH_4^+ production rates can be calculated from changes in inventory values based on measured porewater concentrations of non-steady state, anoxic incubations (e.g., Aller & Mackin 1989; Aller et al 2004 (a) & (b); & Rysgaard et al 1998). Net NH_4^+ production rates must be subsequently adjusted for adsorption losses during incubation by multiplying the calculated net rate by (1 + K). This correction assumes reversible, linear adsorption characterized by a single adsorption coefficient K, the value of which depends on sediment mineralogy, porosity, and salinity.

(ii) N remineralization proxies based on ΣCO_2 production & SOD. Alternately, estimates of N remineralization rates in marine sediments are often based on stoichiometric ratios applied to estimated rates of carbon (C) remineralization (Giblin et al (1997); LaMontagne et al (2002); Eyre & Ferguson (2005)). C remineralization rates, in turn, are estimated either by measurements of sedimentary ΣCO_2 efflux (Giblin et al (1997)) or by applying a stoichiometric ΣCO_2: O_2 ratio to measured SOD (LaMontagne et al (2002)). The first

[3] NH_4^+ production in this investigation is measured in anoxic incubations (as described under the Methods section). To the extent N_2 fixation occurred in these incubations (e.g., by SRB's), the methods followed here by equating NH_4^+ production with N remineralization would double count fixed N (as it would be included as a negative term under N_2 net flux and a positive term under N remineralization).

approaches requires an estimate of C:N in decomposing organic matter and the second requires an additional estimate of ΣCO_2: O_2. If N remineralization is based on a flux rate (either SOD or ΣCO_2 efflux), potential complications arising from faunal entombment in whole cores used for anoxic incubations are avoided.

If reduced products of remineralization are fully oxidized within sediments (e.g., no pyrite burial), SOD should approximate C remineralization (Glud 2008). Depending on the oxidation state of C undergoing remineralization, the ΣCO_2: O_2 ratio should vary between 0.67- 1.0 (Hulth et al 1997). Organic matter with pure carbohydrate composition will have a ΣCO_2: O_2 ratio of 1.0; the higher the lipid content of the organic matter, the closer towards the bottom of the range the ΣCO_2: O_2 (Hulth et al 1997). SOD can decouple from the C cycle seasonally because of reactions between C or O_2 and the sulfur cycle (S). ΣCO_2 flux can exceed SOD during a phase of sulfate reduction and sedimentary sulfide accumulation whereas SOD can exceed ΣCO_2 flux during a phase of sulfide oxidation (e.g., Guld 2008; Eyre & Ferguson 2005; Therkildsen & Lomstein 1993). For this reason, this ratio can vary extensively on a seasonal basis especially in shallow environments (Therkildsen & Lomstein 1993).

Basing N remineralization estimates on ΣCO_2 flux avoids possible complications involved with the contribution of S oxidation to SOD ; however, ΣCO_2 flux may be affected by carbonate dissolution or precipitation.

4.2 METHODS

4.2.1 Production estimates.

Estimates of ΣCO_2 & NH_4^+ production were derived from the “whole core” incubation procedures described in Aller and Mackin (1989). Accordingly, ΣCO_2 & NH_4^+ concentrations were measured in porewater from anoxic incubations generally carried out over 2- 4 weeks. Sediment for whole core incubations was sampled from box-cores collected as described in chapter 2 of this dissertation. Starting (t=0) values were measured from porewater centrifuged from sediment extruded and sectioned from 7.2 cm (ID) sub-cores used to sample box-cores. Sediment for subsequent incubations was sampled from box-cores in 4 cm (ID) gas tight, glass tubes stoppered at each end with silicon plugs and kept in gas tight, metal foil bags containing O_2 scrubbers. At each time point, metal foil bags were opened, sediment was extruded and sectioned by depth intervals; each sediment interval was centrifuged and porewater was retrieved by syringe and filtered (0.2 um polyethersulfone membrane). Processing was carried out in open air at a moderately rapid pace (< 30 min) (Aller and Mackin, 1989). ΣCO_2 samples were measured within several hours; samples for NH_4^+ were immediately frozen for later measurement.

NH_4^+ was measured colorimetrically using the phenolhypochlorite method (Solorzano 1969); ΣCO_2, was measured using a flow injection analysis system with conductivity detection (Hall & Aller 1992). Sediment porosities were determined by the difference in weight of wet and dry sediment extracts at each depth interval assuming a sediment density of 2.65 g/ml

ΣCO_2 & NH_4^+ values at specific depth intervals to 15 cm deep were calculated by multiplying measured ΣCO_2 & NH_4^+ porewater concentrations by porosity and interval thickness. ΣCO_2 & NH_4^+ inventories were calculated by summing these values for each incubation; production values were derived from regressions of inventory values over incubated time-points (Table 3.1) and, in the case of NH_4^+ production, adjusted for adsorption (see below). Several implausibly high inventory values were discarded because of the likelihood they arose from entombment and death of infauna.

4.2.2 N remineralization calculations.

Mass balances were estimated based on NH_4^+ production using 2 separate estimates for adsorption coefficients: one assumed the average of a set of published values (K= 1.3); the other assumed a value from the higher end of the set (K= 1.7) (Mackin & Aller (1984)). Adjusting NH_4^+ production values by K values lower than 1 would lead to mass balances where total N flux exceeded remineralized N over annualized periods. As such outcomes are not realistic, lower K values were excluded from NH_4^+ production calculations. Measurements of NH_4^+ in supernatant of 2N KCl extractions of GPB sediments were made to determine K values. These measurements resulted in the calculation of a K value ~ 1.7; however, this value was not relied on as (1) there was wide scatter in the regression of KCl extracted NH_4^+ against porewater NH_4^+ and (2) some of the KCl extracted NH_4^+ values when adjusted for porewater concentrations were negative and could not be included in the regression.

Total nitrogen flux (TNF) was calculated as the sum of net N_2 flux and DIN flux; methods used to derive flux values are discussed in Chapter 2. Mass balances were calculated based on values from all flux core and benthic chamber incubations (i.e., light & dark). Comparisons between N fluxes based on ΣCO_2 production, ΣCO_2 flux and SOD were derived exclusively from dark incubations. Type (II) geometric mean regressions were used where each data-set was estimated.

Periodic production and flux estimates were aggregated by season and final estimates were based on average values of seasonal averages. This calculation gives equal weight to each seasonal period and thereby mitigates the bias toward periods in which more incubations were measured.

Comparisons of seasonal means of production and flux values were assessed for homogeneity of variance by Barlett's test. Where data showed

homoscedasticity, seasonality of means was assessed by ANOVA; where data showed heteroscedasticity, seasonality of means was assessed by an approximate test of equality of means (Games and Howell method in Rohlf and Sokal (1969)). This test does not require homogeneous variances between seasonal flux values.

4.3 RESULTS

4.3.1 Overall diagenetic setting.

(i) Estimates of ΣCO_2 & NH_4^+ production. Table 4.1 shows ΣCO_2 & NH_4^+ production estimates by sampling period; NH_4^+ production estimated assume an adsorption coefficient of K= 1.3. Values were lowest in winter, increased in spring and summer and decreased in fall but high intra-seasonal variability rendered patterns in seasonal means statistically insignificant for either data-set[4] (Fig. 4.1). C:N production ratios were 7.8 (at K= 1.3) and 6.6 (at K= 1.7) (Fig. 4.2 (a) & (b)). Because marine sourced organic carbon in GPB sediments has previously been found to rapidly remineralize in GPB sediments (Cochran et al 2000) and because ΣCO_2: O_2 ratios were close to one (see below), organic material in GPB sediments is likely characterized by highly labile, carbohydrate content which suggests the correct C:N production may be close to the lower boundary, Redfield-like ratio.

(ii) ΣCO_2 production compared to SOD and ΣCO_2 flux. A geometric mean regression of ΣCO_2 production values against SOD derived from dark flux incubations produced a slope of 0.96 with significant trend (F-stat 17.5, df= 8 & p-value < .01) and correlation (R= 0.83) in spite of the different incubation methods and different sediment samples used to measure the solutes (Fig. 4.3 (a)). The seasonal chart (Figure 4.4 (a)) shows ΣCO_2 production and SOD means were highest in spring and declined through summer, fall and into winter. However, except in fall, differences between ΣCO_2 production and SOD periodic means were small relative to intra-period variability.

A geometric mean regression of ΣCO_2 flux against ΣCO_2 production generated a slope of 0.97 for dark incubation but the regression was not significant ($\alpha > .05$) and values were scattered (Fig. 4.3 (b)). ΣCO_2 flux was higher in summer than spring unlike ΣCO_2 production but both followed roughly similar seasonal patterns; except in fall, differences between ΣCO_2 flux and ΣCO_2 production were small relative to intra-period variability (Fig. 4.4 (b)). Regressions of $\Sigma CO_{2\ flux}$ against SOD reflected similar slope to $\Sigma CO_{2\ production}$ against SOD but was not significant ($\alpha > .05$) (Fig 4.3 (c)). Except in fall, differences between ΣCO_2 flux and SOD periodic means were small relative to

[4] Significance of differences in means analyzed both by ANOVA and equality of means test (Games and Howell).

intra-period variability (Fig. 4.4 (c)). Differences in results in the fall were significant (ANOVA: F-stat = 33.85, df= 8; p-value < .001) and reflected an overall pattern of $\Sigma CO2_{flux}$ > SOD > $\Sigma CO_{2\ production}$.

4.3.2 TNF regressions against N remineralization proxies.

(i) N equivalents based on $\Sigma CO2_{flux}$. Figure 4.5 (a) shows a geometric mean regression of TNF against the N stoichiometric equivalent of $\Sigma CO_{2\ flux}$ (R= 0.91) with a slope = 0.82; i.e., less than the one: one expected. The regression slope varies positively with the C:N ratio used to convert ΣCO2 to N equivalents. The C:N ratio used to convert measured ΣCO_2 for the chart shown was C:N= 6.6 based on an adsorption coefficient of K= 1.7. If a published average K value = 1.3 (Mackin & Aller (1984)) is assumed, the C:N ratio increases to 7.8 and the slope of the regression increases resulting in the equation y= 0.97- 0.28; i.e. the regression yields close to the one: one trend expected. The regression was significant (F-stat = 28.5, df= 6 & p- value < .01); these parameters are not changed by changes in the slope of the regression.

(ii) N equivalents based on SOD. Figure 4.5 (b) shows a geometric mean regression of TNF against the N stoichiometric equivalent of SOD with a slope = 1.05 slope with a C:N= 6.6 based on an adsorption coefficient of K= 1.7; the regression plot had scattered values (R= 0.49) and was not significant (α > .05). Using a C:N ratio of 7.8 (K= 1.3) and holding the ΣCO_2:O_2 ratio = 0.96, TNF slope against SOD increase to 1.24.

(iii) N equivalent based on measured NH_4^+ production. Figure 4.5 (c) shows a geometric mean regression of TNF against measured NH_4^+ production values yielded a slope of 0.82 with a K value= 1.7. If K= 1.3 is assumed, the slope of the regression line increases to 0.96. The regression was not significant (α > .05) and had high scatter (R= 0.46).

(iv) Seasonality. As shown in Fig. 4.6 (a)- (c), the differences between TNF and each of the N remineralization proxies in each seasonal period were small relative to the variation of results themselves within each period.

4.3.3 N mass balances.

Mass balances evaluating TNF against 3 different N remineralization proxies (N_{eqv} SOD; N_{eqv} $\Sigma CO2_{flux}$ & $NH_4^+{}_{production}$) all resulted in either a balance or an excess of N production over N flux which ranged from 0.05 N mmol m^{-2} d^{-1} to 0.65 N mmol m^{-2} d^{-1} over an annualized period and represented 2% to 26% of estimated N remineralized (Table 4.2 (a-c)).

N remineralization based on measured ΣCO_2 fluxes resulted in larger excess balances of production over flux of 0.33 mmol m^{-2} d^{-1} or 12% of N remineralized in the case where C:N = 7.8 (K= 1.3) and of 0.75 mmol m^{-2} d^{-1} or

26% of N remineralized where C:N = 6.6 (K= 1.7) (Table 4.2 (a)). Although an N remineralization equivalent based on ΣCO_2 flux produces the widest annualized mass balance deficit of any the remineralization proxies, its closer correlation with TNF (R= 0.91) suggests it will produce more stable outcomes than the other remineralization proxies.

The N remineralization equivalents of SOD calculated at a C:N of 7.8 and of the measured NH_4^+ production adjusted for an adsorption coefficient of K= 1.3 yielded mass balances of zero and 2% of remineralized N against TNF over an annualized period (Table 4.2 (b) & (c)). N remineralization equivalents based on SOD at C:N of 6.6 and measured NH_4^+ production at K= 1.7 yielded excess balance 15% and 19% of remineralized N over TNF over an annualized period. The correlations between TNF and SOD and between TNF and NH_4^+ production were low (R= 0.46 and R= 0.49 respectively) implying the near balances between N remineralization and flux may have been fortuitous.

Comparisons between TNF and NH_4^+ production may be complicated by artifacts of the different methods used to measure production and flux. Figure 3.10 shows differences in period means between production and flux; the coincidence both in magnitude and direction of the means occurs regardless of whether the measurement involves ΣCO_2 or NH_4^+ production. The re-occurrence of this pattern (6/8 instances) suggest differences in duration or procedures between anoxic whole core incubations and flux incubations may have an influence on mass balance outcomes apart from the individual C or N biogeochemistry.

The quantities of TNF, unadjusted NH4+ production, ΣCO_2 flux and SOD measured were poised so changes between use of published average and upper end NH4+ adsorption coefficients had a significant effect on mass balance outcomes. This sensitivity is apparent in increases in N mass balance excesses (~ 15% of N remineralization) using all 3 of the N remineralization proxies when the adsorption coefficient (K) is changed from 1.3 to 1.7.

4.4 DISCUSSION

4.4.1 ΣCO_2 & O_2 remineralization stoichiometry.

The slopes of the regression lines of ΣCO_2 production against SOD (dark incubations) (Fig. 4.3 (a)) and of ΣCO_2 flux against SOD (dark incubations) (Fig. 4.3 (b)) were close to one which is expected for remineralized C with an oxidation state characteristic of labile, carbohydrate- based, marine source (Hulth et al 1997). These measurements reinforce the conclusion of Cochran et al (2000) that present-day marine-sourced organic matter in GPB sediments is quickly remineralized leaving only residual aged C. Such a characterization also supports the applicability of a C:N ratio close to Redfield in converting ΣCO_2 and

SOD measurements to N remineralization equivalents. However, mass balances using a N remineralization equivalent converted at a C:N of 6.6 (K= 1.7) produce larger excesses of N production over flux than equivalents converted with a C:N ratio of 7.7 (K= 1.3) (Table 4.2 (a)- (c)).

Differences between ΣCO_2 flux, production and SOD were only significant in fall and reflected an overall pattern of $\Sigma CO2_{flux}$ > SOD > $\Sigma CO_{2\ production}$. These data do not support the occurrence of oscillating patterns of accumulation and subsequent oxidation of reduced remineralization products found by Eyre & Ferguson (2005) or Therkildsen & Lomstein (1993). For this pattern to occur both ΣCO_2 production and ΣCO_2 flux would need to oscillate together around SOD. Green and Aller (2001) found seasonally distinct periods of $CaCO_3^-$ dissolution (in winter) and precipitation (in late spring/early summer) in Long Island Sound sediments adjacent to GPB. The associated seasonal shift in Ca^{2+} flux was higher in flux cores than it was in anoxic whole cores using incubation procedures similar to those used here (Green and Aller (2001)). The difference between ΣCO_2 flux (measures in flux cores) and ΣCO_2 production data (measured in anoxic whole cores) as well as the difference between ΣCO_2 flux and SOD found in GPB sediments are consistent with the finding of carbonate dissolution in the fall period. Greater carbonate dissolution in flux cores compared with whole cores in fall could also partly explain the high scatter in the regression of ΣCO_2 production against ΣCO_2 flux (Fig. 4.3 (b)).

4.4.2. N mass balances.

Regardless of the N remineralization term, the above results demonstrate a trade-off between use of adsorption coefficient (K= 1.7) which produces a Redfield C:N and higher excess of production over flux and one (K= 1.3) which produces a higher C:N but lower (or no) excess of production over flux. In all scenarios, remineralized N proxy produced excess of production over TNF on an annualized basis. There are 2 feasible explanations for these mass balance outcomes generally and several explanations specific to use of different N remineralized proxies.

The mass balances were constructed according to Equation 1- a model which assumes (1) no N_2 fixation and (2) accumulation of N by biomass. As discussed in Chapter 3, N_2 fixation may reduce up to 0.125 mmol m^{-2} d^{-1} of N-N_2. Since N_2 estimates in this research are measured by MiMS on a net basis (gross N_2 production less N_2 fixation), this quantity should be added into the flux term if the product of the fixation (i.e. NH_4^+) is included in the remineralization term. Each of the N stoichiometric equivalents (SOD & ΣCO_2 flux) and the measured NH_4^+ would include NH_4^+ from fixation if it occurred. Consequently, for mass balances assuming K= 1.3, N_2 fixation could account for all of the production excesses where SOD or measured NH4+ are used as remineralized N proxies and ~ ½ of these balances where ΣCO_2 flux is used. Using a higher

adsorption coefficient assumption, N_2 fixation could still account for between ~ ⅙ - ½ of the production excess.

Alternately, the seasonal excesses of remineralized N equivalents over TNF could imply assimilation of N by biomass which is accumulated and shunted from the sedimentary N cycle to higher trophic levels as has been reported by Eyre & Ferguson 2005.

Changes in carbonate dissolution could complicate the interpretation of ΣCO_2 flux as an N remineralization equivalent. Specifically, carbonate dissolution could have increased ΣCO_2 flux in fall periods without a corresponding increase in TNF. The associated increase in ΣCO_2 flux could thereby partially explain the higher mass balance deficit associated with use of ΣCO_2 flux as a remineralization proxy compared to those resulting from use of the other two proxies.

As opposed to the mass balance based on N equivalent ΣCO_2 flux in which N production exceeded N flux in every season, the mass balances based on SOD and measured NH_4^+ production reflected excesses of production over flux in winter and spring and excesses of flux over production in summer and fall. These differences are small relative to intra-seasonal variability around period means (Fig. 3. 9 (a)- (c)) and variability precludes drawing any inferences concerning seasonal patterns which might suggest N storage or release as has been observed by other researchers who have allocated excess balances of N remineralization over N flux to N assimilation by either benthic micro-algae or bacteria (e.g., Eyre & Ferguson 2005; Lomstein et al 1998; Blackburn et al 1996).

In conclusion, the mass balance based on measured ΣCO_2 flux demonstrates a tight coupling between N remineralization and individual N flux measurements. Residual N outcomes in mass balances may be attributable to (1) N_2 fixation; (2) assimilation/release of N by biomass and (3) in the case where the remineralized N term is based on ΣCO_2 flux by carbonate dissolution although its occurrence of could only be inferred in the fall. Mass balances based on SOD and measured NH_4^+ production showed only small excesses over TNF; yet, these proxies were only loosely correlated with TNF raising concerns as to the variability of mass balance outcomes using these proxies. In all mass balance iterations, outcomes are dependent on values for the appropriate NH_4^+ adsorption coefficient.

4.5 TABLES & FIGURES

Table 4.1 ΣCO_2 & NH_4^+ production values from anoxic incubations. NH4+ estimates assumed a NH4+ adsorption coefficient of K= 1.3.

Incubation Period	ΣCO_2 (mmol m^{-2} d^{-1})	p- value	NH_4^+ (mmol m^{-2} d^{-1})	p- value	days incubated
GPB0709	16.6	<.01	1.81	0.01	15.0
GPB1009	22.3	0.05	1.55	0.23	14.0
GPB0210	1.23	N-A	0.22	0.22	21.6
GPB0510	10.1	0.03	1.79	0.02	29.8
GPB0910	25.7	0.06	5.78	<.01	19.2
GPB1110	7.13	0.04	0.87	0.01	15.9
GPB1012	4.08	0.02	0.68	0.07	13.0
GPB0613	39.6	0.02	3.25	0.04	18.6
GPB1113	7.37	0.03	1.42	0.07	14.0
GPB0214	5.38	0.09	0.98	0.35	13.8
GPB0514	24.8	0.02	1.95	0.25	16.9
GPB0914	16.6	N-A	2.12	N-A	6.2

Table 4.2 (a) Mass Balance: Comparison of total nitrogen flux (TNF) versus estimates of remineralized N based on ΣCO_2 flux measurements. Correlation coefficient between TNF & ΣCO_2 flux = 0.91.

All units in mmol m^{-2} d^{-1}		$N_{remineralized}$ ΣCO_2 flux $_{eqv}$ C:N = 7.8 & K=1.3		$N_{remineralized}$ ΣCO_2 flux $_{eqv}$ C:N = 6.6 & K=1.7	
	TNF		Balance		Balance
Slope of regression		0.97		0.82	
Winter	0.17	0.39	0.23	0.46	0.30
Spring	1.92	2.25	0.33	2.64	0.72
Summer	4.34	4.50	0.16	5.28	0.94
Fall	1.91	2.50	0.59	2.93	1.02
average	2.08	2.41	0.33	2.83	0.75
Annualized excess (production less flux) as % N remineralized			12%		26%

Table 4.2 (b) Mass Balance: Comparison of total nitrogen flux (TNF) versus estimates of remineralized N based on SOD measurements. Correlation coefficient between TNF & SOD = 0.49.

All units in mmol m^{-2} d^{-1}		$N_{remineralized}$ SOD_{eqv} C:N = 7.8 & K=1.3		$N_{remineralized}$ SOD_{eqv} C:N = 6.6 & K=1.7	
	TNF		Balance		Balance
Slope of regression		1.24		1.05	
Winter	0.17	0.54	0.38	0.64	0.47
Spring	1.92	3.45	1.53	4.05	2.13
Summer	4.34	2.79	-1.55	3.27	-1.06
Fall	1.91	1.52	-0.39	1.79	-0.12
average	2.08	2.08	0.00	2.44	0.36
Annualized excess (production less flux) as % N remineralized			0%		15%

Table 4.2 (c) Mass Balance: Comparison of total nitrogen flux (TNF) versus NH_4^+ production estimates from anoxic incubations.
Correlation coefficient between TNF & NH_4^+ = 0.46.

All units in mmol m^{-2} d^{-1}					
	TNF	NH_4^+ production K= 1.3	Production less flux	NH_4^+ production K= 1.7	Production less flux
Slope of regression		0.96			0.82
Winter	0.17	0.98	0.81	1.13	0.97
Spring	1.92	2.60	0.68	3.02	1.09
Summer	4.34	3.95	-0.38	4.59	0.25
Fall	1.91	0.99	-0.92	1.15	-0.76
average	2.08	2.13	0.05	2.47	0.39
Annualized excess (production less flux) as % N remineralized			2%		19%

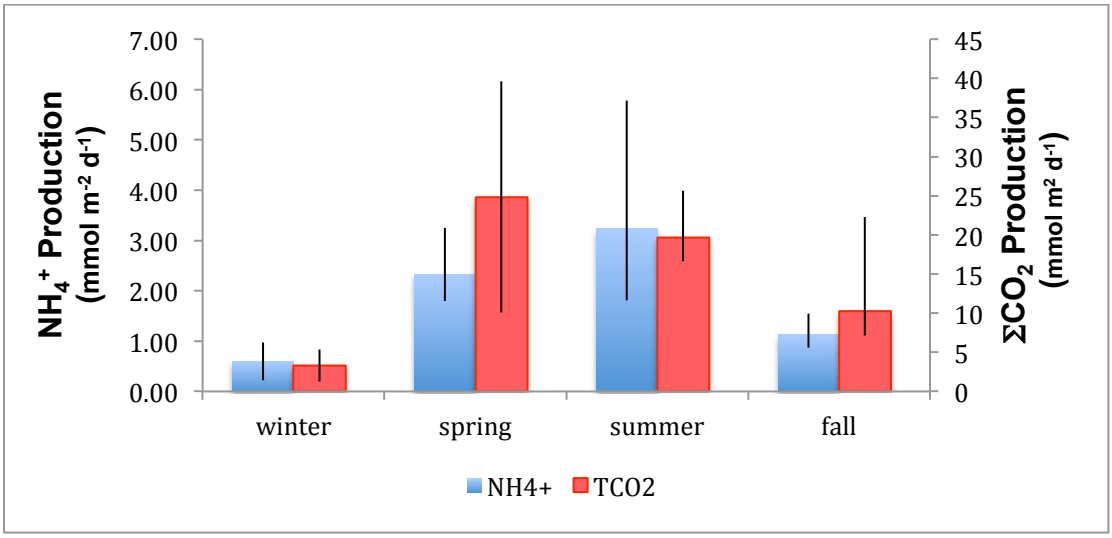

Figure 4.1 Seasonal variations in ΣCO_2 & NH_4^+ production. In the chart shown, NH_4^+ production is calculated at the measured rate adjusted for NH_4^+ adsorption assuming K= 1.3; the patterns in the chart would not look meaningfully different for a K value = 1.7. A Bartlett's test for homogeneity of variance followed by a Games & Howell test showed no differences in seasonal means.

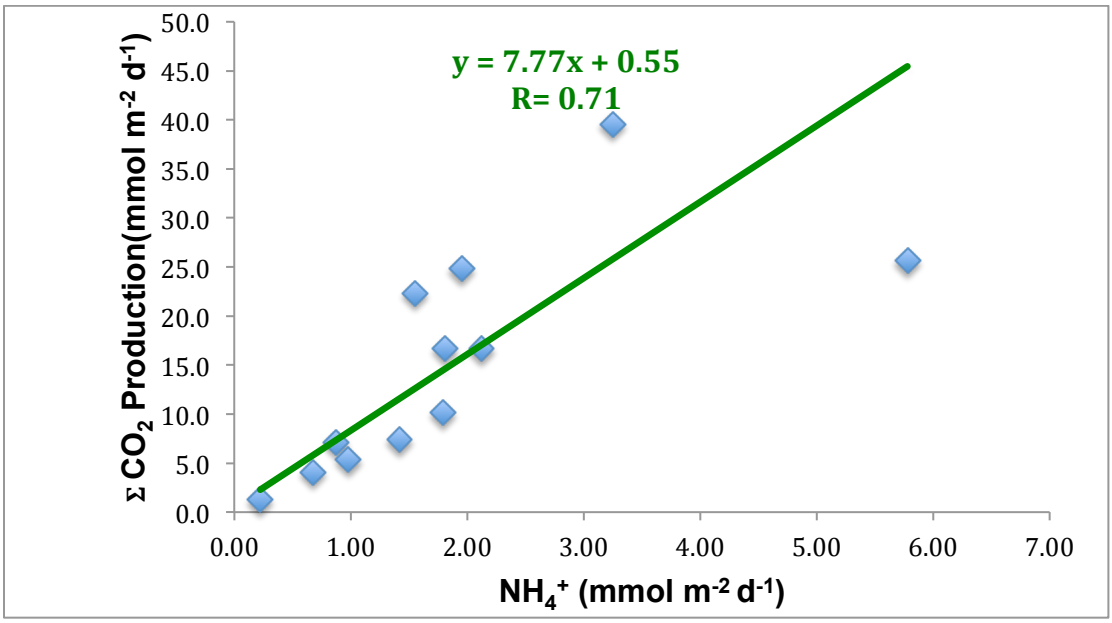

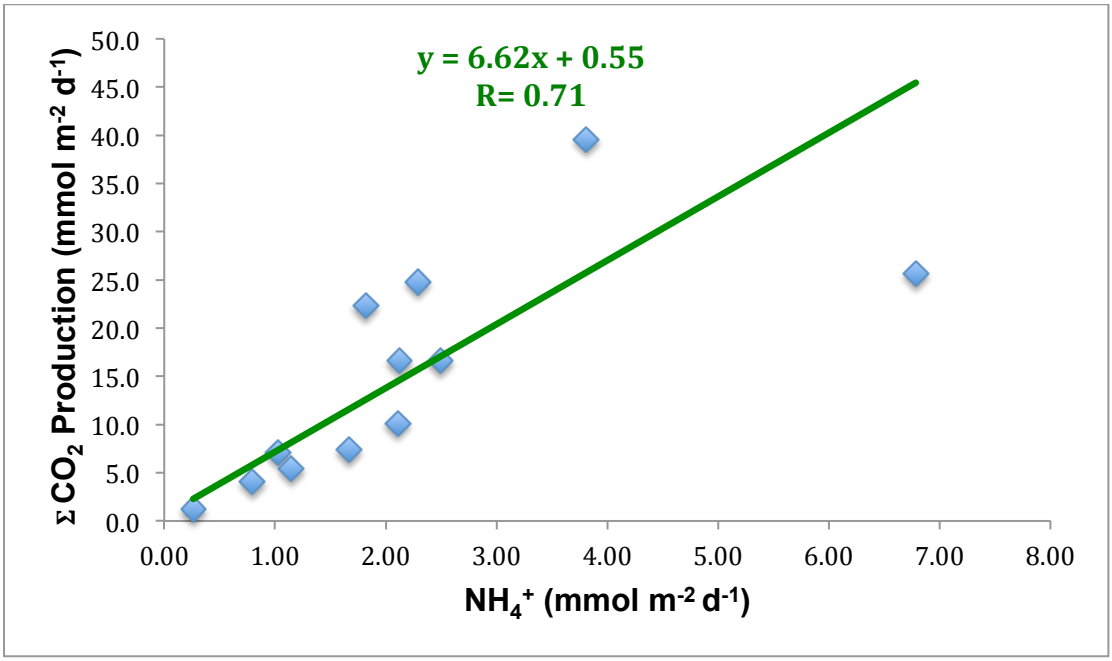

Figure 4.2. (a) Geometric mean regression of ΣCO_2 production against NH_4^+ production using a NH4+ adsorption coefficient K= 1.3 (the average in Mackin & Aller 1984). (b) Geometric mean regression of ΣCO_2 production against NH_4^+ production using a NH4+ adsorption coefficient K= 1.7 (the upper-end of the range of values in Mackin & Aller 1984). By increasing the adsorption coefficient assumption, the C:N production value decreases to the Redfield ratio which describes wholly marine-sourced, carbohydrate- based sedimentary organic material. Changing the adsorption coefficient does not change regression parameters: F-stat 10.4, df= 10 & p-value < 0.01.

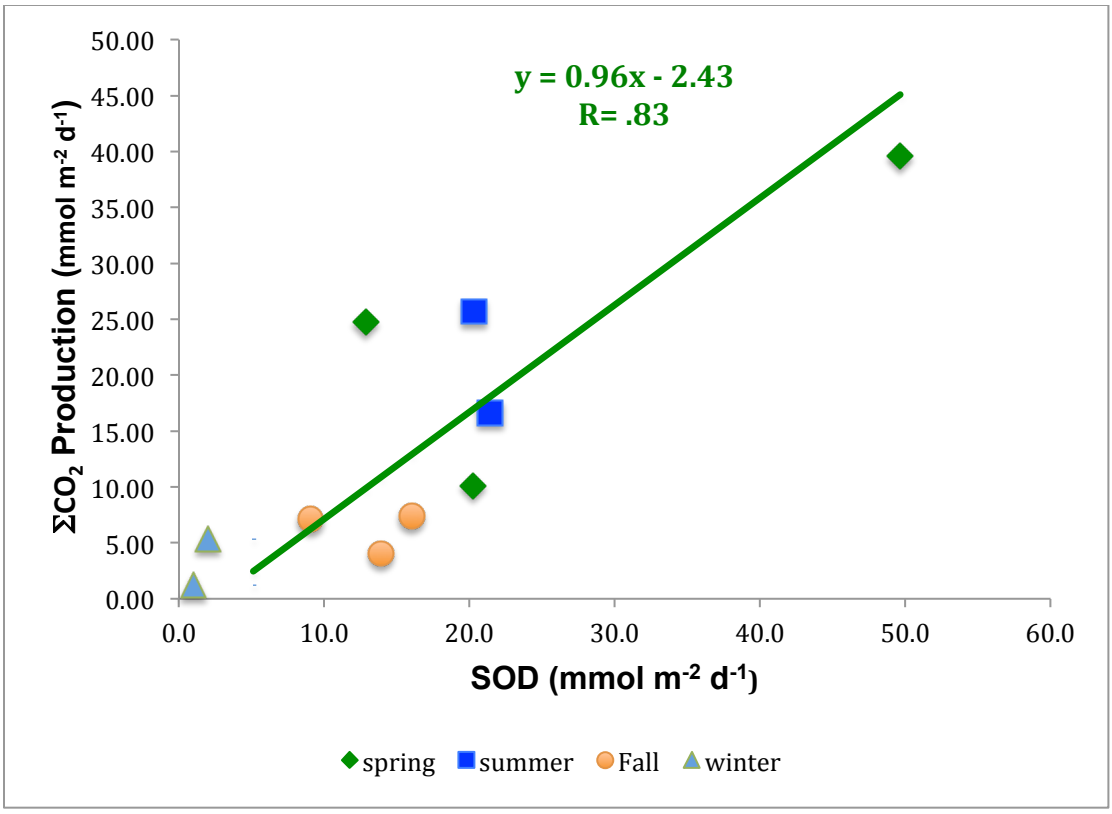
y = 0.96x - 2.43
R= .83
ΣCO2 Production (mmol m-2 d-1)
SOD (mmol m-2 d-1)
50.00
45.00
40.00
35.00
30.00
25.00
20.00
15.00
10.00
5.00
0.00
0.0
10.0
20.0
30.0
40.0
50.0
60.0
spring
summer
Fall
winter

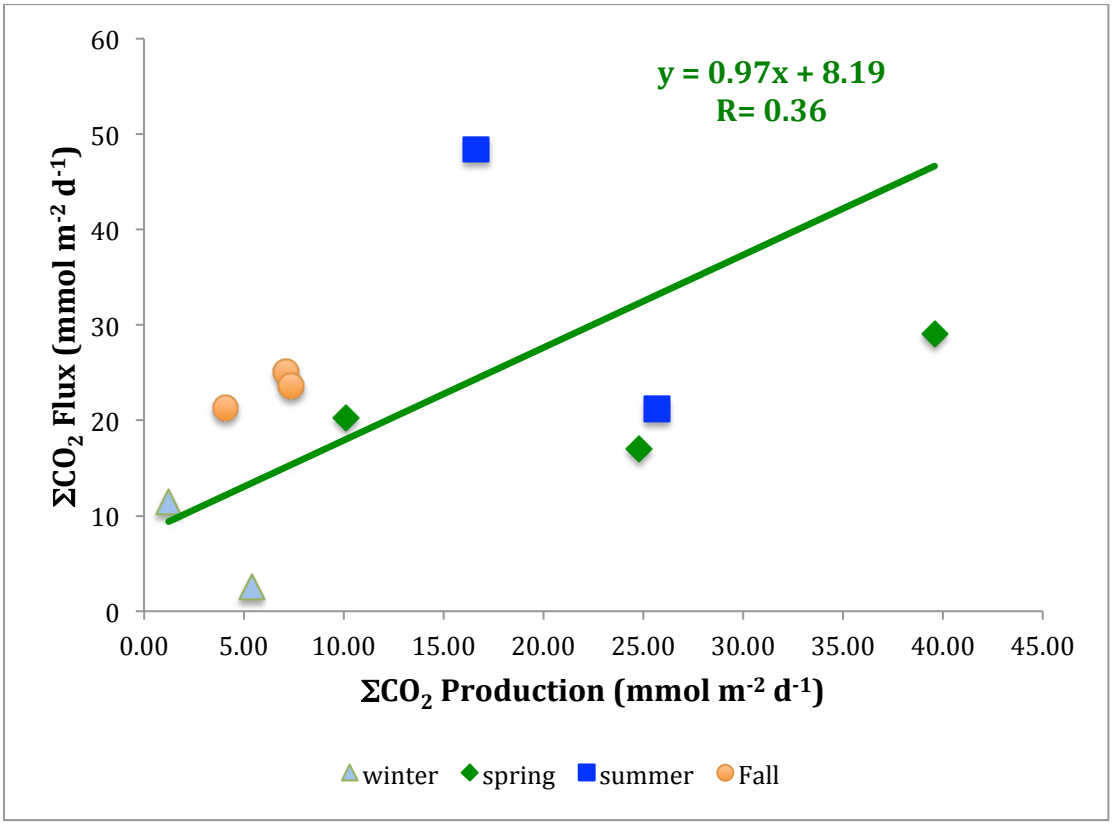
y = 0.97x + 8.19
R= 0.36
ΣCO2 Flux (mmol m-2 d-1)
ΣCO2 Production (mmol m-2 d-1)
60
50
40
30
20
10
0
0.00
5.00
10.00
15.00
20.00
25.00
30.00
35.00
40.00
45.00
winter
spring
summer
Fall

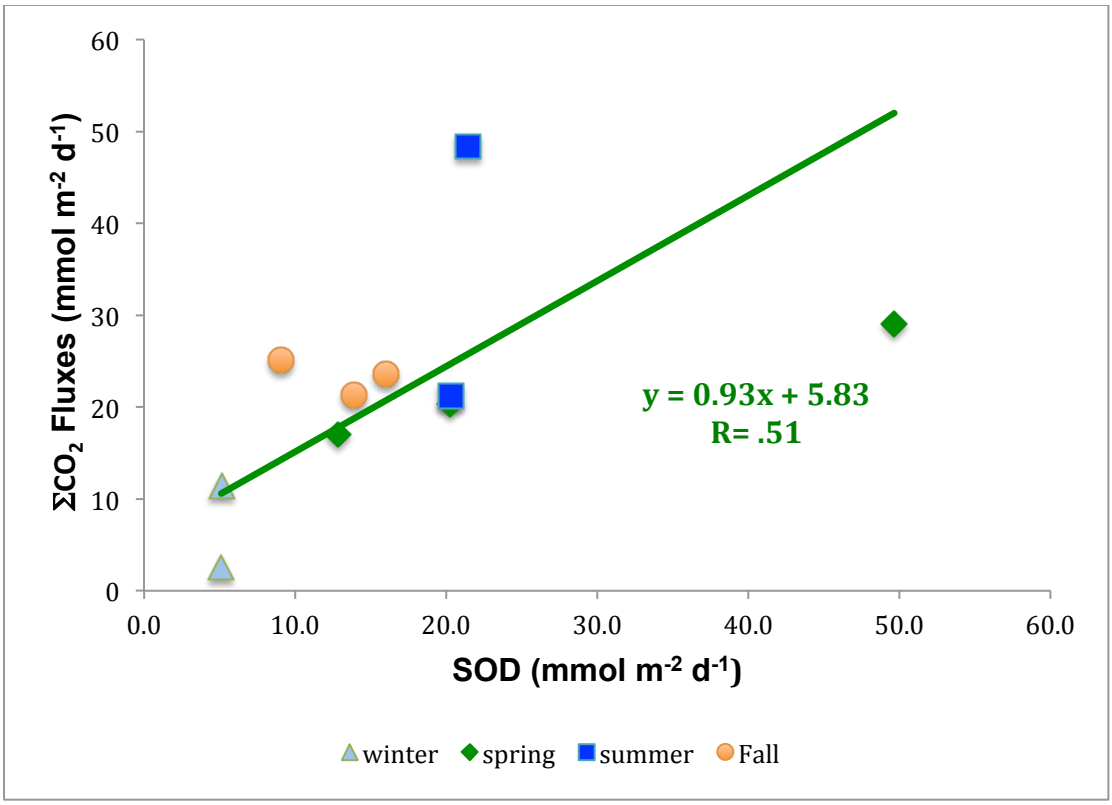

Figure 4.3. (a) Geometric mean regression of ΣCO_2 production and SOD for dark incubations only. (b) Geometric mean regression of ΣCO_2 production against ΣCO_2 flux for dark incubations (c) Geometric mean regression of ΣCO_2 flux against SOD for dark incubations only. ΣCO_2 production and SOD show a higher correlation than the other data-sets despite the different incubation methods and different sediment cores used to generate each measurement.

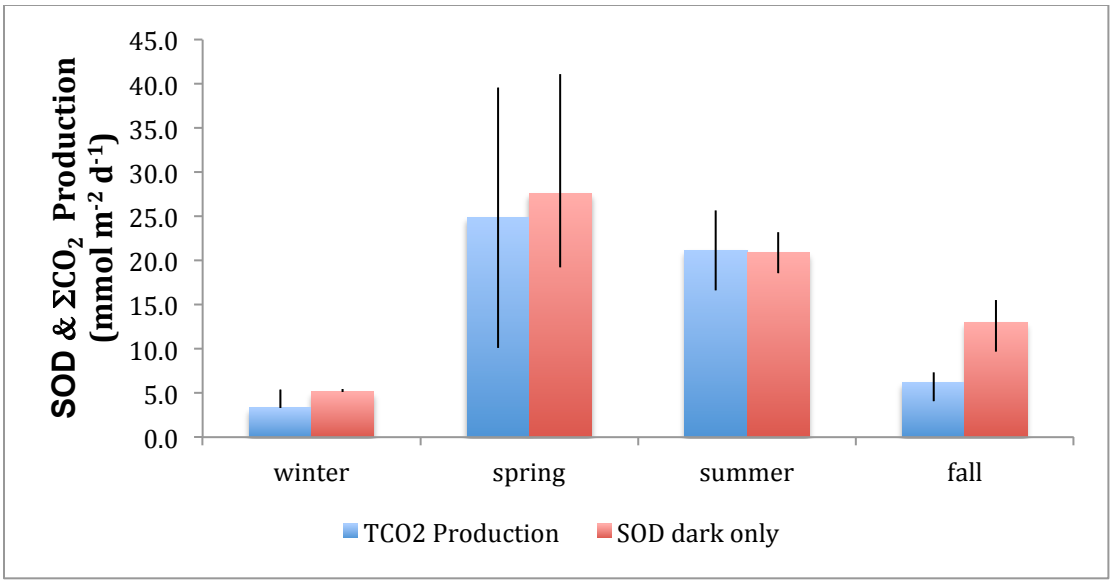
SOD & ΣCO2 Production (mmol m-2 d-1)
45.0
40.0
35.0
30.0
25.0
20.0
15.0
10.0
5.0
0.0
winter
spring
summer
fall
TCO2 Production
SOD dark only

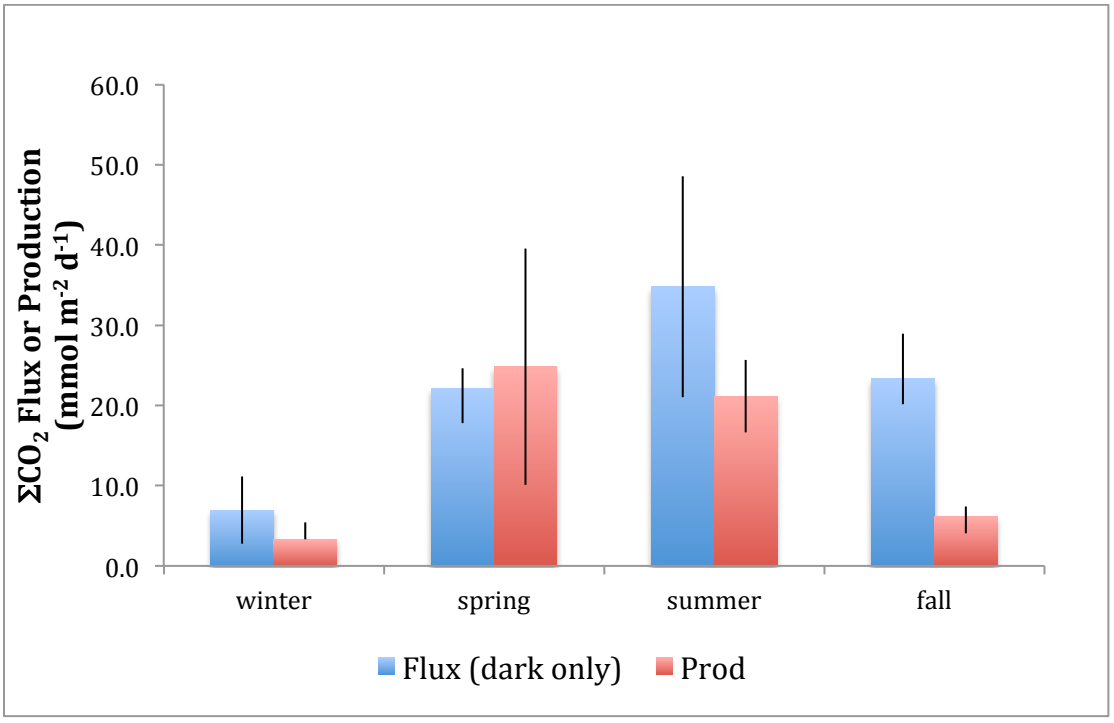
ΣCO2 Flux or Production (mmol m-2 d-1)
60.0
50.0
40.0
30.0
20.0
10.0
0.0
winter
spring
summer
fall
Flux (dark only)
Prod

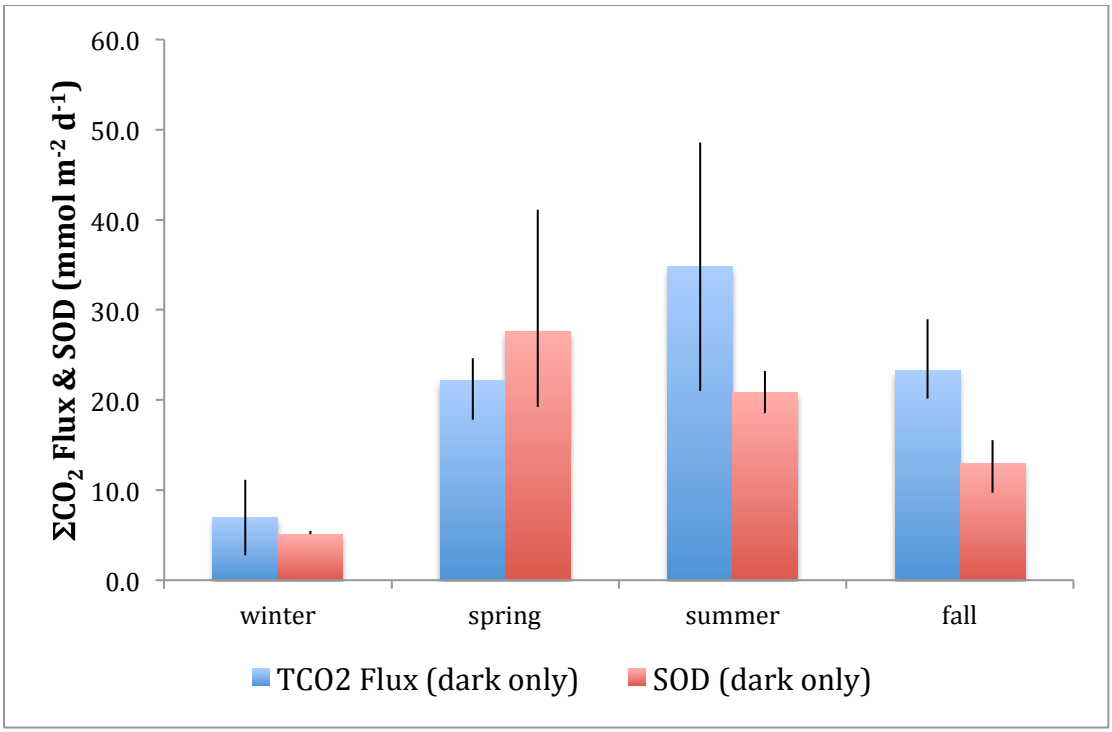

Figure 4.4 (a) Seasonal patterns of ΣCO_2 production & SOD; (b) Seasonal patterns of ΣCO_2 flux & ΣCO_2 production & (c) Seasonal patterns of ΣCO_2 flux & SOD. Except in fall, high intra-period variability limits generalizations about patterns in seasonal differences between production and fluxes.

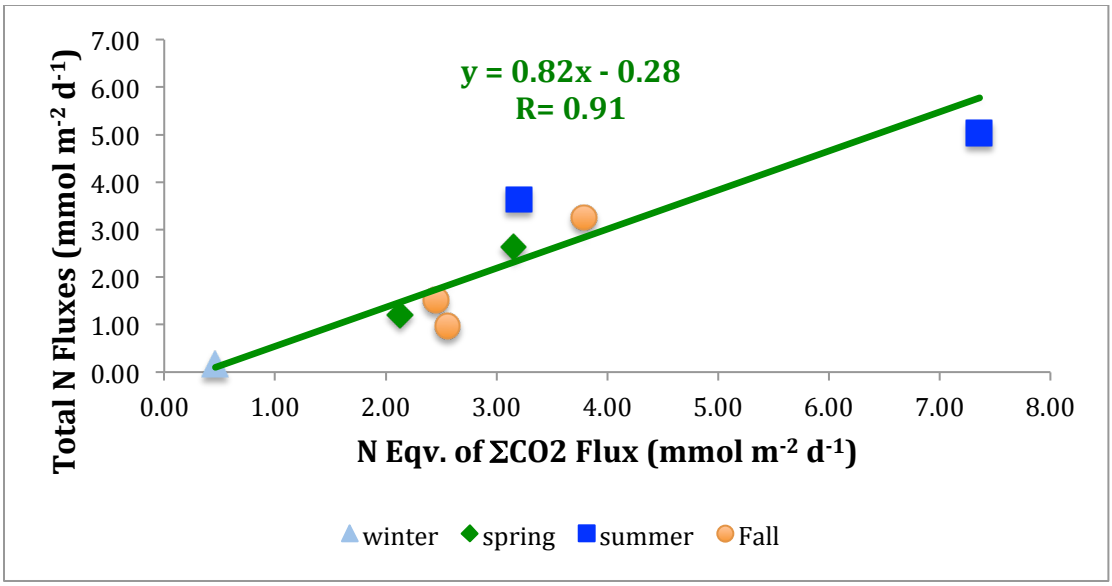
y = 0.82x - 0.28
R= 0.91
Total N Fluxes (mmol m-2 d-1)
N Eqv. of ΣCO2 Flux (mmol m-2 d-1)
7.00
6.00
5.00
4.00
3.00
2.00
1.00
0.00
0.00
1.00
2.00
3.00
4.00
5.00
6.00
7.00
8.00
winter
spring
summer
Fall

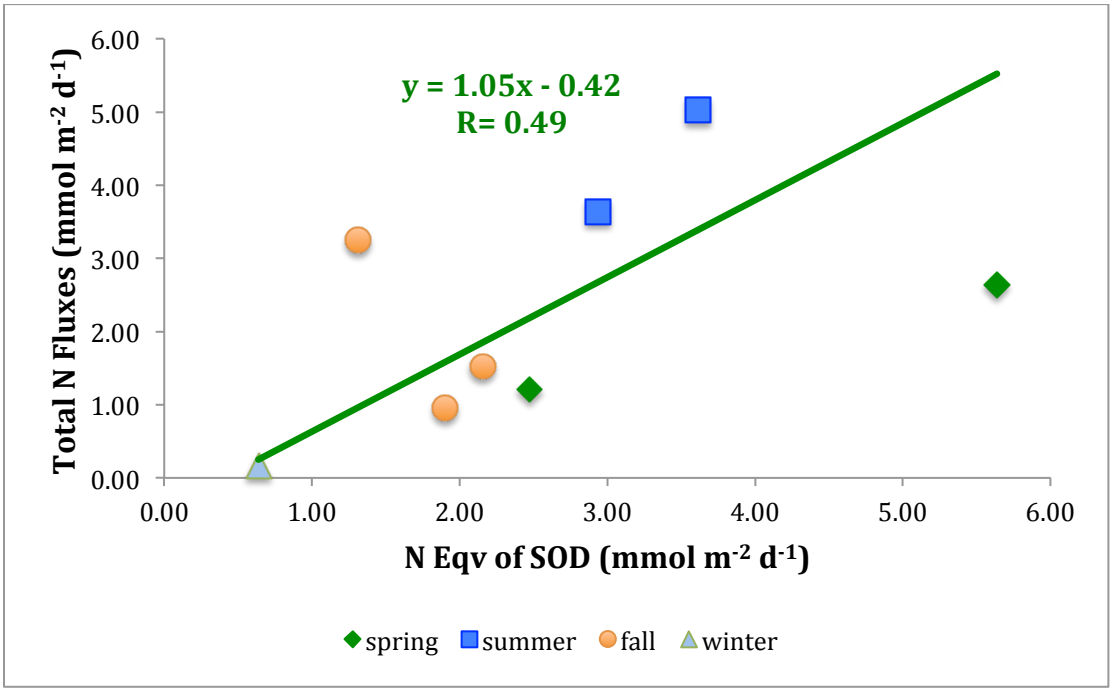
y = 1.05x - 0.42
R= 0.49
Total N Fluxes (mmol m-2 d-1)
N Eqv of SOD (mmol m-2 d-1)
6.00
5.00
4.00
3.00
2.00
1.00
0.00
0.00
1.00
2.00
3.00
4.00
5.00
6.00
spring
summer
fall
winter

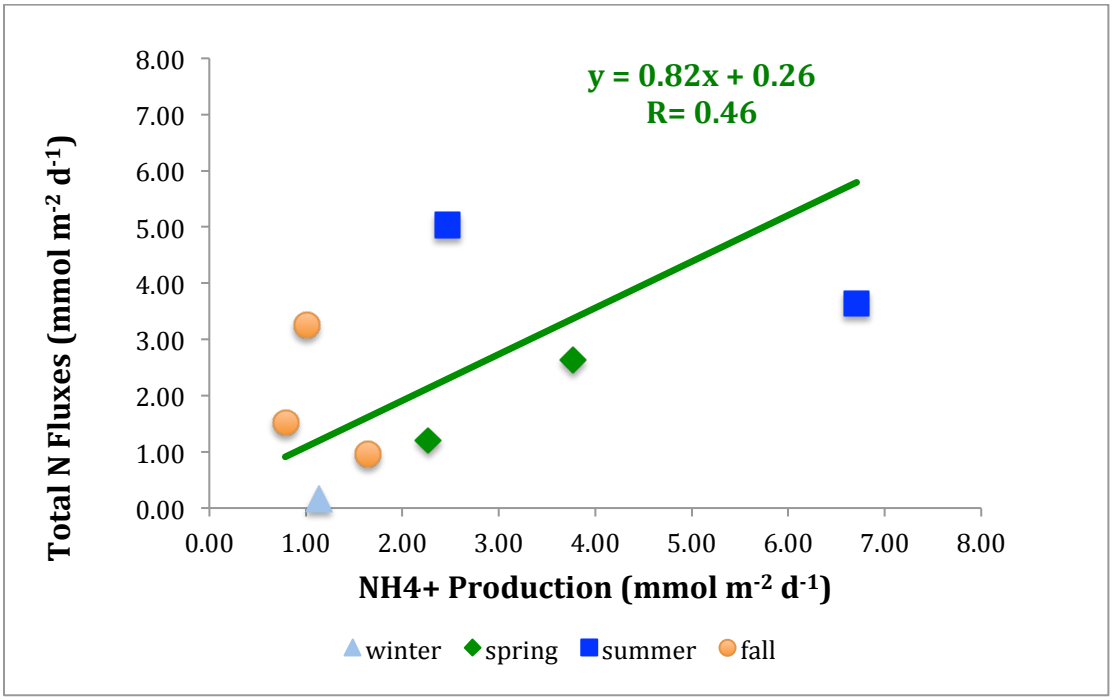

Figure 4.5 (a) **Geometric mean regressions of TNF against stoichiometric N remineralization equivalents of ΣCO2 flux**. **(b) Geometric mean regressions of TNF against stoichiometric N remineralization equivalents of SOD with a measured C:N ratio of 6.6 at an assumed adsorption coefficient of K= 1.7**. If the published average K value (K= 1.3) Mackin & Aller (1984)) is assumed, the C:N ratio increases to 7.77 and the slope of the regression trends increase so the resulting equations are (a) **y= 0.97- 0.28** and (b) **y= 1.24 x – 0.42**. **(c) Geometric mean regressions of measured TNF against measured NH_4^+ production assuming K= 1.7.** If K= 1.3, the regression equation is **y= 0.96x + 0.26**. Correlation coefficients do not change with changes in slope.

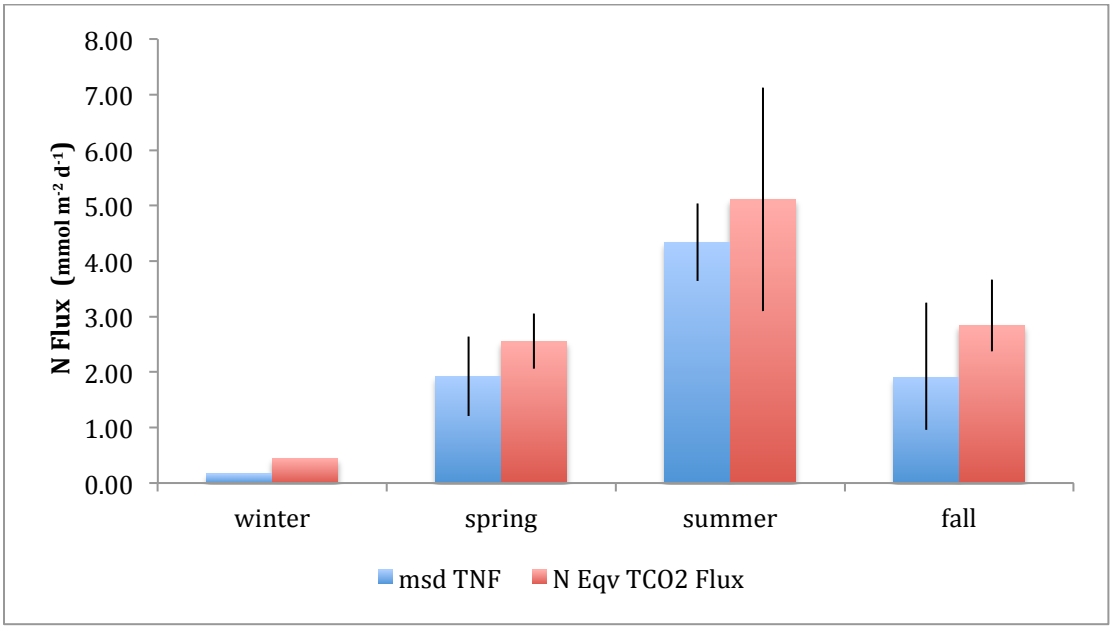
8.00
7.00
6.00
5.00
4.00
3.00
2.00
1.00
0.00
N Flux (mmol m-2 d-1)
winter
spring
summer
fall
msd TNF
N Eqv TCO2 Flux

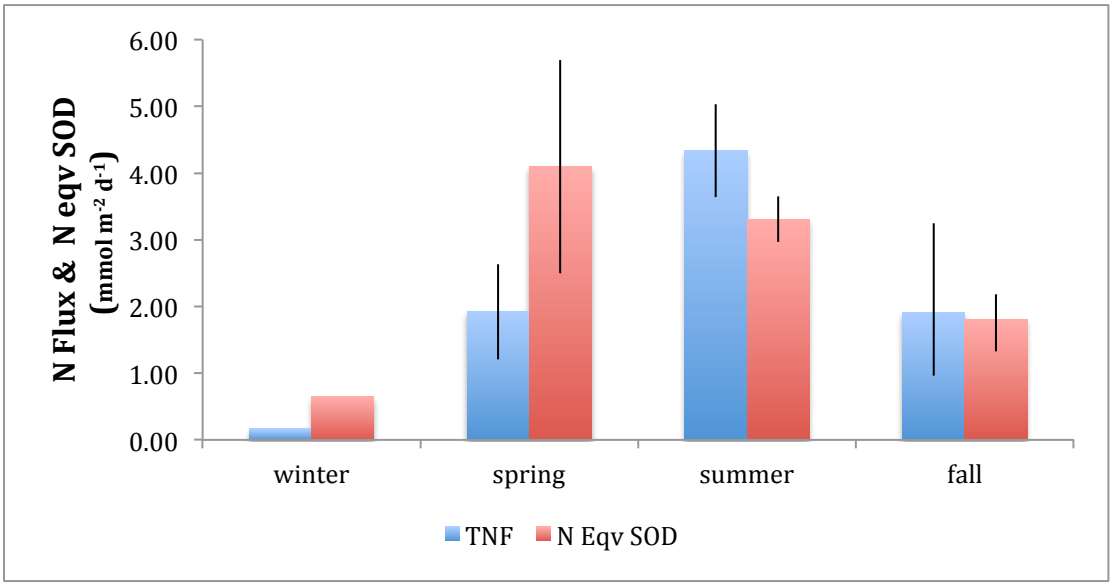
6.00
5.00
4.00
3.00
2.00
1.00
0.00
N Flux & N eqv SOD (mmol m-2 d-1)
winter
spring
summer
fall
TNF
N Eqv SOD

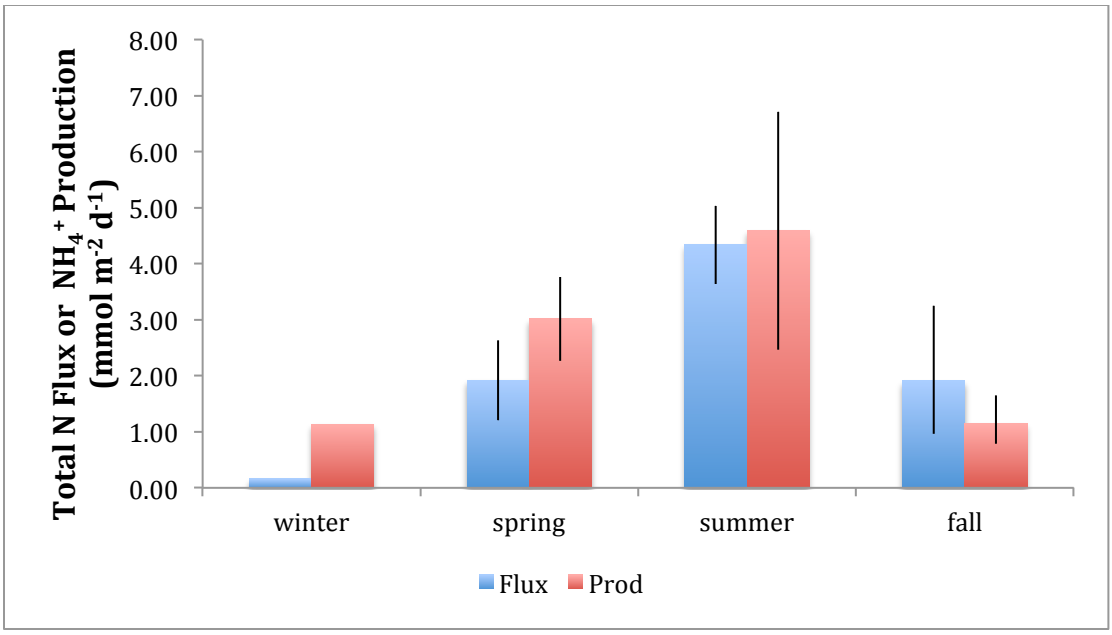

Figure 4.6 (a) Seasonal comparison of TNF and stoichiometrically equivalent measured ΣCO2 flux at C:N= 6.6 (K= 1.7); (b) Seasonal comparison of TNF and stoichiometrically equivalent measured SOD at C:N= 6.6 (K= 1.7) and a measured C:O_2 = 0.96. (c) Seasonal comparison of TNF and measured NH_4^+ production (K= 1.7). Chart patterns and intra-period variability do not change in any material way if NH_4^+ production values are estimated at C:N= 7.8 (K= 1.3).

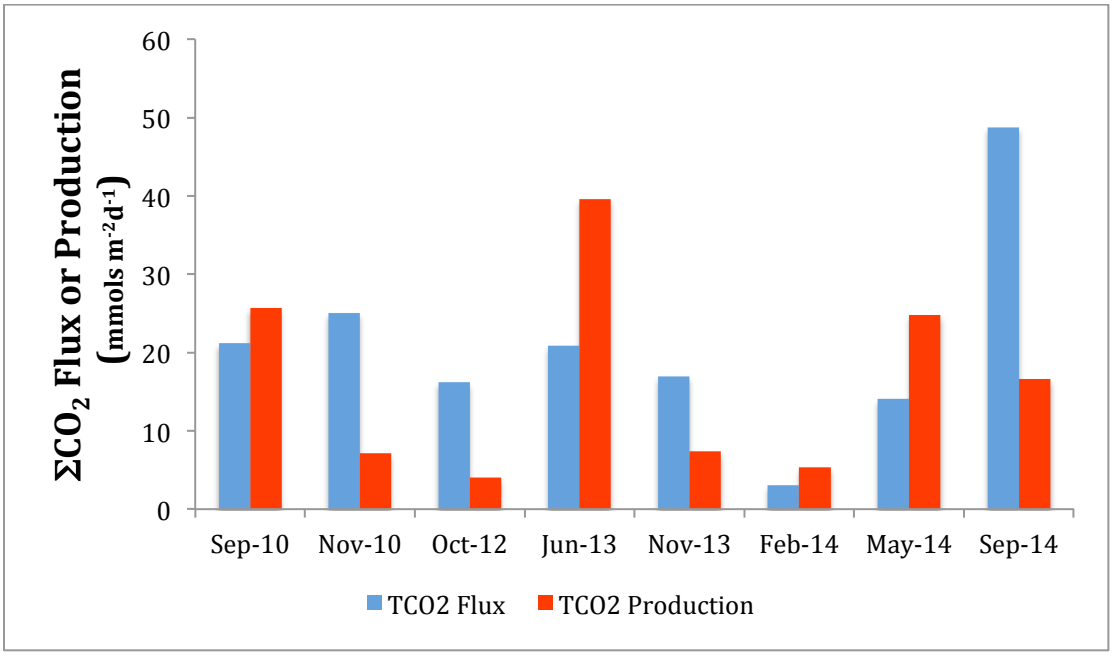

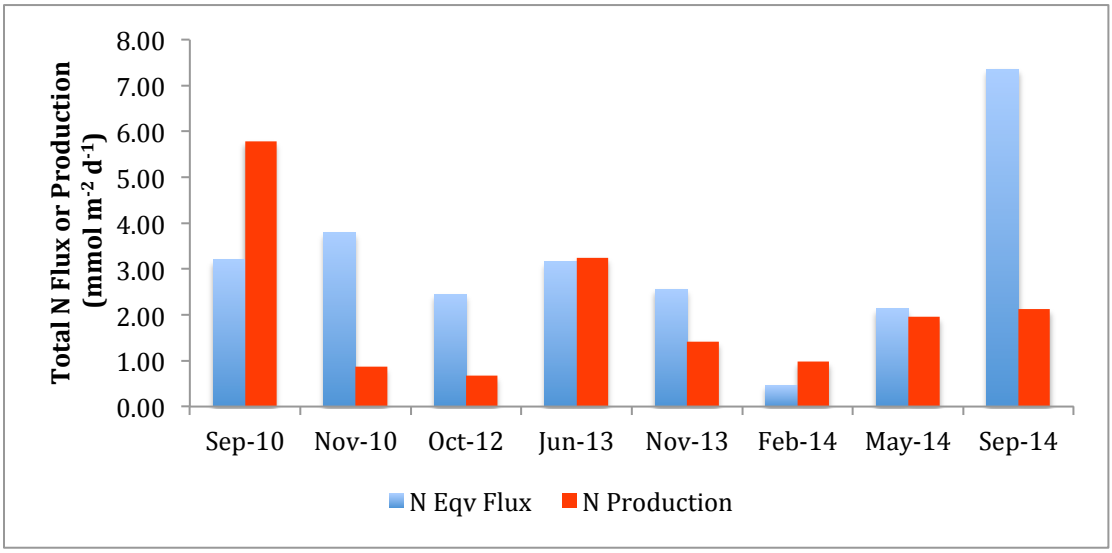

Figure 4.7 (a) Comparison of ΣCO_2 production (mean values) and ΣCO_2 flux by incubation period. (b) Comparison of NH_4^+ production (mean values) and TNF by incubation period. Co-incidence of differences between means of production and flux terms for ΣCO_2 and N in magnitude and direction (6/8 instances) suggest differences in duration or procedures between anoxic whole core incubations and flux incubations have an influence on mass balance outcomes apart from the individual C or N biogeochemistry. Only for spring periods does the similarity of these patterns not hold; in spring periods, ΣCO_2 production exceeds flux whereas TNF is approximately the same as N production.

CHAPTER 5: MACROFAUNAL INFLUENCES ON NET N_2 PRODUCTION

5.1 INTRODUCTION

Macrofaunal irrigating activity extends O_2 penetration depth, creates additional redox gradients around burrow walls and thereby enables greater diffusive solute fluxes across a greater area of sediment: water interface ((Aller (1988); Aller & Aller (1998); Gilbert et al (1998); Aller (2001)). As NH_4^+ concentration gradients generally increase with sediment depth, deeper O_2 penetration increases nitrification potential and porewater NO_3^- concentrations. Diffusion of NO_3^- into reducing sediments and oscillations of redox gradients allow for reduction of the additional NO_3^- supplied by burrow irrigation. Sediment incubations with bio-irrigating macro-fauna have shown enhanced production of N_2 or intermediates associated with denitrification compared to non-irrigated controls; e.g., for the estuarine polycheate *Nereis virens* (Kristensen et al 1991); for the amphipods of the genus *Corophium* (Pelegri et al (1994) and Rysgaard et al (1995); and for *Thalassinidean* shrimp (Howes et al (2004).

Spacing of irrigated burrow structures influences rates of N_2 production coupled to nitrification by determining not only the quantity of redox zones within the sediment but also the types of redox reactions which occur (Aller 2001; Gilbert et al 2003). If proximity is too close, sediment between burrows will become fully oxygenated displacing oxic/anoxic boundaries where dentrification would otherwise occur; if spacing is far apart, less sediment volume is occupied by suboxic zones and O_2 supplied from the burrow irrigation will be largely consumed by reduced metabolites such as sulfide (Aller 1988; Gilbert et al 2003).

Although active macro-faunal burrows in coastal sediments support redox zones which enhance N_2 production, sediments proximate to such sites may also provide biogeochemical conditions which enable N_2 fixation (Bertics et al (2010)). Although O_2 and NH_4+ are inhibitors of N_2 fixation (Capone 1998) and active burrows are irrigated with oxygenated water and surrounded by NH_4^+ gradients, N_2 fixation may occur nearby redox gradients surrounding burrows where O_2 has been consumed and coupled nitrification- denitrification limits availability of NH_4^+ (Bertics et al (2010)). Bertics et al (2010) measured C_2H_4 by ARAs in sediments proximate to and in the burrows of *Neotrypaea californiensis*. This shrimp actively irrigates chambered burrows averaging 0.2 m deep (but can extend burrows to .8 m depth) with multiple surface openings and may engage in wall-grazing and burrow gardening of microbes growing on introduced organic substrate (Bertics et al (2010) and references therein). The additional of labile organic matter

proximate to areas of low O_2 and denitrification (or anammox) may provide the carbon necessary for the energy required for N_2 fixation. N_2 fixation rates calculated from these measurements produced were similar to rates from sea-grass meadows or microbial mats (Bertics et al (2010)). Subsequently, Bertics et al (2012) estimated N_2 production by ARAs in these sediments and found rates similar to the N_2 fixation rates measured 2 years earlier. They argued for a critical role of N_2 fixation associated with burrow structures in the sedimentary N cycle.

Dense populations of the ophiuroid, *Amphioplus abditus,* and the stomatopod, *Squilla empusa,* were observed in GPB muds over a six year period. These infauna are responsible for a two-tiered bioturbation regime, an upper tier dominated by *Amphioplus* extending ~ 20 cm into deposits and a lower, deeper tier dominated by *Squilla* potentially extending up to ~ 3 m. This study investigated the effects of bio-irrigation by *A. abditus* on N_2 production and compared net N_2 concentrations in burrow-water of *S. empusa,* and overlying bottomwater to determine if net N_2 fixation was likely in the upper ~ 5- 10 cm of the burrows.

A. abditus has 5 arms, at least one of which extends above the sediment-water interface and undulates bottom-water into the rest of its multi-channel burrow structure (Woodley 1975). The animal's arms are covered with tiny tube feet which move food particles along its arms to the animal's mouth in its central disk; the animal obtains particles from bottomwater, the sediment surface and from the sediments themselves (Woodley 1975). Arms can extend several centimeters out from the sediment either into the bottomwater or along the sediment surface to gather food-particles. The result of arm undulation is *A. abditus* effectively ventilates the sediments to at least 6 cm (Woodley 1975) and can be expected to enlarge the oxic: anoxic boundary of bulk sediments and create redox gradients along the burrow-segments of each feeding arm. In this study, animals have often been found active to ~ 15 – 20 cm in GPB sediment. Greater oxygenation of the sediment enables greater nitrification of available NH_4^+ and therefore greater substrate for N_2 production, the area for which is enhanced by the redox gradients created by the animal's burrows.

S. empusa inhibits burrows with 2 different seasonal architectures in the northern end of its habitat range (Maine to Surinam). Winter burrows are vertical shafts to ~ 4 m depth; summer burrows are U-shaped with 2 vertical limbs (15-50 cm deep) and with a horizontal channel parallel to the sediment surface up to 2 m long (Meyers 1979). In each case, diameters are from 1- 10 cm (Meyer 1979). *S. empusa* are predatory shrimp which leave their burrows to hunt at night (Wortham- Neal (2002)) whereas *N. californiensis* are deposit- feeders (Bertics et al (2010)). Although both animals irrigate their burrows, no published information about the rate for either animal has been found. Burrow irrigation rates by other relatively large infaunal crustaceans such as *Callianassa* range from ~ 30 – 100 mL hr^{-1} (Koike and Mukai, 1983; Forster and Graf, 1995). The objective of this

investigation was to determine whether there was evidence of net N_2 fixation in *Squilla* burrows rather than to directly compare potential N_2 fixation rates between *S. empusa* and *N. californiensis* burrows.

5.2 METHODS

(i) Measurement of *A. abditus* influence on sedimentary fluxes. N_2 production, NH_4^+ and NO_3^- fluxes and SOD were compared with *Amphioplus* densities counted in sediment cores and benthic chambers. Data were collected from lab sub-cores used to measure fluxes in June & October 2013 and February, May & September 2014 and from benthic chambers in June 2013 and May & September 2014. As these incubations were designed to replicate *in-situ* conditions, the effect of *Amphioplus* on N fluxes was not isolated. These incubations were carried out in triplicate. In an effort to further resolve patterns between N_2 production and ventilating activity, a series of incubations of sieved, homogenized sediments amended with different numbers of *Amphioplus* were carried out with sediment collected in February and May 2014. Amendments consisted of 0 (control), 1 & 2 animals representing densities of 0, 144 and 288 animals per square meter. These incubations were carried out in duplicate.

Incubation procedures, sample processing and measurement methods were the same as those described in chapter 2.

(ii) Measurement of N_2 & O_2 in *S. empusa* burrow-water. Samples of burrow-water (~ 6 replicates) and overlying bottomwater (~ 3 replicates) were taken seasonally by scuba- divers with 12 cm Tygon tubes (1/4" OD; 1/8" ID) attached to a 30 ml (N_2) and 10 ml (O_2) syringes. Samples were collected from between 5 and 10 cm depth in the burrows; sampling tubes were marked with white tape at 5 and 10 cm intervals to guide divers. N_2 & O_2 samples were measured in November 2013, February & May 2014 and N_2 samples only were measured in May 2015. Analytical methods were the same as those described in chapter 2. 12.6 ml Exetainers for N_2 measurements were immediately over-filled (bottom to top) from syringes upon divers return onboard and reagents for the Winkler titration were then injected into 10 ml syringes. All samples were stored at in-situ bottom-water temperatures until returned to the lab.

5.3 RESULTS & DISCUSSION

(i) The effect of *A. abditus* on SOD, N_2, NH_4^+ & NO_3^- fluxes. The number of *A. abditus* recovered from completed incubations reflected densities averaging 211 individuals (S.D. 260) m^{-2} in cores and 88 (S.D. 174) m^{-2} in chambers. The comparison of density counts against sedimentary fluxes shows the highest N_2 production and NH_4^+ fluxes occurred at densities below 300 m^{-2} whereas SOD and NO_3^- fluxes were similar across all densities (Fig. 5.1 (a- d)).

When *ex-situ* and *in-situ* results within individual periods were examined, a pattern emerges whereby incubations with higher animal densities have higher fluxes of N_2 and SOD regardless of whether the incubations were carried out *ex-situ* and *in-situ*; these values do not include incubations with high animal densities (Table 5.1). This pattern does not repeat in NH_4^+ & NO_3^- fluxes.

The February 2014 incubations were first incubated at *in-situ* temperatures approaching 0° C. Animals in these intact cores were uniformly found buried at depths between 4- 10 cm and were not noticeably ventilating; neither N_2 or O_2 fluxes showed differences correlated with animal densities (Fig. 5.2 (a)). Subsequently, core temperatures were allowed to increase to ~ 22° C. After amendments with green algae, animals were observed to ventilate burrows. Incubations showed average N_2 production and SOD increased linearly (R^2 = 0.99 and .92 respectively) with increases in *A. abditus* densities (Table 5.2 & Fig. 5.2 (a)). Subsequently, the experiment was repeated with fresh sediment collected in May 2014 and similar results were obtained (Table 5.2 & Fig. 5.2 (b)).

All incubations produced results implying *A. abditus* enhanced N_2 production and SOD and corroborate the importance of irrigating infauna documented by Kristensen et al (1991); Pelegri et al (1994) and Rysgaard et al (1995) among others. On a seasonal scale, however, the impact of irrigation by these animals could not be analyzed because of overlapping animal densities between periods. Even if specific animal densities could be linked to specific seasonal periods, interpretation of such results would be difficult because there is no necessary link between animal number and ventilating activity.

(ii) Measurements of net N_2 flux in *Squilla* burrows. *S.empusa* burrows were sampled seasonally and showed consistent, significantly higher N_2 concentrations over ambient seawater levels (Fig. 5.3). Burrow-water was supersaturated with respect to N_2 at a broad range of temperatures, implying net N_2 production. Because of N_2 loss into overlying water near the burrow entrance, N_2 concentrations in deeper burrow water may be far higher than measured values in the upper ~10 cm. However, *S. empusa* burrows are large and clearly net N_2 fixation could occur deeper down in the burrow channel or burrow walls around redox zones with low O_2 and high rates of denitrification (which would reduce inhibitory NH_4^+). There are reports of concomitant N_2 production and N_2 fixation in proximate sediments (e.g., Haines et al (1981); Fulweiler et al (2007); Fulweiler et al (2013); this study- chapter 3).

Because all measurements made in this study demonstrate excess N_2 near the burrow overlying water boundary and presumably correspond to random times within possible irrigation cycles of multiple individuals, it seems highly likely that net denitrification within the burrow system dominates the net flux. If we assign a general irrigation rate of ~ 1 L d^{-1} (~ 50 mL hr^{-1}) based on other crustacean species, an estimated burrow volume of ~1 – 4 L (summer – winter

burrows; Myers, 1979), and a N_2 concentration difference of 5 µM, then the net flux rate from the burrows is ~ 1 - 5 µM/d (winter – summer). Normalized to the entrance surface area (~20 cm^2), these rates correspond to N_2 fluxes across the sediment – water interface of 0.05 – 0.25 umol cm^{-2} d^{-1} or ~ 0.5 – 2.5 mmol m^{-2} d^{-1}, in the range of those measured away from *Squilla* burrows. Interestingly, because *Squilla* burrow surface area is far greater than the burrow entrance alone, when normalized to burrow surface area this flux range actually implies that net denitrification is smaller around lower tier burrows than in upper tier and thus a possible relatively greater importance of N_2 fixation in the lower tier.

Comparisons of O_2 concentrations in burrow-water and bottom-water in February and May strongly support Meyers (1979) interpretation of the purpose of seasonal burrow architecture adopted by *S. empusa* in the northern end of its habitat range (Fig. 5.4). In winter, *S. empusa* constructs deep, vertical burrows (~ 4 m) and likely slows metabolic activity to minimize mixing of colder overlying bottom-water with warmer burrow-water. From spring thru fall, the animal inhabits a shallow, chambered burrow with multiple openings.

The dense populations of *Amphioplus* within the upper 15- 20 cm depth interval and *Squilla* within the upper .5 – 4 m depth interval create a 2 tier sedimentary structure whereby oxygenated surface water is extensively irrigated deeply into GPB sediments thereby creating redox gradients capable of enhancing N_2 production.

5.4 TABLES & FIGURES

Table 5.1 N_2 Production, SOD, NH_4^+ & NO_3^-/NO_2^- fluxes sorted by sampling period and *A. abditus* densities. Within specific measurement periods, incubations with higher densities of *A. abditus* produced higher fluxes of N_2, O_2 and NH_4^+ than those with lower densities. O_2 data for benthic chambers was comprised in processing in June 2013 and therefore SOD values are not shown for the period.

All fluxes in mmol/m^2-d.

	Amphioplus density	N_2 flux	SOD	NH_4^+ flux	NO_3^- flux
June 2013 bc	370	0.15		1.95	0.00
June 2013 lab	432	0.36		1.93	-0.15
May 2014 bc	87	1.95	24	-1.49	-0.16
May 2014 lab	48	-0.08	11	0.17	-0.07
Sep 2014 bc	109	1.23	25	5.80	0.03
Sep 2014 lab	0	0.55	19	3.82	0.35

Table 5.2 Animal density experiment in sieved homogenized sediment w/ additions of *A. amphioplus*

Units: mmol m^{-2} d^{-1}

	Feb 2015 sediment at 22° C		**May 2015 sediment at 15.7° C**	
Animal density	**N-N_2**	**SOD**	**N-N_2**	**SOD**
0	0.54	10.6	0.82	11.7
144	0.95	12.2	0.92	12.8
288	1.2	12.7	1.3	12.8

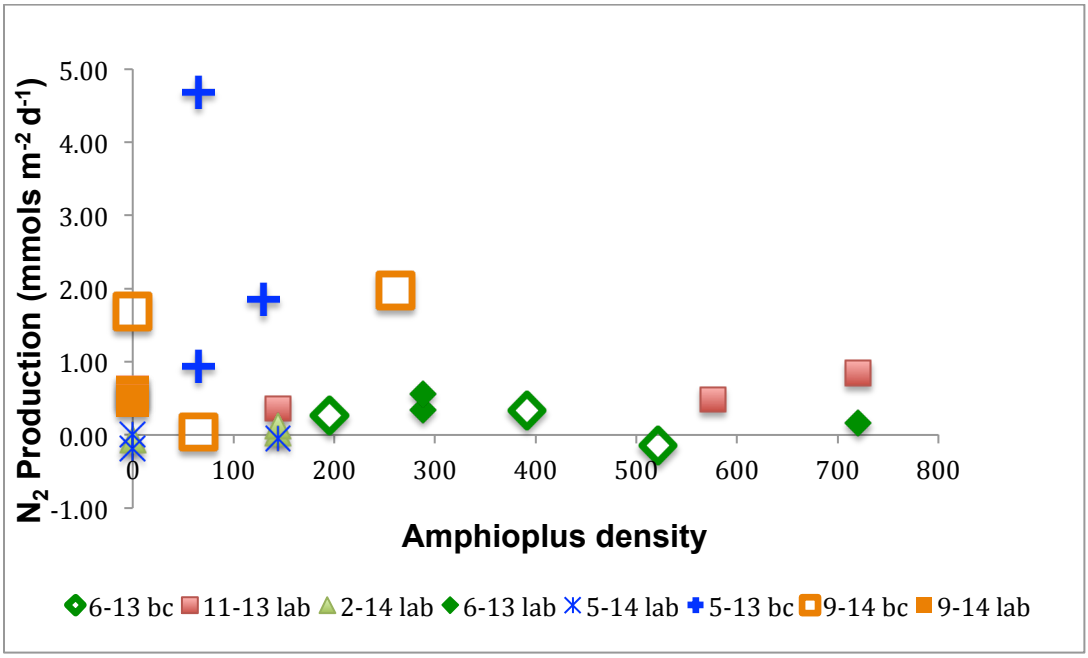
5.00
4.00
3.00
2.00
1.00
0.00
-1.00
0
100
200
300
400
500
600
700
800
N2 Production (mmols m-2 d-1)
Amphioplus density
6-13 bc
11-13 lab
2-14 lab
6-13 lab
5-14 lab
5-13 bc
9-14 bc
9-14 lab

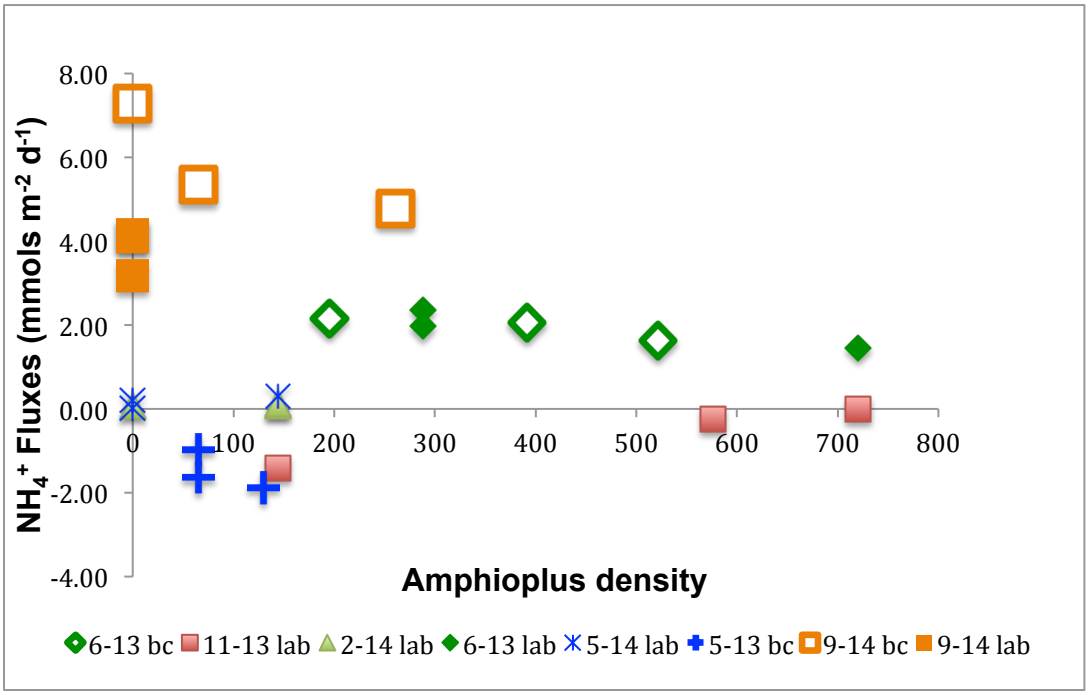
8.00
6.00
4.00
2.00
0.00
-2.00
-4.00
0
100
200
300
400
500
600
700
800
NH4+ Fluxes (mmols m-2 d-1)
Amphioplus density
6-13 bc
11-13 lab
2-14 lab
6-13 lab
5-14 lab
5-13 bc
9-14 bc
9-14 lab

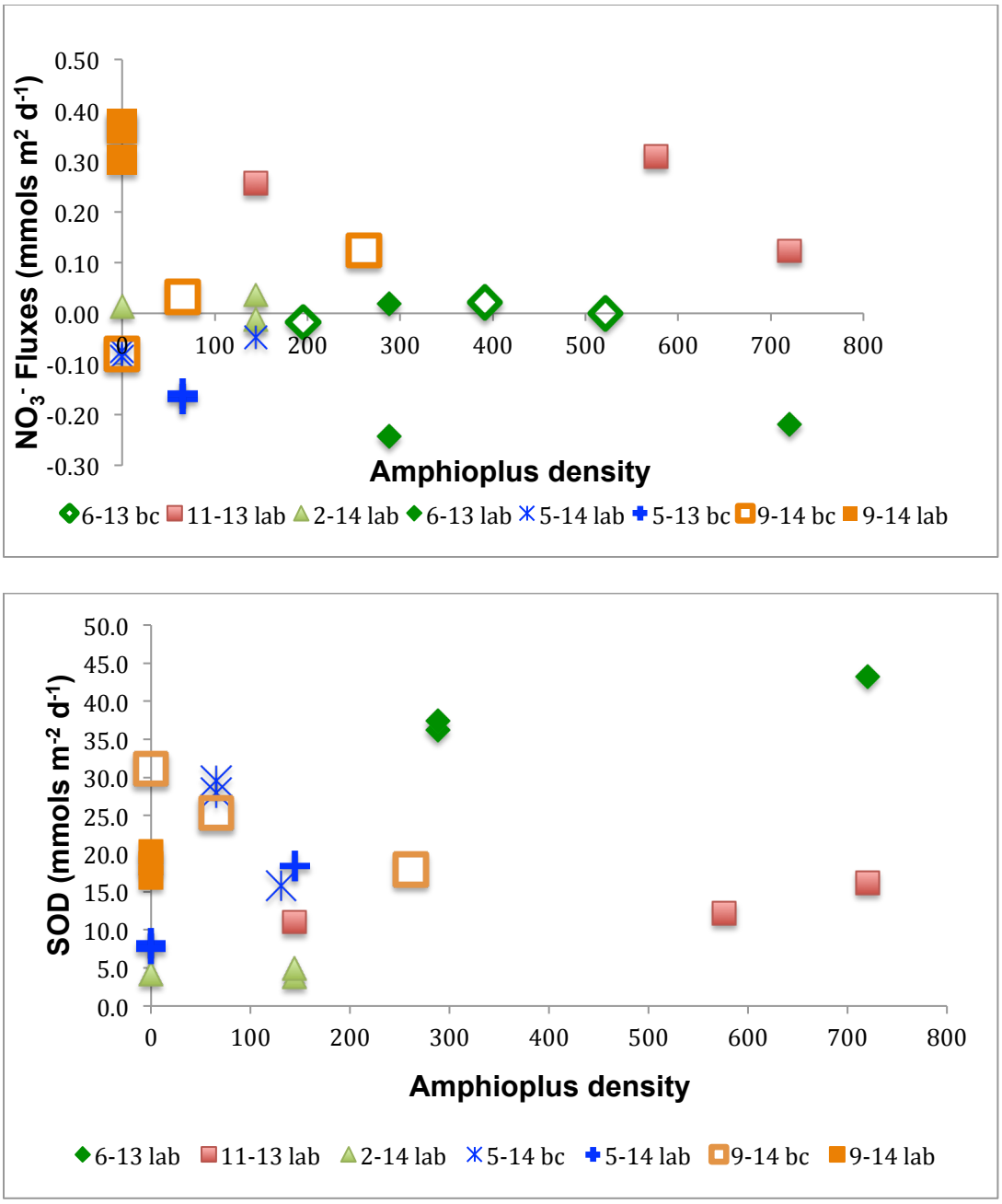

Fig. 5. 1 (a) N_2 fluxes compared to *Amphioplus* densities; (b) NH_4^+ fluxes compared to *Amphioplus* densities; (c) NO_3^- fluxes compared to *Amphioplus* densities; and (d) SOD compared to *Amphioplus* densities. The highest N_2 production and NH_4^+ fluxes occur at animal densities below 300 m^{-2} whereas there is no apparent relationship between SOD and NO_3^- fluxes in these incubations.

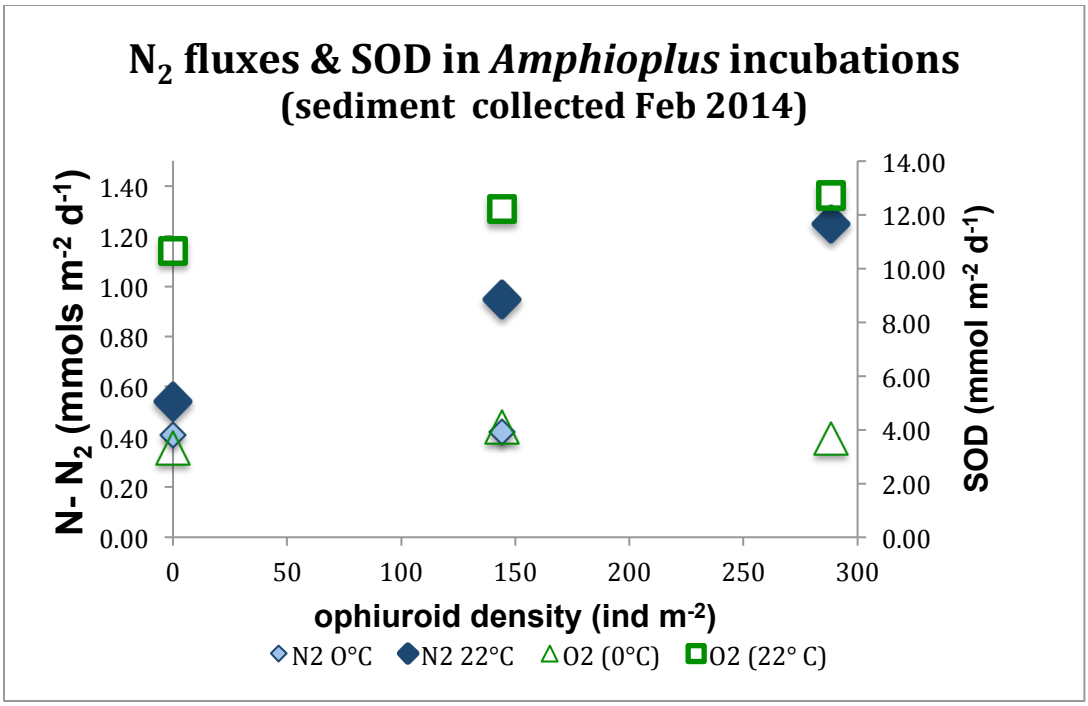

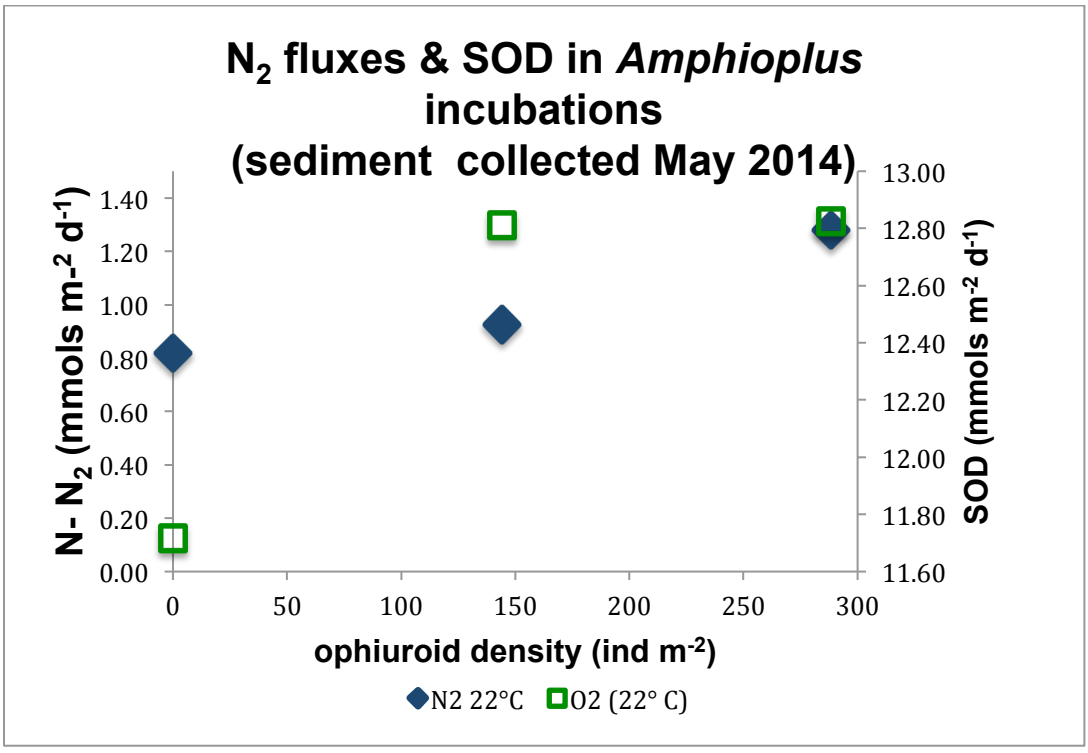

Fig. 5.2 (a) N_2 fluxes & SOD in Feb 2014 sediment incubations with *Amphioplus* additions; (b) N_2 Production & SOD in May 2014 sediment incubations with *Amphioplus* additions. February sediments were incubated at 0° C & 22° C. Sediments were sieved & homogenized sediments prior to additions.

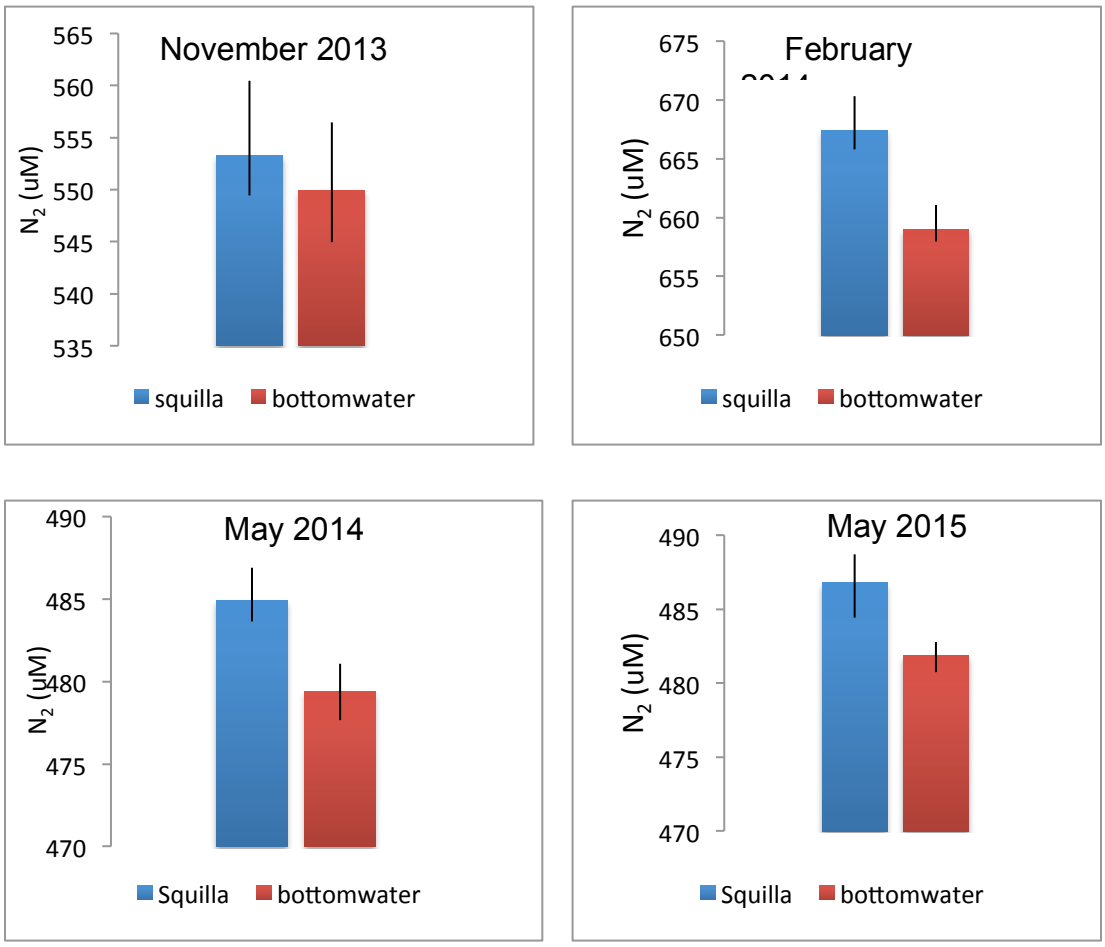

Fig. 5.3 Seasonal N_2 concentrations in bottom water and *Squilla* burrows in central Great Peconic Bay, NY. Burrow water N_2 exceeds bottom water during all sampled seasons.

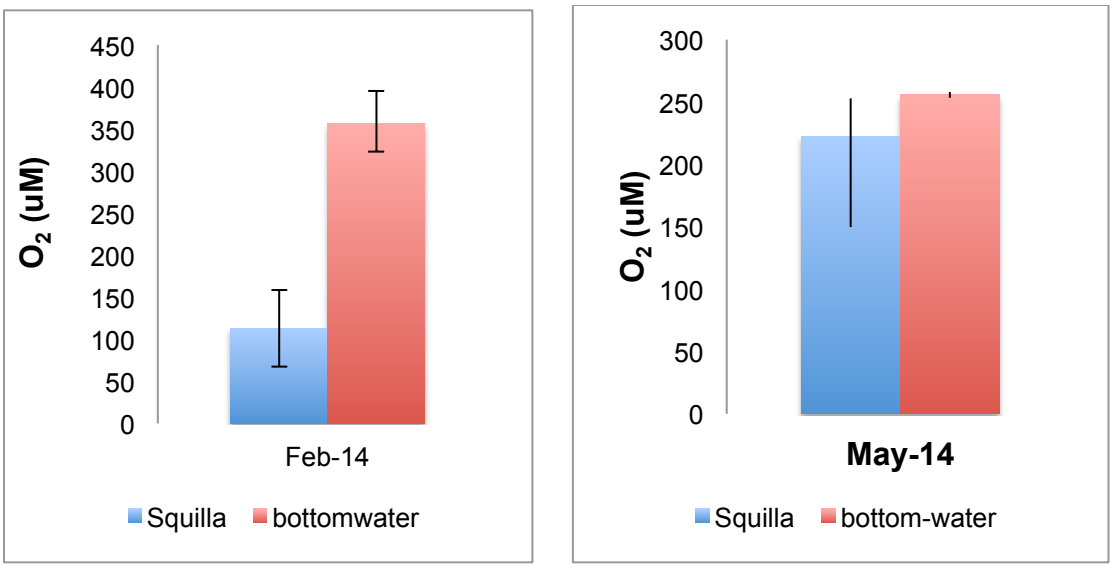

Fig. 5.4 O_2 concentrations in burrow-water and bottomwater in February and May 2015. The large difference in relative O_2 concentrations between burrow-water and bottomwater in February compared with May likely reflects seasonal changes to burrow architecture engineered by *S. empusa* to adapt to winter temperatures (5° C) which would otherwise be lethal (Meyer 1979).

CHAPTER 6: EFFECTS OF $CuCl_2$ AND ATMAC 12, SINGLY AND COMBINED, ON SEDIMENTARY N_2 PRODUCTION

6.1 INTRODUCTION

There is evidence from multiple areas of research that denitrification is susceptible to environmental contaminants. The aim of the present investigation was to determine what impacts environmentally relevant concentrations of different classes of the commonly used quaternary ammonium surfactant compounds (QACs) and the heavy metal contaminant Cu - alone and in combination- have on denitrification overall and on specific steps of its reductive pathway in estuarine sediments and in particular muds from Great Peconic Bay.

While copper (Cu) in trace amounts is an essential component of nitrous oxide reductase, the metalloenzymene facilitating the reduction of N_2O to N_2 (Granger & Ward 2003), several studies have demonstrated Cu, among other heavy metals, is inhibitory to N_2 production in soils and sediments by interfering with the final step of denitrification in which N_2O is reduced to N_2 (Bollag & Barabasz (1979); Holtan-Hartwig et al (2002); Magalhaes et al (2011)). These studies linked incremental Cu additions (in the range of 4 – 250 µg Cu g^{-1} sed.) with increases in N_2O inventories relative to N_2 production. Quantitative PCR analysis of the functional genes for nitrite reductase (*nirS & nirK*) and nitrous oxide reductase (*nosZ*) showed decreases in the abundance of these genes with increasing Cu additions (Magalhaes et al. 2011).

In addition to inhibiting reductive steps in the denitrification sequence, Cu may inhibit production of nitrate. Nitrification is susceptible to compounds which interfere with (1) the functioning of enzymes (NH_3 monooxygenase & oxidoreductase) which catalyze oxidation of NH_3 to NO_3^- or (2) the availability of copper which is a component of NH_3 monooxygenase (Ward 2008). Cu additions have been shown to inhibit nitrification in waste treatment streams at 10 mg L^{-1} (e.g., Lee et al 2009) and in soils from 100 µg Cu g^{-1} (Bääth 1989 and references therein).

Quaternary ammonium compounds (QAC) are a class of cationic surfactants widely used in industrial and household applications including commercial disinfectants, anti-microbial soaps, detergents, fabric softeners, and cosmetics. Discharged to the environment through wastewater, these hydrophobic ion-pair complexes adsorb strongly to sediments. Because of their high sorption capacity (Hand et al 1990), QACs may persist in marine sediments at concentrations above those commonly associated with organic contaminants

(Li & Brownawell 2010); for instance, dialkyldimethylammonium (DADMAC), benzylalkyl- dimethylamonium (BAC) and alkyltrimethylammonium (ATMAC) compounds have been reported at median concentrations levels of 26, 1.5 & 0.52 μg g^{-1} in urban estuaries along the NY and NJ coasts (Li & Brownawell 2010) and total BAC compounds have been reported to reach 5.8 μg g^{-1} in sediments of a European river (Kreuzinger et al 2007).

Toxicity of QACs in sediments depends on their bioavailability which is controlled by partitioning bewteen solid and aqueous phases (Ismail et al 2010) but little research has been published describing QAC toxicity in or adsorption to sediments. Sakar et al (2011) found potential nitrification was inhibited in incubations of different soil types at additions of 50 μg QAC g^{-1} soil. Tezel and co-researchers found (1) didecyl ammonium chloride (DDAC) concentrations above 50 mg L^{-1} (Tezel et al 2008) and (2) benzalkonium chlorides (BAC) above 50 mg L^{-1} (Tezel et al 2009) inhibited the final step of the denitrification reductive pathway in food processing waste streams resulting in N_2O accumulations. Alternately, Hajaya et al (2011) found BAC inhibited coupled nitrification denitrification primarily at the nitrite reduction step at 50 mg L^{-1} in food processing waste cultures. But total suspended solids in these aqueous solutions were always < 7 g L^{-1} and therefore presented close to a multiple of 100 times less particle surface area compared to muddy sediments with a porosity ~ .80 used in this study. Also these toxicity thresholds are above the aqueous- phase levels at which QACs are likely to be bio-available based on equilibrium with solid-phase quantities presently found in urban marine sediments (Li & Brownawell 2010).

Harrison et al (2008) demonstrated increased antimicrobial efficacy of certain classes of QACs when used in combination with copper (Cu^{2+}) to eradicate six different strains of bacterial biofilms. While the synergistic effect was demonstrated at QAC concentrations greater than those currently present in the environment and at Cu^{2+} concentrations at the upper range of those present in some polluted estuaries, the experiments were carried out on *Pseudomonas aeruginosa* biofilms which were specifically chosen because they are highly resilient to antimicrobials (Harrison et al 2008). The synergistic effect of Cu^{2+} and the QAC cocktail may exert itself at lower concentrations with less robust bacteria. But any research into the effect of Cu^{2+} or other metals present within the sedimentary matrices on the toxicity of QACs to denitrifying bacteria in marine sediments has not been publically reported.

The research cited above provides credible evidence that (1) a number of species of heavy metals and classes of QACs inhibit overall denitrification; (2) nitrous oxide reductase may be more susceptible to toxic effects from these contaminants than other enzymes or cellular mechanisms in the denitrification pathway, and consequently, (3) at least the final step of the denitrification process may be inhibited by environmentally relevant concentrations of metal and QACs alone or in combination. In light of the ecological importance of

denitrification, the evidence to date suggests risk assessments on the effects of QACs and Cu^{2+} - both alone and in combination- on denitrification in different soil and sediment matrices need to be carried out. Were antimicrobial or metal interference in the denitrification pathway described here to occur over a regional scale, nitrate reduction could provide a source of N_2O to the atmosphere rather than a sink for anthropogenic nitrogen inputs to the ocean. Because most marine denitrification occurs in sediments of estuaries, shelves and continental margins (Seitzinger et al 2006), well within reach of anthropogenic influence, the impact of QAC and metals pollution on denitrification could be significant on a global scale.

The hypothesis that QACs & Cu synergistically or individually inhibit denitrification was tested by amending sediments with variable concentrations of ATMAC 12 and $CuCl_2$ and measuring denitrification responses. If N_2 fluxes from sediments amended with combinations of ATMAC 12 and $CuCl_2$ are lower than N_2 fluxes from sediments singly amended, then support will be gained for the idea Cu & QACs synergistically inhibit denitrification. If either CuC_{l2} or ATMAC 12 singly amended sediments generate lower N_2 fluxes than non-amended sediments, then support will be gained for the idea Cu and/or QACs alone exert a control on denitrification.

GPB sediments retrieved on 9-23-2014 were incubated with amendments of 500 ppm of ATMAC 12, 200 ppm of $CuCl_2$ and 3 combinations of these compounds (ATMAC 12: CuCl2 500: 200 ppm; 250:100 ppm & 125:50 ppm). ATMAC 12 additions were higher than concentrations reported in present-day urban estuaries; e.g., in Jamaica Bay, total ATMAC concentrations were reported between 360 to 6,750 ng ATMAC g^{-1} sediment (Lara- Martin et al (2010) and across a broad swath of sediments in greater NY Harbor, ATMAC concentrations were reported between 0.98- 5,300 ng ATMAC g^{-1} (Li & Brownawell 2010). Total concentrations of QACs in urban impacted estuaries reach ~ 76 µg g^{-1} (Li & Brownawell 2009). $CuCl_2$ was added at concentrations near levels found in urban estuaries in the developed world; e.g., mean concentrations found in industrial, mangrove and storm-water impacted sediments in Sydney, Australia were 481, 261 & 200 µg g^{-1} (Shaike et al (2014)); concentration in the upper 2 cm of sediment (reflecting deposition after sewage outfall was moved offshore) were ~ 70 µg $g^{-}1$ at Hingham Bay in Boston Harbor and 115 µg g^{-1} in deeper sediments (Kalnejais et al (2015)). The Cu amendment levels in this study reflected realistic, present day urban estuary solid-phase values; the amendments levels for ATMAC 12 were higher (but not by orders of magnitude) based on uncertainty about their bioavailability in fine grained- GPB sediments for which there was no published reference (see discussion).

6.2 METHODS

To investigate the toxicity of QAC and Cu amendments to N_2 production, sediment incubations were carried out in June and September-October 2014.

The earlier set was carried out to explore the scale of amended concentrations relevant to establishing toxicity; the second set was designed to quantify the statistical significance of its results. The first set of incubations included amendments of 2 QACs, dodecyl trimethyl (ATMAC 12) and a mix of benzyl-alkyl ammonium chloride 12 & 14 (BAC) as well as $CuCl_2$. BAC amendments were not included in the second set of incubations due to practical considerations. The first set of incubations included a range of amendments with higher concentrations than the second set and, except for blanks, replicate measurements were not made. Finally, measurements in the first set of incubations were made on days 2 and 20. Otherwise, procedures followed in the first set of incubations were similar to those described below for the second set. Descriptions of the quantities of amendments added in each incubation set are contained in Table 6.1 (a) & (b).

For the second set of incubations, amendments dissolved in methanol were added to 8.2 cm acrylic cylinders (subcores) containing 25 g of < 10 μm spherical glass beads; methanol was then evaporated from the subcores in a hood. The upper 3 cm of GPB sediment was removed by spoon from the box-cores in which it was collected and homogenized. ~ 150 g (wet weight) of this sediment was added to each subcore and mixed with the glass beads. Subcores were then filled with filtered GPB seawater (44 μm mesh), stirred with a glass stirring rod; sediment was then allowed to settle and subsequently the cores were placed in aerated buckets filled with filtered GPB seawater at room temperature. Incubations of amended sediment and un-amended blanks were carried out in triplicate.

Grain size from samples taken with a van Veen grab near where the incubated sediment was collected have phi (Φ) values ~ 8.1 – 8.5 and were characterized as mud (Cerrato et al 2010). These grain size samples likely closely approximate the characteristic of the sediment incubated. The glass beads used to mix the amendments into the sediment have diameters approximately 1 to 3 times the ~ 3 μm mean nominal diameter of the sediment particles. The density of the glass beads was measured as 1.3 g/cc and the dry sediment density is assumed at 2.65 g/cc. Since 25 g of glass beads was mixed into ~ 150 g of wet sediment, total volume of glass beads was calculated as ~ 19 cc versus ~ 23 cc of dry sediment using a measured dry:wet sediment ratio of 0.41. The glass beads were mixed into the sediment by hand before the overlying seawater was added and again afterwards.

Measurements of SOD, N_2, NH_4^+ and NO_3- fluxes were made on day 4, 10 and 22 of the oxic incubation period by removing the cores from the buckets, sealing them and subsequently sampling the overlying water with syringes thru Leur-lock fittings at 4 time-points over ~ 24 hour periods. N_2 was measured using MiMS (Kana 1994); O_2 by Winkler titration; NH_4^+ by the phenolhypochlorite method (Solorzano 1969) ; and NO_3^- by VCl_3 reduction and Griess reagent (Doane & Horwath (2003).

N_2O fluxes were not monitored in this study. Inhibition of the last step of the denitrification process as described by (Holtan- Hartwig et al (2002), Magalhaes et al (2011) and Tezel et al (2008) & (2010) could have resulted in diversion of oxidized N to N_2O instead of N_2. However, in the experimental set-up used in this study, any N_2O (g) would have been measured as N_2 because a copper-reduction furnace was included in the MiMS used.

Sedimentary flux rates were calculated by regression of measured values (O_2, N_2, NH_4^+ & NO_3^-/NO_2^-) by normalizing slopes to surface area of incubation cores; regressions were analyzed for significance and results reported in Table 6.2. Means of incubated replicates (O_2, N_2 & NH_4^+ flux rates) were analyzed by single factor ANOVA for significant differences. Significant results were subsequently assessed by Tukey tests. Results of ANOVA with insignificant p-values were analyzed for homogeneity of variance by the Barlett's test; in these cases analyzed, no heterogeneity in variance was identified and consequently no further analysis of differences in means was carried out.

Results from exploratory incubations (June 2014) for a 20 day period showed N_2 production in sub-cores amended with combinations of 500:200 ppm QACs (both ATMAC and BAC): $CuCl_2$ were significantly ($\alpha = .05$; *t- tests*) lower than N_2 production in singly- amended and un-amended sediments collectively. No incubations for this period showed significant differences in N_2 production against the un-amended sediment as results from the two blanks were widely dispersed (Fig. 6.1). N_2 production from these exploratory incubations measured on day 2 showed no significant differences between un-amended and amended sediments; (Fig. 6.1). Based on these results, the second stage incubations were designed with maximum amendments of 500 ppm ATMAC 12 and 200 ppm $CuCl_2$; two sets of combined additions (250 ppm ATMAC & 100 ppm $CuCl_2$; 125 ppm ATMAC & 50 ppm $CuCl_2$) were diluted from this stock. l.

6.3 RESULTS

(i) Regression analysis of measured values. Regressions of N_2 ,NH_4^+ & SOD time-point values in day 4 and 10 incubations in September-October 2014 yielded significant trends (Table 2.2 (a) & (b)). Values at day 22 yielded insignificant trends except in the case of SOD. Because of this lack of significance in N_2 & NH_4^+ flux rates, results from day 22 incubations were not analyzed for differences among differently amended sediments. In all sets of incubations (controls & amended sediments), NO_3^- fluxes were all close to zero (day 4 $\mu = -.007$ & $\sigma = .016$; day 10 $\mu = .026$ & $\sigma = .034$; day 22 $\mu = .002$ & $\sigma = .037$) and fluxes were not further analyzed.

(ii) N_2 production. The results of the incubations did not confirm the hypothesis that sediments amended with combinations of ATMAC 12 and $CuCl_2$ would show lower N_2 production than un-amended (blank) or singly amended

sediment. Single factor ANOVAs for day 4 and 10 incubations showed no significant differences among controls and amendments (Fig. 6.2 & Fig. 6.3).

Although the day 4 N_2 production rates were not significantly different compared to controls, all rates in amended sediments were lower than controls except for those from the combined incubations with the lowest amendments (Table 6.2 (a); Fig. 6.2 (a) & Fig 6.3 (a) & (b)). These results are different for the day 10 incubations when N_2 production rates from all AMTAC 12 amended sediments were higher than controls (Table 6.2 (a); Fig. 6.2). Day 22 N_2 production rates were all ~ ½ of day 4 rates and reflect a slowing of sediment metabolism also evident in other fluxes (Table 6.2 (a); Fig. 6.2).

Although the difference in N_2 production between singly amended $CuCl_2$ cores and controls was not statistically significant, in the 3 sets of incubations of 3 replicates each, only once did a $CuCl_2$ amended replicate produce N_2 at a greater rate than the lowest N_2 production rate of the controls (data not shown). Further, cumulative N_2 production in the $CuCl_2$ amended sediments was 21% lower than in the un-amended sediments over the 22 day course of the experiment (Fig. 6.8 (b)). However, SOD was lower in $CuCl_2$ amended cores than in controls or ATMAC 12[5] amended cores (Fig. 6. 9) and, if N_2 production is normalized to SOD, $CuCl_2$ amended sediments reflected higher rates of N_2 flux than did controls (Fig 6.10)

Amended sediments (both $CuCl_2$ & ATMAC 12) showed greater variability in N_2 flux results than un-amended cores, a pattern which did not extend to O_2 & NH_4^+ fluxes (Fig. 6.11).

(iii) NH_4^+ flux. Amended day 4 incubations reflected significantly higher rates of NH_4^+ flux than controls (ANOVA & Tukey test) (Table 6.2 (b); Table 6.3 (a); Fig. 6.4 & Fig. 6.5 (a) & (b)). NH_4^+ fluxes increased linearly with increases in the quantity of amended N from ATMAC additions in the day 4 incubations (Fig. 6.6). NH_4^+ concentrations at t=0 on the day 4 incubations roughly followed the gradient of ATMAC 12 additions (data not shown). Incubations amended with the highest concentrations of $CuCl_2$ and ATMAC 12 also had significantly higher rates of NH_4^+ flux than controls in the 10 day incubations (Table. 6.2 (b); Table 6.3 (b) & Fig 6.4). The two incubations with the lower mixes of ATMAC 12 and Cu had lower (near zero) rates of NH_4^+ flux on the day 10 incubation; however, regressions producing these fluxes had insignificant p-values (Table 6.2 (b)). All day 22 incubations had near zero or negative rates of NH_4^+ flux on day 22 incubations and regressions had insignificant p-values except for controls (Table 6.2 (b) & Fig. 6.4). These negative or low rates likely indicate most labile proteinaceous organic matter had been remineralized during the period since

[5] N_2 production and SOD were similar in un-amended and ATMAC amended sediments (Fig 6.10).

sediment retrieval. At day 22, SOD was ~ ½ of its rate in the day 4 incubations indicating a substantial decrease in overall sediment metabolism (Table 6.2 (c)).

Higher partitioning of N substrate to NH_4^+ export than to N_2 resulted in lower denitrification efficiency ratios (DE= N_2/ (N_2 + DIN)) in amended compared with un-amended cores in day 4 incubations (Fig 6.7). Only DE ratios in incubations with the lowest amendments (Atmac: Cu 125: 50) were not different from those of controls. In 10 and 22 day incubations, this pattern in DE ratios was confounded as some incubations generated negative NH_4^+ fluxes; nevertheless, incubations with the highest amendments (e.g., $CuCl_2$, ATMAC 12 alone and combined at 500:200 ppm) also showed lower DE ratios than controls in day 10 incubations. Because day 22 flux rates in amended sediments were low and no significant, DE values were not calculated.

6.4 DISCUSSION

While N_2 production results were not significantly lower in amended than un-amended sediments (Fig 6.2), the amendments clearly affected N processes in the incubations. Day 4 and all but 2 day 10 results reflected consistent partitioning toward NH_4^+ fluxes in amended sediments compared with controls. In the day 10 incubations, sediments with two lowest combined amendments showed almost no NH_4^+ fluxes; however, regressions of these NH4+ flux values showed high p-values raising doubts as to how to interpret these results. Day 22 results reflected substantially lower sediment metabolism (SOD ~ ½ of day 4 rates) and less pronounced differences in N outcomes. The decreased SOD is consistent with the loss of labile OM substrate over a several week period and with typical reactivities ($1/t_{1/2}$) of relatively fresh planktonic material (e.g. Middleburg and Meysman, 2007).

The ATMAC 12: $CuCl_2$ mix with the lowest amendments (125: 50 ppm) showed similar results to the un-amended sediments in N_2 production, NH_4^+ flux and in DE ratios in almost all instances. In this case, the amendments appear to have had little effect.

Before examining the preferential partitioning of N substrate to NH_4^+ flux in amended sediments, the next two sections address the lack of significant differences in N_2 production between amended and un-amended sediments and the likely sources of NH_4^+ inventories in different amendment categories. As the reasons for these results in the singly amended sediments are likely the same as in sediments with combined amendments, only outcomes in the singly amended sediments are discussed.

6.4.1 N_2 production outcomes.

(i) Singly amended $CuCl_2$ incubations. Although CuC_{l2} amended cores always produced lower N_2 fluxes than controls and over the course of 22 days produced an estimated 20% less cumulative N_2, normalized to SOD $CuCl_2$ amended cores produced more N_2 than controls.

Cu has been shown to inhibit denitrification in soils and sediments[6] at amendment concentrations comparable to those added in this study (Bollag & Barabasz (1979); Holtan-Hartwig et al (2002) & Magalhaes et al (2011)). Differences between soil/ sediment matrices used in this study and earlier research may have determined the difference in the statistical significance of the results achieved. The soil used by Holtan-Hartwig et al (2002) had a cation exchange capacity (CEC) of 70.2 µmol g^{-1} which is typical for sand. Magalhaes et al (2011) did not report a CEC but added $CuSO_4^-$ to permeable sediments with a high sand content. GPB sediment used in these incubations consisted of fine silt (~ 3 µm diameter) and likely had a CEC at least twice a CEC typical of sand (Langmuir 1997). Since sediment CEC exerts a substantial control on the fraction of Cu bioavailable, the difference in sediment matrices may explain the difference in the statistical robustness of results achieved by Holtan-Hartwig et al (2002) and Magalhaes et al (2011) compared to this study. Sulfide was never obvious in GPB sediments; however, acid volatile sulfides (AVS) (Ankley et al 1996) may have dampened toxicity by complexing with dissolved Cu to reduce its bioavailability. As the primary objective of these incubations was to investigate whether Cu and ATMAC 12 combined inhibited N_2 production more than either amendment alone, neither estimation of CEC nor AVS was considered in the experimental design.

(ii) Singly amended ATMAC 12 incubations. For QACs to inhibit N_2 production, they must be bioavailable to denitrifying bacteria; i.e., their toxicity is controlled by their adsorption equilibrium between solid (unavailable) and aqueous (bioavailable) phases. QACs adsorb to sediments both through ion exchange and hydrophobic interactions of their hydrocarbon tails; because of its shorter chain length, ATMAC 12 adsorbs less strongly than other QACs (Ismail et al 2010).

Tezel and colleagues whose work constitutes the only published research on QAC inhibition of denitrification consistently reported total QAC amendments of 50 mg L^{-1} are necessary to achieve inhibition of denitrification (Tezel et al (2008); Tezel et al (2010); Hajaya et al (2011)). However, this amendment does not reflect aqueous bioavailable concentration of their amendments because QACs partition to total dissolved solids in the waste water streams used in their incubations. For example, Hajaya et al (2011) reported a 100 mg L^{-1} BAC

[6] Although no published results were found which normalized N_2 production to SOD.

addition resulted in a dissolved concentration of 11.8 mg L^{-1} BAC aqueous phase concentration at the end of the incubation at 22° C.

Cations partition differently in settled sediments (ø= 0.80) in seawater compared to municipal or industrial waste-water where total dissolved solids were in the range of low mg g^{-1} and S= 0 ‰ (Tezel et al (2008); Tezel et al (2010); Hajaya et al (2011)). Nevertheless, in order to derive a minimum estimate of the bioavailable fraction of the 500 ppm ATMAC addition in this study, published Freundlich isotherm coefficients derived for ATMAC 12 in cultures of municipal sludge (Ismail et al (2010)) were used to compare solid-phase additions used in this investigation with the aqueous phase toxicity levels reported in the work of Tezel's group (i.e. 50 mg L^{-1}). The isotherm understates the aqueous phase QAC concentrations for 2 reasons: (1) the higher solid: aqueous phase in the settled sediment in this study will decrease adsorption equilibrium (Hand 1990) and (2) the ionic strength of seawater will keep more cations in the dissolved phase than in freshwater. The relevant equation was:

$$q_e = 1.28 * C^{0.64}$$

where q_e is the solid-phase concentration (mg g^{-1} particles) and C is the aqueous phase concentration (mg L^{-1}). Adjusting for seawater matrix by a multiple of 5 (Brownawell *pers. comm.*) yields a aqueous equilibrium value of ~ 1 mg L^{-1} for the highest 500 ppm ATMAC 12 amendment. This estimate is conservative because it does not take into account the higher sediment: aqueous phase mix in these amendments compared to Ismail et al (2010). An alternate estimate of equilibrium aqueous concentration corresponding to the 500 ppm amendments was calculated based on a minimum partition coefficient (i.e. maximum aqueous value) in sediment: river-water (440L = kg) from Hand et al (1990). This ratio corresponded to an aqueous phase concentration of ~ 5 mg L^{-1}. Consequently, the amendments used in this study likely produced bioavailable ATMAC 12 in the low-end of the range of the amendments used by Tezel to ascribe toxicity.

6.4.2 NH_4^+ fluxes between amended and un-amended sediments.

In the day 4 incubations, higher NH_4^+ exports versus controls could have been due to one or some combination of (1) diffusion of exchangeable NH_4^+ from initial additions; (2) remineralization of bioavailable ATMAC 12; (3) efflux of intra-cellular NH_4^+ brought about by ATMAC 12 microbial toxicity or (4) inhibition of nitrification. The last possibility is discussed in section 6.4.3. Sources of excess NH_4^+ fluxes may have differed depending on the type of amendment.

(i) Ion exchange with exchangeable NH_4^+ upon ATMAC 12 & Cu additions. Additions of $CuCl_2$ and ATMAC likely released exchangeable, adsorbed NH_4^+ into the slurry during mixing. As such ion exchange is rapid (~2 hrs) (Rosenfeld 1979; Fitzsimons et al 2006), most desorbed exchangeable NH_4^+ probably remained in the overlying water as sediment settled. Yet some fraction

of exchangeable NH_4^+ may have desorbed after sediment settling. To test whether diffusion of porewater inventories of desorbed exchangeable NH_4^+ could have contributed to NH_4^+ fluxes from the amended sediments in the day 4 incubations, sediment transport and N reactions were modeled assuming a maximum-case pulse of 100 µM exchangeable ammonia to porewater on mixing (i.e. 4 days before the initial incubation) and no re-adsorption of exchangeable NH_4^+ or adsorption of freshly remineralized NH_4^+. This model showed initial available exchangeable NH_4^+ had largely escaped from the surficial sediment by day 4 (Aller *pers. comm.*) and therefore the initial behavior did not directly affect NH_4^+ flux at 4 days.

(ii) Singly amended ATMAC 12 sediments. While N additions from ATMAC amendments did not total more than 1% of estimated in-situ N_{org} in any incubation (Table 1 (c)), they represented a substantial inventory of labile N. The strong linear relationship between the level of ATMAC 12 additions and the rate of NH_4^+ efflux from the sediments in the day 4 incubations (Fig. 6.6 (a)) suggests the excess of NH_4^+ flux in ATMAC amended cores over controls derives either from (1) remineralization of ATMAC 12 amendments themselves or (2) ATMAC 12 induced microbial toxicity and release of cellular NH_4^+. The lack of significance in SOD between controls and amended sediments in day 4 and 10 is not consistent with overall microbial toxicity and cell lysis.

ATMAC 12 is only known to biodegrade aerobically (Ying et al 2006; Doherty PHD dissertation (2013)). Although O_2 penetration depth was not measured in incubated sediments, overlying water was aerated and even at the final time-point (~24 hrs) of the sealed incubations remained > 60% of equilibrium. Although at 19°C, *in-situ* oxygen penetration depth in fine silt with a porosity of ~ .8 (characteristic of GPB surficial sediment) may be expected at < ~ 3 mm, in these incubations, 3mm depth is most likely a conservative estimate of O_2 penetration depth because SOD in 5 cm deep cores is much lower than *in-situ* rates. Using this value as oxygen penetration depth and assuming ATMAC 12 amendments were mixed homogenously ~ 1.26 umol/m^2 of ATMAC 12 would be available for aerobic biodegradation in the singly amended sediments. Since the excess N flux in these cores over controls cumulatively amounted to ~ 0.6 mmol m^{-2} (i.e., (1.68 – 1.53 mmol m^{-2} d^{-1}) X 4 days in Table 2(b)), the fraction of ATMAC 12 remineralized after 4 days would be ~ 0.5 (0.13 d^{-1}) if no cellular NH_4^+ contributed to the N flux. This remaining fraction contrasts with a remaining fraction of ~ 0.25 after 4 days for ATMAC 12 in sediment incubations in Doherty (PhD dissertation 2013). At this linear rate, N from remineralization of ATMAC 12 additions would be consumed by the day 10 incubations; ATMAC 12 would have to be remineralized at a substantially lower rate to explain the excess N fluxes versus controls at the day 10 incubations.

(iii) Singly amended $CuCl_2$ sediments. Higher NH_4^+ production in the day 4 incubations occurred concomitant with lower SOD in $CuCl_2$ amended cores (6.7 O_2 mmol m^{-2} d^{-1}) than in controls (7.7 O_2 mmol m^{-2} d^{-1}) (Fig 6.9). The co-

occurrence could reflect a general biocidal impact in the $CuCl_2$ amended sediment which slowed sediment metabolism and precipitated release of intra-cellular NH_4^+ from lysis of microbial cells. However, SOD was not significantly different in ANOVAs in day 4 or day 10 incubations. Further, SOD was higher in $CuCl_2$ amended sediments than controls in day 10 incubations and higher SOD is not consistent with the release of intracellular NH_4^+ due to biocidal impacts.

6.4.3 Partitioning of N substrate between N_2 & NH_4^+ fluxes.

Regardless of the incremental N source, NH_4^+ concentrations in amended cores were not oxidized to NO_3^- or subsequently denitrified in the proportions they were in controls. In the day 4 incubations, higher NH_4^+ fluxes correspond to lower N_2 production in all amended cores (Table 6.2). As O_2 levels in overlying seawater were similar in all cores and never fell below 60% of air saturated values during incubations, the difference in NH_4^+ fluxes was not due to O_2 limitation on nitrification.

As described in the chapter introduction, Cu additions to sediments in a range of 100- 500 µg Cu g^{-1} sediment (Baath 1989 and references therein) have been found to inhibit nitrification in soil. Jacinthe & Tedesco (2009) reported amendments of 100 µg Cu g^{-1} sediment reduced nitrification by ~20- 60% in lake sediments. The Cu amendments in this study were in the range of or higher than this previous work. Although no published reports of ATMAC 12 inhibition of nitrification were found, Sarkar et al (2012) demonstrated the QACs, hexadecyltrimethyl ammonium bromide (HDTMA) and octadecyltrimethyl ammonium bromide (ODTMA), inhibited nitrification at 50 mg kg^{-1} in soil. So inhibition of nitrification perhaps because of interference with enzyme conformations may have resulted in a build-up of NH_4^+ inventories in porewater (& subsequently higher NH_4^+ efflux) in amended sediments versus controls.

6.5 SUMMARY

The results of these investigations did not confirm the hypothesis sediment incubations amended with combinations of ATMAC 12 and $CuCl_2$ would show lower N_2 production than singly amended incubations and consequently did not support an inference of synergistic effects which would inhibit N_2 production in sediments. Although N_2 production was not significantly lower in amended sediment versus controls, the results generally showed amended sediments partitioned N substrate preferentially toward NH_4^+ fluxes instead of N_2 production compared with un-amended sediments. Clearly, the amendments affected the oxidation of remineralized N.

Lack of statistically significant differences in N_2 production in $CuCl_2$ amended sediments versus controls was attributed to CEC of fine grained GPB

sediments. The bioavailability of ATMAC 12 in these incubations was not quantified although at least the highest quantities amended appear close to those of Tezel et al (2008); (2010) and Hajaya et al (2011).

Greater variability in N_2 production outcomes in amended cores compared to controls reflected disturbance of the additions to sedimentary N cycling. Results of some replicates suggest additions provided excess (relative to controls) N substrate which was oxidized and subsequently reduced to N_2; other results of other replicates suggest inhibitory effects on denitrification.

The source of the higher NH_4^+ production in amended sediments was not resolved. The reason excess (versus controls) NH_4^+ was effluxed instead of further oxidized to NO_3^- was attributed to inhibition of nitrification by Cu (Baath 1989; Jacinthe & Tedesco (2009)) and ATMAC 12 (Sakar et al (2011).

6.6 TABLES & FIGURES

Table 6.1 (a). QAC & CuCl2 additions to preliminary incubations, June 2014

	Weight Added (mg/ sample)	Target Added (mg/sample)	PPM
CuCl2 (heavy)	172	64	1,069
CuCl2 (light)	64	24	398
ATMAC 12 (h)	162	162	2,700
ATMAC 12 (l)	60	60	1,000
BAC (h)	167	167	2,775
BAC (l)	60	60	1,000
ATMAC: $CuCl_2$	30 + 32	30 + 12	500: 199
BAC: $CuCl_2$	30 + 32	30 + 12	500: 199
Sediment Weight ~ 160 g (wet); estimated dry:wet ratio 0.375 and calculated dry sediment weight 60 g/sample. Mol fraction Cu in $CuCl_2$ ~ 0.373			

Table 1 (b). ATMAC 12 & CuCl2 additions to Sep- Oct 2014 incubations.

	Target (ppm)	Atmac:Cu Addition/ Sample (mg)	N add/ sample (umol)	N add mmol/m^2	Addition as % est. N_{org} (C_{org}=2%)
Blank	0				
$CuCl_2$	200	32			
Atmac 12 singly amended	500	30	113	21	0.9%
Atmac: Cu (high)	500:200	30:32	113	21	0.9%
Atmac: Cu (medium)	250:100	15:16	56	11	0.5%
Atmac:Cu (low)	125:50	7.5:8	28	5	0.2%

Table 6.2 (a). N_2 fluxes from Sep- Oct 2014 sediment incubations. NO_3^- fluxes not shown as values were too low to change outcomes (i.e., average period NO_3^- flux 0.007 mmol m^{-2} d^{-1}; (+/- 0.029)). P-values refer to significance of trend in incubated values (df= 2).

	triplicate averages (mmol/m^2-d) (+/- std dev)					
	4 days	p-value	10 days	p-value	22 days	p-value
blank	0.68 (+/- .08)	0.012	0.47 (+/- .09)	0.008	0.30 (+/- .07)	0.048
CuCl2	0.59 (+/- .04)	0.023	0.37 (+/- .18)	0.066	0.18 (+/- .07)	0.223
Atmac (all)	0.62 (+/- .21)	0.031	0.56 (+/- .22)	0.04	0.28 (+/- .09)	0.095
Atmac (500)	0.52 (+/- .15)	0.008	0.64 (+/- .29)	0.039	0.29 (+/- .14)	0.142
c 500:200	0.64 (+/- .22)	0.067	0.53 (+/- .14)	0.009	0.23 (+/- .11)	0.079
c 250:100	0.62 (+/- .18)	0.019	0.55 (+/- .14)	0.005	0.28 (+/- .09)	0.090
c 125:50	0.69 (+/- .28)	0.030	0.54 (+/- .29)	0.120	0.30 (+/- .03)	0.070

Table 6.2 (b). NH_4^+ fluxes from Sep- Oct 2014 sediment incubations. P-values refer to significance of trend in incubated values (df= 2).

	triplicate averages (mmol/m^2-d) (+/- std dev)					
	4 days	p-value	10 days	p-value	22 days	p-value
blank	0.18	0.088	0.16	0.000	-0.06	0.024
CuCl2	0.44	0.000	0.22	0.001	-0.01	0.697
Atmac (all)	0.47	0.016	0.18	0.228	0.01	0.413
AtMAC (500)	0.65	0.000	0.34	0.089	-0.04	0.536
c 500:200	0.52	0.007	0.49	0.001	0.12	0.258
c 250:100	0.44	0.000	-0.02	0.569	-0.02	0.417
c 125:50	0.28	0.004	-0.10	0.255	-0.02	0.440

Table 6.2 (c). SOD from Sep- Oct 2014 sediment incubations. P-values refer to significance of trend in incubated values (df= 2).						
	triplicate averages (mmol/m^2-d) (+/- std dev)					
	4 days	p-value	10 days	p-value	22 days	p-value
blank	7.73	0.012	5.28	0.007	3.44	0.060
CuCl2	6.68	0.023	5.63	0.041	3.90	0.032
Atmac (all)	7.14	0.026	5.66	0.024	3.92	0.047
AtMAC (500)	7.39	0.060	4.98	0.038	4.20	0.051
c 500:200	7.41	0.024	6.52	0.008	3.99	0.034
c 250:100	6.60	0.023	5.81	0.023	3.84	0.065
c 125:50	7.16	0.016	5.73	0.025	3.67	0.039

Table 6.3 (a) ANOVA: day 4 incubations NH4+ flux rates w/ Tukey multiple comparisons test						
Source of Variation	***SS***	***df***	***MS***	***F***	***p-level***	***F crit***
Between Groups	0.422	5	0.08	13.10	0.00	4.16
Within Groups	0.077	12	0.01			
Total	0.500	17				
Tukey Multiple Comparisons Test						
addition>	**control**	**c 125:50**	**c 250:100**	**CuCl 2**	**c 500:200**	**AtMAC 12**
mean	0.18	0.28	0.44	0.44	0.52	0.65
SE	0.046					
critical value q (.05,12,6)						
						Equality of means
	Addition a	**Addition b**	**Difference In means**	**q**	**q (.05,12,6)**	
	control	Atmac 12	0.470	10.14	4.751	Reject
	c 125:50	Atmac 12	0.371	8.01	4.751	Reject
	c 250:100	Atmac 12	0.214	4.62	4.751	Accept
	control	c 500:200	0.338	7.30	4.751	Reject
	c125: 50	c 500:200	0.239	5.16	4.751	Reject
	c 250:100	c 500: 200	0.083	1.78	4.751	Accept
	control	CuCl2	0.261	5.63	4.751	Reject
	c125: 50	CuCl2	0.162	3.49	4.751	Accept
	control	c 250:100	0.256	5.52	4.751	Reject
	c125: 50	c 250:100	0.157	3.38	4.751	Accept

Table 6.3 (b) ANOVA: day 12 incubations NH4+ flux rates w/ Tukey multiple comparisons test						
Source of Variation	***SS***	***df***	***MS***	***F***	***p-level***	***F crit***
Between Groups	0.722	5	0.144	11.2	0.000	4.16
Within Groups	0.155	12	0.0129			
Total						
Tukey Multiple Comparisons Test						
addition>	c 125:50	c 250:100	control	CuCl2	AtMAC 12	c 500:200
mean	-0.097	-0.024	0.156	0.222	0.337	0.488
SE	0.066					
critical value q (.05,12,6)						
			Differenc e In means			**Equality Of means**
	Addition a	**Addition b**		**q**	**q (.05,12,6)**	
	c 125: 50	c500:200	0.586	8.93	4.75	Reject
	c 250:100	c500:200	0.513	7.82	4.75	Reject
	control	c 500:200	0.333	5.07	4.75	Reject
	CuCl2	c 500:200	0.267	4.07	4.75	Accept
	c125: 50	Atmac 12	0.435	6.63	4.75	Reject
	c 250:100	Atmac 12	0.362	5.51	4.75	Reject
	control	Atmac 12	0.182	2.77	4.75	Accept
	c125: 50	CuCl2	0.319	4.86	4.75	Reject
	c 250:100	CuCl2	0.246	3.75	4.75	Accept
	c125: 50	control	0.253	3.86	4.75	Accept

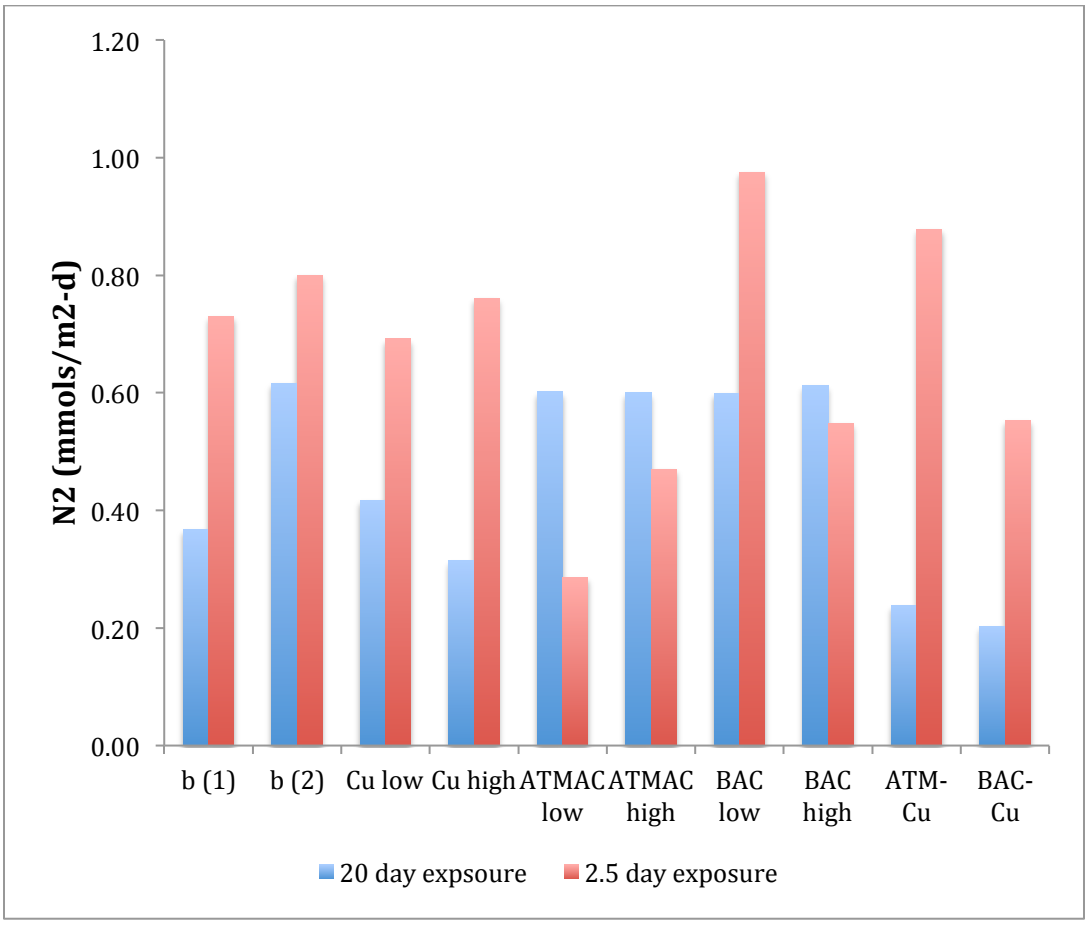

Fig. 6.1. Preliminary incubations June 2014: N_2 production after QAC & Cu additions to GPB sediment. Results for 2.5 day exposure are not significant. For the 20 day incubation, combined results from ATMAC 12- CuCl2 and Bac-$CuCl_2$ amendments are significantly different (t-test $\alpha < .05$) than all other results but not significantly different than controls due to dispersion of results between duplicate blanks.

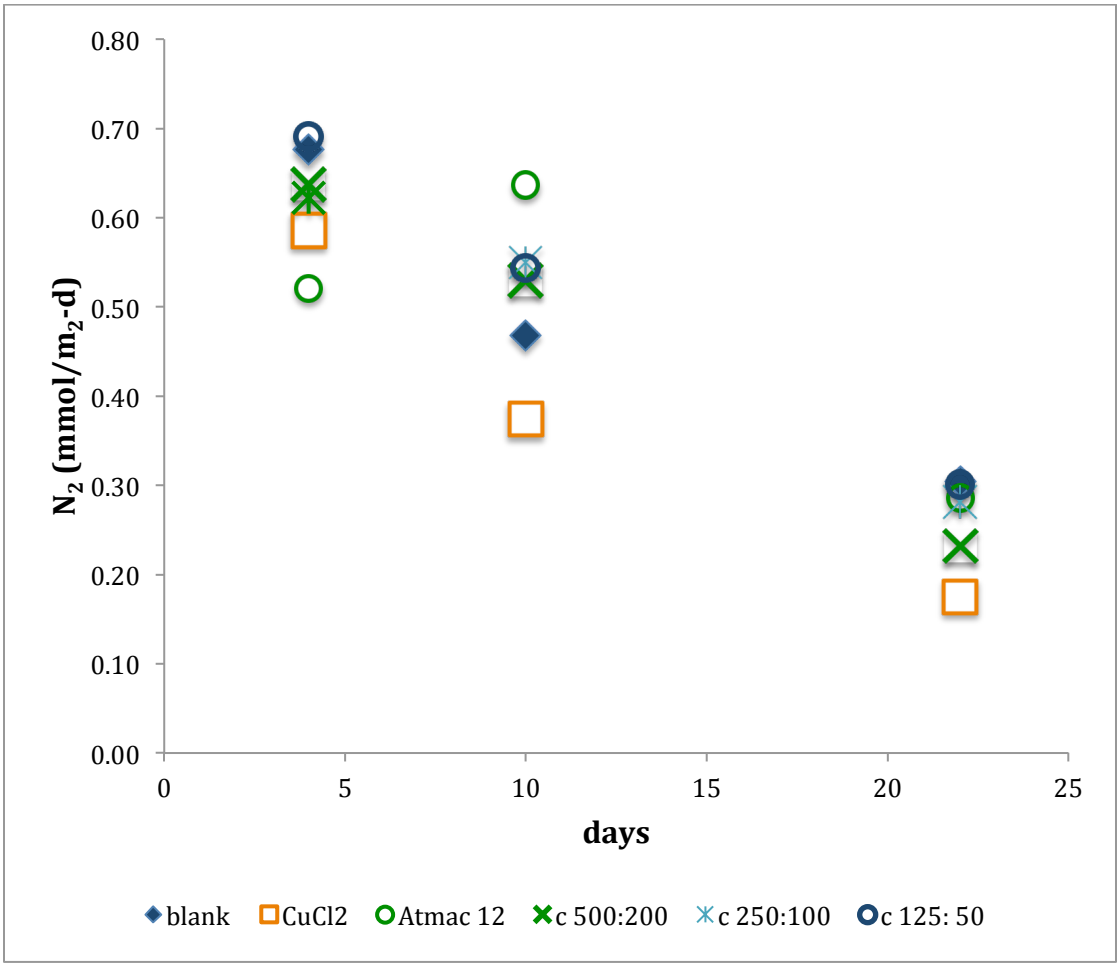

Fig. 6.2. N_2 production from cores incubated w/ $CuCl_2$ & ATMAC 12 amendments. Each symbol= average flux rate of triplicate incubations. Although net N_2 production from un-amended sediments and sediments with low additions of ATMAC & Cu was higher at 4 and 22 days compared with cores receiving concentrated amendments of ATMAC 12 and/or $CuCl_2$, variability of replicates rendered differences between controls and amended means not statistically significant (ANOVAs) (4 day incubations: F- stat= 0.38, df= 17 & p- value= 0.85; 10 day incubations: F- stat= 1.44, df= 17 & p- value= 0.28).

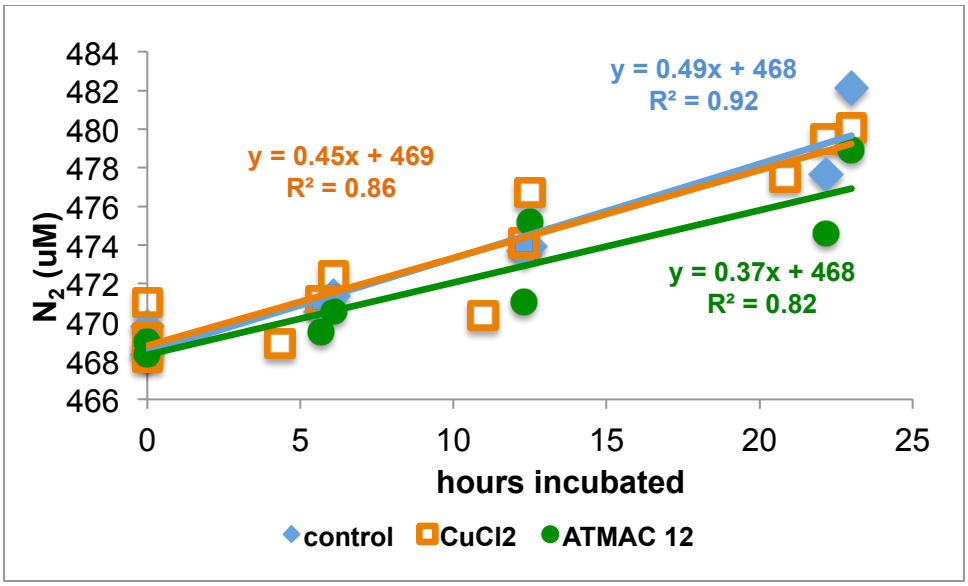

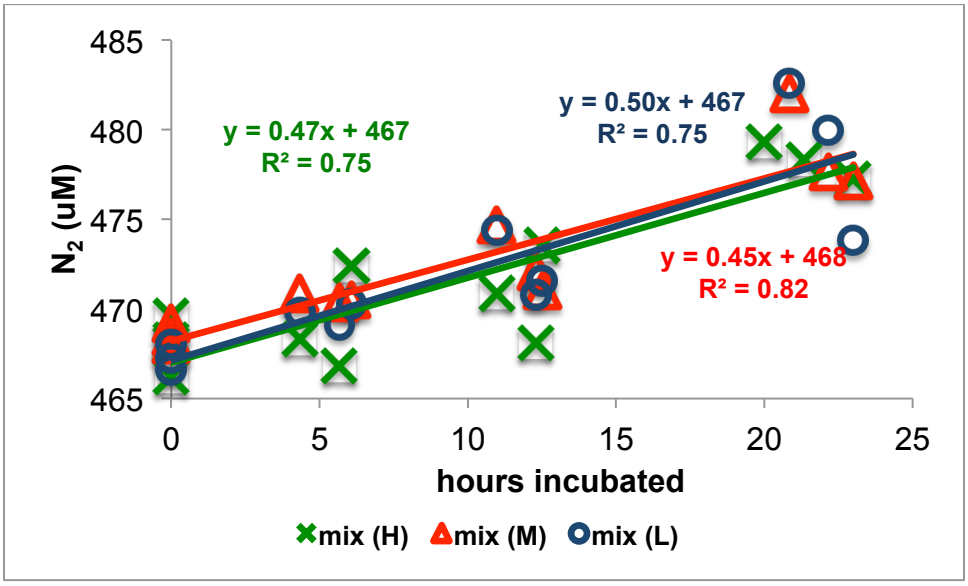

Fig. 6.3 (a) Day 4 incubation time-series of N_2 values: control & singly amended sediments. (b) Day 4 incubation time-series of N_2 values: combined amended sediments. Mixes (Cu: ATMAC): (H)= 200:500; (M)= 100:250 & (L)= 50: 125.

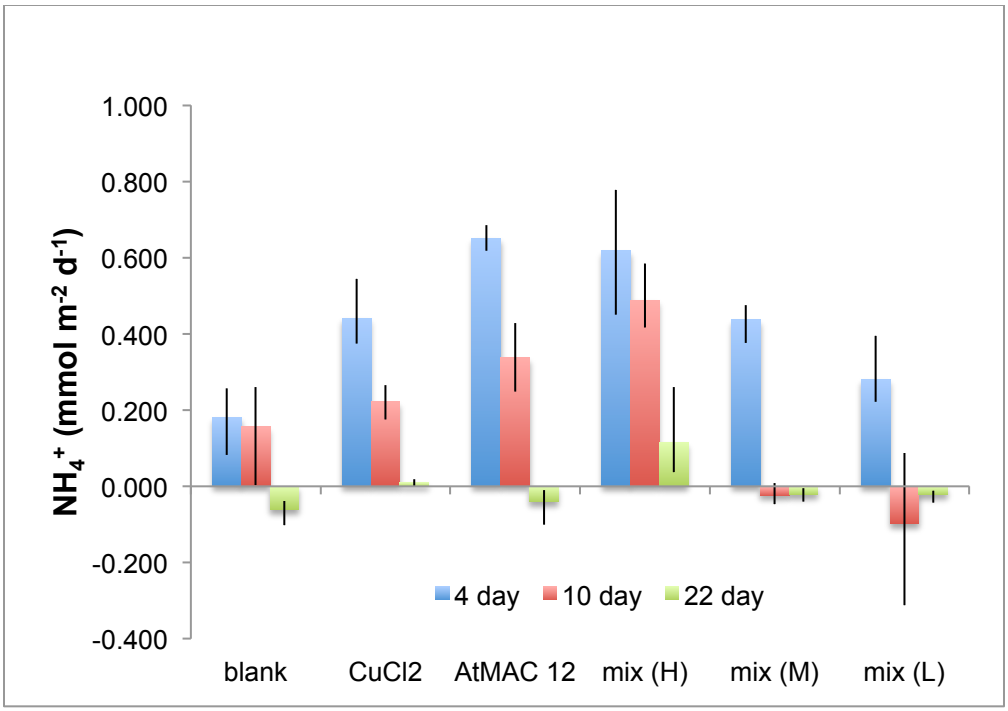

Fig. 6.4 NH_4^+ fluxes from $CuCl_2$ & ATMAC 12 incubations. NH_4^+ fluxes from controls significantly lower than from amended incubations in day 4. Significance of differences varies in day 10 and in 22 day incubations (see Table 2 (c)). Mixes (Cu: ATMAC): (H)= 200:500; (M)= 100:250 & (L)= 50: 125.

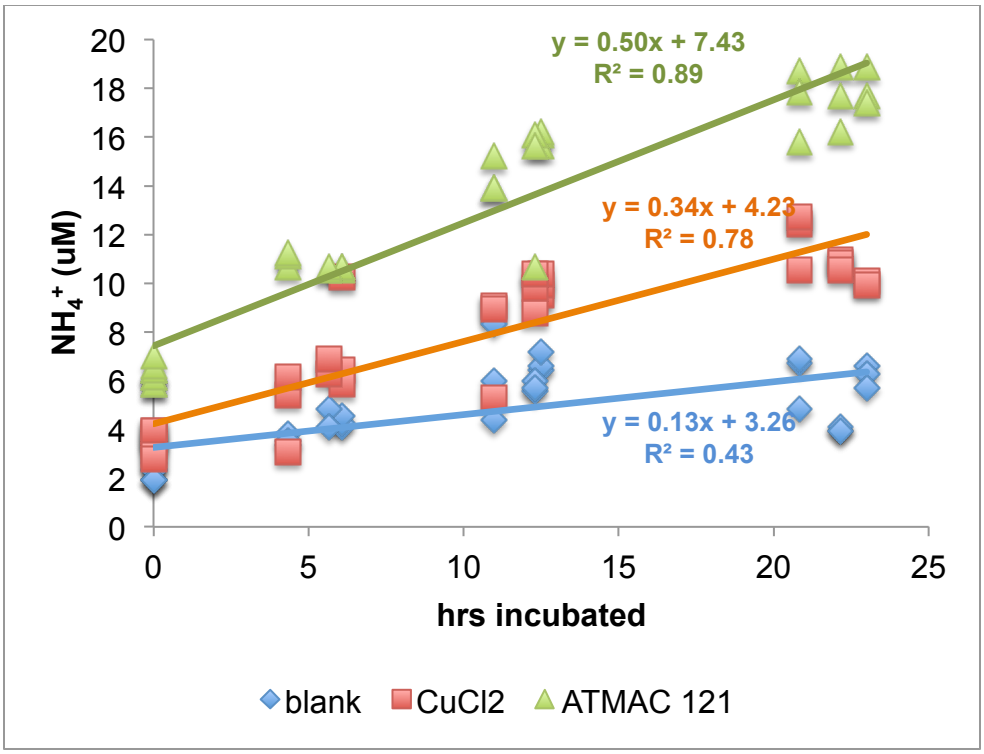

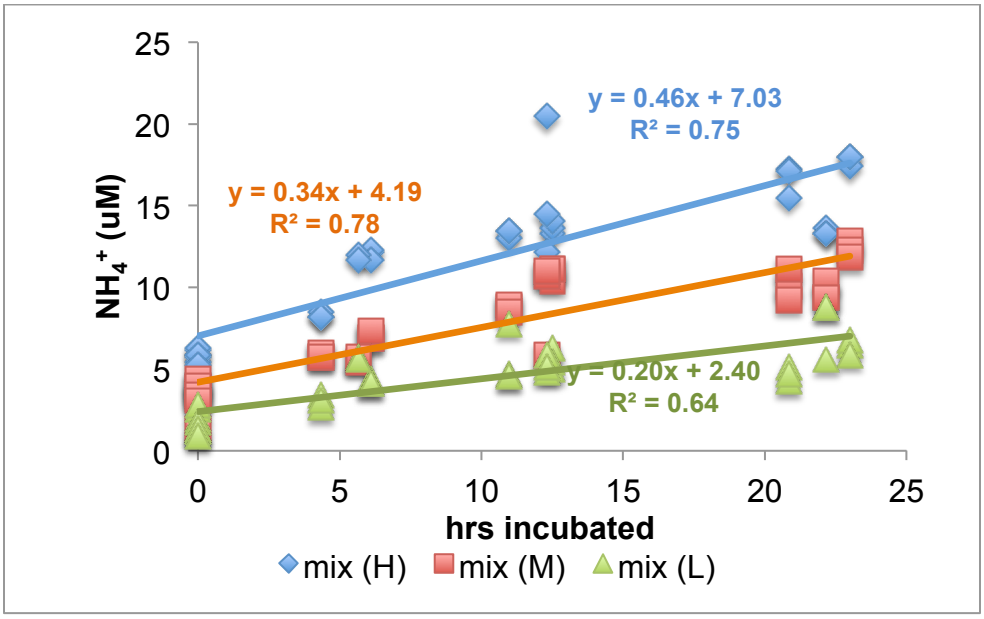

Fig. 6.5 (a) Day 4 incubation time-series of NH_4^+ values: control & singly amended sediments. (b) Day 4 incubation time-series of NH_4^+ values: combined amended sediments. NH_4^+ production in all amended incubations except for lowest additions of ATMAC: Cu is significantly higher than NH_4^+ production in control. Initial (t= 0) NH4+ values are also higher in amended sediments than controls and- in the case of sediments amended with ATMAC 12- followed a gradient corresponding to the quantity of ATMAC 12 additions. Mixes (Cu: ATMAC): (H)= 200:500; (M)= 100:250 & (L)= 50: 125

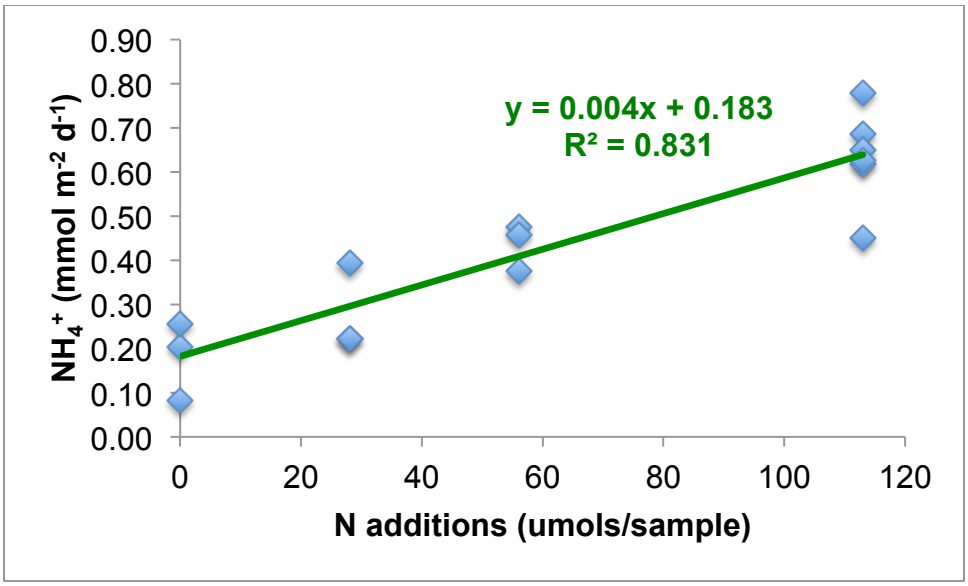

Fig. 6.6. **Influence of N additions on NH_4^+ fluxes in day 4 incubations.** NH_4^+ fluxes show statistically significant relationships with ATMAC amendments across all measurement periods (F-stat= 53.1, df= 13 & p- value < .001).

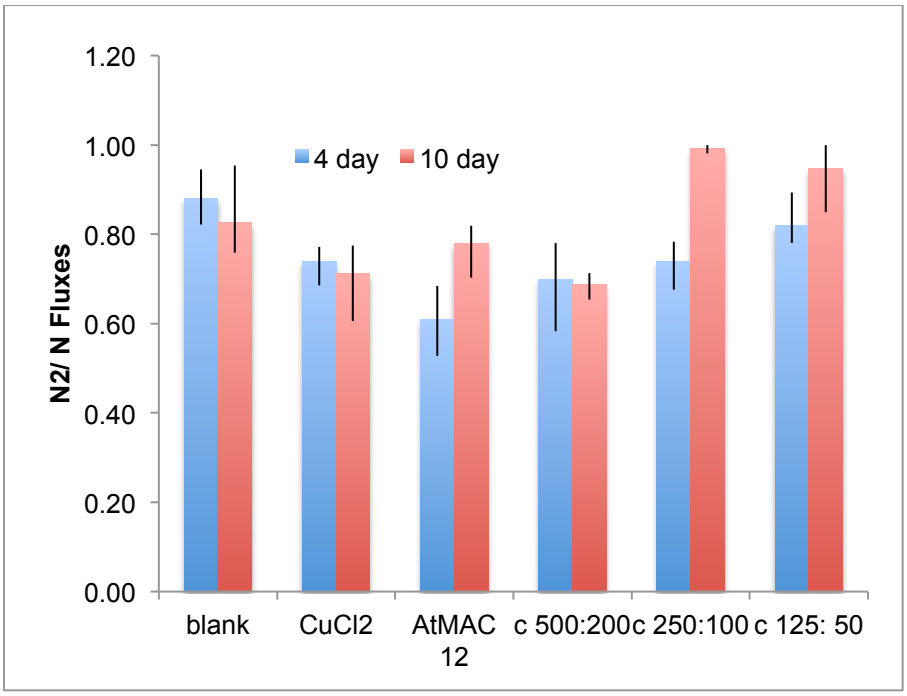

Fig. 6.7. Denitrification efficiency in day 4 & 10 incubations.
Partitioning of N substrate between NH_4^+ export and N_2 gas production favors NH_4^+ in amended cores relative to un-amended sediment in day 4 but not in day 10 incubations.

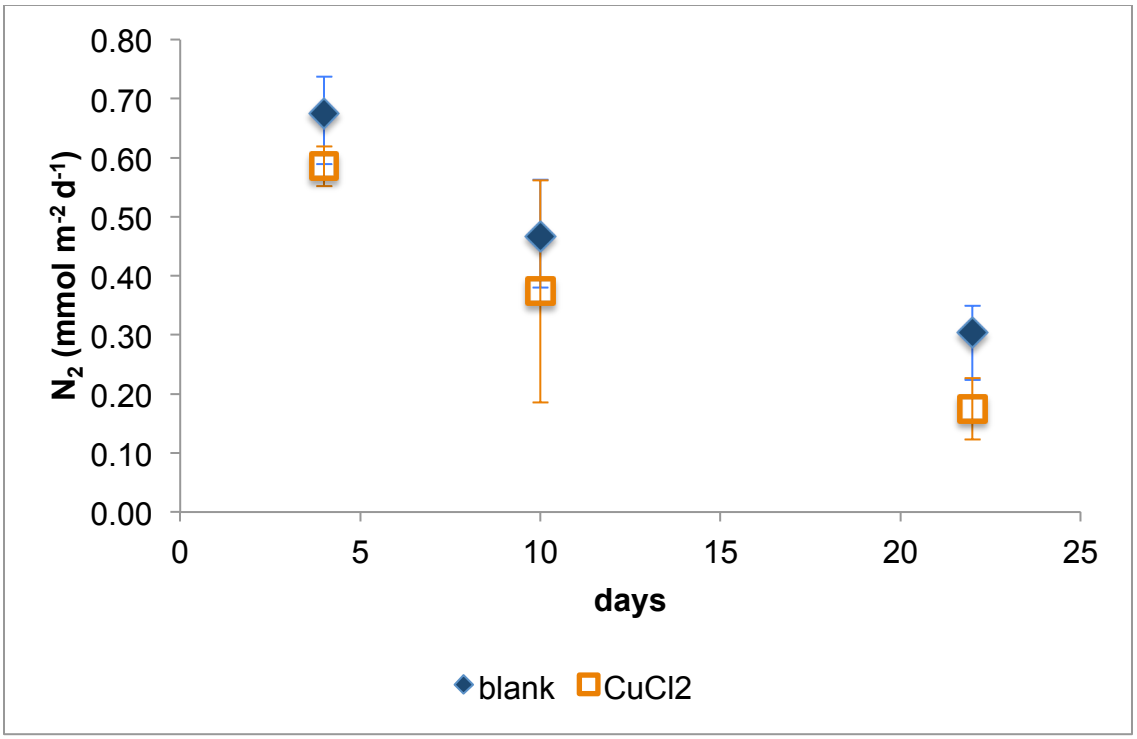

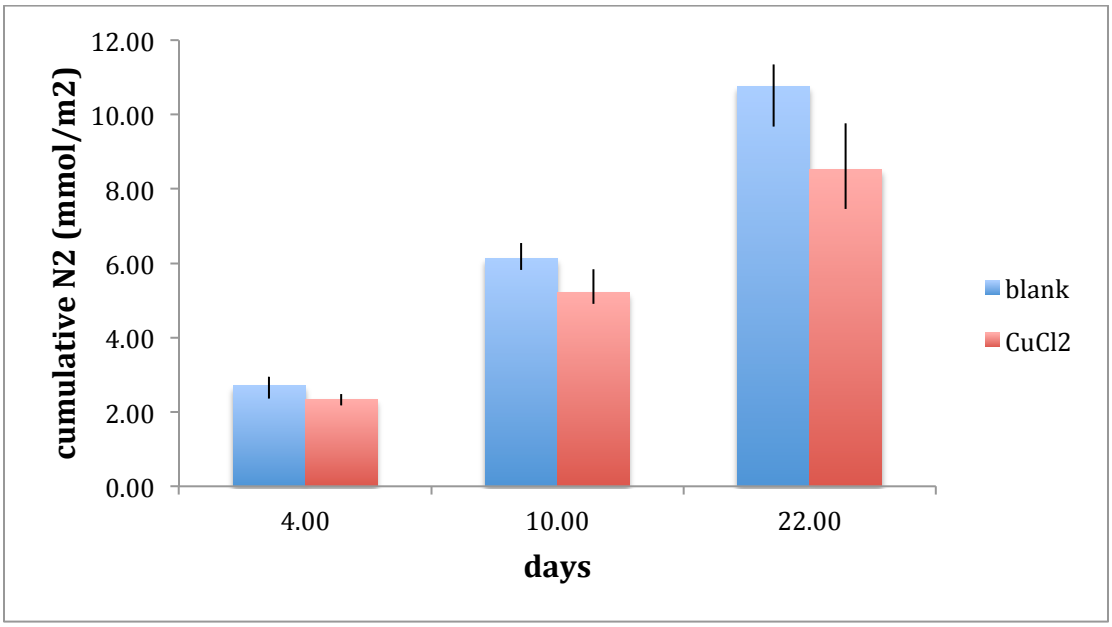

Fig. 6.8. (a) Inhibitory effects of $CuCl_2$ amendments on N_2 sedimentary fluxes: controls versus amended sediments. (b) Cumulative N_2 production in controls & CuCl2 amended sediments. Over the 22 day period, mean cumulative N_2 production was over 20% lower in the $CuCl_2$ amended sediment compared with un-amended cores.

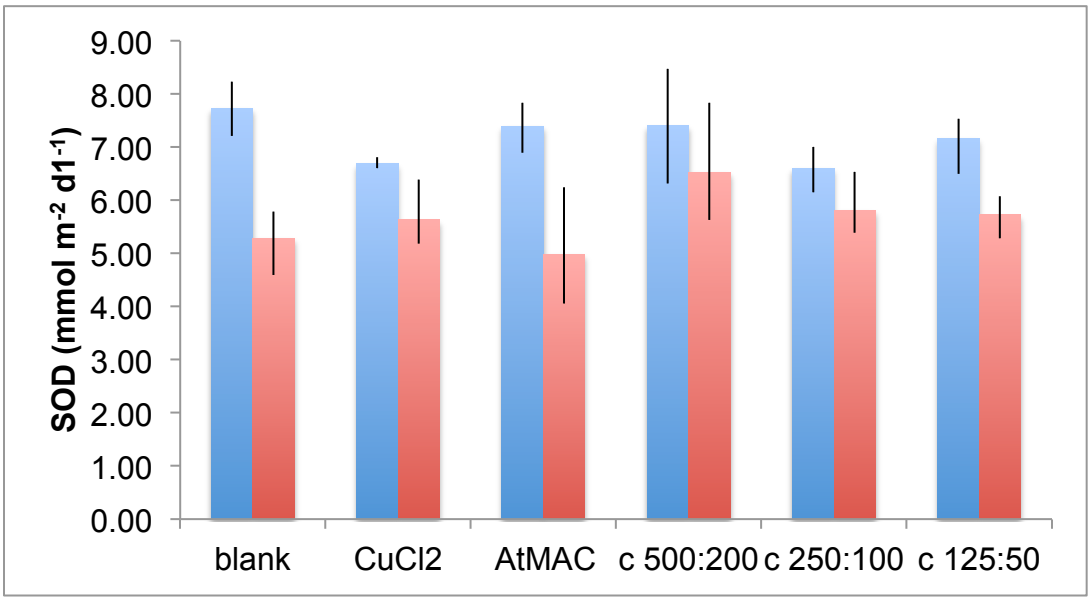

Fig. 6.9. SOD day 4 & 10 incubations. Lower SOD may reflect a general toxicity in the CuCl2 amended sediments in day 4 incubations; in this case, no enzyme-specific inhibition would be implicated in explaining lower N_2 production in $CuCl_2$ amended sediment compared with un-amended sediment. But SOD was not significantly different among fluxes among all 4 and 10 day incubations (ANOVA day 4: F-stat= 1.64, df= 17 & p- value=0.223; day 10: F-stat = 1.23, df= 17 & p-value= 0.35).

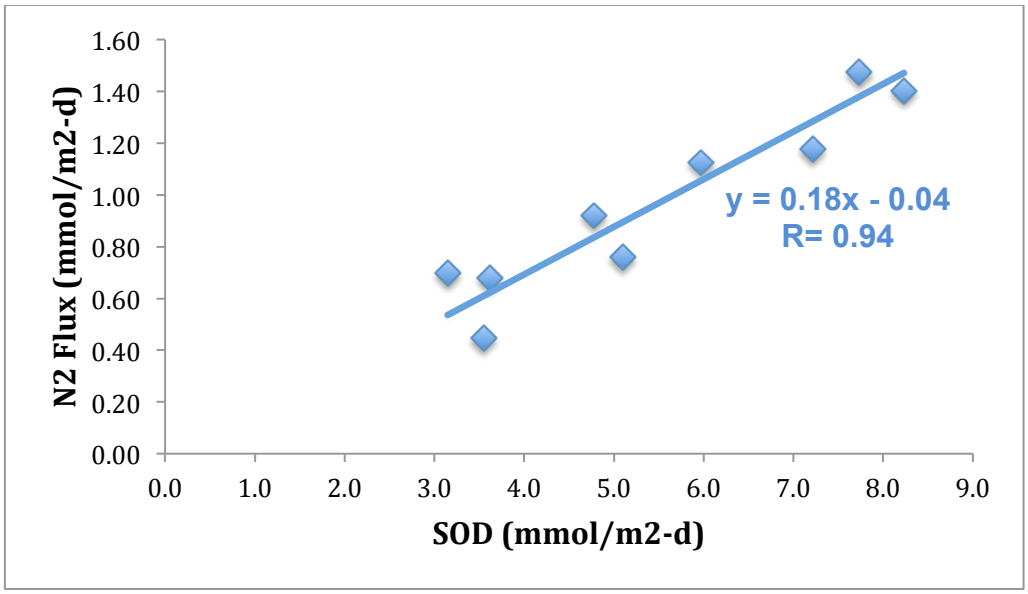
1.60
1.40
1.20
1.00
0.80
0.60
0.40
0.20
0.00
N2 Flux (mmol/m2-d)
y = 0.18x - 0.04
R= 0.94
0.0
1.0
2.0
3.0
4.0
5.0
6.0
7.0
8.0
9.0
SOD (mmol/m2-d)

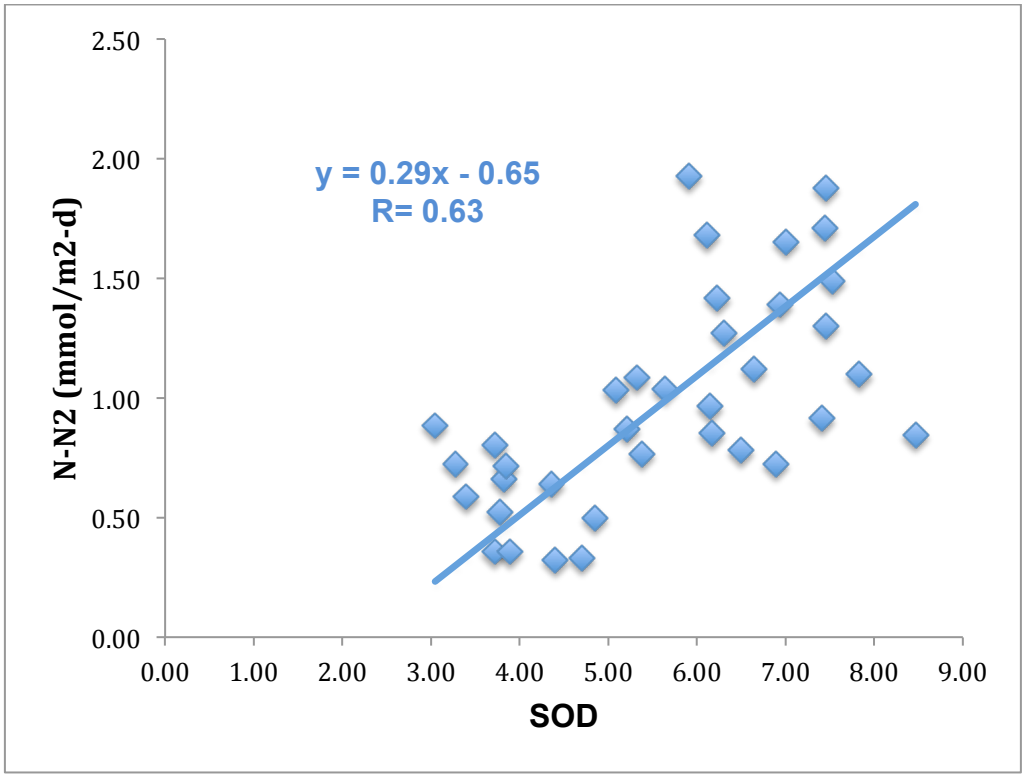
2.50
2.00
1.50
1.00
0.50
0.00
N-N2 (mmol/m2-d)
y = 0.29x - 0.65
R= 0.63
0.00
1.00
2.00
3.00
4.00
5.00
6.00
7.00
8.00
9.00
SOD

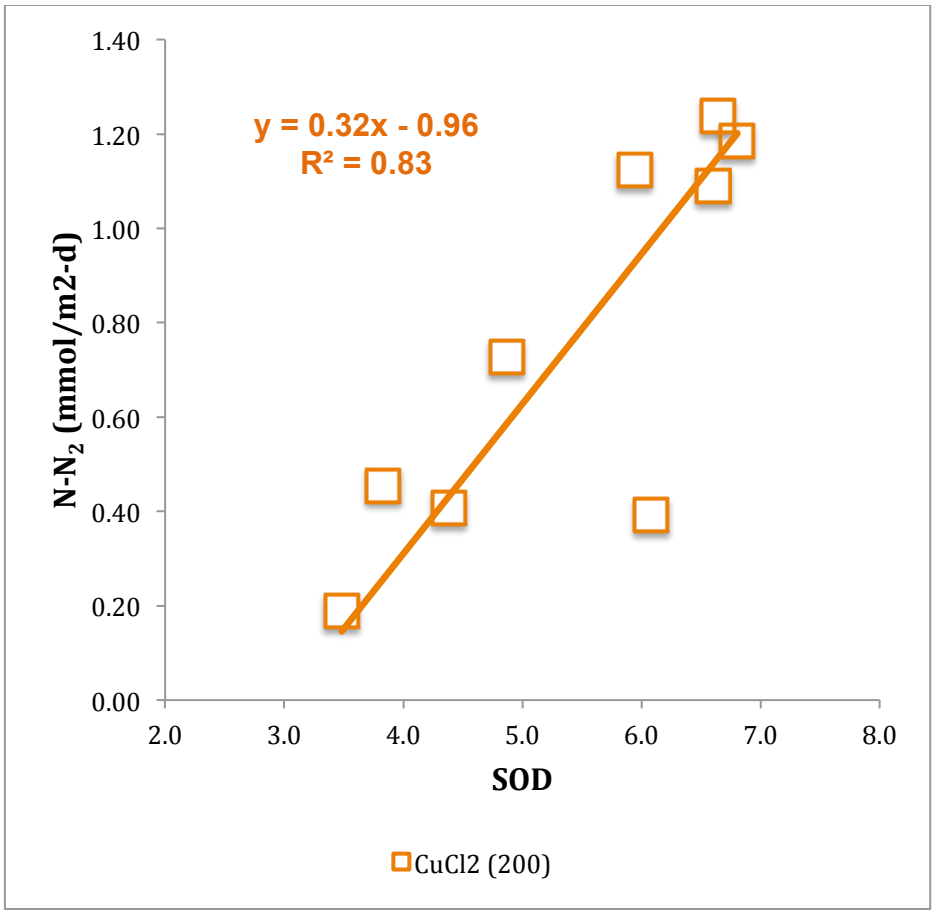

Fig. 6.10. (a) N_2 production versus SOD in un-amended sediment; (b) N_2 production versus SOD in ATMAC & ATMAC/$CuCl_2$ amended sediment; & (c) N_2 production versus SOD in $CuCl_2$ amended sediment. Generally, SOD is low (and therefore regression coefficients high) compared with *in-situ* measurements most likely reflecting the abbreviated core height (~ 5cm) of the amended incubations. All regressions are calculated by geometric mean method.

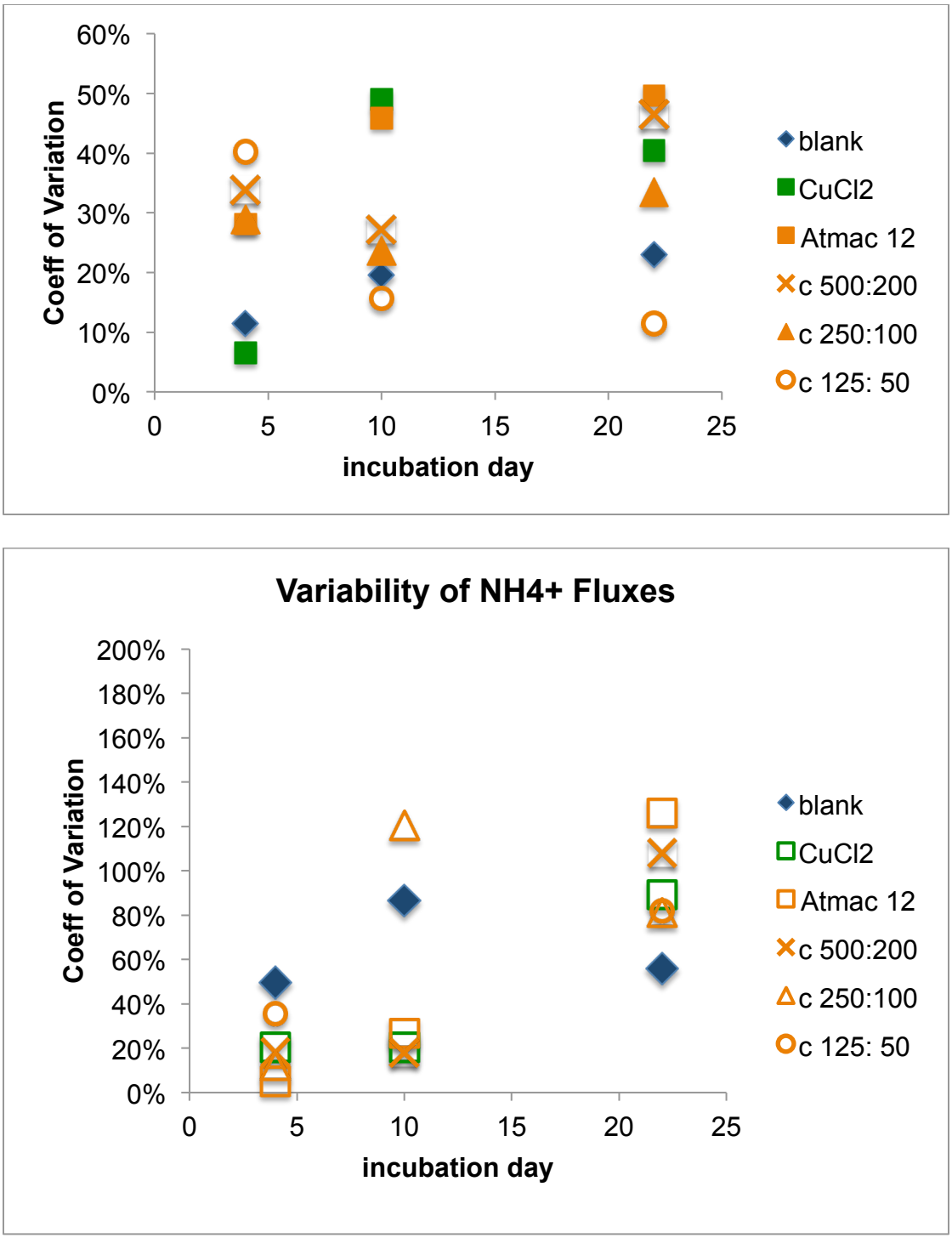

Fig. 6.11. (a) Variance in N_2 fluxes. (b) Variance in NH_4^+ fluxes. Amended sediments showed greater variability compared to controls ("blank") in N_2 production but not in NH_4^+ fluxes.

CHAPTER 7: DISSERTATION FINDINGS

7.1 SUMMARY

GPB sedimentary fluxes were studied over the 2009- 2015 period by *in-situ* and *ex-situ* incubations. Multiple ancillary experiments were made to elucidate rates of remineralization, N reaction pathways and biogeochemical processes behind these fluxes. These investigations led to the following findings:

I. Net N_2, NH_4^+ & NO_3^- estimates were close to published average values for comparable sediments. Seasonal flux patterns in GPB muds were low in winter, highly variable in spring and steady at higher rates in summer and fall.

II. Controls on N_2 production were found to include temperature, reactive substrate availability, benthic microalgae, and infaunal irrigation by *A. amphioplus*. No relationships were found between seasonal average N_2 flux rates and bottomwater O_2 or porewater NO_3^- concentrations. N_2 production may have been constrained by O_2 availability when sediment metabolism was high but rates were not well correlated with SOD.

III. In some instances, *in-situ* measurements were found to provide a more dynamic picture of changes in diurnal flux patterns than was obtained from *ex-situ* incubations.

IV. N flux estimates reflected a tight coupling with N remineralization as calculated by multiple proxies (ΣCO2 flux, SOD & changes in NH_4^+ porewater in anoxic incubations). NH_4^+ production estimates reflected C:N production ratios of 6.6 to 7.7 depending on the adsorption equilibrium value assumed for exchangeable NH_4^+. This range is consistent with marine organic matter as the primary N source.

V. The results of ^{15}N tracer experiments reflected a low contribution of anammox (< 5 - 10%) and a dominant role of dentrification in N_2 production. These results confirm expectations based on a number of published studies investigating the relative importance of anammox to N_2 production in coastal sediments over the last 13 years.

VI. Acetylene reduction assays demonstrated GPB sediments have the capacity to reduce C_2H_2 to C_2H_4. Based on a 3:1 C_2H_4: N_2 conversion, N_2 fixation rates from the upper 2 cm of sediment measured in May 2015 represented ~ 10% of measured net N_2 production. Integrating this rate to

the 15 cm depth of a flux core shows N_2 fixation could have accounted for roughly ½ of measured net spring N_2 production (gross production ~ 1.5× net). This fraction likely represents a maximum as (1) the measured net N_2 production rate for May 2015 incubations was particularly low compared with annualized and summer/fall rates and (2) because in spring N_2 fixation benefits from higher availability of labile carbon than in other periods.

VII. Incubations designed to analyze the toxicity of commonly used surfactants and $CuCl_2$ did not demonstrate a synergistic inhibition of N_2 production when amended to sediment incubations in combination. However, the amendments affected the partitioning of N substrate between NH_4^+ and N_2 fluxes supporting the conclusion QACs and Cu inhibit nitrification.

7.2 ADDENDUM

Net N_2 production estimates in the context of modern, anthropogenic N loadings into the Peconic estuary.

Population growth and consequent urbanization of the Peconic Estuary's watershed have altered the structure of its ecosystem in recent decades. Changes to the estuary include large declines in eelgrasses and frequent instances of harmful algal blooms including brown-tides which decimated shellfish populations in the 1980's (EPA 2007). The NY State DEC has determined that several areas of the western estuary proximate to GPB fail to meet standards for dissolved O_2 due to nutrient loadings (Peconic Estuary Program 2007).

As part of a plan to address concerns arising from these developments, the Peconic Estuary Program (PEP), a partnership between the U.S. E.P.A., the N.Y. State D.E.C. and others, published estimates of N loadings to separate areas within the overall estuary in 2007. Table 7.1 compares relevant estimates from this survey with total annual net N_2 production based on flux estimates from this study. Total annual net N_2 production is calculated assuming (1) annualized flux estimates from station one can be applied to total GPB surface area (i.e the central mud basin & fringing sand deposits) (~ $52 * 10^6$ m^2) and (2) these estimates can only be applied to the central mud basin (~ $23 * 10^6$ m^2). The comparison illustrates GPB sediments can remove most direct N loadings from groundwater & atmospheric deposition only if fringing sand deposits produce N2 at the same rate as the sediments investigated in the central mud basin. The rate of net N2 production in these fringing sand deposits is not known. Western areas

of the Peconic estuary experience seasonal O_2 depletion due to nitrogen input in groundwater discharge and from a sewage treatment plant in Riverhead (PEP 2007). The surface area of the sediment bottoms in these creeks and embayments is unlikely to be large enough for denitrification to remove these N loadings which likely empty into adjacent GPB. The table makes clear sedimentary net N2 production in GPB can not remove direct N loadings plus additional loadings from western rivers and creeks. Unless this N is removed by tidal fluxes from GPB, water quality in the estuary can not improve without remediation in its western creeks.

Table 7.1 N_2 Flux Estimates Compared with Total Nitrogen Loads to GPB

Peconic Estuary Program (2007)*
Baseline Total Annual Nitrogen Loads

Great Peconic Bay:	lbs yr^{-1}
Atmospheric Deposition	379,951
Groundwater	313,133
Direct N Load to GPB	693,084
Peconic River & Impaired Western Creeks	344,273
Total GPB & western river & creeks	1,037,357
Annualized net N-N_2 flux total GPB**	644,504
Annualized net N-N2 flux GPB central mud basin only **	285,069

* Peconic Estuary Program (2007) Total Maximum Daily Load for Nitrogen in the Peconic Estuary Program Study Area, Including waterbodies currently impaired due to low dissolved oxygen: the lower Peconic River and tidal tributaries; Western Flanders Bay, Lower Sawmill Creek, Meetinghouse Creek, Terrys Creek and tributaries.

** based on net N-N_2 flux = 1.1 mmol m^{-2} d^{-1}

REFERENCES

Aller R.C. (1988) Benthic fauna and biogeochemical processes in marine sediments: the role of burrow structures. in *Nitrogen Cycling in Coastal Marine Environments* (Blackburn T.H. & J. Sorensen eds.) John Wiley & Sons Ltd. 301-338

Aller R.C. (2001) Transport and reactions in the bioirrigated zone. *The Benthic Boundary Layer: Transport processes and biogeochemistry* (Boudreau B. & B.B. Jorgensen eds.) Oxford University Press 269- 301

Aller R.C. & J. Aller (1998) The effect of biogenic irrigation intensity and solute exchange on diagenetic reaction rates in marine sediments. *J. Mar. Res.* 56 (4): 905-936

Aller R.C., A. Hannides, C. Heilbrun & C. Panzeca (2004) Coupling of early diagenetic processes and sedimentary dynamics intropical shelf environments: the Gulf of Papua deltaic complex. *Cont. Shelf Res.* 24 2455- 2486

Aller R.C., C. Heilbrun, C. Panzeca, Z. Zhu & F. Baltzer (2004) Coupling between sedimentary dynamics, early diagenetic processes and biogeochemical cycling in the Amazon- Guianas mud belt: coastal French Guiana. *Mar. Geol.* 208 331- 360

Aller R.C. & J.E. Mackin (1989) Open-incubation, diffusion methods for measuring solute reaction rates in sediments. *J. Mar. Res.* 47 411-440

An S. & S.B. Joye (2001) Enhancement of coupled nitrification-denitrification by benthic photosynthesis in shallow estuarine sediments. *Limnol. Oceangr.* (46)(1) 62- 74

Ankley G.T., D.M. Di Toro, D. J. Hansen & W. J. Berry (1996) Technical basis and proposal for deriving sediment quality criteria for metals. *Environ. Toxicol. Chem.* (15) (12): 2056- 2066

Anschutz, P., B. Sundby, L. Lefrancois, G. W. Luther, III, and A. Mucci. 2000.
Bääth E. (1989) Effects of heavy metals in soil on microbial processes and populations. *Water, Air and Soil Pollution* 47: 335-379

Bertics V.J., C.R. Loscher, I. Salonen, A.W. Dale, J. Gier, R. A. Schmitz & T. Treude (2013) Occurrence of benthic nitrogen fixation coupled to sulfate reduction in the seasonally hypoxic Eckernforde Bay, Baltic Sea. *Biogeosciences* 10 1243- 1258

Bertics V.J., J.A. Sohm, C. Magnabosco & W. Ziebis (2012) Denitrification and nitrogen fixation dynamics surrounding an individual ghost shrimp (*Neotrypaea californiensis*) burrow system. *Appl. & Environ. Microb.* 78 3864-3872

Bertics V.J., J.A. Sohm, T. Treude, C-E. T. Chow, D.G. Capone, J.A. Fuhrman & W. Ziebis (2010) Burrowing deeper into benthic nitrogen cycling: the impact of bioturbation on nitrogen fixation coupled to sulfate reduction. *Mar. Ecol. Prog. Ser.* 409 1- 15

Blackburn T.H., P.O.J. Hall, S. Hulth & A. Landen (1996) Organic N loss by efflux and burial associated with a low efflux of inorganic N and with nitrate assimilation in Arctic sediments (Svalbard, Norway). *Mar. Ecol. Prog. Ser.* 141: 283- 293

Bollag, J-M., W. Barabasz (1979) Effect of heavy metals on denitrification process in soil. *J. Environ. Qual.* 8 (2): 196- 201

Boynton W.R. & W. M. Kemp (2008) Estuaries. *Nitrogen in the marine environment.* (2nd ed.) Capone D.G., E.J. Carpenter, D. Bronk. Academic Press 199- 260

Breitbarth, E. (2004) The Bunsen gas solubility coefficient of ethylene as a function of temperature and salinity and its importance for nitrogen fixation assays. *Limnol. Oceangr. Methods* 2: 282- 288

Brin L.D., A.E. Giblin & J.J. Rich (2014) Environmental controls of anammox and denitrification in southern New England estuarine and shelf sediments. *Limnol. Oceanogr.* 59 (3) 851- 860

Capone D.G. (1988) Benthic nitrogen fixation; in *Nitrogen Cyclng in Coastal Marine Environments*. eds. Blackburn, T.H. & J. Sorensen J. Wiley & Sons Ltd. 87- 123

Capone D.G. (1993) Determination of nitrogenase activity in aquatic samples using the acetylene reduction procedure; in *Handbook of Methods in Aquatic Microbial Ecology*. eds. Kemp P.F., B.F. Sherr, E.B. Sherr & J.J. Coles; CRC Press, Boca Raton, FL 621- 631

Capone D.G. & E.J. Carpenter (1982 (a)) Perfusion method for assaying microbial activities in sediments: applicability to studies of N_2 fixation by C_2H_2 reduction. *Appl. and Environ. Microbiol.* 43 (6) 1400- 5

Cerrato R., R. Flood & L. Holt (2010) Benthic Mapping for Habitat Classification in the Peconic Estuary: Phase III Ground Truth Studies. A final report prepared for Suffolk County Department of Health Services. Marine Science Research Center Special *Report # 137*

Cochran, J.K., D. Hirschberg & D. Amiel (2000). Particle mixing and sediment accumulation rates of Peconic Estuary sediments: A sediment accretion study in support of the Peconic Estuary Program. Final Report of Project #0014400498181563. Marine Sciences Research Center

Cornwell J.C., W.M. Kemp & T.M. Kana (1999) Denitrification in coastal ecosystems: methods, environmental controls and ecosystem level controls, a review. *Aquatic Ecology* 33: 41-54

Currin C.A., S.B. Joye & H.W. Paerl (1996) Diel rates of N_2 fixation & dentrification in a transplanted *Spartina alternifora* marsh: implication for N- flux dynamics. *Estuar. Coast. Shelf S.* 42 597- 616

Dalsgaard, T. and B. Thamdrup 2002. Factors controlling anaerobic ammonium oxidation with nitrite in marine sediments. *App. Environ. Microb*. 68 (8): 3802-3808.

Dalsgaard, T., B. Thamdrup, and D. E. Canfield. 2005. Anaerobic ammonium oxidation (anammox) in the marine environment. *Res. Microbiol.* 156, 457-464.

Dedieu K., C. Rabouille, F. Gilbert, K. Soetart, F. Metzger, C. Simonucci, D. Jezequel, F. Prevot, P. Anschutz, S. Hulth, S. Ogier & V. Mesnage (2007) Coupling of carbon, nitrogen and oxygen cycles in sediments from a Mediterranean lagoon: a seasonal perspective. *Mar. Ecol. Prog. Ser.* (346) 45-59

Devol A.H. (2015) Denitrification, anammox and N_2 production. *Annu Rev. Mar. Sci.* 7: 403-23

Doane T.A. & W.R. Horwath (2003) Spectrophotometric Determination of Nitrate with a Single Reagent. *Spectrometry Analytical Letters* (36): 12 2713- 2722

Doherty AC (2013) The distribution, fate and application as tracers of quaternary ammonium compounds (QACs) in sewage impacted estuaries. Ph.D. dissertation; School of Marine & Atmospheric Sciences, Stony Brook University

Engström P., T. Dalsgaard, S.Hulth and R. C. Aller. 2005. Anaerobic ammonium oxidation by nitrite (anammox): implications for N_2 production in coastal marine sediments. *Geochim. Cosmochim. Acta* 69, 2057-2065

Environmental Protection Agency (2007) National Estuary Program Coastal Condition Report. Chapter 3: Northeast National Estuary Program Coastal Condition, Peconic Bay Estuary Program

Eyre B.D. & A.J.P. Ferguson (2005) Benthic metabolism and nitrogen cycling in a subtropical eastern estuary (Brunswick): temporal variability and controlling factors. *Limnol. Oceangr*. 50 (1) 81- 96

Eyre, B.D., D.T. Maher & P. Squire (2013) Quantity and quality of organic matter (detritus) drives N_2 effluxes (net denitrification) across seasons, benthic habitats and estuaries. Global Biogeochemical Cycles (27) 1083- 1095

Fennel et al (2009) Modeling denitrification in aquatic sediments. *Biogeochemistry* (93) 150- 178

Ferguson A. & B. Eyre (2013) Interaction of benthic microalgae and macrofauna in the control of benthic metabolism, nutrient fluxes and denitrification in a shallow, sub-tropical coastal embayment (western Moreton Bay, Australia). *Biogeochemistry* (112) 423- 400

Ferguson A.J.P., B.D.Eyre & J.M.Gay (2004) Benthic nutrient fluxes in euphotic sediments along shallow sub-tropical estuaries, northern New South Wales, Australia. *Aquat Microb Ecol* 37: 219- 235

Fitzsimons M.F., G.E. Millward, D.M. Revitt & M.D. Dawit (2006) Desorption kinetics of ammonium and methylamines from estuarine sediments: consequences for the cycling of nitrogen. *Mar. Chem.* 101: 12-26

Forster S. & G. Graf (1995) Impact of irrigation on oxygen flux into the sediment-intermittent pumping by Callianassa subterranean and piston-pumping by Lanice-Conchilega. *Mar. Biol.* 123 (2): 335-346

Fulweiler & Nixon (2012) Net sediment N_2 fluxes in asouthern New England estuary: variations in space and time. *Biogeochemistry* (111) 111-124

Fulweiler R.W. & E.M. Heiss (2014) (Nearly) a decade of directly measured sediment N_2 fluxes. What can Narragansett Bay tell us about the global ocean nitrogen budget? *Oceanography* 27(1): 184- 195

Fulweiler R.W., E.M. Heiss, M.K. Rogener, S.E. Newell, G.R. LeCleir, S.M. Kortbein & S.M. Welheim (2015) Examing the impact of acetylene on N-fixation and the active sediment microbial community. *Front. Microbiol.* 6:418. doi: 10.3389/fmicb.2015.00418

Fulweiler R.W., S.W. Nixon, B.A. Buckeley & S.L. Granger (2007) Reversal of the dinitrogen gas flux in coastal marine sediments. *Nature* 448, 180-182

Garcia M.T., I. Ribosa, T. Guindulain, J. Sanchez- Leal & J. Vives- Rego (2001). Fate and effect of monoalkyl quaternary ammonium surfactants in the aquatic environment. *Environ. Pollut.* 111: 169-175

Gardner W.S. & M.J. McCarthy (2009) Nitrogen dynamics at the sediment water interface in shallow, subtropical Florida Bay: why denitrification efficiency may decrease with increased eutrophication. *Biogeochemistry* (95) 185- 198

Gardner W.S., M.J.McCarthy, S. An & D. Sobolev (2006) Nitrogen fixation and dissimilatory reduction to ammonium (DNRA) support nitrogen dynamics in Texas estuaries. *Limnol. Oceangr.* 51(1): 558- 568

Giblin A.E., C. S. Hopkinson & J. Tucker (1997) Benthic metabolism and nutrient cycling in Boston Harbor, Massachusetts. *Estuaries* 20 (2) 346- 364

Giblin A.E., C.R. Tobias, B. Song, N. Weston, G.T. Banta & V.H. Riveria-Monroy (2014) The importance of dissimilatory nitrtate reduction to ammonium (DNRA) in the nitrogen cycles of coastal ecosystems. *Oceanograpghy* 26 (3): 124- 131

Gilbert F., G. Stora & P. Bonin (1998) Influence of bioturbation on denitrification activity in Mediterranean coastal sediments: an *in-situ* experimental approach. *Mar. Ecol. Prog. Ser.* 163: 99-107

Gilbert F., R.C. Aller & S. Hulth (2003) The influence of macrofaunal burrow spacing and diffusive scaling on sedimentary nitrification and denitrification: An experimental simulation and model approach. *J. Mar. Res.* (61) 101-125

Glud, N.R., O. Holby, F. Hoffmann & D.E. Canfield (1998) Benthic mineralization and exchange in Arctic sediments (Svalbard, Norway). *Mar. Ecol. Prog. Ser.* (173) 237- 251

Glud, R.N. (2008) Oxygen dynamics in marine sediments. *Mar. Biol. Res.* 4 243- 289

Goa Y., J.M. O'Neill, D.K.Stoecker & J.C. Cornwell (2014) Photosynthesis and nitrogen fixation during cyanobacterial blooms in oligiohaline and tidal freshwater estuary. *Aquat. Microb. Ecol.* 72: 127-142

Granger J. & B. Ward (2003) Accumulation of nitrogen oxides in copper- limited cultures of denitrifying bacteria. *Limnol. Oceanogr*. 48 (1): 313- 318

Green M.A., R.C. Aller (2001) Early diagenesis of calcium carbonate in Long Island Sound sediments: Benthic fluxes of Ca^{2+} and minor elements during seasonal periods of net dissolution. *J. Mar. Res.* 59 (5): 769-794

Haines J.R., R.M. Atlas, R.P. Griffiths & R.Y. Morita (1981) Denitrification and N2 fixation in Alaskan contintental shelf sediments. *Appl. and Environ. Microbiol.* 41 (2) 412- 421

Hajaya M.G., U. Tezel, S.G. Pavlostathis (2011) Effect of temperature and benzylkonium chloride on nitrate reduction. *Bioresource Technol.* 102: 5039-5047

Hall P.O. & R.C. Aller (1992) Rapid, small-volume, flow injection analysis for SCO_2 and NH_4^+ in marine and freshwater. *Limnol Oceanogr*. 37(5) 1113-1119

Hamme R.C. & S.R. Emerson (2004) The solubility of neon, nitrogen and argon in distilled water and seawater. *Deep-Sea Res. I* 51 1517-1528

Hammond D.E., J. McManus, W.M. Berelson, T.E. Kilgore & R.H. Pope (1996) Diagenesis of organic material in equatorial Pacific sediments: stoichiometry and kinetics. *Deep- Sea Res.* II 43 4-6 1365- 1412

Hansen J. I., K. Henriksen & T.H. Blackburn (1981) Seasonal distribution of nitrifying bacteria and rates of nitrification in coastal marine sediments. *Microb. Ecol*. (7) 297- 304

Harrison J., R.J. Turner, D.A. Joo, M.A. Stan, C.S. Chan, N.D. Allan, H.A.Vrionis, M.E.Olson & H. Ceri (2008) Copper and Quaternary Cations Exert Synergistic Bactericidal and Antibiofilm Activity against *Pseudomanas aeruginosa Antimicrobial Agents and Chemotherapy* (52) 8: 2870- 2881

Herbert, R.A. (1999) Nitrogen cycling in coastal marine ecosystems. *FEMS Microbiol. Rev.* 23: 563-590

Holtan- Hartwig L., M. Bechmann, T. R. Hoyas, R. Linjordet & L.R. Bakken (2002) Heavy metals tolerance of soil denitrifying communities: N_2O dynamics. *Soil Biol. & Biochem.* 34 (2002) 1181- 1190

Howarth R.W., R. Marino & J.J. Cole (1988) Nitrogen fixation in fresh water, estuarine and marine ecosystems. 2. Biogeochemical controls. *Limnol. Oceangr.* 33 (4 (2)) 688- 701

Howarth R.W., R. Marino, J. Lane & J.J. Cole (1988) Nitrogen fixation in fresh water, estuarine and marine ecosystems. 1. Rates and importance. *Limnol. Oceangr.* 33 (4 (2)) 669- 687

Howes et al (1998) Oxygen uptake and nutrient regeneration in the Peconic Estaury. A final report prepared for Suffolk County Department of Health Serivices

Howes R.L., A.P. Rees & S. Widdecombe (2004) The impact of two species of bioturbating shrimp (*Callianassa subterranean* and *Upogebia deltaura*) on sediment denitrification. *J. Mar. Biol. Ass. UK* 84 629- 632

Hulth S., A. Tengberg, A. Landen & P.O.J. Hall (1997) Mineralization and burial of organic carbon in sediments of the southern Weddell Sea (Antarctica). *Deep-Sea Res.* 44 (6) 955- 981

Hulth S., R.C. Aller, D.E. Canfield, T. Dalsgaard, P. Engstrom, F. Gilbert, K. Sundback & B. Thamdrup (2005) Nitrogen removal in marine environments: recent findings and future research challenges. *Mar. Chem.* 94: 125- 145

Jenkins M.C. & W.M. Kemp (1984) The coupling of nitrification and denitrification in two estuarine sediments. *Limnol. Oceangr.* 29(3) 609- 619

Jones, K. (1982) Nitrogen fixation in the temperate estuarine intertidal sediments of the River Lune. *Limnol. Oceangr.* 27 (3) 455- 60

Joye S. B. & H.W. Paerl (1993) Contemporaneous nitrogen fixation and denitrification in intertidal microbial mats: rapid response to run- off events. *Mar. Ecol. Prog. Ser.* 94 267- 274

Joye S.B. & I.C. Anderson (2008) Nitrogen Cycling in Coastal Sediments. Nitrogen Cycling in the Marine Environment 2nd. (Capone D.G., E. H. Carpenter & D.A. Bronk ed.) *Academic Press* 868- 918

Joye S.B. & J.T. Hollibaugh (1995) Influence of Sulfide Inhibition of Nitrification on Nutrient Regeneration in Sediments. *Science* 270 (5236): 623- 625

Kana T.M., C. Darkangelo, M.D. Hunt, J.B. Oldham, G.E. Bennett & J.C. Cornwell (1994) A membrane inlet mass spectrometer for rapid high precision determination of N_2, O_2 and Ar in environmental water samples. *Anal. Chem*. 66: 4166- 4170

Kemp W.M., P. Sampou, M. Mayer, K. Henrikson & W.R. Boynton (1990) Ammonium recycling versus denitrification in Chesapeake Bay sediments. *Limnol. Oceangr.* 35 (7) 1545- 1563

Koike I. & H. Mukai (1983) Oxygen and inorganic nitrogen contents in burrows of the shrimps *Callianasa japonica* and *Upogebia major. Mar. Ecol. Prog. Ser.* 12: 185-190

Koop-Jacobsen, K. & A.E. Giblin (2009) Anammox in tidal marsh sediments: the role of salinity, nitrogen loading and marsh vegetation. *Estuaries & Coasts* 32: 238- 245

Kreuzinger N., M. Fuerhacker, S. Scharf, M. Uhl, O. Gans & B. Grillitsch (2007) Methodological approach towards environmental significance of uncharacterized substances- quaternary ammonium compounds as an example. *Desalination* 215: 209- 222

Kristensen E., M.H.Jensen & R.C. Aller (1991) Direct measurement of dissolved inorganic nitrogen exchange and denitrification in individual polychaete (*Nereis virens*) burrows. *J. Mar. Res.* 49: 355- 377

Laima M.J.C., M.F. Girard, F. Vouve, G.F. Blanchard, D. Goleau, R. Galois & P. Richard (1999) Distribution of absorbed ammonium pools in two intertidal sedimentary structures, Marennes- Oleron Bay, France. *Mar. Ecol. Prog. Ser.* 182 29- 35

LaMontagne M.G., V. Astorga, A.E. Giblin & I. Valiela (2002) Denitrificiation and the stoichiometry of nutrient regeneration in Waquoit Bay, Massachusetts. *Estuaries* 26 (2) 272- 281

Langmiur D. (1997) Aqueous Environmental Chemistry. *Prentice- Hall Inc.* Upper Saddle River, NJ p. 353

Lara- Martin P.A., X. Li, R. Bopp & B. Brownawell (2010) Occurrence of Alkyltrimethylammonium Compounds in Urban Estuarine Sediments: Behentrimonium as a new emerging contaminant. *Environ. Sci. Technol.* 44: 7569- 7575

Laverock B., J.A. Gilbert, K. Tait, A.M. Osborn & S. Widdecombe (2011) Bioturbation: impact on the marine nitrogen cycle. *Biochem. Soc. Trans.* 39 315-320

Lee Y., Q. Tian, S.K. Ong, C. Sato &J. Chung (2009) Inhibitory effects of copper on nitrifying bacteria in suspended and attached growth reactors. *Water Air Soil Pollution* 203: 17- 27

Li X. & B.J. Brownawell (2010) Quaternary Ammonium Compounds in Urban Estuarine Sediments- A Class of Contaminants in Need of Increased Attention? *Environ Sci. Technol*. 44: 7561- 7568

Lomstein B.A., A-G. U. Jensen, J.W. Hansen, J.B. Andreasen, L.S.Hansen, J. Berntsen & H. Kunzendorf (1998) Budgets of sediment nitrogen and carbon cycling in the shallow water of Knebel Vig, Denmark. *Aqua.t Microb. Ecol.* 14: 69-80

Luther, G.W. III, B. Sundby, B.L. Lewis, P.J. Brendel and N. Silverberg. 1997. Interactions of manganese with the nitrogen cycle: Alternative pathways to dintrogen. *Geochim. Cosmochim. Acta* 61:4043-4052.

Mackin, J.E. & R.C. Aller (1984) Ammonium adsorption in marine sediments. *Limnol. Oceangr*. 29 (2) 250- 257

Macreadie P.I., D.J. Ross, A.R. Longmore & M.J. Keough (2006) Denitrification measurements of sediments using cores and chambers. *Mar. Ecol. Prog. Ser.* (326) 49- 59

Magalhaes C.M., A.Machado, P. Matos & A.A. Bordalo (2011) Impact of copper on the diversity, abundance and transcription of nitrite and nitrous oxide reductase genes in an urban European estuary. FEMS *Microbiol Ecol* 77 274-284

McCarthy M.J., K.S. McNeal, J.W.Morse & W.S.Gardner (2008) Bottomwater hypoxia effects on sediment- water interface nitrogen transformations in a seasonally hypoxic, swallow bay (Corpus Christi Bay, TX, USA) *Estuaries & Coasts* 31: 521- 531

McCarty, G.W. (1999) Modes of action of nitrification inhibitors. *Biol Fertil Soils* (29) 1-9

McGlathery K.J., N. Risgaard- Petersen & P. B. Christensen (1998) Temporal and spatial variation in nitrogen fixation activity in the eelgrass *Zostera marina* rhizosphere. *Mar. Ecol. Prog. Ser.* 168: 245- 258

Meyers, A.C. (1979) Summer and winter burrows of mantis shrimp, Squilla empusa, in Narragansett Bay, RI (USA). *Estuaries & Coastal Marine Science* 8: 87-98

Neubacher E.C., R.E. Parker & M.Trimmer (2011) Short-term hypoxia alters the balance of nitrogen cycling in coastal sediments. *Limnol Oceangr.* 56 (2): 651-665

Nicholls, J.C. & M. Trimmer (2009) Widespread occurrence of the anammox reaction in estuarine sediments. *Aquat Microb Ecol* 55: 103-113

Nielsen L.P. & R.N. Glud (1996) Denitrification in a coastal sediment measured *in-situ* by the isotope pairing technique applied to a benthic flux chamber. *Mar. Ecol. Prog. Ser.* (137) 181- 186

Pearl H.W., M. Fitzpatrick & B.M. Bebout (1996) Seasonal nitrogen fixation dynamics in a marine microbial mat: potential roles of cyanobacteria and microheterotrophs. *Limnol. & Oceangr.* 41(3): 419- 427

Peconic Estuary Program (2007) Total Maximum Daily Load for Nitrogen in the Peconic Estuary Program Study Area, Including Waterbodies Currently Impaired Due to Low Dissolved Oxygen: the Lower Peconic River and Tidal Tributaries; Western Flanders Bay and Lower Sawmill Creek; and Meetinghouse Creek, Terrys Creek and Tributaries.

Pelegri S.P., L.P. Nielsen, T.H. Blackburn (1994) Denitrification in estuarine sediment stimulated by the irrigation activity of the amphipod *Corophium volutator*. *Mar. Ecol. Prog. Ser.* (105): 285- 290

Porubsky W.P., L.E.Velasquez & S.B. Joye (2008) Nutrient- replete benthic microalgae as a source of dissolved organic carbon to coastal waters*. Estuaries & Coasts* (31) 860- 876

Postgate J.R. (1982) Biological nitrogen fixation: the fundamentals. *Phil. Trans. R. Soc. Lond. B* (296): 375- 85

Riderer- Hendersen M-A. & P.W. Wilson (1971) Nitrogen fixation by sulphate-reducing bacteria. *J. Gen. Microbiol.* 61: 27- 31

Risgaard- Petersen N. (2003) Coupled nitrification-denitrification in autotrophic and heterotrophic estuarine sediments: On the influence of benthic microalgae. *Limnol Oceangr.* 48 (1): 93- 105

Risgaard- Petersen N., M.H. Nicolaisen, N.P. Revsbech & B.A. Lomstein (2004) Competition between ammonia-oxidizing bacteria and benthic microalgae. *Appl. Environ. Microb.* 70 (9): 5528- 5537

Risgaard- Petersen N., R.L. Meyer & N.P. Revsbech (2005) Denitrification and anaerobic ammonium oxidation in sediments: effects of microphytobenthos and NO_3^-. *Aquat. Microb*. Ecol. (40): 67- 76

Risgaard- Petersen N., S. Rysgaard, L.P. Nielsen & N.P. Revsbech (1994) Diurnal Variation of denitrification and nitrification in sediments colonized by benthic microphytes. *Limnol Oceangr.* (39) (3) 573- 579

Rosenfeld J.K. (1979) Ammonium adsorption in near shore anoxic sediments. . *Limnol. Oceangr*. 24 (2) 356- 364

Rysgaard S., P. Thastum, T. Dalsgaard, P.B. Christensen, N. P. Sloth (1999) Effects of salinity on NH_4^+ adsorption capacity, nitrification and denitrification in Danish estuarine sediments. *Estuaries* (22)(1): 21- 30

Rysgaard S., B. Thamdrup, N. Risgaard- Petersen, H. Fossing, P. Berg, P.B. Christensen & T. Dalsgaard (1998) Seasonal carbon and nutrient in a high Arctic coastal marine sediment, Young Sound, Northeast Greenland. *Mar. Ecol. Prog. Ser.* 175 261- 276

Rysgaard S., N. Risgaard-Petersen, NP Sloth, K. Jensen & L.P. Nielsen (1994) Oxygen regulation of nitrification and denitrification in sediments. *Limnol Oceangr.* 39: 1643- 1652

Rysgaard, S., P.B. Christensen & L.P. Nielsen (1995) Seasonal variation in nitrification and denitrification in estuarine sediment colonized by benthic microalgae and bioturbating infauna. *Mar. Ecol. Prog. Ser.* (128) 111-124

Sakadevan K., H. Zheng & H.J. Bavor (1999) Impact of heavy metals on denitrification in surface wetland sediments receiving wastewater. *Water Sci. Technol.* 40: 349- 355

Sarkar B., M. Megharaj, Y. Xi, G.S.R. Krishnamurati & R. Naidu (2010) Sorption of quaternary ammonium compunds in soils: implications to the soil microbial activities. *J. Hazard. Mater.* 184: 448-456

Sayama M. (2001) Presence of nitrate-accumulating sulfur bacteria and their influence on nitrogen cycling in a shallow coastal marine sediment. *Applied and Environmental Microbiology* 67 (8): 3481- 3487

Seitzinger S.P. (1988) Denitrification in freshwater and coastal ecosystems: Ecological and geochemical signhificance. *Limnol. Oceanogr.* 33 (4)(2): 702- 724

Seitzinger S.P. & A.E. Giblin (1996) Estimating denitrification in North Atlantic contintental shelf sediments. *Biogeochemistry* (35) 235- 260

Shimp R.J. & R.L. Young (1988) Availability of organic chemicals for biodegradation in settled bottom sediments. *Ecotox. Environ. Safe.* 15: 31- 45

Sloth, N.P., H. Blackburn, L.S. Hansen, N. Risgaard-Petersen & B.A. Lomstein (1995) Nitrogen cycling in sediments with different organic loading. *Mar. Ecol. Prog. Serv.* (110) 163- 170

Sokal R.R. & F.J. Rohlf (1981) Biometry; 2nd ed. *W.H. Freeman & Co*. NY

Solorzano L. (1969) Determination of ammonia in natural waters by the phenolhypochlorite method. *Limnol. Oceanogr*. 13 799-801

Steppe T.F. & H.W. Paerl (2002) Potential N2 fixation by sulfate-reducing bacteria in a marine intertidal microbial mat. *Aquat. Microb. Ecol.* 28 1-12

Strickland J.D.H. & T.R. Parsons (1972) A practical handbook of seawater analysis, 2nd ed. *Fisheries Research Board of Canada*. Ottowa

Strous M., J.A. Fuerst, E.H.M. Kramer, S. Logemann, G. Muyzer, K.T. van de Pas- Schoonen, R. Webb, J.G. Kunen & M.S.M. Jetten (1999) Missing lithotroph identified as new *Planctomycete*. *Nature* 400: 446- 449

Sundback K. & A. Miles (2000) Balance between denitrification and microalgal incorporation of nitrogen in microtidal sediments, NE Kattegat. *Aquat Microb Ecol* 22: 291- 300

Tezel U. & S.G. Pavlostathis (2009) Transformation of benzylkonium chloride under nitrate Reducing Conditions. *Environ Sci. Technol*. 43: 1342- 1348

Tezel U., J.A. Pierson, S.G. Pavlostathis (2008) Effect of didecyl dimethyl ammonium chloride on nitrate reduction in a mixed methanogenic culture. *Water Sci. & Technol* 57 541-546

Thamdrup, B. (2012) New pathways and processes in the global nitrogen cycle. *Annu. Rev. Ecol. Evol. Syst.* 43:407-428

Thamdrup, B. and T. Dalsgaard (2002). Production of N_2 through anaerobic ammonium oxidation coupled to nitrate reduction in marine sediments. *Applied Environ. Microbiol*., 68: 1312-1318.

Therkildsen, M.S. & B.A. Lomstein (1993) Seasonal variation in net benthic C-mineralization in a shallow estuary. *FEMS Micrbiology Ecology* 12 131-142
Trimmer M., P. Engstrom & B. Thamdrup (2013) Stark contrast in denitrification and anammox across the deep Norwegian trench in Skagerrak. *Appl. & Environ. Microb.* 79 (23): 7381- 7389

Van Duyl F.C., W. van Raaphorst, A.J. Kop (1993) Benthic bacterial production and nutrient sediment-water exchange in sandy North Sea sediments. *Mar. Ecol. Prog. Ser.* 100 85-95

Van Raaphorst W. & J.F.P. Malschaert (1996) Ammonium adsorption in superficial North Sea sediments. *Cont. Shelf Res.* 16 (11) 1415- 1435

Vopel K., D. Thistle & R. Rosenberg (2003) “Effect of the brittle star *Amphiura filiformis* (Amphiuridae, Echinodermata) on oxygen flux into the sediment” *Limnol Oceangr.* 48 (5) 2034- 2045

Ward, B.B. (2008) Nitrification in the marine environment. *Nitrogen in the marine environment.* (2^{nd} ed.) Capone D.G., E.J. Carpenter, D. Bronk. Academic Press 199- 260

Welsh D.T., S. Bourgues, R. Dewitt & R.A. Herbert (1996) Seasonal variations in N_2 fixation (acetylene reduction) and sulphate-reduction rates in the rhizosphere of *Zostera noltii*: nitrogen fixation by sulphate reducing bacteria. *Mar. Biol.* 125: 619- 628

Woodley, J.D. (1975) The behavior of some amphiurid brittlestars. J*. Exp. Mar. BioL.Ecol.* (18): 29- 46.

Wortham-Neal J.L. (2001) Intraspecific agonistic interactions of *Squilla empusa* (Crustacea Stomatopoda) *Behaviou*r 1 39: 463-486

Ying G-G (2006) Effects of surfactants and their degradation products in the environment. *Environ. Int.* 32: 417- 431

Yoch D.C. & G. J. Whiting (1985) Evidence for NH_4^+ switch-off regulation of nitrogenase activity by bacteria in salt marsh sediments and roots of the grass *Spartina alternofora*. *Appl. and Environ. Microbiol.* 51 (1): 143- 149

Zumft W.G. (1997) Cell Biology and Molecular Basis of Denitrification. *Microbiology and Molecular Biology Reviews* 61 (4) 533-616

APPENDICES:

Appendix 1. Table of N_2, NH_4^+, NO_3^-/NO_2^- & O_2 flux values and corresponding regression p- values

GPB0914 (all fluxes in mmol m^{-2} d^{-1})

Incubation Conditions		replicate	N2	p-value	O2	p-value	NH4+	p-value	NO3-	p-value
in-situ	daylight	X	1.97	.17	-18	.00	4.77	.01	0.12	.17
in-situ	daylight	Y	0.40	.72	-20	.11	6.80	.01	-0.10	.01
in-situ	daylight	Z	0.04	.93	-25	.01	5.34	.00	0.03	.46
in-situ	daylight	W	1.68	.04	-31	.01	7.28	.01	-0.08	.02
in-situ	daylight	core avg	1.17	.19	-25	.00	6.01	.00	0.00	.87
in-situ	daylight	K	-0.93	.56	-7.2	.21	0.42	.79	-0.32	.19
bc- lab	light	X	0.70	.04	-26	.06	0.73	.09	-0.28	.11
bc- lab	light	Y	0.93	.04	-43	.01	1.77	.18	0.04	.73
bc- lab	light	Z	0.24	.04	-46	.01	3.72	.03	0.10	.53
bc- lab	light	core avg	0.62	.02	-37	.00	2.04	.06	-0.06	.19
bc- lab	light	K	0.29	.17	-15	.01	2.79	.14	0.79	.10
bc- lab	dark	X	0.35	.04	-23	.01	1.55	.06	-0.06	.06
bc- lab	dark	Y	0.56	.04	-27	.02	1.55	.25	-0.03	.32
bc- lab	dark	Z	0.31	.03	-29	.02	1.43	.11	-0.10	.16
bc- lab	dark	core avg	0.40	.00	-27	.00	1.53	.09	-0.06	.01
bc- lab	dark	K	0.15	.24	-5.3	.02	5.88	.15	0.64	.48
lab	light	X	0.84	.00	-13	.08	1.94	.01	0.19	.39
lab	light	Y	0.31	.00	-16	.06	3.85	.01	-0.07	.78
lab	light	Z	0.34	.14	-18	.07	3.85	.00	0.12	.16
lab	light	core avg	0.37	.01	-16	.06	3.20	.00	0.20	.56
lab	light	K	0.51	.28	4.3	.32	0.38	.61	0.08	.47
lab	dark	X	0.33	.04	-20	.00	4.42	.01	0.54	.04
lab	dark	Y	0.87	.00	-22	.00	4.49	.01	0.67	.06
lab	dark	Z	0.60	.01	-22	.03	4.37	.08	0.62	.01
lab	dark	core avg	0.60	.00	-21	.00	4.46	.02	0.61	.00
lab	dark	K	0.20	.03	-5.3	.01	-0.68	.13	0.06	.24

GPB0514 (all fluxes in mmol m^{-2} d^{-1})

Incubation Conditions		replicate	N2	p-value	O2	p-value	NH4+	p-value	NO3-	p-value
bc	light	X	4.69	.03	-30	.03	-0.98	.61	-0.17	.29
bc	light	Z	1.85	.03	-39	.14	-1.87	.38	-0.16	.13
lab	light	X	-0.42	.03	-1.2	.77	-0.08	.00	-0.08	.50
lab	light	Y	-0.04	.80	-20	.07	0.12	.60	-0.04	.72
lab	light	Z	-0.02	.88	-9.1	.08	-0.11	.43	-0.26	.17
lab	light	core avg	-0.17	.36	6.0	.10	-0.02	.79	-0.13	.36
lab	light	K	0.13	.24	-5.7	.52	0.05	.60	0.06	.71
lab	dark	X	0.05	.77	-15	.10	0.10	.05	-0.07	.46
lab	dark	Y	-0.06	.45	-17	.03	0.48	.13	-0.06	.05
lab	dark	Z	0.03	.77	-5.9	.22	0.52	.40	0.09	.66
lab	dark	core avg	0.01	.67	-12	.00	0.37	.25	-0.01	.62
lab	dark	K	0.12	0.13	6.3	0.11	0.18	0.26	-0.03	0.73

Table of N_2, NH_4^+, NO_3^-/NO_2^- & O_2 flux values and corresponding p- values

GPB0214 (all fluxes in mmol m^{-2} d^{-1})

Incubation Conditions		replicate	N2	p-value	O2	p-value	NH4+	p-value	NO3-	p-value
lab	light	X	0.00	.99	-2.87	.10	0.007	.88	-0.02	N-A
lab	light	Y	-0.05	.45	-3.94	.05	0.031	.35	0.02	N-A
lab	light	Z	0.14	.21	-3.85	.02	0.208	.95	0.05	N-A
lab	light	core avg	0.08	.35	-3.71	.01	0.082	.60	0.02	N-A
lab	light	K	0.00	.20	0.78	.56	0.026	.69	0.02	N-A
lab	dark	X	0.06	.06	-4.87	.07	0.154	.08	0.00	.92
lab	dark	Y	-0.08	.00	-4.55	.24	0.120	.28	0.01	.79
lab	dark	Z	0.10	.02	-5.96	.09	0.052	.16	0.02	.41
lab	dark	core avg	0.02	.06	-5.11	.13	0.112	.13	0.01	.61
lab	dark	K	-0.10	.09	-0.74	.29	0.042	.59	-0.02	.26

GPB1113 (all fluxes in mmol m^{-2} d^{-1})

Incubation Conditions		replicate	N2	p-value	SOD	p-value	NH4+	p-value	NO3-	p-value
lab	light	X	0.87	<.01	-13.5	.02	0.18	.71	0.07	.21
lab	light	Y	0.29	.09	-9.26	.02	-1.4	.21	0.16	.25
lab	light	Z	0.52	<.01	-8.04	.07	-0.24	.62	0.24	.02
lab	light	core avg	0.56	.03	-10.2	.02	-0.50	.41	0.16	.01
lab	light	K	0.00	.98	-1.82	.35	-0.16	.51		
lab	dark	X	0.83	<.01	-18.9	.02	-0.18	.87	0.18	.12
lab	dark	Y	0.44	<.01	-12.7	.04	-0.47	.31	0.35	<.01
lab	dark	Z	0.45	.23	-16.4	.03	-0.26	.23	0.38	<.01
lab	dark	core avg	0.57	<.01	-16.0	<.01	-0.30	.59	0.30	<.01
lab	dark	K	0.19	.24	-2.66	.23	-.02	.21	0.05	.41

GPB0613 (all fluxes in mmol m^{-2} d^{-1})

Incubation Conditions		replicate	N2	p-value	SOD	p-value	NH4+	p-value	NO3-	p-value
bc	24 hrs	X	-0.15	.43	**		1.64	0.01	0.00	0.98
bc	24 hrs	Y	0.33	**	**		2.05	0.01	0.02	0.47
bc	24 hrs	Z	0.27	.07	**		2.16	0.13	-0.02	0.71
bc	daylight	X	0.26	*	**		2.19	0.18	-0.04	0.78
bc	daylight	Y		**	**		2.81	0.01	-0.08	0.45
bc	daylight	Z	0.40	*	**		6.14	0.23	0.18	0.17
bc	night	X	-0.18	*	**		1.52	*	0.00	*
bc	night	Y		**	**		1.82	**	0.05	**
Bc	night	Z	0.18	*	**		0.73	*	-0.08	*
lab	light	X	0.16	0.23	-35.9	0.05	2.45	0.09	-0.31	0.38
lab	light	Y	0.18		-17.6	0.03	1.77	0.01	-0.02	0.96
lab	light	Z	0.59	0.01	-34.2	0.00	2.04	0.10	-0.19	0.55
lab	light	core avg	0.31	0.03	-29.2	0.00	2.09	0.07	-0.15	0.57
lab	light	K	0.00	1.00	2.09	0.22	0.28	0.65	-0.35	0.30
lab	dark	X			-50.7	0.04	0.46	0.28	-0.14	0.79
lab	dark	Y	0.51	0.10	-54.9	0.07	2.16	0.04	-0.47	0.23
lab	dark	Z	0.54	0.32	-40.7	0.02	2.68	0.25	0.18	0.17
lab	dark	core avg	0.51	0.18	-49.7	0.02	1.76	0.10	-0.14	0.29
lab	dark	K	-0.16	0.81	0.09	0.99	0.26	0.56	0.09	0.86

Table of N_2, NH_4^+, NO_3^-/NO_2^- & O_2 flux values and corresponding p- values

GPB1012 (all fluxes in mmol m^{-2} d^{-1})

Incubation Conditions		replicate	N2	p-value	SOD	p-value	NH4+	p-value	NO3-	p-value
bc	24 hrs	X	1.45	.03	-11.7	.02	0.69	0.35	0.04	0.82
bc	24 hrs	Y	0.55	.65	-16.5	.00	1.08	0.11	0.04	0.43
bc	24 hrs	Z	1.01	.44	-16.5	.01	1.32	0.03	0.27	0.16
bc	daylight	X	3.10	.17	-10.4	.56	-2.50	0.45	-0.17	0.89
bc	daylight	Y	7.40	.14	-23.7	.09	-1.50	0.22	0.30	0.25
bc	daylight	Z	4.74	*	-11.8	.45	-0.14	0.82	-0.26	0.76
bc	night	X	1.19	*	-10.9	*	1.51	*	0.16	*
bc	night	Y	-0.68	*	-15.4	*	1.64	*	0.00	*
bc	night	Z	0.25	*	-16.6	*	1.65	*	0.43	*
lab	dark	X	0.32	.02	-17.7	0.12	-0.21	<.01	0.06	0.06
lab	light	X	0.46	.00	-15.3	<.05	-0.96	<.01	-0.21	0.06
lab	light	Y	0.21	.04	-15.5	<.01	-0.91	<.01	-0.09	0.19

Dark lab incubations Fall 2010 (all fluxes in mmol m^{-2} d^{-1})

Incubation Conditions	replicate	N2	p-value	SOD	p-value	NH4+	p-value	NO3-	p-value
GPB1110	X	1.62	.08	-8.69	.47	-0.08	.80	0.12	0.50
GPB1110	Y	1.32	.03	-9.55	.05	0.81	.03	0.02	0.75
GPB1110	Z	1.18	.23	-8.92	.42	0.46	.50	0.09	0.12
GPB0910	X	0.86	0.24	-25.0	<.01	2.27	.08	0.00	0.98
GPB0910	Y	0.84	0.15			0.73	<.01	0.07	0.56
GPB0910	Z			-15.6	<.03	2.86	.02	0.11	0.06

Appendix notation:

* fluxes calculated from 2 incubation time-points;
** measurements suspect & discarded.

Appendix 2: Depth profiles of porewater NH_4^+ & NO_3^-. Charts illustrate maximum NO_3^- concentrations generally occur in the upper 0.5 cm of sediment; however, apparent infaunal irrigation introduces spikes in NO_3^- concentrations to lower depth intervals.

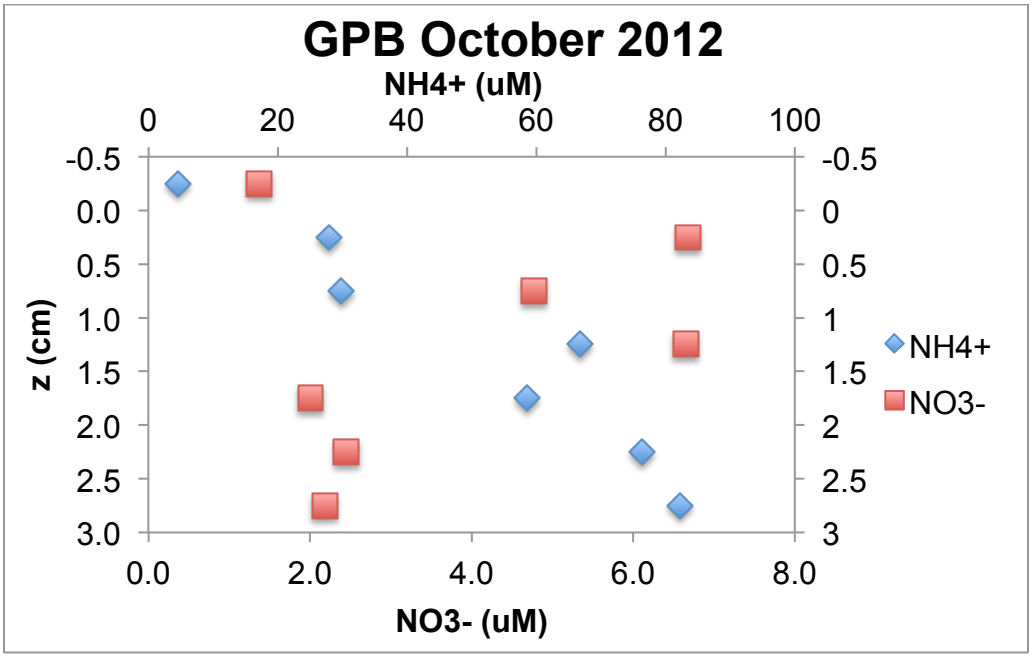

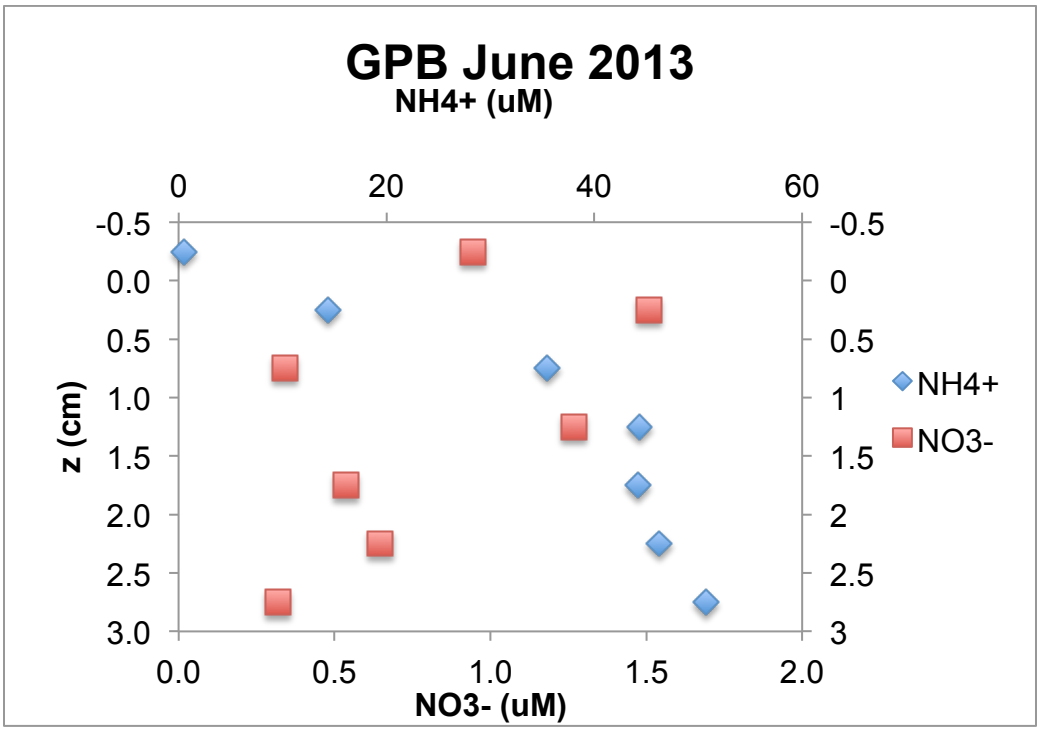

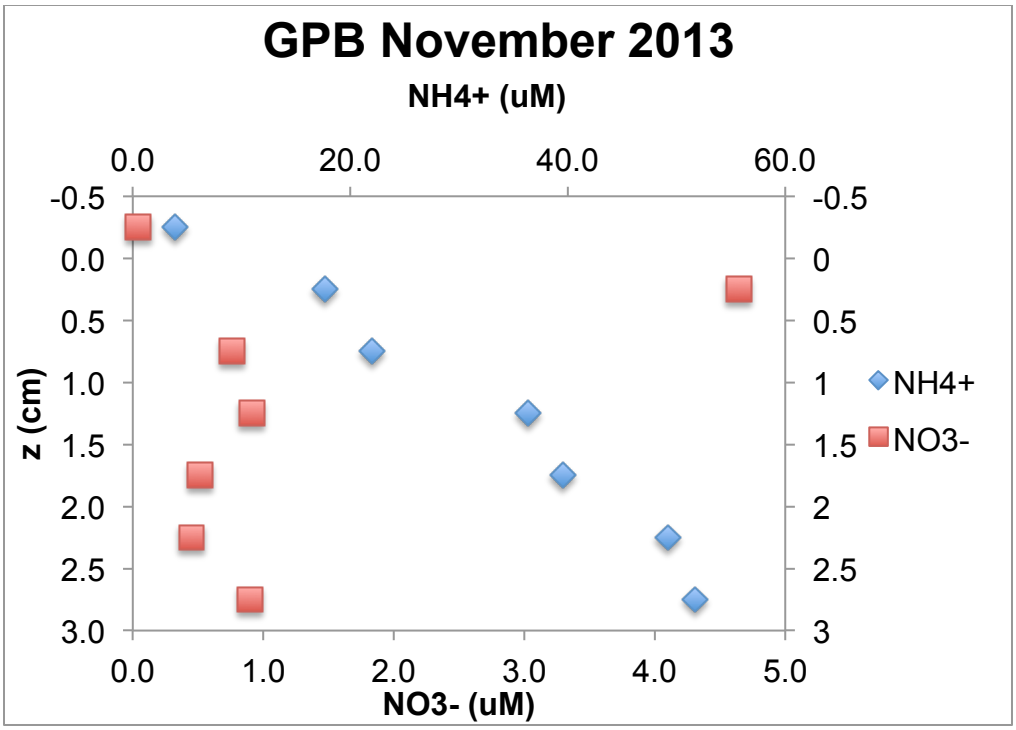
GPB November 2013
NH4+ (uM)
0.0
20.0
40.0
60.0
-0.5
0.0
0.5
1.0
1.5
2.0
2.5
3.0
z (cm)
0.0
1.0
2.0
3.0
4.0
5.0
NO3- (uM)
NH4+
NO3-

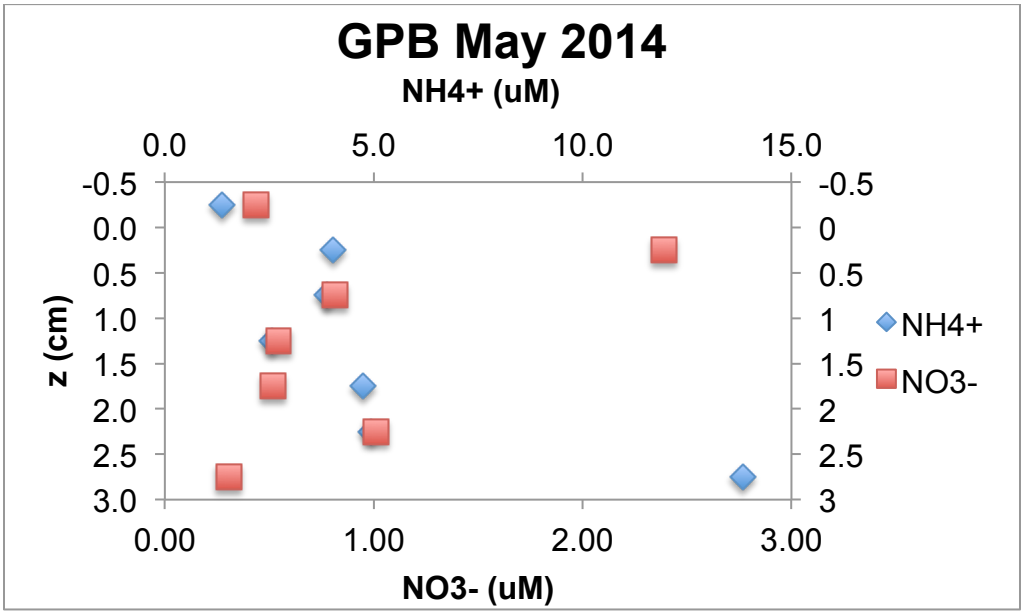
GPB May 2014
NH4+ (uM)
0.0
5.0
10.0
15.0
-0.5
0.0
0.5
1.0
1.5
2.0
2.5
3.0
z (cm)
0.00
1.00
2.00
3.00
NO3- (uM)
NH4+
NO3-

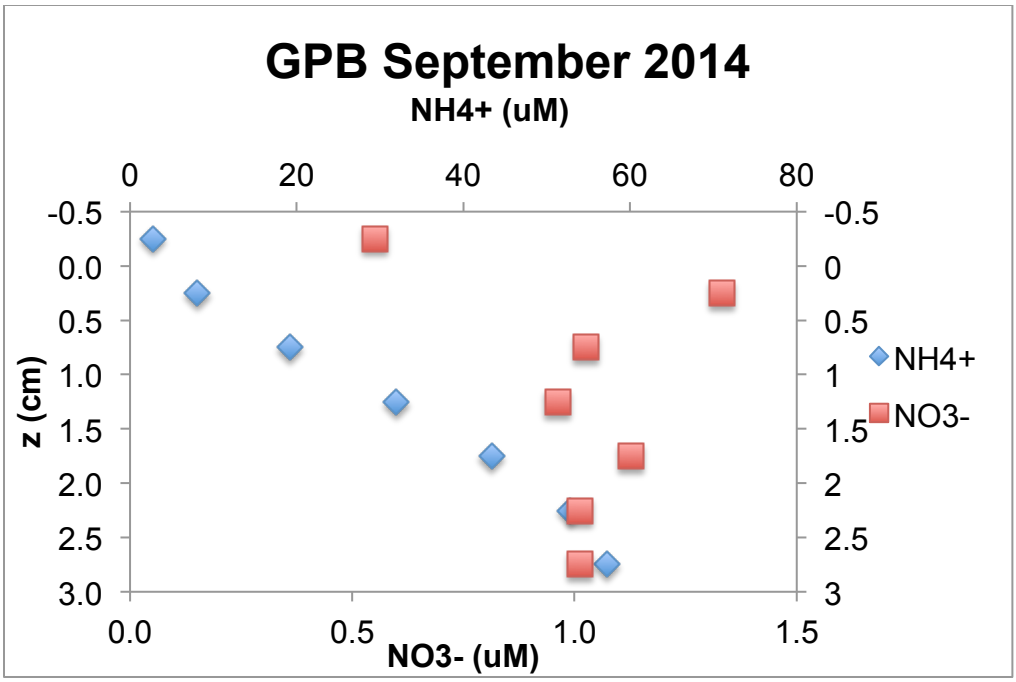
GPB September 2014
NH4+ (uM)
0
20
40
60
80
-0.5
0.0
0.5
1.0
1.5
2.0
2.5
3.0
z (cm)
0.0
0.5
1.0
1.5
NO3- (uM)
NH4+
NO3-

Appendix 3: (a) Sequential depth profiles for ΣCO_2 & $NH4^+$ porewater concentrations during anoxic incubations & (b) Trendlines of ΣCO_2 & $NH4^+$ porewater inventories to 15 cm during anoxic incubations

Charts follow in chronological order. Charts for September 2014 incubations are not shown as only 2 time-points were used due to the effects of obvious entombment of animals.

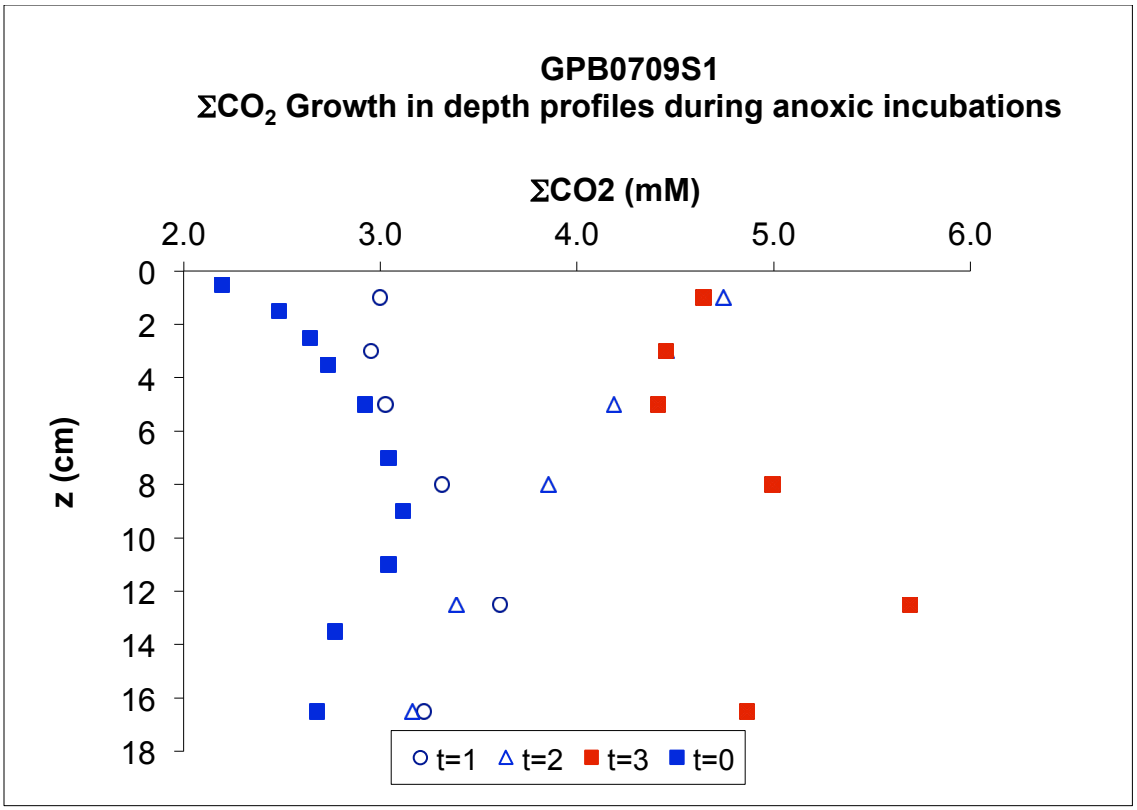
GPB0709S1
ΣCO2 Growth in depth profiles during anoxic incubations
ΣCO2 (mM)
2.0
3.0
4.0
5.0
6.0
z (cm)
0
2
4
6
8
10
12
14
16
18
t=1
t=2
t=3
t=0

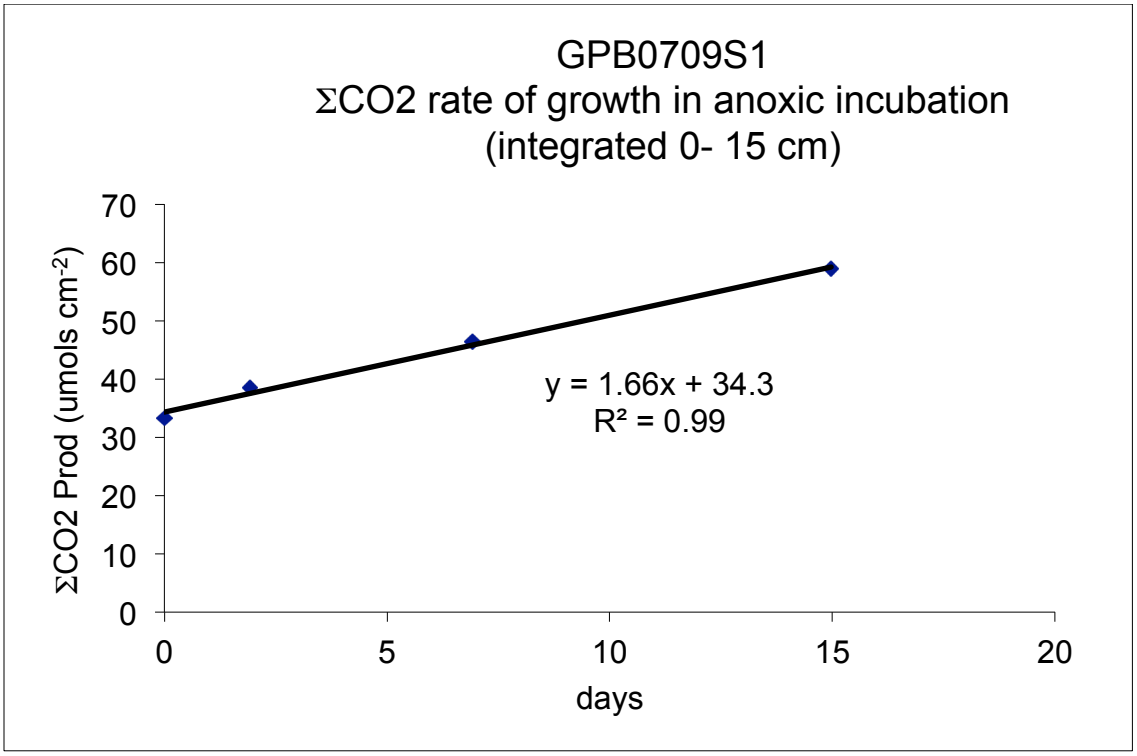
GPB0709S1
ΣCO2 rate of growth in anoxic incubation
(integrated 0- 15 cm)
ΣCO2 Prod (umols cm-2)
70
60
50
40
30
20
10
0
0
5
10
15
20
days
y = 1.66x + 34.3
R² = 0.99

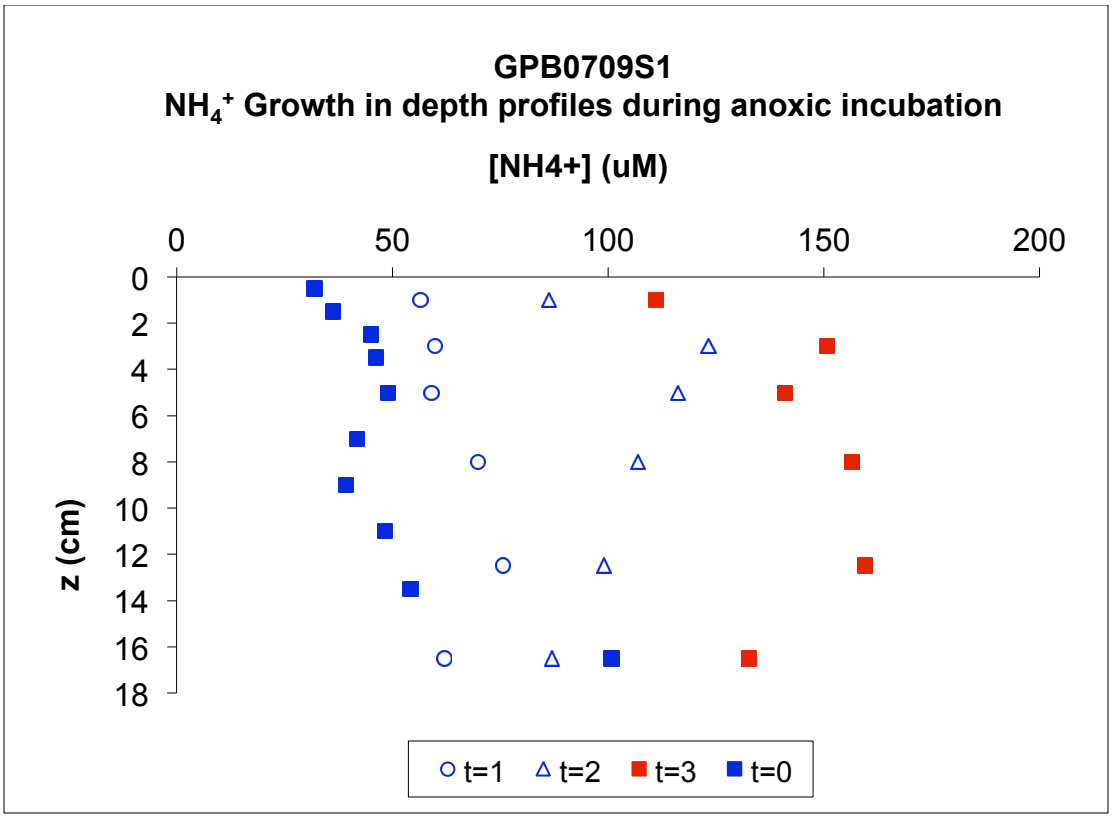
GPB0709S1
NH4+ Growth in depth profiles during anoxic incubation
[NH4+] (uM)
0
50
100
150
200
z (cm)
0
2
4
6
8
10
12
14
16
18
t=1
t=2
t=3
t=0

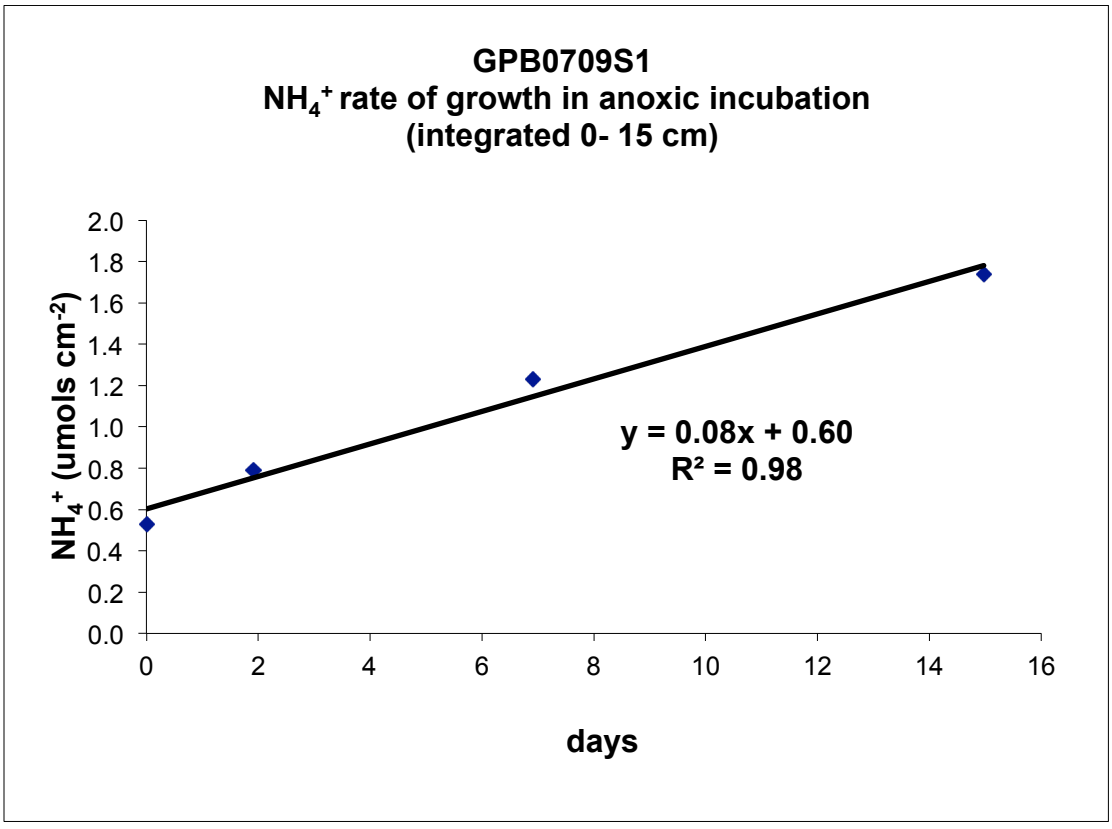
GPB0709S1
NH4+ rate of growth in anoxic incubation
(integrated 0- 15 cm)
NH4+ (umols cm-2)
2.0
1.8
1.6
1.4
1.2
1.0
0.8
0.6
0.4
0.2
0.0
0
2
4
6
8
10
12
14
16
y = 0.08x + 0.60
R² = 0.98
days

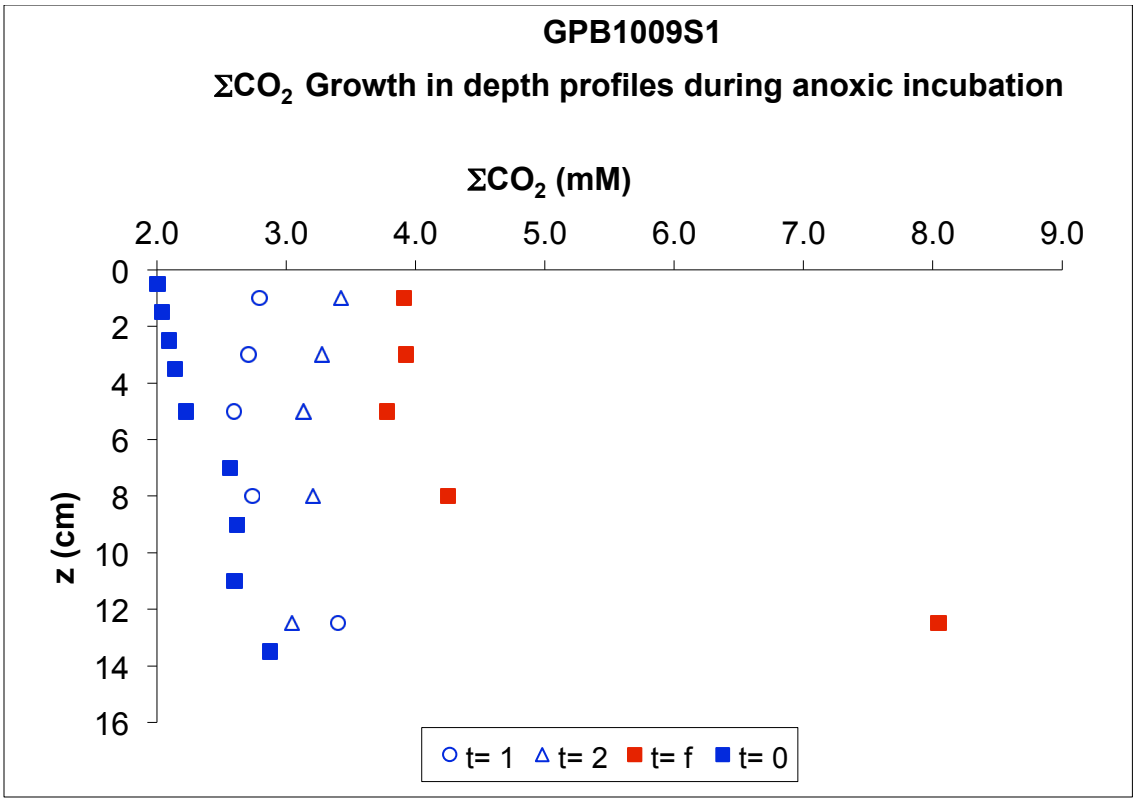
GPB1009S1
ΣCO2 Growth in depth profiles during anoxic incubation
ΣCO2 (mM)
2.0
3.0
4.0
5.0
6.0
7.0
8.0
9.0
z (cm)
0
2
4
6
8
10
12
14
16
t= 1
t= 2
t= f
t= 0

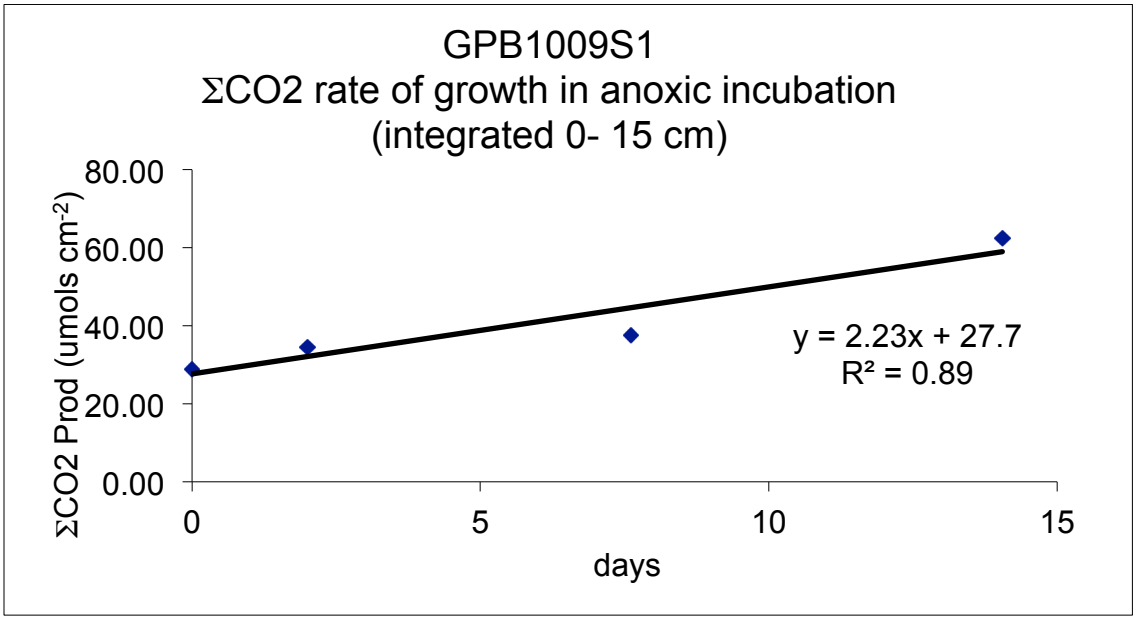
GPB1009S1
ΣCO2 rate of growth in anoxic incubation
(integrated 0- 15 cm)
ΣCO2 Prod (umols cm-2)
80.00
60.00
40.00
20.00
0.00
y = 2.23x + 27.7
R² = 0.89
0
5
10
15
days

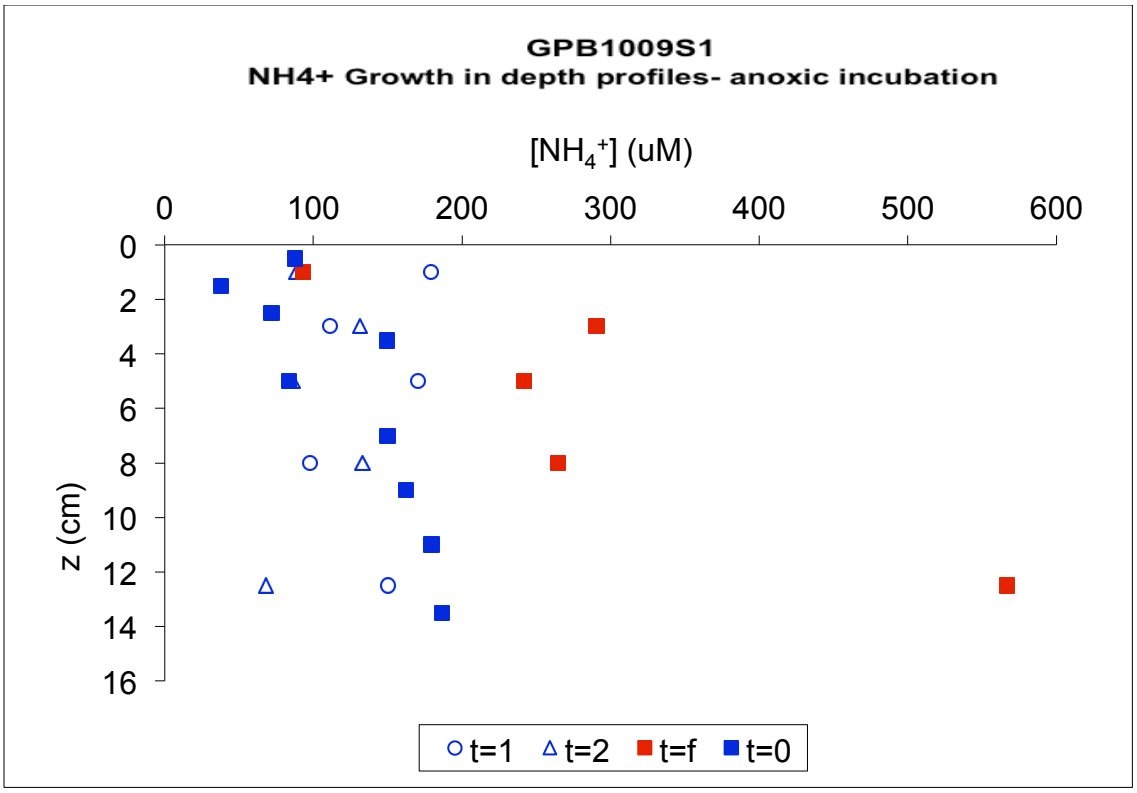
GPB1009S1
NH4+ Growth in depth profiles- anoxic incubation
[NH4+] (uM)
0
100
200
300
400
500
600
z (cm)
0
2
4
6
8
10
12
14
16
t=1
t=2
t=f
t=0

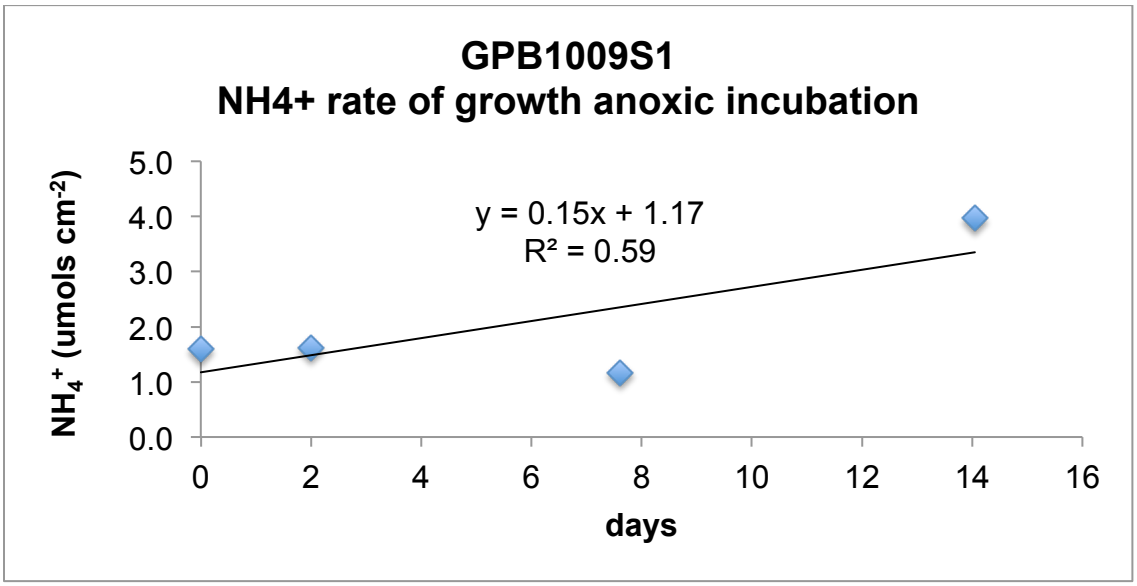
GPB1009S1
NH4+ rate of growth anoxic incubation
NH4+ (umols cm-2)
5.0
4.0
3.0
2.0
1.0
0.0
y = 0.15x + 1.17
R² = 0.59
0
2
4
6
8
10
12
14
16
days

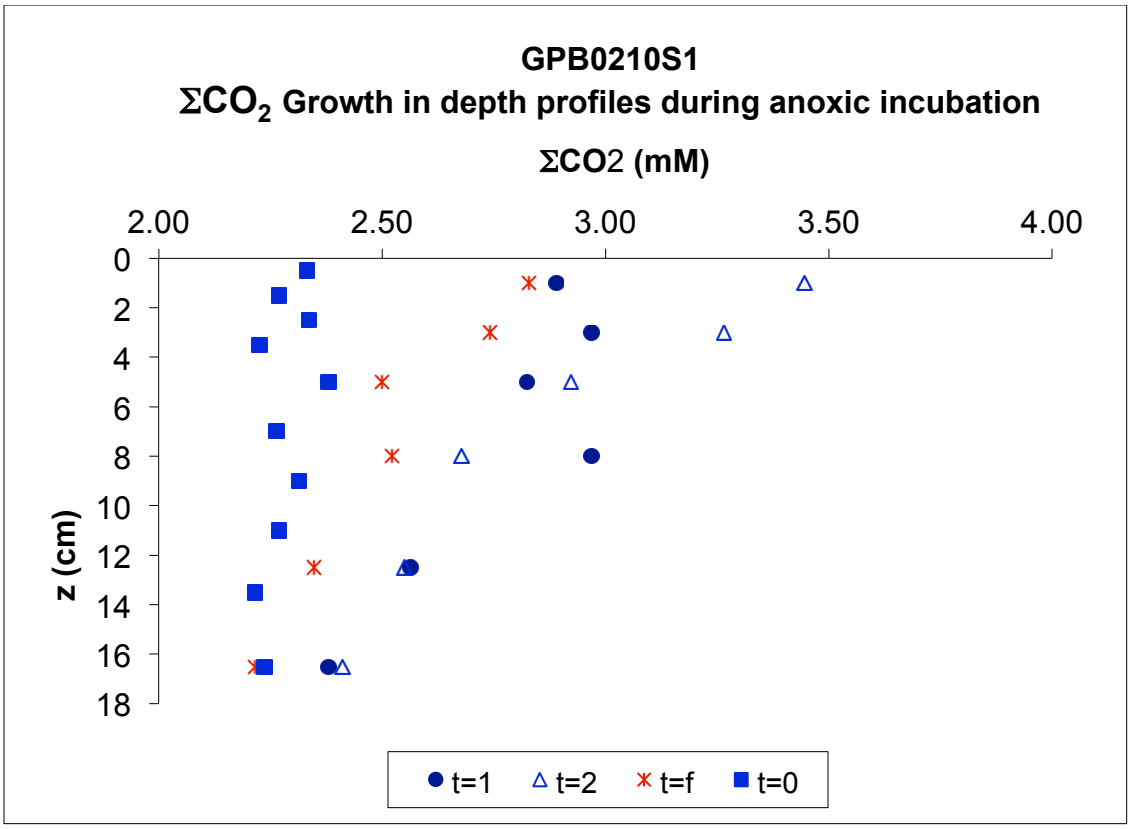
GPB0210S1
ΣCO2 Growth in depth profiles during anoxic incubation
ΣCO2 (mM)
2.00
2.50
3.00
3.50
4.00
0
2
4
6
8
10
12
14
16
18
z (cm)
t=1
t=2
t=f
t=0

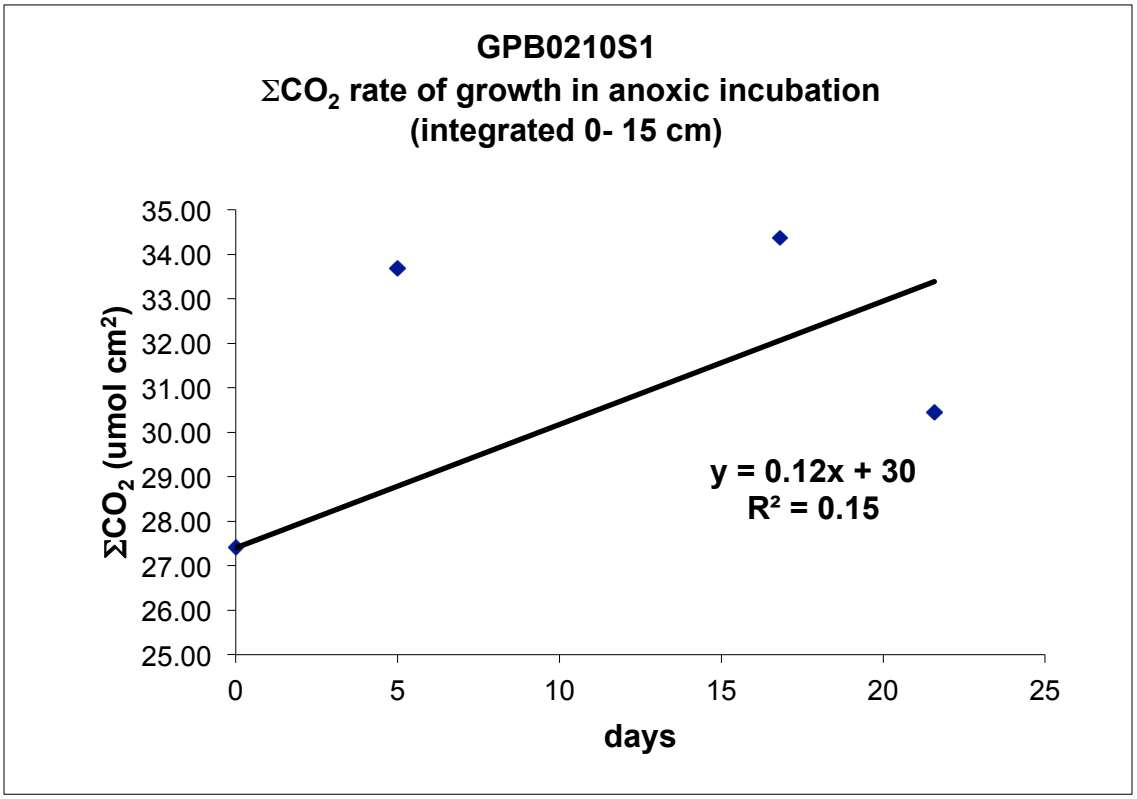
GPB0210S1
ΣCO2 rate of growth in anoxic incubation
(integrated 0- 15 cm)
35.00
34.00
33.00
32.00
31.00
30.00
29.00
28.00
27.00
26.00
25.00
ΣCO2 (umol cm2)
0
5
10
15
20
25
days
y = 0.12x + 30
R² = 0.15

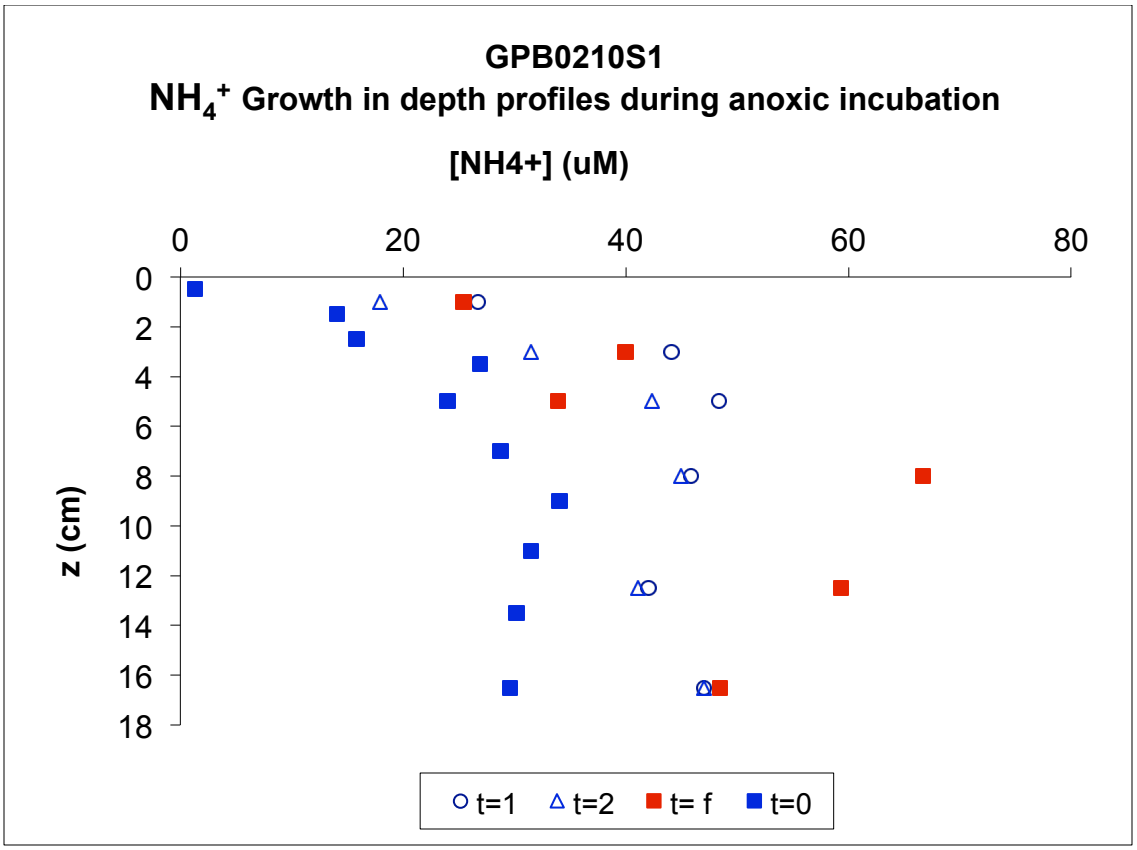
GPB0210S1
NH4+ Growth in depth profiles during anoxic incubation
[NH4+] (uM)
0
20
40
60
80
z (cm)
0
2
4
6
8
10
12
14
16
18
t=1
t=2
t= f
t=0

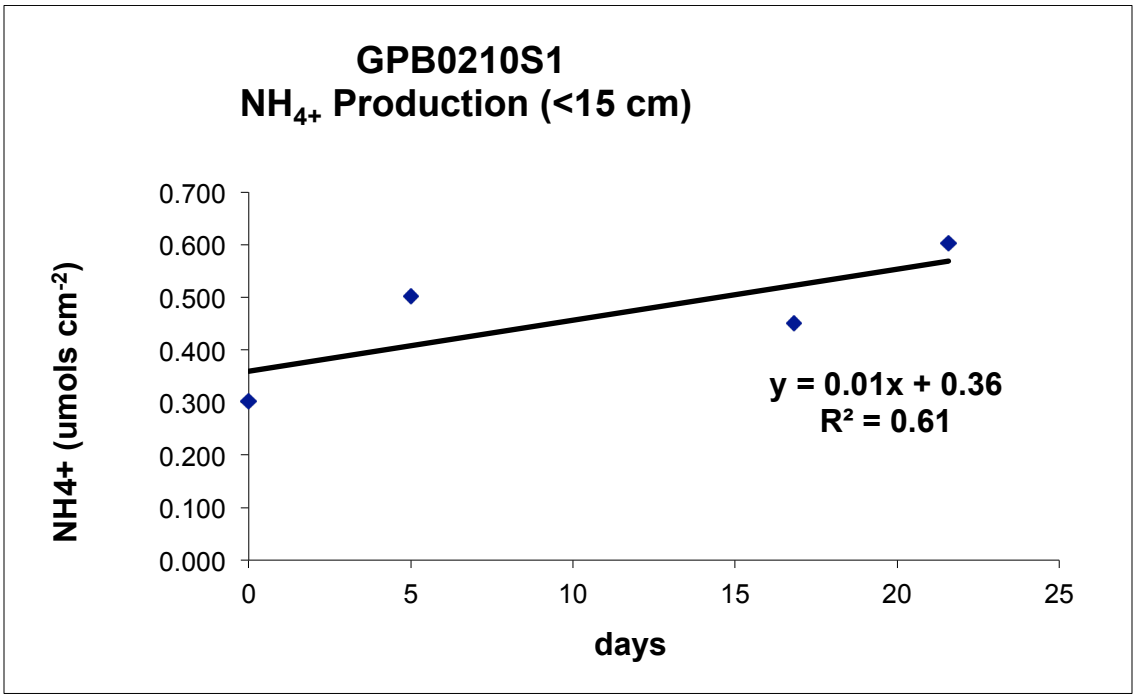
GPB0210S1
NH4+ Production (<15 cm)
NH4+ (umols cm-2)
0.700
0.600
0.500
0.400
0.300
0.200
0.100
0.000
0
5
10
15
20
25
days
y = 0.01x + 0.36
R² = 0.61

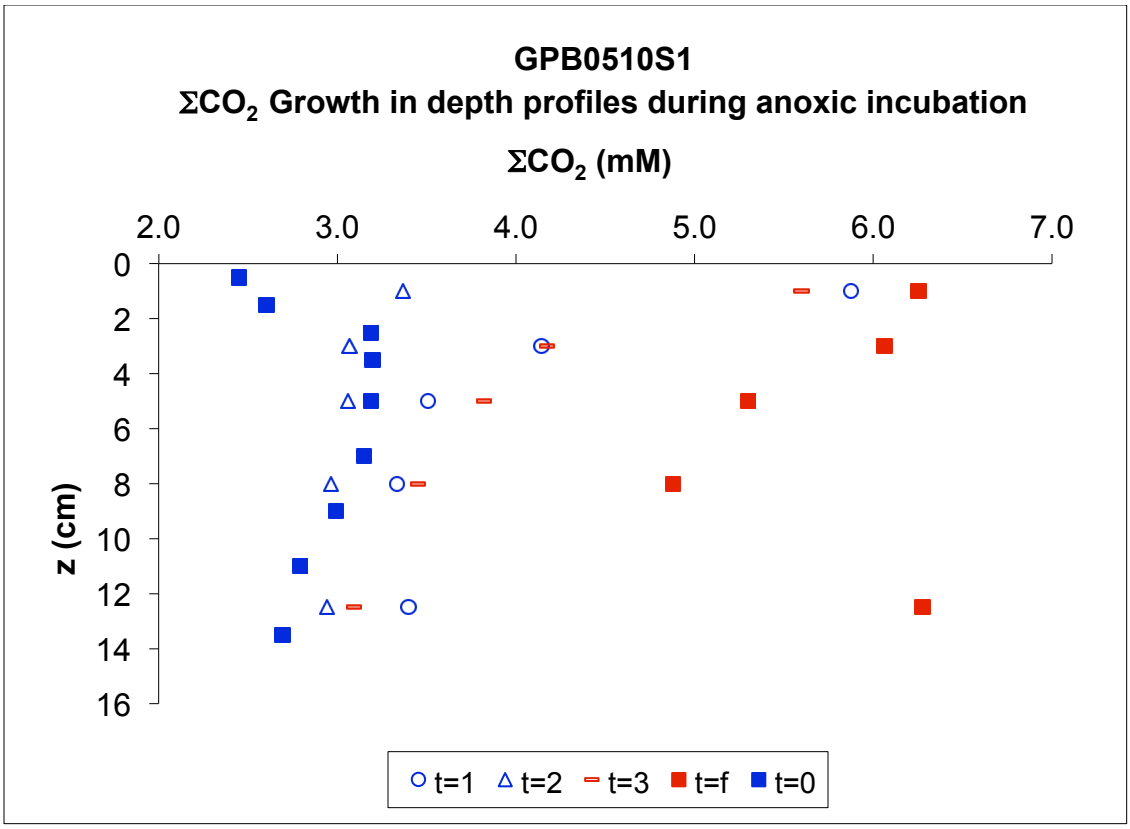
GPB0510S1
ΣCO2 Growth in depth profiles during anoxic incubation
ΣCO2 (mM)
2.0
3.0
4.0
5.0
6.0
7.0
0
2
4
6
8
10
12
14
16
z (cm)
t=1
t=2
t=3
t=f
t=0

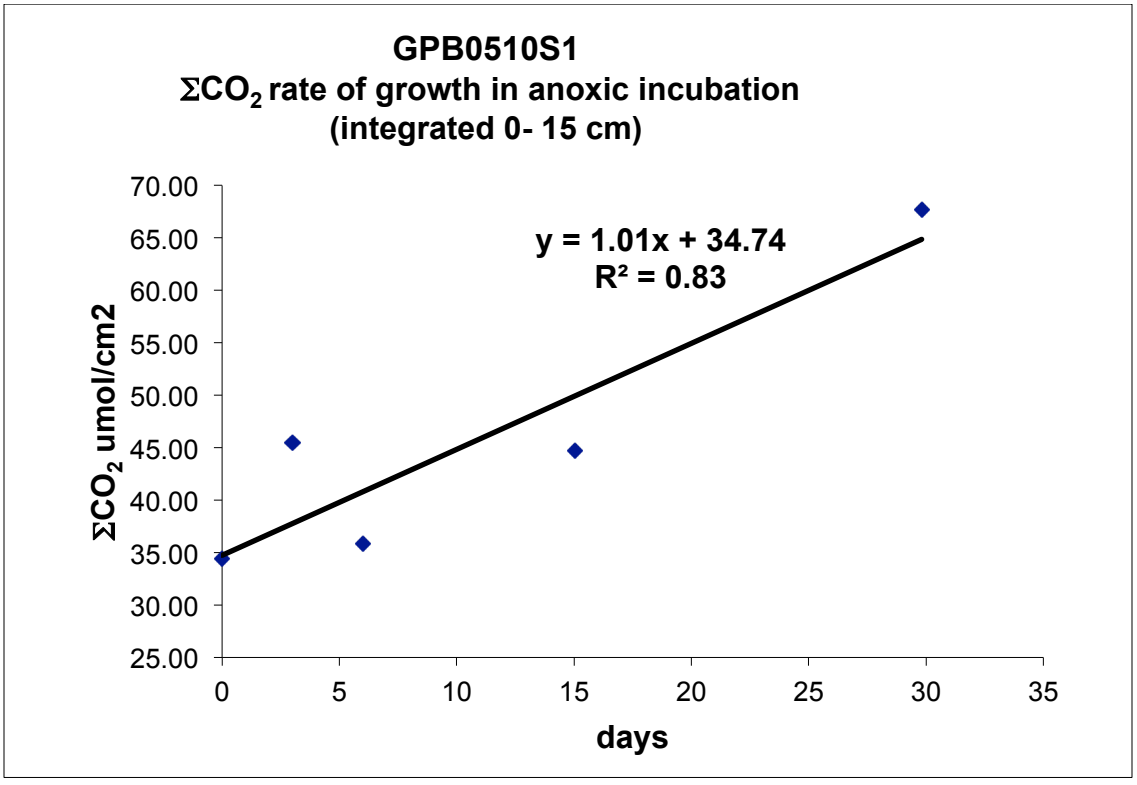
GPB0510S1
ΣCO2 rate of growth in anoxic incubation
(integrated 0- 15 cm)
y = 1.01x + 34.74
R² = 0.83
70.00
65.00
60.00
55.00
50.00
45.00
40.00
35.00
30.00
25.00
ΣCO2 umol/cm2
0
5
10
15
20
25
30
35
days

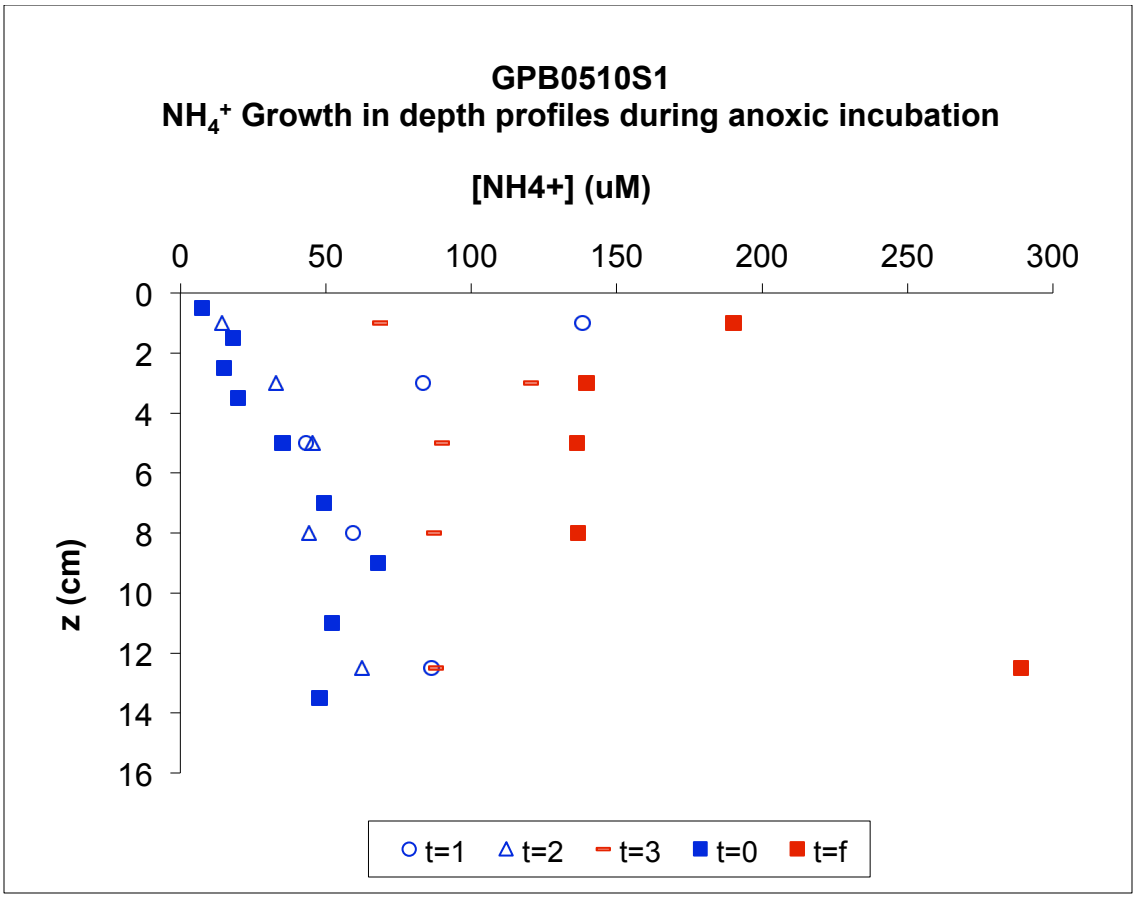
GPB0510S1
NH4+ Growth in depth profiles during anoxic incubation
[NH4+] (uM)
0
50
100
150
200
250
300
z (cm)
0
2
4
6
8
10
12
14
16
t=1
t=2
t=3
t=0
t=f

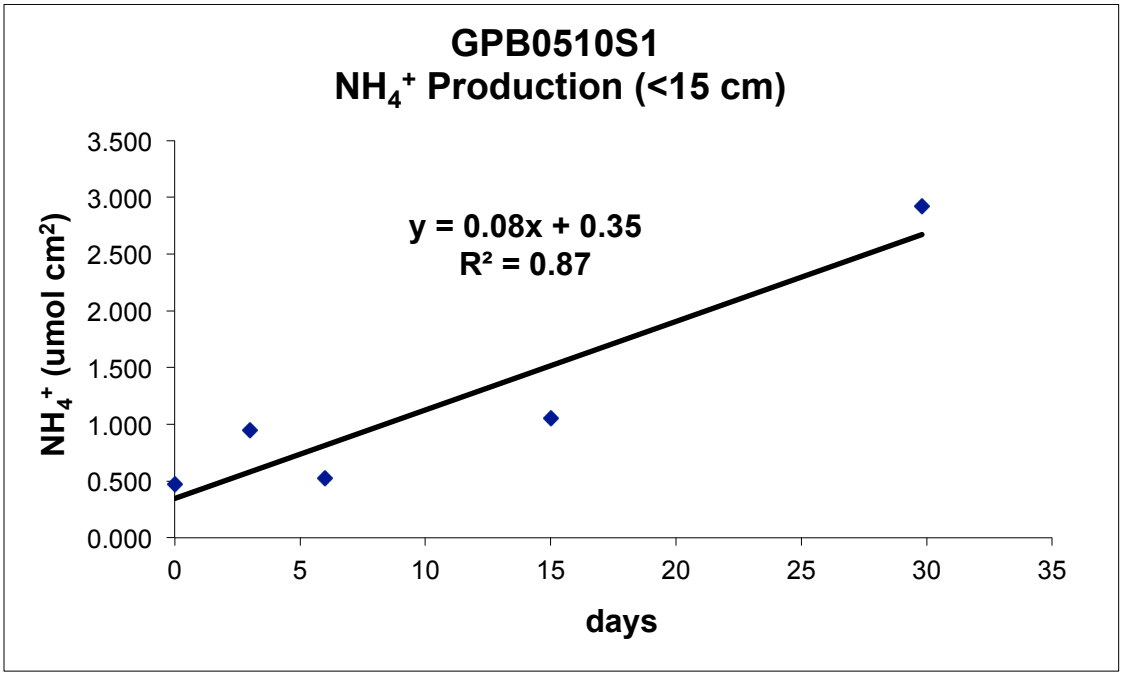
GPB0510S1
NH4+ Production (<15 cm)
y = 0.08x + 0.35
R² = 0.87
NH4+ (umol cm2)
3.500
3.000
2.500
2.000
1.500
1.000
0.500
0.000
0
5
10
15
20
25
30
35
days

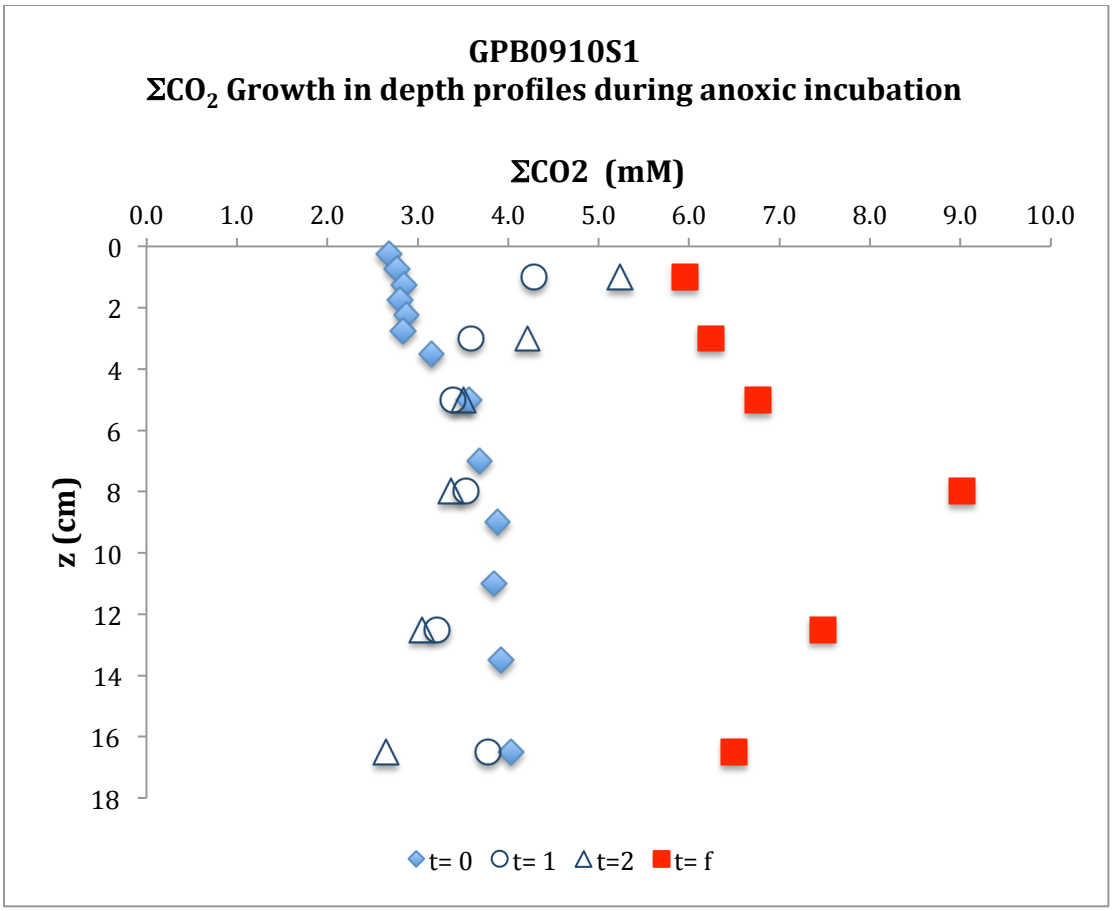
GPB0910S1
ΣCO2 Growth in depth profiles during anoxic incubation
ΣCO2 (mM)
0.0
1.0
2.0
3.0
4.0
5.0
6.0
7.0
8.0
9.0
10.0
z (cm)
0
2
4
6
8
10
12
14
16
18
t= 0
t= 1
t=2
t= f

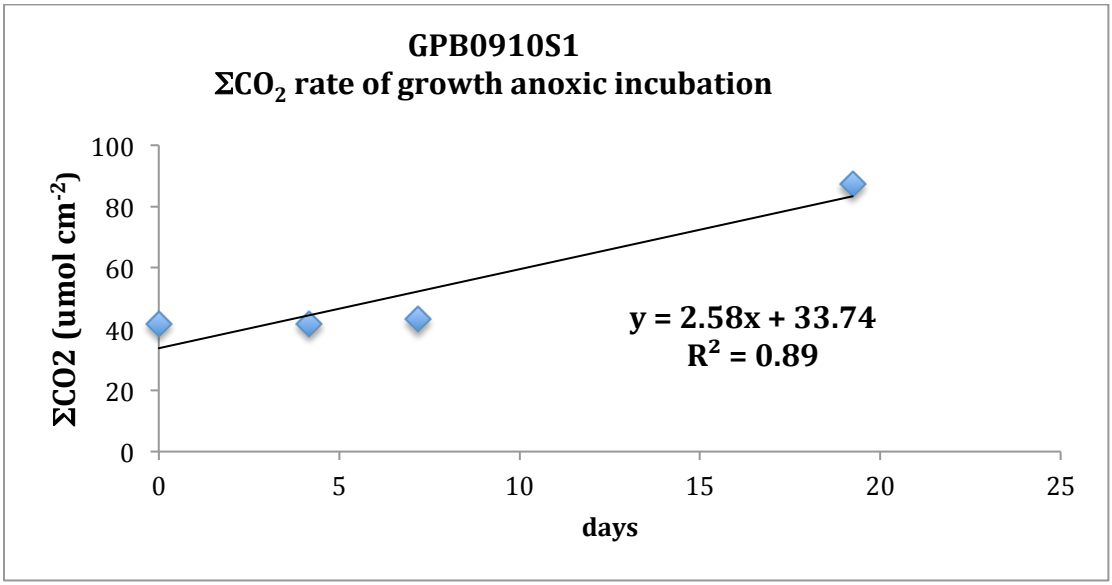
GPB0910S1
ΣCO2 rate of growth anoxic incubation
ΣCO2 (umol cm-2)
100
80
60
40
20
0
0
5
10
15
20
25
days
y = 2.58x + 33.74
R2 = 0.89

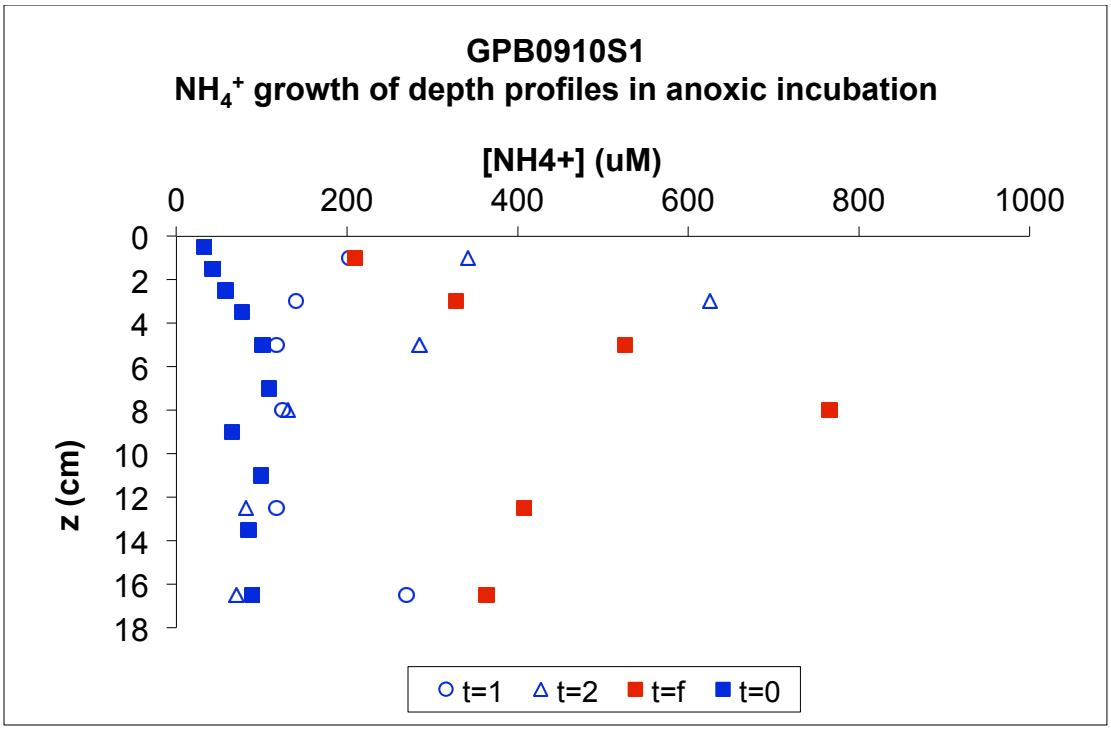
GPB0910S1
NH4+ growth of depth profiles in anoxic incubation
[NH4+] (uM)
0
200
400
600
800
1000
z (cm)
0
2
4
6
8
10
12
14
16
18
t=1
t=2
t=f
t=0

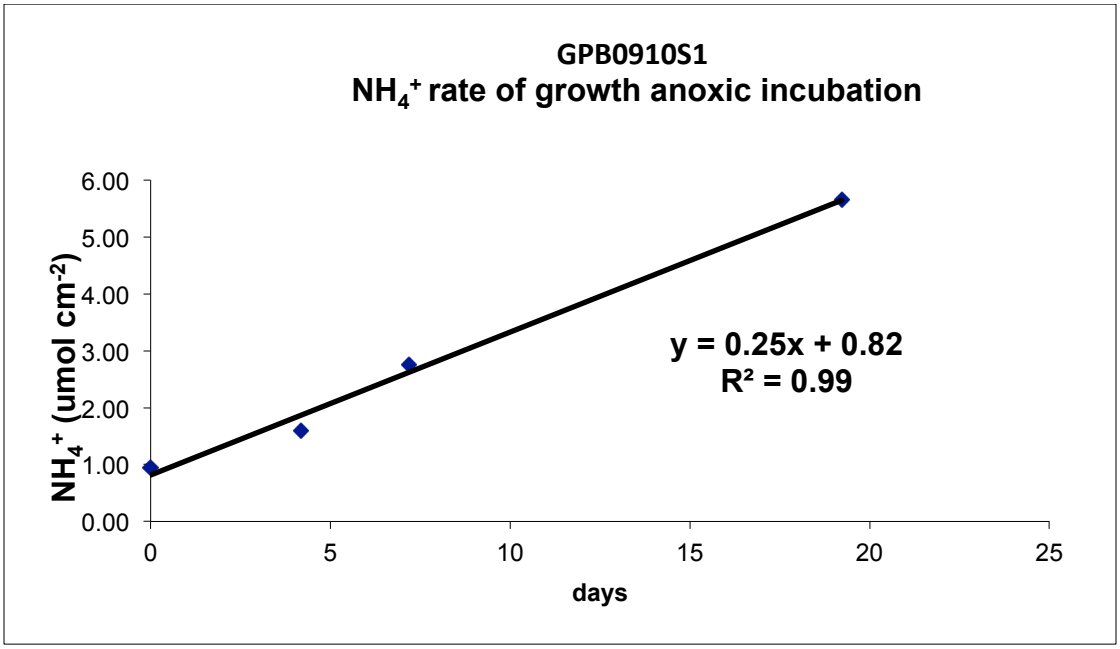
GPB0910S1
NH4+ rate of growth anoxic incubation
NH4+ (umol cm-2)
6.00
5.00
4.00
3.00
2.00
1.00
0.00
0
5
10
15
20
25
days
y = 0.25x + 0.82
R² = 0.99

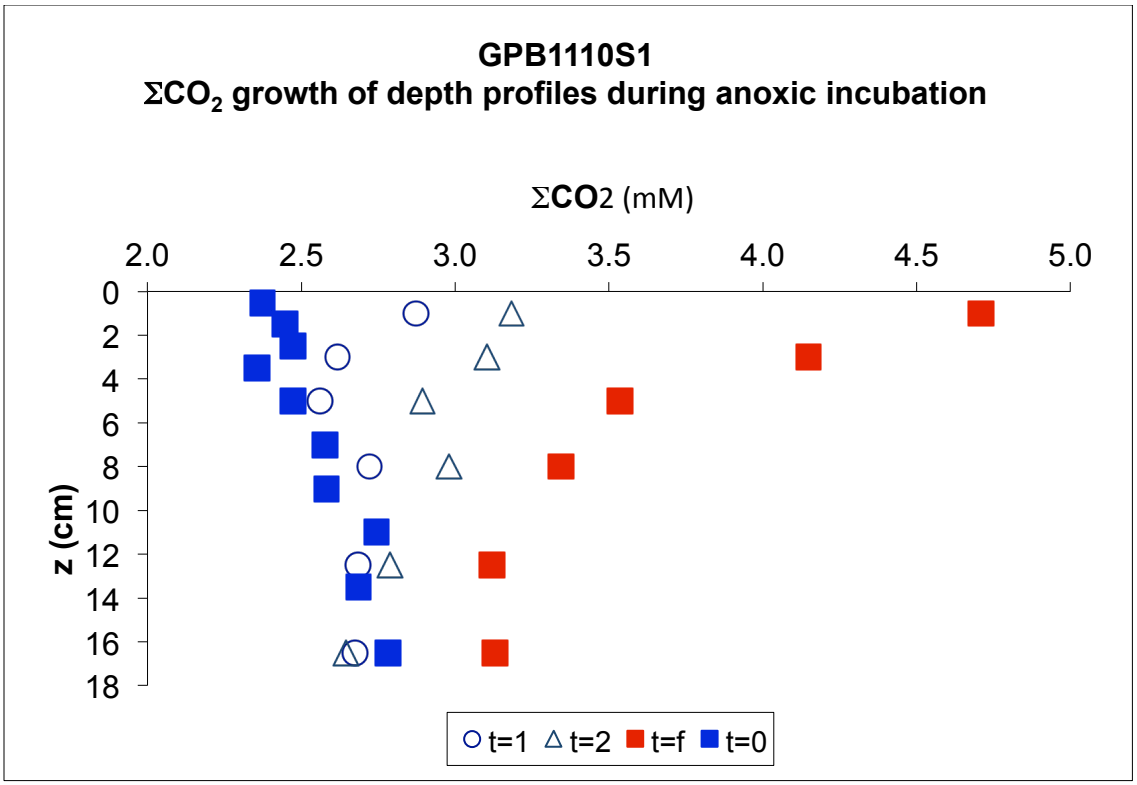
GPB1110S1
ΣCO2 growth of depth profiles during anoxic incubation
ΣCO2 (mM)
2.0
2.5
3.0
3.5
4.0
4.5
5.0
z (cm)
0
2
4
6
8
10
12
14
16
18
t=1
t=2
t=f
t=0

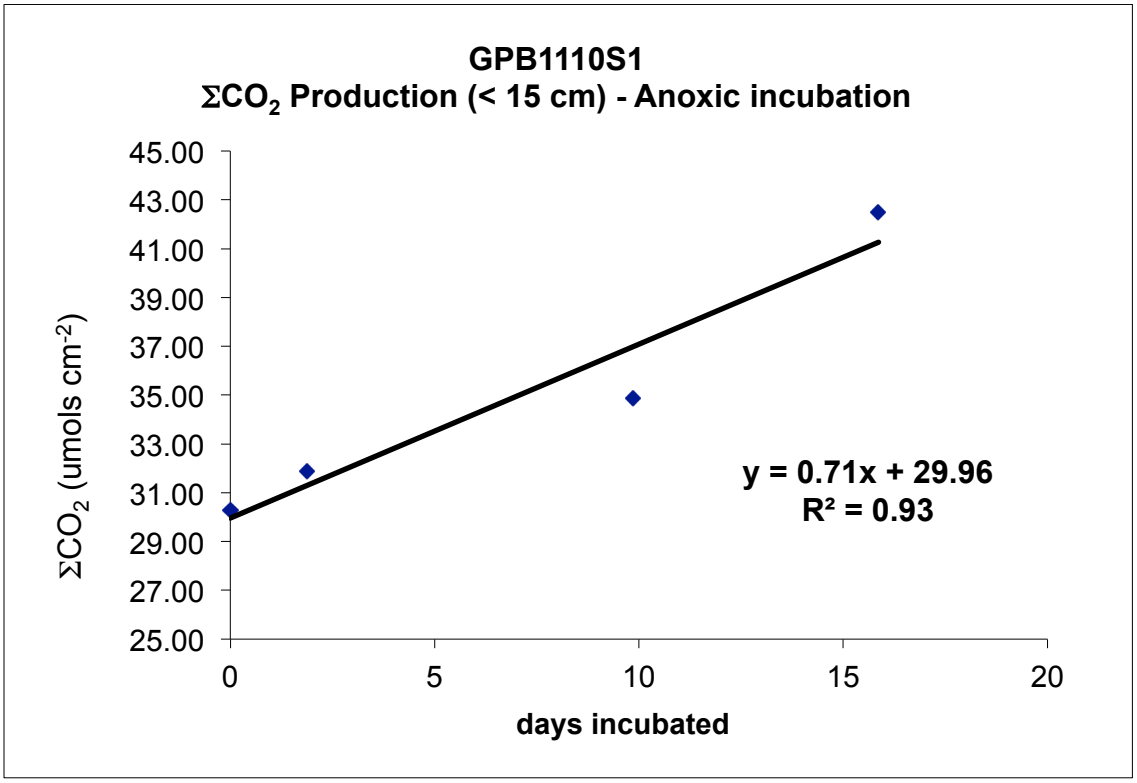
GPB1110S1
ΣCO2 Production (< 15 cm) - Anoxic incubation
ΣCO2 (umols cm-2)
45.00
43.00
41.00
39.00
37.00
35.00
33.00
31.00
29.00
27.00
25.00
0
5
10
15
20
days incubated
y = 0.71x + 29.96
R² = 0.93

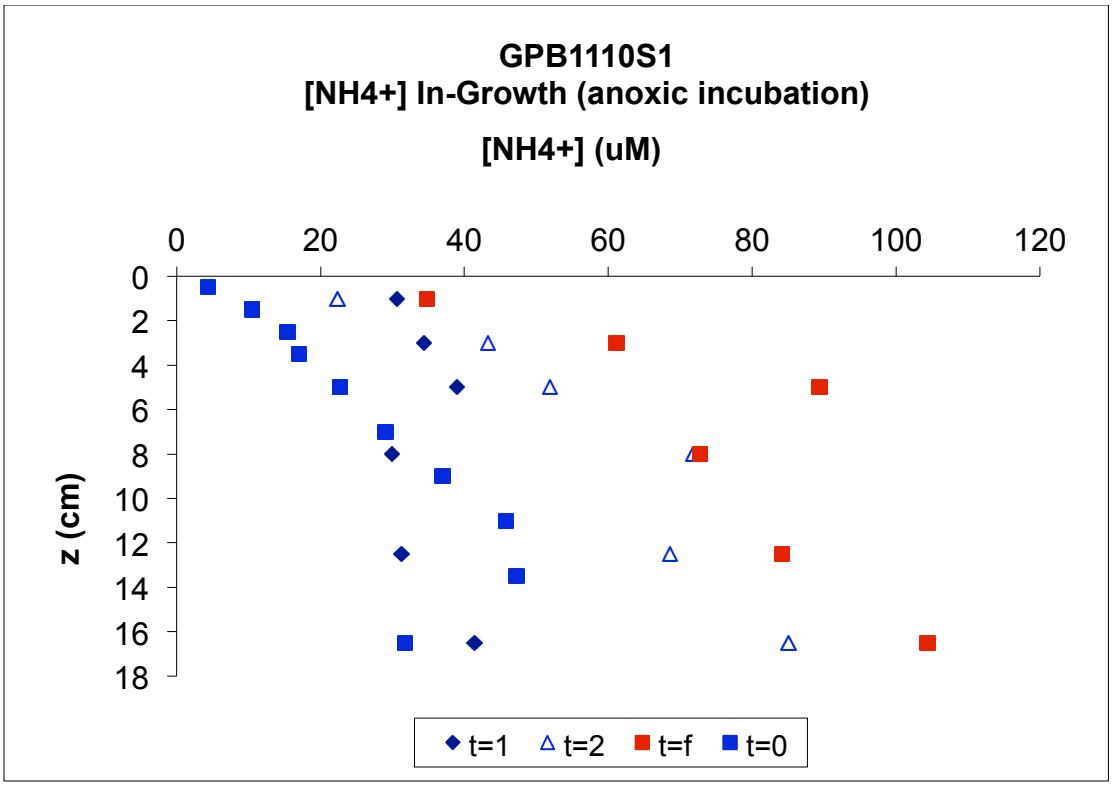
GPB1110S1
[NH4+] In-Growth (anoxic incubation)
[NH4+] (uM)
0
20
40
60
80
100
120
z (cm)
0
2
4
6
8
10
12
14
16
18
t=1
t=2
t=f
t=0

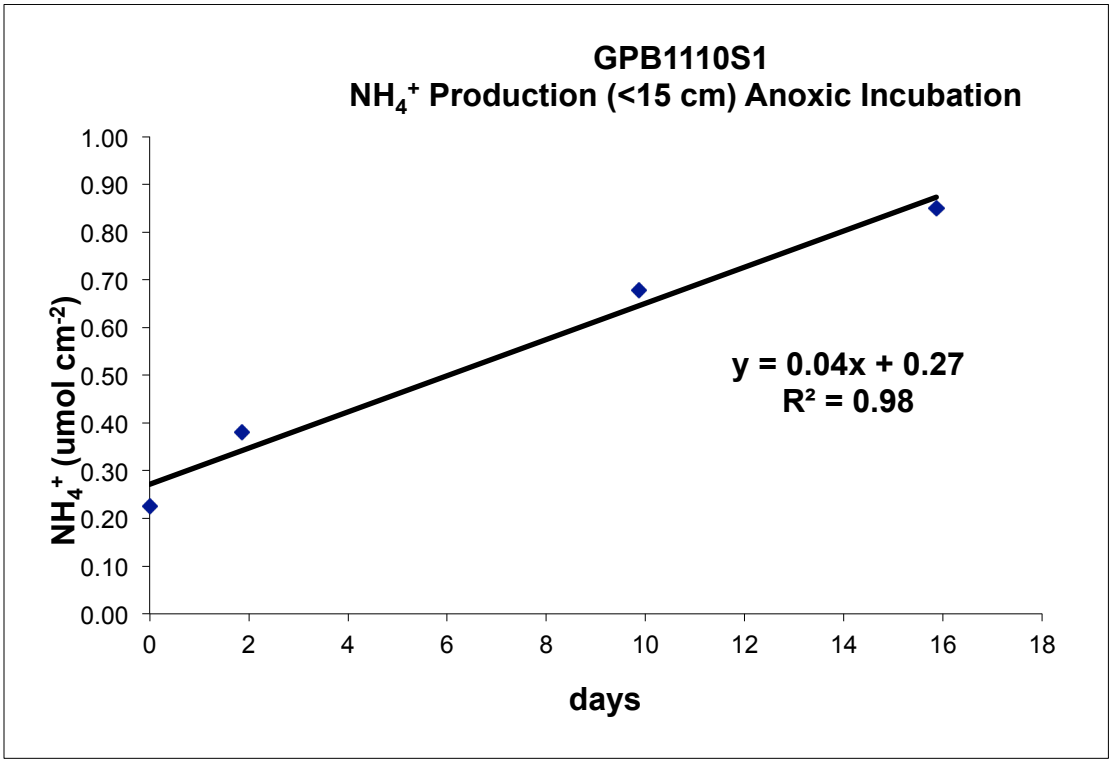
GPB1110S1
NH4+ Production (<15 cm) Anoxic Incubation
NH4+ (umol cm-2)
1.00
0.90
0.80
0.70
0.60
0.50
0.40
0.30
0.20
0.10
0.00
0
2
4
6
8
10
12
14
16
18
days
y = 0.04x + 0.27
R² = 0.98

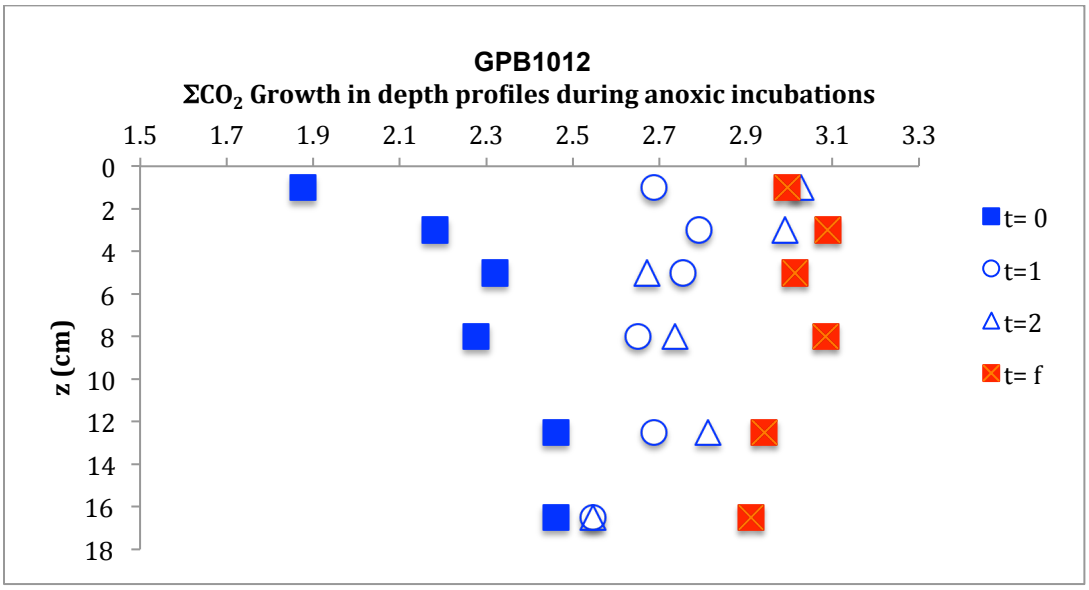
GPB1012
ΣCO2 Growth in depth profiles during anoxic incubations
1.5
1.7
1.9
2.1
2.3
2.5
2.7
2.9
3.1
3.3
0
2
4
6
8
10
12
14
16
18
z (cm)
t= 0
t=1
t=2
t= f

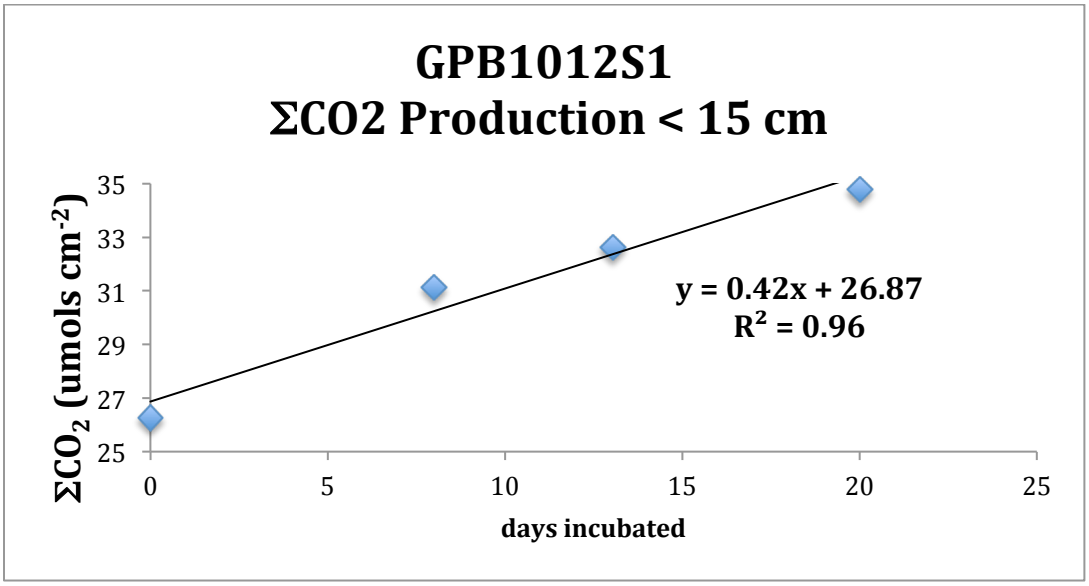
GPB1012S1
ΣCO2 Production < 15 cm
35
33
31
29
27
25
ΣCO2 (umols cm-2)
0
5
10
15
20
25
days incubated
y = 0.42x + 26.87
R2 = 0.96

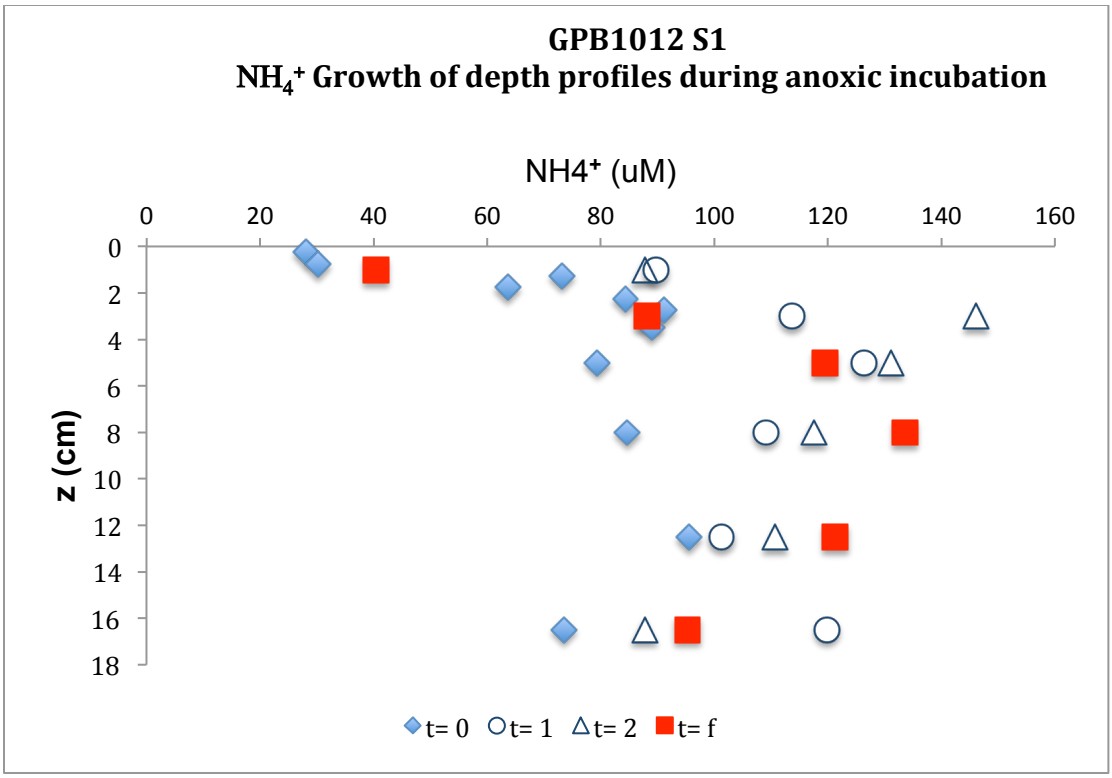
GPB1012 S1
NH4+ Growth of depth profiles during anoxic incubation
NH4+ (uM)
0
20
40
60
80
100
120
140
160
z (cm)
0
2
4
6
8
10
12
14
16
18
t= 0
t= 1
t= 2
t= f

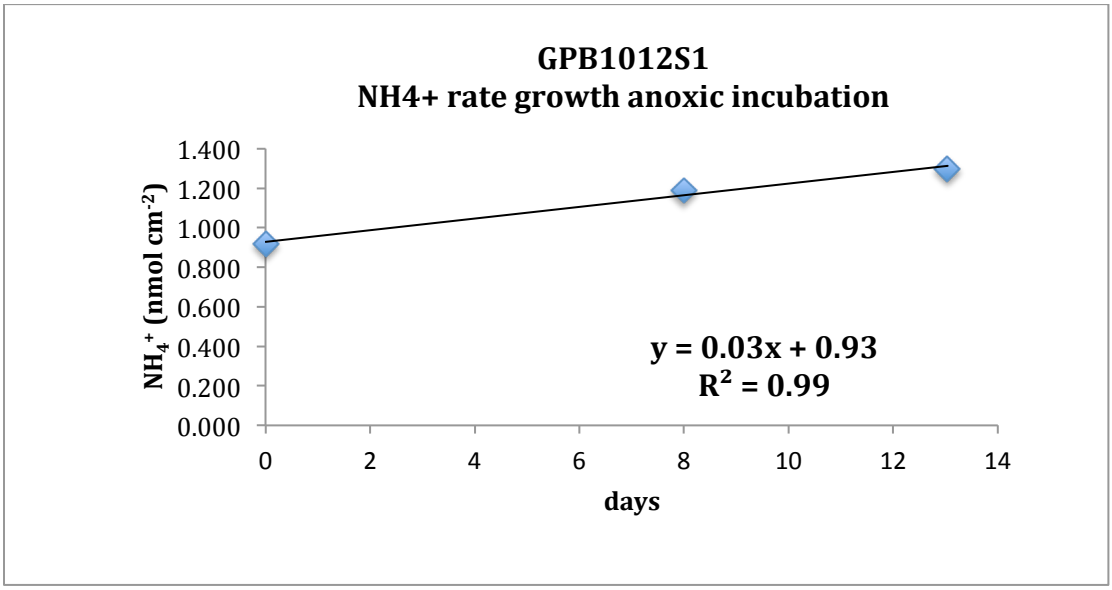
GPB1012S1
NH4+ rate growth anoxic incubation
NH4+ (nmol cm-2)
1.400
1.200
1.000
0.800
0.600
0.400
0.200
0.000
y = 0.03x + 0.93
R2 = 0.99
0
2
4
6
8
10
12
14
days

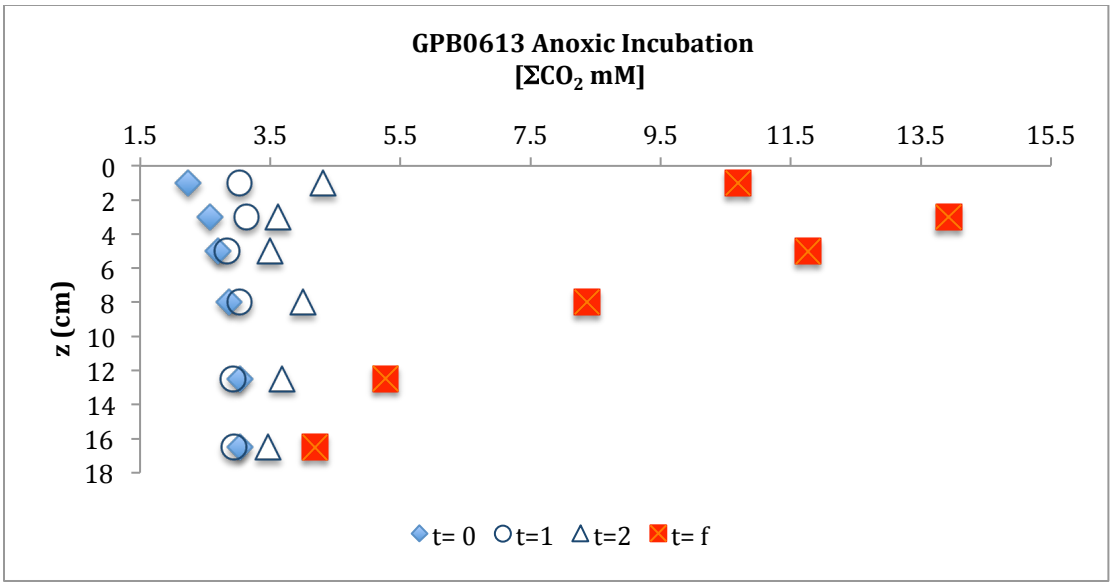
GPB0613 Anoxic Incubation
[ΣCO2 mM]
1.5
3.5
5.5
7.5
9.5
11.5
13.5
15.5
0
2
4
6
8
10
12
14
16
18
z (cm)
t= 0
t=1
t=2
t= f

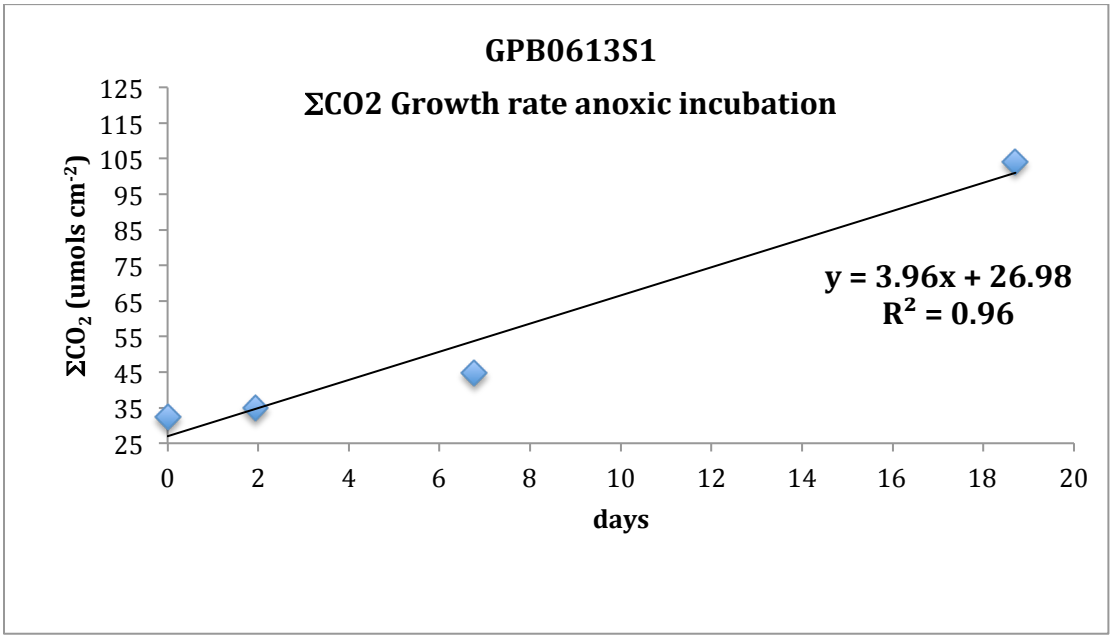
GPB0613S1
ΣCO2 Growth rate anoxic incubation
125
115
105
95
85
75
65
55
45
35
25
ΣCO2 (umols cm-2)
y = 3.96x + 26.98
R2 = 0.96
0
2
4
6
8
10
12
14
16
18
20
days

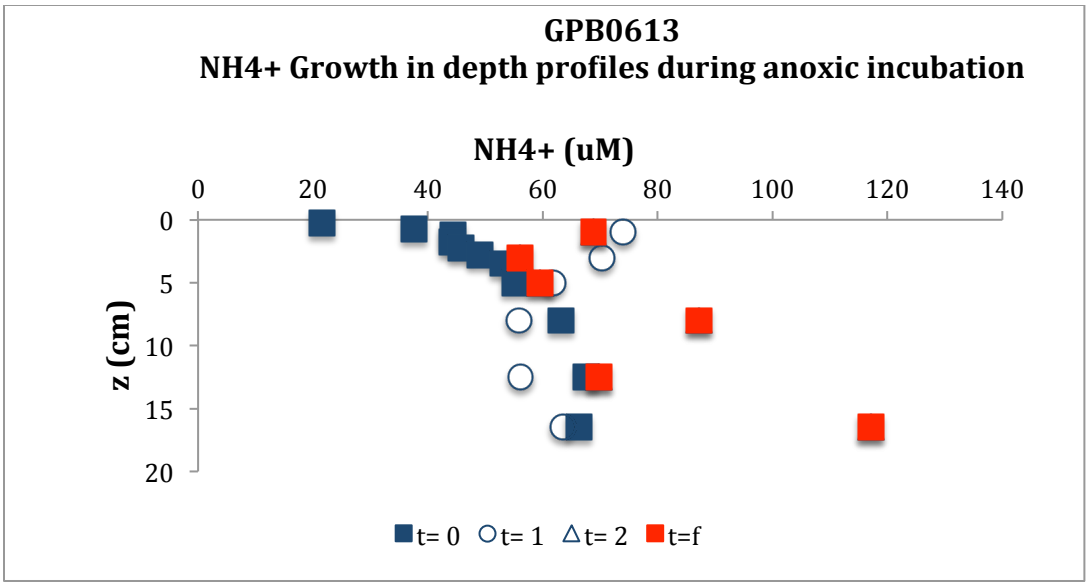
GPB0613
NH4+ Growth in depth profiles during anoxic incubation
NH4+ (uM)
0
20
40
60
80
100
120
140
z (cm)
0
5
10
15
20
t= 0
t= 1
t= 2
t=f

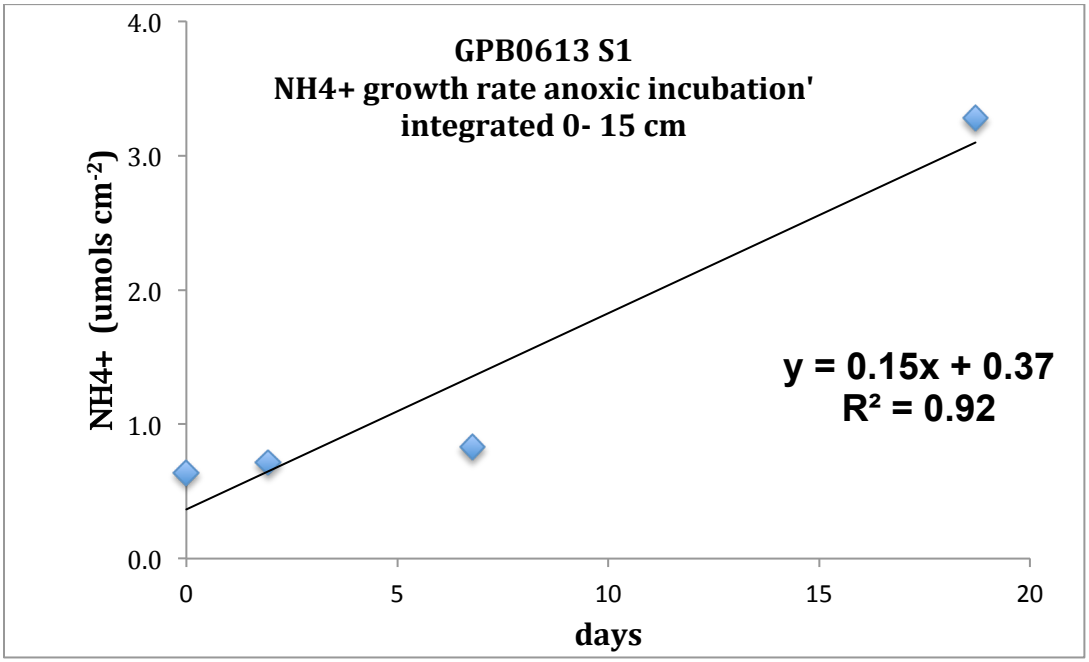
GPB0613 S1
NH4+ growth rate anoxic incubation'
integrated 0- 15 cm
NH4+ (umols cm-2)
4.0
3.0
2.0
1.0
0.0
y = 0.15x + 0.37
R² = 0.92
0
5
10
15
20
days

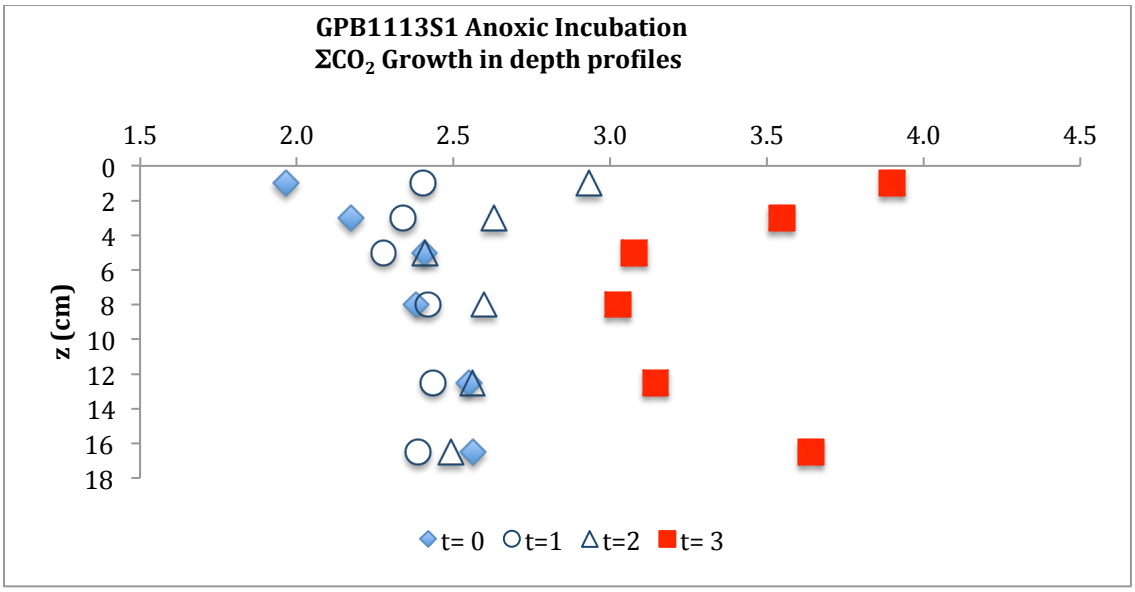
GPB1113S1 Anoxic Incubation
ΣCO2 Growth in depth profiles
1.5
2.0
2.5
3.0
3.5
4.0
4.5
0
2
4
6
8
10
12
14
16
18
z (cm)
t= 0
t=1
t=2
t= 3

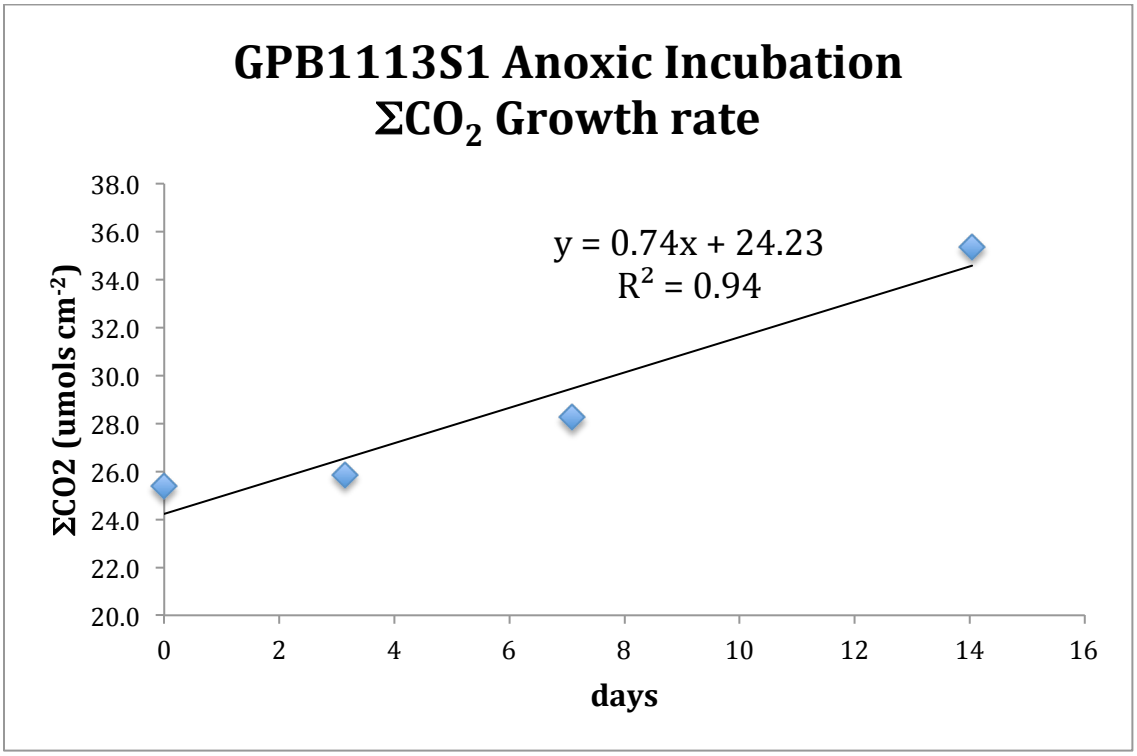
GPB1113S1 Anoxic Incubation
ΣCO2 Growth rate
y = 0.74x + 24.23
R2 = 0.94
38.0
36.0
34.0
32.0
30.0
28.0
26.0
24.0
22.0
20.0
ΣCO2 (umols cm-2)
0
2
4
6
8
10
12
14
16
days

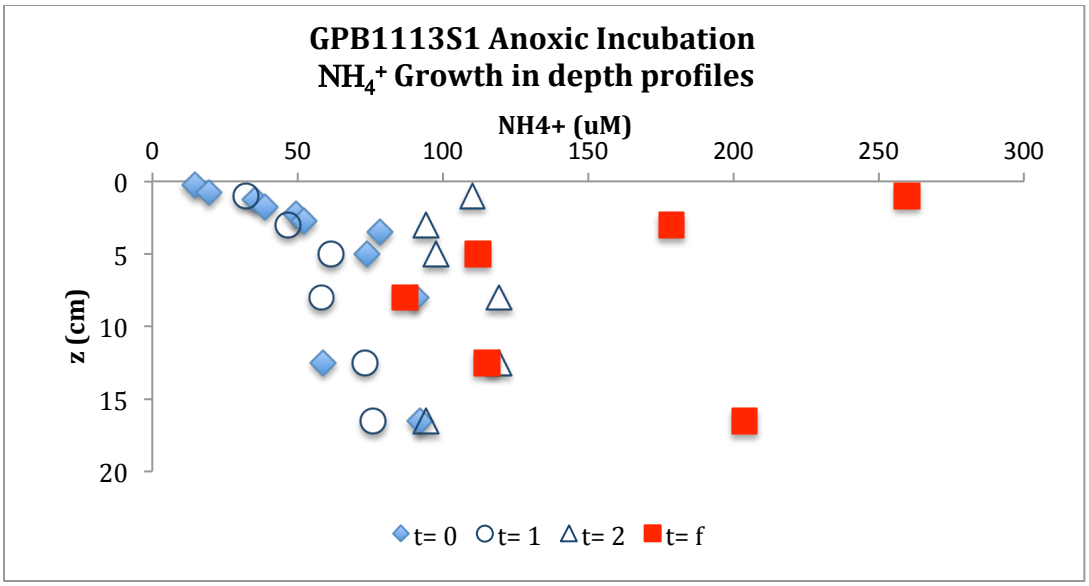
GPB1113S1 Anoxic Incubation
NH4+ Growth in depth profiles
NH4+ (uM)
0
50
100
150
200
250
300
z (cm)
0
5
10
15
20
t= 0
t= 1
t= 2
t= f

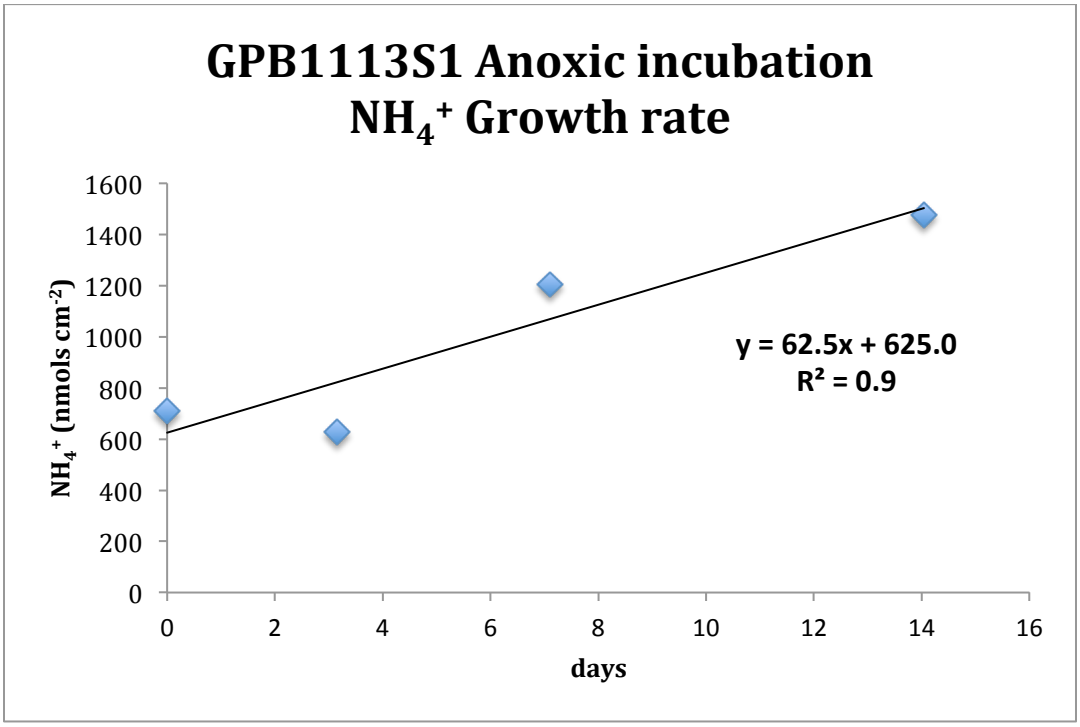
GPB1113S1 Anoxic incubation
NH4+ Growth rate
NH4+ (nmols cm-2)
1600
1400
1200
1000
800
600
400
200
0
0
2
4
6
8
10
12
14
16
days
y = 62.5x + 625.0
R² = 0.9

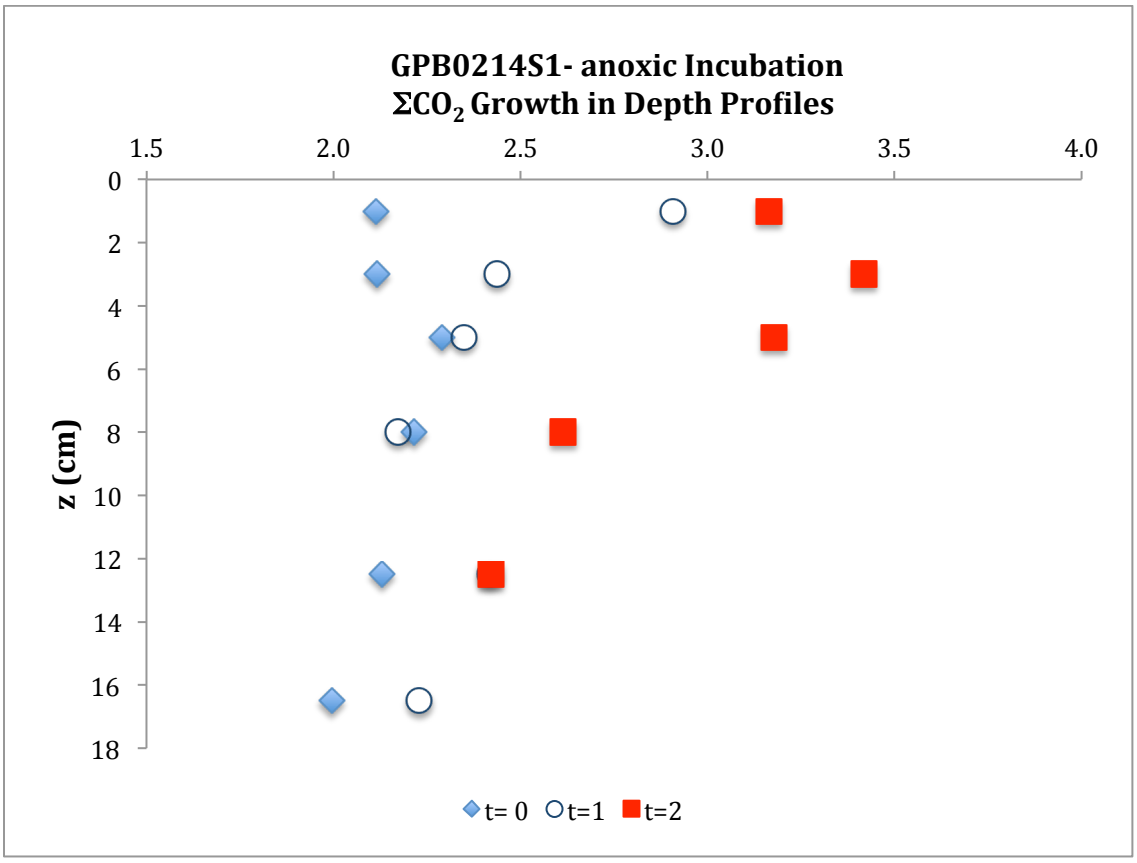
GPB0214S1- anoxic Incubation
ΣCO2 Growth in Depth Profiles
1.5
2.0
2.5
3.0
3.5
4.0
0
2
4
6
8
10
12
14
16
18
z (cm)
t= 0
t=1
t=2

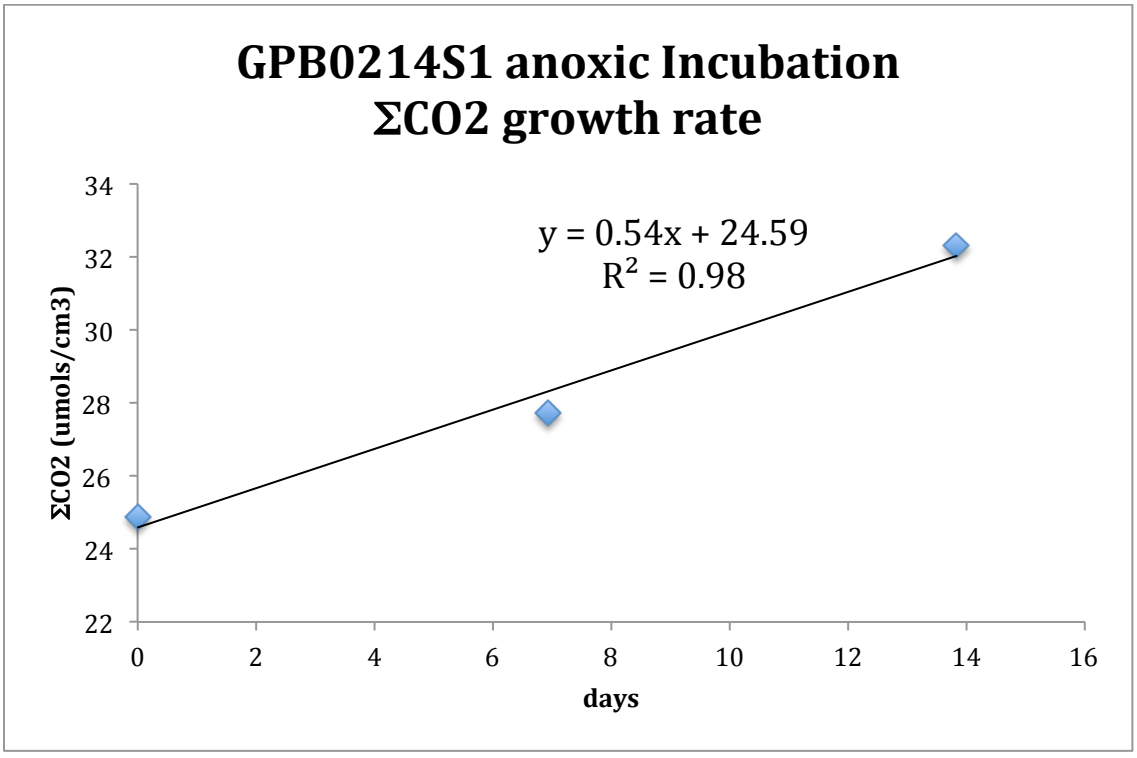
GPB0214S1 anoxic Incubation
ΣCO2 growth rate
y = 0.54x + 24.59
R² = 0.98
34
32
30
28
26
24
22
ΣCO2 (umols/cm3)
0
2
4
6
8
10
12
14
16
days

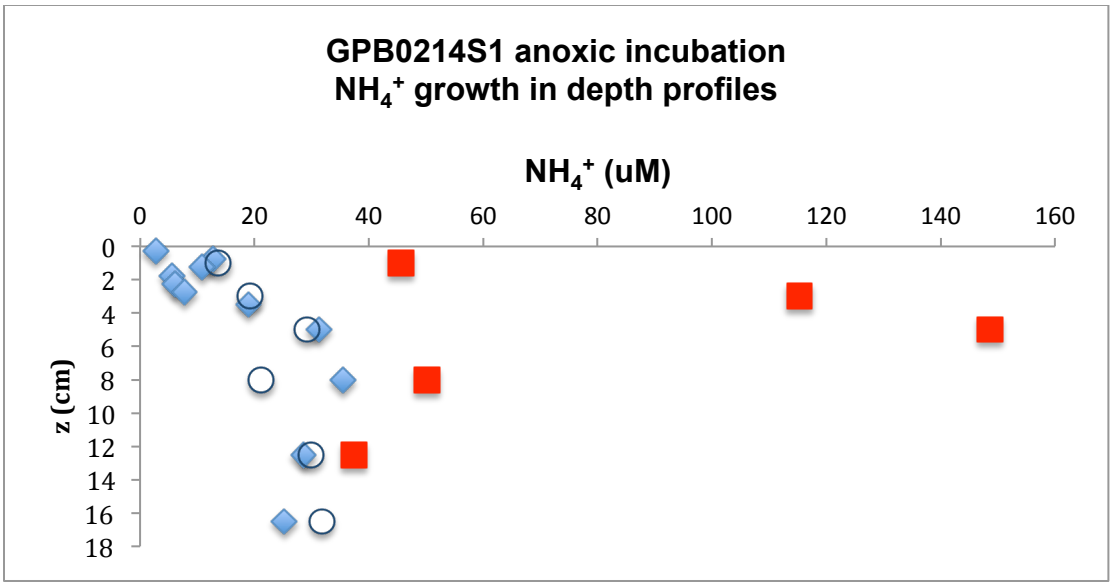
GPB0214S1 anoxic incubation
NH4+ growth in depth profiles
NH4+ (uM)
0
20
40
60
80
100
120
140
160
z (cm)
0
2
4
6
8
10
12
14
16
18

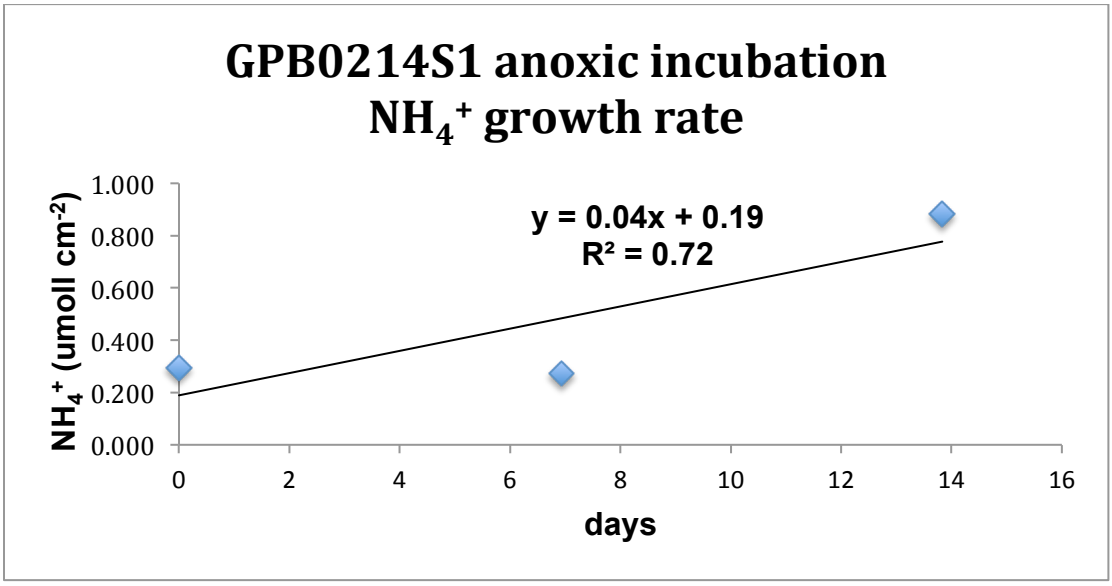
GPB0214S1 anoxic incubation
NH4+ growth rate
NH4+ (umoll cm-2)
1.000
0.800
0.600
0.400
0.200
0.000
y = 0.04x + 0.19
R² = 0.72
0
2
4
6
8
10
12
14
16
days

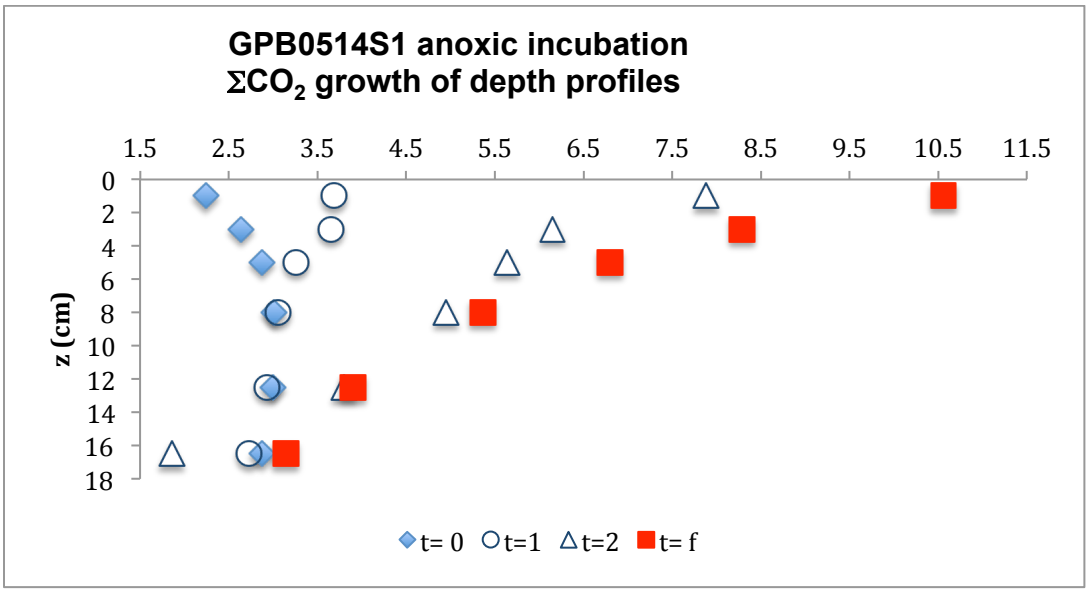
GPB0514S1 anoxic incubation
ΣCO2 growth of depth profiles
1.5
2.5
3.5
4.5
5.5
6.5
7.5
8.5
9.5
10.5
11.5
0
2
4
6
8
10
12
14
16
18
z (cm)
t= 0
t=1
t=2
t= f

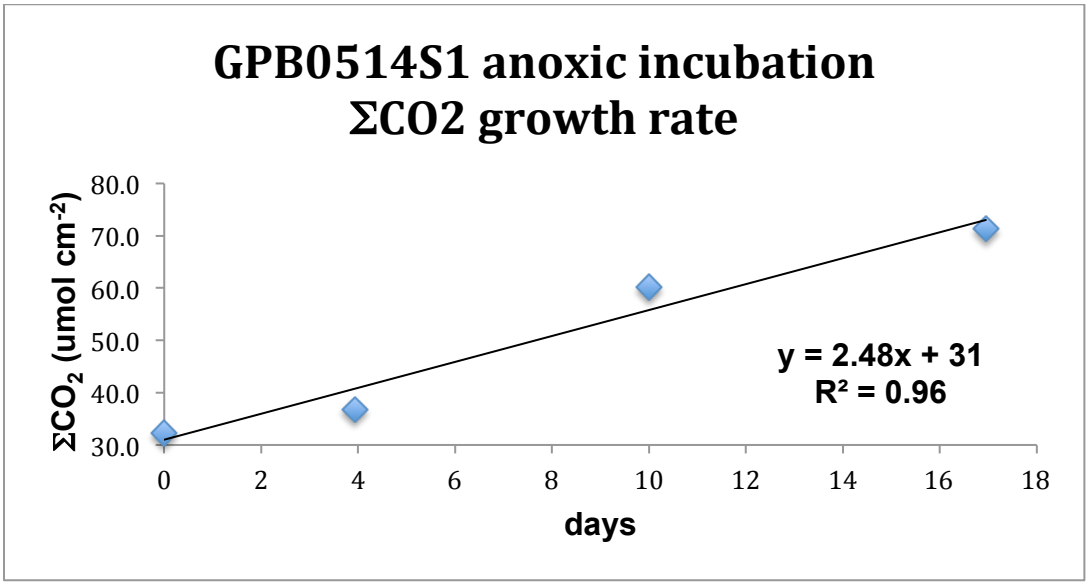
GPB0514S1 anoxic incubation
ΣCO2 growth rate
80.0
70.0
60.0
50.0
40.0
30.0
ΣCO2 (umol cm-2)
0
2
4
6
8
10
12
14
16
18
days
y = 2.48x + 31
R² = 0.96

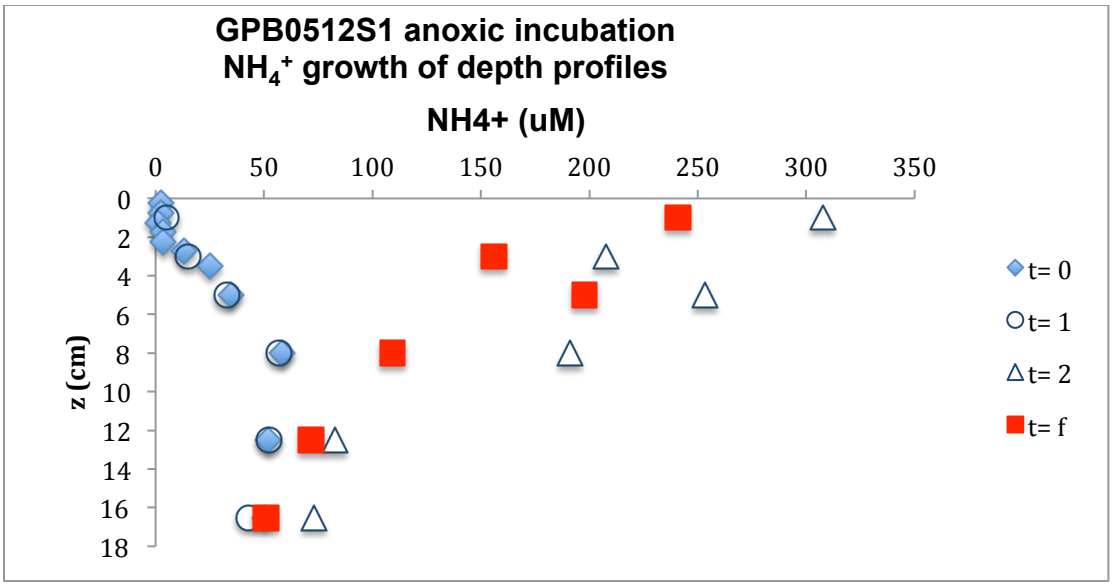
GPB0512S1 anoxic incubation
NH4+ growth of depth profiles
NH4+ (uM)
0
50
100
150
200
250
300
350
z (cm)
0
2
4
6
8
10
12
14
16
18
t= 0
t= 1
t= 2
t= f

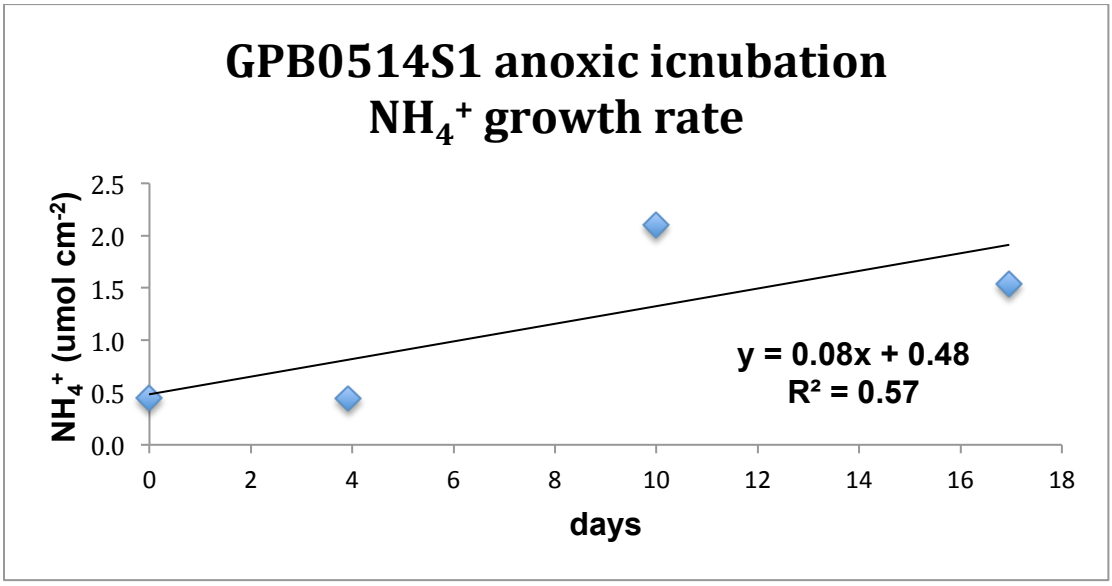
GPB0514S1 anoxic icnubation
NH4+ growth rate
NH4+ (umol cm-2)
2.5
2.0
1.5
1.0
0.5
0.0
0
2
4
6
8
10
12
14
16
18
days
y = 0.08x + 0.48
R² = 0.57